1-1-2002

Rammed aggregate pier soil reinforcement: group load tests and settlement monitoring of large box culvert

Kenneth Keith Hoevelkamp
Iowa State University

Rammed aggregate pier soil reinforcement: group load tests and settlement monitoring of large box culvert

by

Kenneth Keith Hoevelkamp

A thesis submitted to the graduate faculty

in partial fulfillment of the requirements for the degree of

MASTER OF SCIENCE

Major: Civil Engineering (Geotechnical Engineering)

Program of Study Committee:
David J. White (Major Professor)
John M. Pitt
Igor Beresnev

Iowa State University

Ames, Iowa

2002

Graduate College
Iowa State University

This is to certify that the Master's thesis of

Kenneth Hoevelkamp

has met the thesis requirements of Iowa State University

Signatures have been redacted for privacy

TABLE OF CONTENTS

LIST OF FIGURES

LIST OF TABLES

INTRODUCTION

Background

The construction of infrastructure and embankments on soft soils has long been a primary challenge to the geotechnical engineer. Past solutions to this problem often result in significantly increased construction costs, which can impact the overall scope and schedule of construction. Recently, the application of rammed aggregate pier soil reinforcement has emerged as ground improvement that precludes the need for deep foundations, over-excavation and replacement, or pre-loading. This method offers some solutions to the concerns of significant construction delay and uneconomical applications by working as a soil improvement method. The improvement of soft soils is primarily gained by replacing soft compressible soils with stiffer granular pile elements. In addition to increased stiffness, rammed aggregate pier foundation elements, being permeable, provide drainage paths for water, thus facilitating consolidation settlement.

Rammed aggregate piers, also known as Geopier™ foundation elements, a patented variation of the granular pile, were installed beneath the footprint of a 4.2 m wide x 3.6 m high box culvert installed on Iowa Highway 191 south of Neola, Iowa. Rammed aggregate piers were installed in an effort to reduce total and differential. The box culvert was installed beneath an existing bridge as an alternative to bridge replacement. After construction of the box culvert fill was placed over the culvert up to the existing bridge deck, as a result it was necessary to ensure that settlement of the soft layer under the box culvert did not affect the existing bridge piers by inducing downdrag. The rammed aggregate pier grid spacing and depth was designed to address these settlement concerns.

Construction at the site began in late July 2001. Filling operations began the last week of November 2001, and were completed the first week of December 2001. The fill height at the center of the culvert is 7.5 m and the total amount of fill placed was roughly 6500 m^3. The focus of the investigation was to document the implementation and performance of the *Geopier* soil reinforcement method used to mitigate settlement.

Objectives and Scope of Study

The overall objective of this research is to document and assess the performance of *Geopier* soil reinforcement in a transportation application in Iowa soils. The box culvert installation project south of Neola on Iowa Highway 191, was the primary research site.

Site investigation consisted of an in-situ testing program including piezocone penetrometer (CPT), pressuremeter (PMT), dilatometer (DMT) and borehole shear (BST). This testing was designed to characterize the subsurface, and also to define the parameters of the alluvial clay layer. Laboratory testing was conducted utilizing consolidated drained triaxial (CD), unconsolidated undrained triaxial (UU), oedometer and Atterberg limit testing. Testing was used to define strength and consolidation parameters as well as to classify the soft alluvial clay layer.

Vibrating wire instrumentation installed within the embankment includes total stress cells, settlement cells, and piezometers. Monitoring began during pier installations and continued for a period of about 6 months following box culvert construction and fill placement. In addition, survey pins were installed along the floor of the culvert to monitor the full settlement profile. Focus in the instrumentation program was placed on changes within the alluvial clay layer during and immediately after fill placement in an effort to closely monitor settlements.

Load testing on *Geopier* elements at the site utilized instrumentation to better characterize their behavior. Inclinometer, tell-tale, and stress cell data were obtained during testing operations to facilitate characterization under load. Individual and group load tests were performed to compare and contrast load-deformation behavior. A focus of these operations was the investigation of a "group effect". This phenomenon is a comparison of the strength of an individual pier with that of a pier within a group. The effect is considered in design for other applications such as driven piles. Instrumentation data also aided in concluding failure modes, observing stress concentration and the vertical stress distribution within a pier.

LITERATURE REVIEW

Introduction

A better understanding of the behavior of rammed aggregate piers is prefaced by an examination of the analogous concepts of granular piles. Significant research on granular piles, specifically stone columns, has attempted to characterize the mechanical concepts of bearing capacity and settlement. Methods vary from rigorous finite element analysis (Balaam and Booker, 1981) to approaches based on empirical data gathered by past experience (Castelli and Maugeri, 2002). Although these have met with some success, predictions of pile behavior under load are still on a case-to-case basis.

It is instructive to note here that the prediction of standard driven pile performance is still a wide area of research. Design methods based on site investigation tools such as CPT (Robertson and Campanella, 1983) and SPT (Meyerhof, 1956) testing are still widely debated. When one considers the additional uncertainties involved with granular pile construction including: diameter of the installed pier, angle of internal friction of the compacted pier material, soil-pier interaction, in-situ lateral stress development, etc., it is readily seen that prediction of performance is a complex undertaking.

Granular piles are considered a ground improvement method. Their feasibility lies in applications where only moderate strength increases of soft and compressible soils are necessary. Bearing capacity increases of 2 to 5 times are typical (Bergado et al., 1984). Installations are grid arrangements, typically in a square or triangular spacing pattern. The low load carrying capacity, high number of piles, and uncertainty in performance of piles, lends pile design to one based on an arbitrary factor of safety, usually three in relation to bearing capacity, and questionable correlations. This is much the same situation with driven piles.

The introduction of rammed aggregate piers has changed this. Their application as foundation elements for concentrated loads beneath mid-rise buildings has demanded control of bearing capacity and settlement. Significant research effort has been put forth to effectively characterize and predict the behavior of the rammed aggregate pier. It will be seen in this research that rammed aggregate piers have been successfully used to control total settlement as well as the more difficult differential settlement.

Particular concepts have been found to be more significant in granular pile design methodology and are the basis for current design. In order to analyze the load test data and settlement behavior of the reinforced clay layer, a thorough treatment of past and recent research on these concepts is developed herein.

Individual Pile Behavior

Bearing capacity

The capacity of a single pile is inherently tied to its failure mechanism, consistent with the classical mechanics of foundation design. The primary mechanisms in the granular pile are bulging, shear and punching type failure. Figure 1 is a graphic of each failure type in a homogeneous soft layer, such as the one present in this research. The mechanism induced is determined by several factors including: diameter of the pile, length of the pile, internal friction angle of the pile, shear strength of the soil, passive resistance of the soil and the homogeneity of the soil surrounding the pile, e.g., the presence of a stiff underlying layer.

The failure modes of interest here are bulging and punching type as they are most

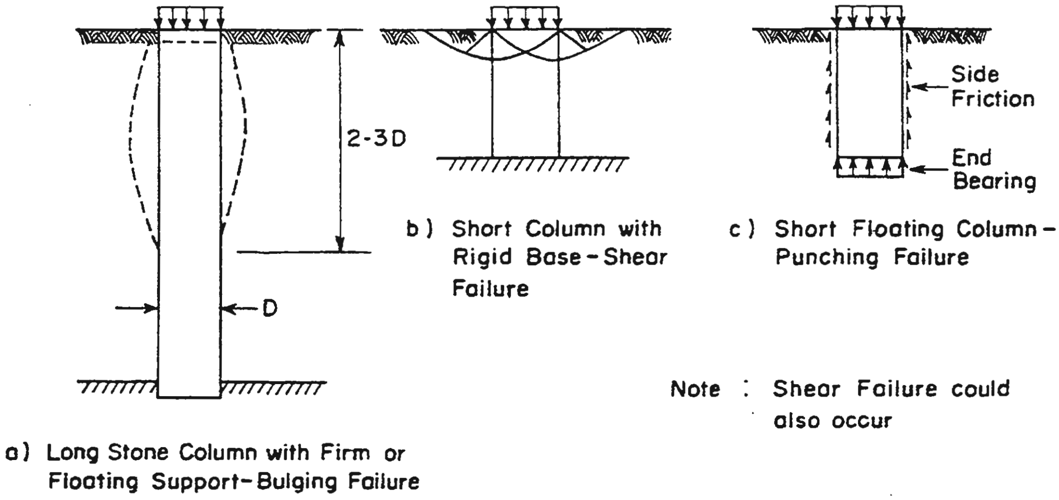

Figure 1. Failure modes of individual granular pile (Barksdale and Bachus, 1983)

likely in soft soil conditions. Each of these is observed in the load testing data presented later in this paper. The lateral confining stress of the pile, defined as the ultimate passive resistance that the soil can mobilize, controls bulging failure. A majority of the relationships derived to describe bulging behavior have been founded on this assumption (Bergado et al., 1996). Hughes and Withers (1974) have proposed to predict the bearing capacity based on confining resistance with the following relationship:

$$q_{ult} = (\sigma_{ro} + 4s_u)*(1 + \sin\phi_s / 1 - \sin\phi_s) \quad (1)$$

where σ_{ro} is the initial in-situ radial stress, s_u is the undrained shear strength, and ϕ_s is the angle of internal friction for the granular pile material. Punching type failure is controlled by the same calculation associated with driven piles described in the following relationship:

$$q_{ult} = 4Ls_u/d + 9s_u \quad (2)$$

where L is pile depth and d is pile diameter. In this case it is assumed that undrained strength of the clay is equal to shaft friction.

Beyond a certain critical depth of pier, bulging becomes the most likely failure mode (Hughes et al., 1975). The concept of critical pile depth is an important one in regard to failure mechanism and also load carrying capacity. Critical pile depth is defined as that depth corresponding to equilibrium of bearing capacity given by bulging and punching type failure modes. Hence at depths less than critical, punching type failure is most likely and at depths greater than critical, bulging type is most likely. The implication is that load carrying capacity is not increased as pile depth extends beyond the critical length, i.e., the ultimate resistance offered by a pile will not increase beyond that offered by bulging failure. The design capacity of both granular piles and rammed aggregate piers takes advantage of the increased resistance offered by the radial expansion preceding bulging failure in a soft cohesive soil. Figure 2 offers a method to estimate critical pile depth using the unit weight, diameter (d_p) and friction angle (ϕ) of the pile along with the undrained shear strength of the soil. Figure 3 is a diagram representing the relationships used by *Geopier* to estimate bulging depths. They are:

$$d = d_g[\tan(45+\phi/2)] + z \qquad (3)$$

$$d_m = \{d_g[\tan(45+\phi/2)]\}/2 + z \qquad (4)$$

where d is the maximum depth of bulging, d_m is the mid-height of bulging, d_g is the diameter of the pier, ϕ is the friction angle of the pier material, and z is the footing depth.

It should be noted that rammed aggregate piers are typically constructed with a length of approximately three times their diameter, roughly 2.74 m (Lawton et al., 1994). Not penetrating to a stiff underlying layer, commonly referred to as a "floating" pile, is characteristic of their construction. Granular piles are routinely installed to depths of 10-15 m, often for the purpose of penetrating a stiff layer.

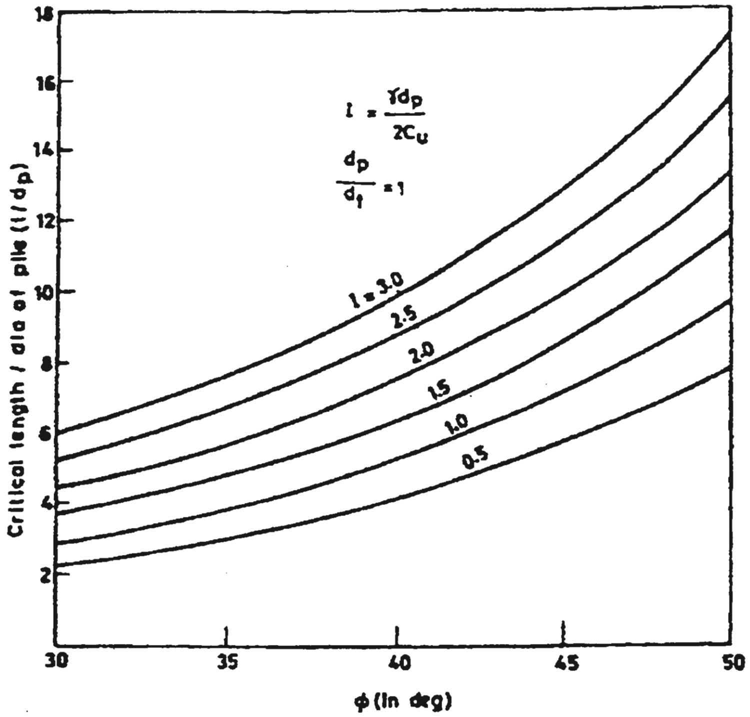

Figure 2. Critical length of granular pile (Madhav and Vitkar, 1978)

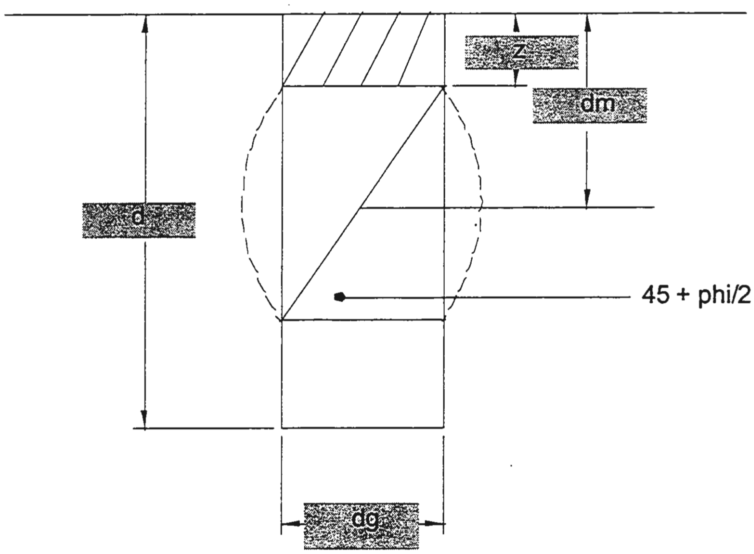

Figure 3. Graphic of *Geopier* bulging dimensions (*Geopier* Technical Bulletin No. 2)

Settlement

Several methods have been proposed to predict the settlement behavior of an individual pile. These have met with varied success. An elastic approach and a method based on the radial stress-strain properties of the soil will be discussed here.

Elastic continuum approach

Mattes and Poulos (1969) presented a solution for the settlement of a single compressible pile. The assumption is that the pile deformation behaves elastically. The settlement is given by:

$$S = P/(E_s L_p) * I_p \tag{5}$$

where P is load, E_s is soil modulus, L_p is length of pier, and I_p is a displacement influence factor given as a function of the pile stiffness factor:

$$k = E_p/E_s \tag{6}$$

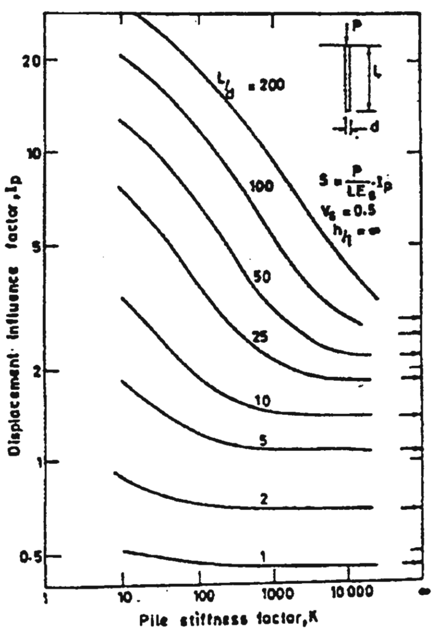

Figure 4. Displacement influence factors (Mattes and Poulos, 1969)

where E_p is the deformation modulus of the pile. Figure 4 is a graph that indicates that I_p increases as the length to diameter ratio increases. Although the method seems counter-intuitive with respect to prior knowledge of pile deformation modulus being required, it allows the flexibility of varying soil and pier dimensions and parameters. The key concept in this approach is the use of the modular ratio between the pile and soil.

Radial stress-strain approach

Hughes et al. (1975) proposed a method for predicting settlement based on the radial stress-strain properties of the soil. The necessary parameters listed in the report are given below.

1. Undrained shear strength of the soil.
2. The in-situ lateral stress in the soil.
3. The radial pressure/deformation characteristics of the soil.
4. The angle of internal friction of the column material.
5. The initial diameter of the column. -Hughes, Withers and Greenwood (1975)

It was rationalized that the bulging mechanism of the pile could be directly analogized to the radial expansion of a pressuremeter. The pile is then assumed to expand at constant volume, translating the radial expansion directly into settlement. Dividing the pile into layers and summing the settlement contribution from each layer provides the calculation of total settlement. The radial expansion is estimated directly from a pressuremeter curve containing stress on the ordinate and radial strain on the abscissa. The relationship is expressed by:

$$S = \sum_{i=1}^{m} 4H_i\delta_{ri}/d_p \qquad (7)$$

where H_i is the layer thickness, d_p is the diameter of the pile, and $2\delta_{ri}/d_p$ represents the radial strain of the i^{th} layer.

In addition to predicting settlement, Hughes et al. (1975) show that vertical stress distribution within the pier can be estimated through an idealization of shear stress build-up along the pile-soil boundary. This is represented in Figure 5. It can be seen that the shear stress is not allowed to exceed the capacity of the soil and that maximum shear stress is only transmitted to a depth coinciding with the critical length of the pier.

The final consideration is that bulging does not occur unless the passive resistance of the soil has been realized and full shear resistance has been mobilized throughout the critical length of the pier. The concepts learned here will become important in the analysis of load test data later in this thesis.

Group Pile Behavior

The basic behavior of an individual pile is the same as a pile within a group. Failure mechanisms remain the same, with the addition of global failures that involve failure planes

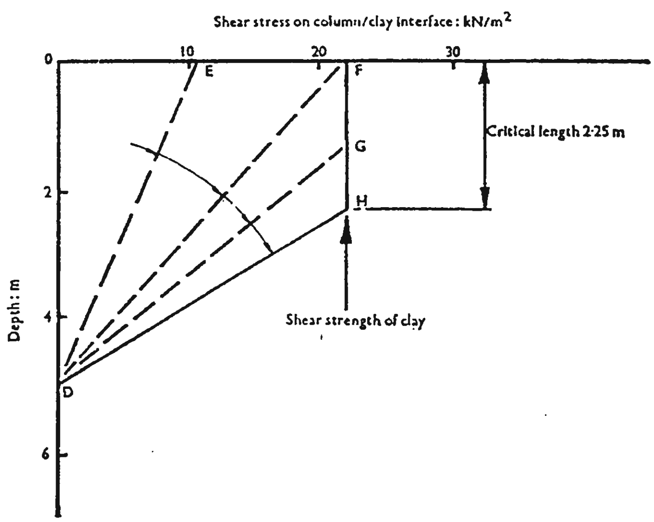

Figure 5. Idealized shear stress distribution with load (Hughes et al., 1975)

extending through several piles whether on a circular or planar surface. Complications arise when evaluating bearing capacity and settlement as a result of the loading mechanism. Either a flexible raft or a rigid raft loads a group of piles. Examples are an embankment for the former, and a mat foundation for the latter. In these cases load is now transferred not only to the pile but also directly to the matrix soil between. The conglomeration of the two units, pile and soil, necessitates a characterization of the entire system. Present methods for analysis and design include semi-empirical methods based on experience, and finite element method. A discussion of the key concepts used in current design methodology follows.

Tributary area

Groups of granular piles are typically placed on a grid with a triangular or rectangular spacing arrangement. A cylinder with an effective diameter dependent on the grid spacing approximates the unit cell (tributary area), including pile and matrix soil. Figure 6 illustrates the unit cell for both triangular and square grid spacing along with their effective diameters.

Barksdale and Bachus (1983) presented a method of design based on the unit cell concept. It was found that the amount of matrix soil replaced with aggregate within the area tributary to the pile had a significant correlation to the performance of the improved ground. Thus an equation was posed to define area replacement ratio:

$$a_s = A_s/A \tag{8}$$

where A_s is the area of the pile and A is the total area within the unit cell. Coupling this with the equations for unit cell area obtains the ratio for triangular and square arrangements as follows, respectively:

$$a_s = 0.907\,(D_s/s)^2 \tag{9}$$

$$a_s = 0.783\,(D_s/s)^2 \tag{10}$$

where D_s is the diameter of the pile and s is spacing of the grid. Typical ratios used are in the range of 0.10 to 0.40 (Barksdale and Bachus, 1983).

The volume of soil replaced is important in relation to composite stiffness. The piles represent a stiffer element, so that higher replacement ratios of aggregate would work to stiffen the pile-soil composite grid. Improvement ratios for settlement and bearing capacity are based on the area replacement ratio.

Stress concentration

As mentioned previously, the granular piles represent a stiffer element within the soil-pile matrix. When load is applied through a rigid raft the pier and matrix soil settle

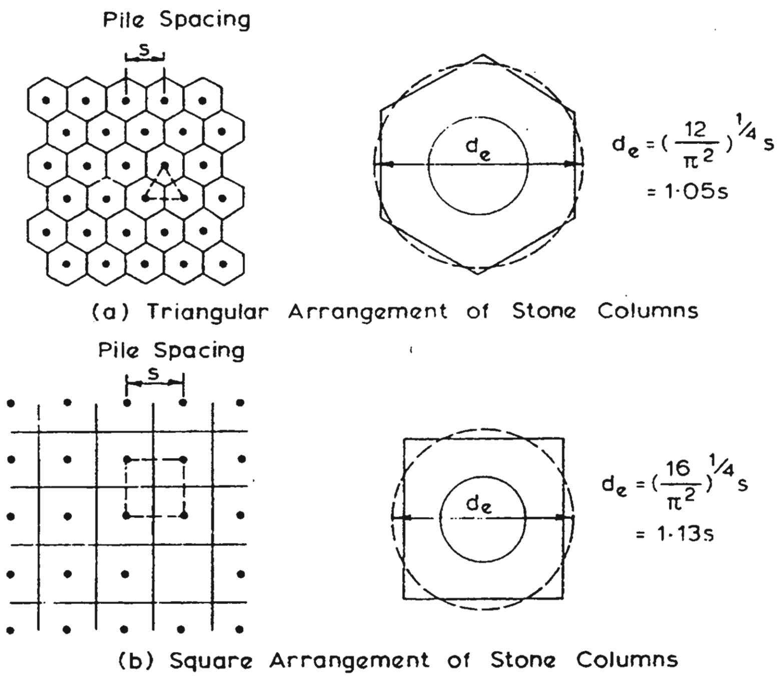

Figure 6. Pile arrangements with influence of each pile (Balaam and Booker, 1981)

an equal amount. Due to the higher stiffness of the pile, elastic theory prescribes a higher stress applied to the pile. The magnitude of this stress concentration is then directly proportional to the ratio in stiffness of the pier to the matrix soil. This effect can be less pronounced in the case of a flexible raft where each element can settle somewhat independently. The stress concentration factor is defined as:

$$n_s = \sigma_s/\sigma_c \qquad (11)$$

where σ_s is the stress in the pile and σ_c is the stress in the soil. The variation of stress concentration with area replacement ratio listed for stone columns by Barksdale and Bachus (1983) ranged from 2 to 5. Gaul (2001) indicates stiffness ratios of rammed aggregate piers to stone columns ranging from 10 to 15 based on load test results. From this it is reasonable to surmise that rammed aggregate piers generate higher stress concentrations than stone columns.

Once again using elastic theory, it is possible to calculate the stresses on the pile and soil using the area replacement ratio and stress concentration factor. The stresses in the pile and clay are:

$$\sigma_s = n\sigma/[1+(n-1)a_s] \qquad (12)$$

$$\sigma_c = \sigma/[1+(n-1)a_s] \qquad (13)$$

where σ is the overburden.

It has been posed that stress concentration ratios should increase with time in a cohesive soil (Juran and Guermazi, 1988, Han and Ye, 1991, Lawton, 1999). As consolidation proceeds due to the increase in vertical stress, the soil will further compress. This compression should theoretically be accompanied by a proportionate decrease in stress concentration on the matrix soil.

Bearing Capacity

Barksdale and Bachus (1983) have posed that different methods for bearing capacity be used when encountering soft to very soft cohesive soils as opposed to firm and stronger cohesive soils. The assumption is that the failure mechanisms differ, requiring separate analyses. Very soft soils consider the possibility of local bulging failure so that ultimate capacity is based on the strength of a single isolated column within a group multiplied by the number of piles. This is expressed as:

$$q_{ult} = s_u N_c \qquad (14)$$

where N_c is the composite bearing capacity factor for the granular pile which ranges from 15-22. The composite bearing capacity factor is correlated to the area replacement ratio. This method is assumed representative whether the loading is through a rigid or flexible foundation.

The question of group efficiency is an elusive one in the study of pile group capacity. The concept under scrutiny is whether piles within groups have a capacity less than that of an isolated one due to the influence of adjacent piles. This becomes important when design considers a smaller group of piles supported by a concrete raft. The raft may be freestanding in the case of some driven piles, or in contact with the ground, as is the case with some driven piles and all granular piles. The ASCE Committee on Deep Foundations report [CDF (1984)] recommends not using group efficiency as a description of group action. It suggests that only piles driven in cohesionless soils be assigned an efficiency greater than one, as densification resulting from pile driving increases skin friction. Barksdale and Bachus(1983) suggest group efficiency in the range of 0.8 to 1.0 for small groups of stone columns. These recommendations and findings from several studies of driven piles reviewed in Zhang

Table 1. Experimental values of group efficiency from Zhang et al. (2001) and Barksdale and Bachus (1983)

	Driven Piles	Mean	Standard
Soil Type	Raft Type	Efficiency	Deviation
Cohesive	Free	0.84	0.10
	Free	0.83	0.12
	Free	0.88	0.11
	Ground	1.04	0.13
	Ground	1.19	0.17
Cohesionless	Free	1.41	0.34
	Free	1.41	0.28
	Free	1.30	0.27
	Ground	1.40	0.18
	Ground	1.54	0.16
	Granular Piles		
Cohesive	Ground	0.8-1.0	N/A

et al. (2001) are listed in Table 1. The contribution of the raft to capacity is indicated by a comparison between the freestanding and ground rafts on cohesive soil.

The assumption of a firm soil begins with the measurement of undrained shear strength greater than 30-40 kPa. Barksdale and Bachus (1983) then prescribe that the angle of internal friction of the soil and the cohesion in the pile are negligible. Once the full strength of the soil-pile system has been mobilized a failure surface with two planar lines is estimated. This is shown in Figure 7. Using equilibrium of the wedge in Figure 7 the ultimate bearing capacity is expressed as:

$$q_{ult} = \sigma_3 \tan^2\beta + 2c_{avg}\tan\beta \qquad (15)$$

where:

$$\sigma_3 = \frac{1}{2}\gamma_c B\tan\beta + 2c \qquad (16)$$

$$\beta = 45 + \phi_{avg}/2 \qquad (17)$$

$$\phi_{avg} = \tan^{-1}(\mu_s a_s \tan\phi_s) \qquad (18)$$

$$c_{avg} = (1\text{-}a_s)c \qquad (19)$$

where γ_c=saturated or wet unit weight of soil; B=foundation width; β=failure surface inclination; c=undrained shear strength within the unreinforced cohesive soil; ϕ_s=angle of internal friction of the pile; ϕ_{avg}=composite angle of internal friction; c_{avg}=composite cohesion on the shear surface; μ_s=stress ratio of pile to soil.

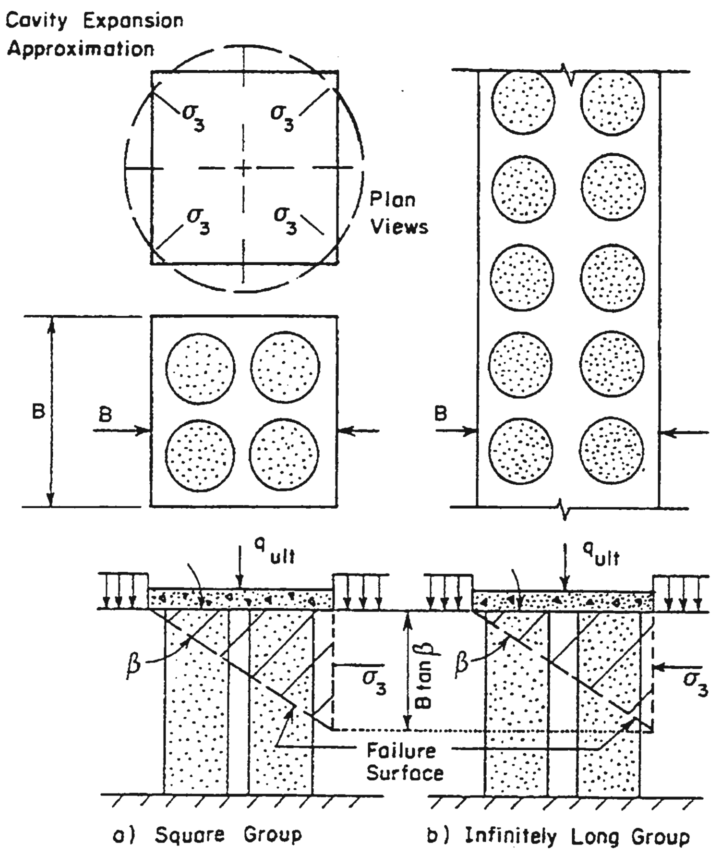

Figure 7. Granular pile group shear failure (Barksdale and Bachus, 1983)

Settlement

Decreased magnitude in settlement is often the purpose of granular pile installation. In this capacity embankments and other infrastructure not tolerable of excessive settlement can be constructed on what would otherwise be unsuitable soils. Increased rate of consolidation in cohesive soils is a benefit that was first posed theoretically and has subsequently been proven through field observations (Stewart and Fahey, 1984). A discussion of each aspect of settlement follows.

Total Settlement

Several methods have been investigated to predict settlement of reinforced soil. These analyses do not predict absolute settlement, rather a quantity relative to the unreinforced condition called the settlement reduction ratio. This is expressed as:

$$SR = \frac{Sr}{Su} \tag{20}$$

where S_r is settlement of the reinforced soil and S_u the settlement of the unreinforced soil. Settlement in the unreinforced condition is calculated by conventional methods. From this an improvement factor is defined as:

$$IF = 1/SR \tag{21}$$

Aboshi and Suematsu (1985) have compiled several of the settlement reduction ratio prediction methods. The methods are functions of area replacement ratio with varying other factors such as stress concentration factor, modular ratio, and pile material friction angle. The compilation is shown in Figure 8. Balaam and Booker (1981) suggested a method relying on elastic theory, modular ratio, and pile spacing. Their analysis is summarized in Figure 9.

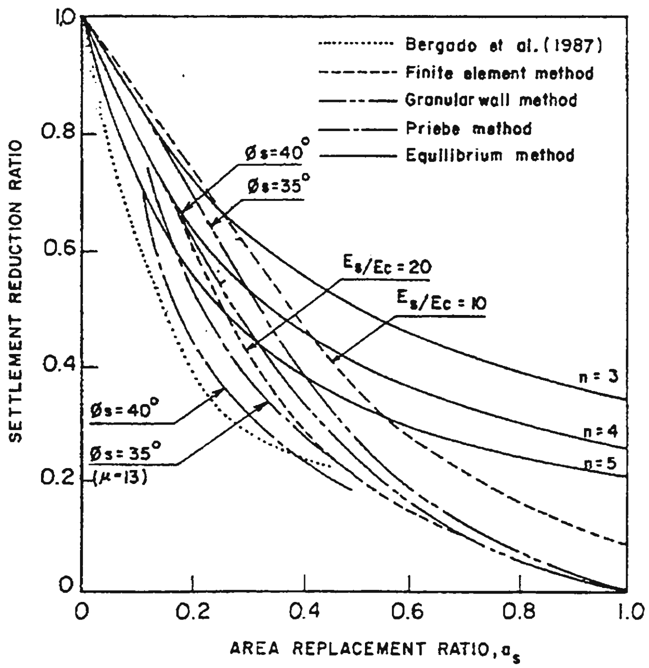

Figure 8. Compilation of settlement prediction methods using area replacement (Aboshi and Suematsu, 1985)

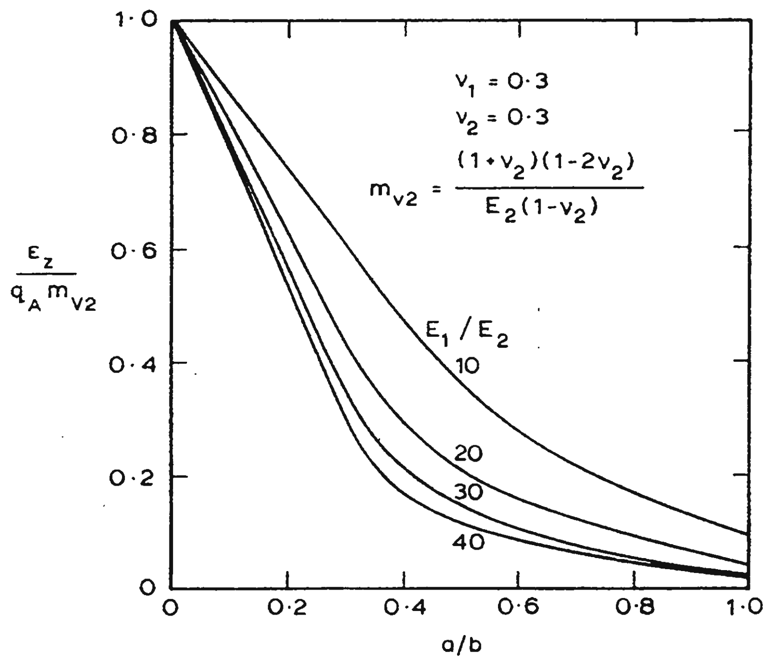

Figure 9. Settlement prediction using modular ratio and effective area (Balaam and Booker, 1981)

Rate of settlement

Sand drains had long been used as means to speed up consolidation before the advent of granular piles. Barron (1947) derived a solution for drain wells that considered both radial and vertical drainage. It was initially thought that granular piles would have the same properties of drainage, but consideration to strain and modulus inequalities between soil and pile led to varying assumptions for analysis. Each solution is based on the concept of decreasing the total drainage distance.

Han and Ye (2001) have posed a simplified solution that resolves the issues of soil-pile modular ratio and stress transfer to the pile with the dissipation of excess pore pressure. Their analysis is based on the following assumptions excerpted from the paper.

1. Stone columns are free-draining at any time. Each stone column has a circular influence zone.
2. The surrounding soil is fully saturated, and water is incompressible.
3. Stone columns and the surrounding soil only deform vertically and have equal strain at any depth.
4. The load is applied instantly through a rigid foundation and maintained constant during the consolidation period. At the moment of the load being applied, uniform excess pore water pressures within the surrounding soil carry all the loads. At the moment of loading, however, the saturated soil is under an undrained condition. The undrained elastic modulus of the saturated soil is theoretically infinite under a condition with full confinement, which results from the preceding assumption of one-dimensional deformation.
5. Total vertical stresses with stone columns and the surrounding soil, respectively, are averaged and uniform. - from Han and Ye (2001)

Modified coefficients of vertical and radial consolidation are calculated based on stress concentration factor and a diameter influence ratio. The expressions are:

$$c'_r = c_r(1 + n_s(1/(N^2-1))) \qquad (22)$$

$$c'_v = c_v(1 + n_s(1/(N^2-1))) \qquad (23)$$

where c'_r and c'_v are the modified coefficients of consolidation and N is:

$$N = d_{inf} / d_{col} \quad (24)$$

where $d_{inf,col}$ are the effective diameter of the pile and the actual diameter, respectively. It can be seen in these relationships that a higher stress concentration factor would lead to a higher modified coefficient of consolidation. The increased stiffness in a rammed aggregate pier should increase consolidation rates accordingly.

A modified time factor is then calculated with the modified coefficients of consolidation. These are found by substituting the modified coefficients directly into Terzaghi's 1-d time rate of consolidation equation:

$$T'_r = c'_r t / d_e^2 \quad (25)$$

Han and Ye (2001) provided two figures to calculate relative amount of consolidation using the time factors. These are shown in Figures 10 and 11. An overall amount of consolidation is calculated using an expression posed by Carillo (1942):

$$U_{rv} = 1 - (1 - U_r)(1 - U_v) \quad (26)$$

where U represents the correspondent percentage of total consolidation.

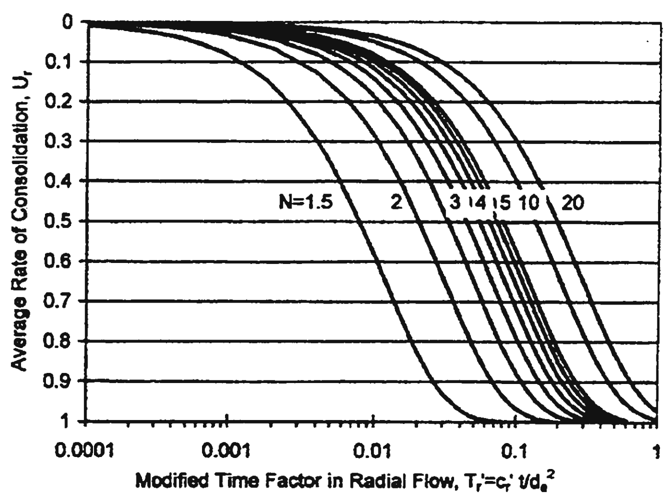

Figure 10. Consolidation with modified coefficient of consolidation (Han and Ye, 2001)

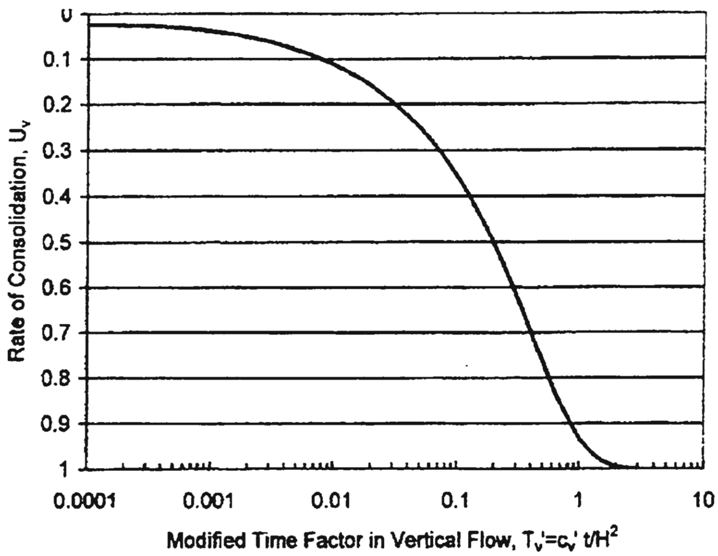

Figure 11. Consolidation amount with modified vertical coefficient of consolidation (Han and Ye, 2001)

PROJECT LOCATION AND DESCRIPTION

Rammed aggregate piers were installed beneath a culvert on Iowa Highway 191 south of Neola, Iowa. The piers were installed in an effort to reduce total and differential settlement of the culvert and embankment due to the presence of a soft alluvial clay layer. Routing of the stream was diverted while earthwork, construction of the culvert and subsequent backfill was performed. The culvert was located beneath a bridge as part of a remediation project resulting from anticipation of structural disrepair in the aging bridge. Construction at the site began in late July 2001 and was finished by mid-December 2001. The embankment reached a maximum depth of 7.5 m beneath the bridge.

In-situ testing was conducted prior to construction to effectively characterize soil parameters of the soft alluvial clay. Vibrating wire instrumentation was installed within the embankment to monitor change during filling operations and consolidation. A self-contained data-logging console was installed on site to provide automatic logging of data twice each day. Load testing was also performed on site with the objective of further characterizing rammed aggregate pier behavior under load.

Backfilling operations began in late November 2001 and were finished within 3 weeks. Continuous monitoring was maintained to verify total and differential settlement performance of the soft soil reinforcement. Settlement of the bridge was also monitored to verify that consolidation of the clay layer did not threaten the stability of the existing timber bridge piles. Figures 12 and 13 are pictures of the project site.

Figure 12. Project site looking north-east during pier installation

Figure 13. Project site showing spoils of soft alluvial clay layer from drilling

SUBSURFACE INVESTIGATION

In order to assess conditions at the site, a comprehensive testing program including in-situ and laboratory testing was completed. In-situ testing included Cone Penetrometer testing (CPT), Flat Dilatometer testing (DMT), Borehole-Shear testing (BST) and Pressuremeter testing (PMT). The in-situ testing took place prior to the beginning of construction at the site. The laboratory testing was conducted on representative samples obtained through Shelby-tube sampling. Laboratory testing included particle size distribution, moisture content, Atterberg Limits, drained and undrained triaxial, and one-dimensional consolidation tests. Laboratory results were compared to soil parameters obtained from each of the different in-situ testing methods employed on the site and described herein.

CPT was the first in-situ testing performed at the site. Figure 14 shows a schematic of the site indicating three soundings labeled CPT1, CPT2 and CPT3. The locations of subsequent drilling and in-situ testing were at CPT1, CPT2, and the load testing area located on the southwest corner of the site. Testing was performed at CPT1 and CPT2 to aid in the correlation of data by comparing it with that obtained by the CPT. Testing in the load test area was used to obtain soil parameters for analysis with load test data. A description of all test results follows.

In-Situ Testing Program

CPT data

Three soundings were performed on the site prior to construction. The locations of the soundings are labeled CPT1 through 3 in Figure 14. The soundings were placed at the corners of the site to obtain subsurface information concerning the thickness of the natural

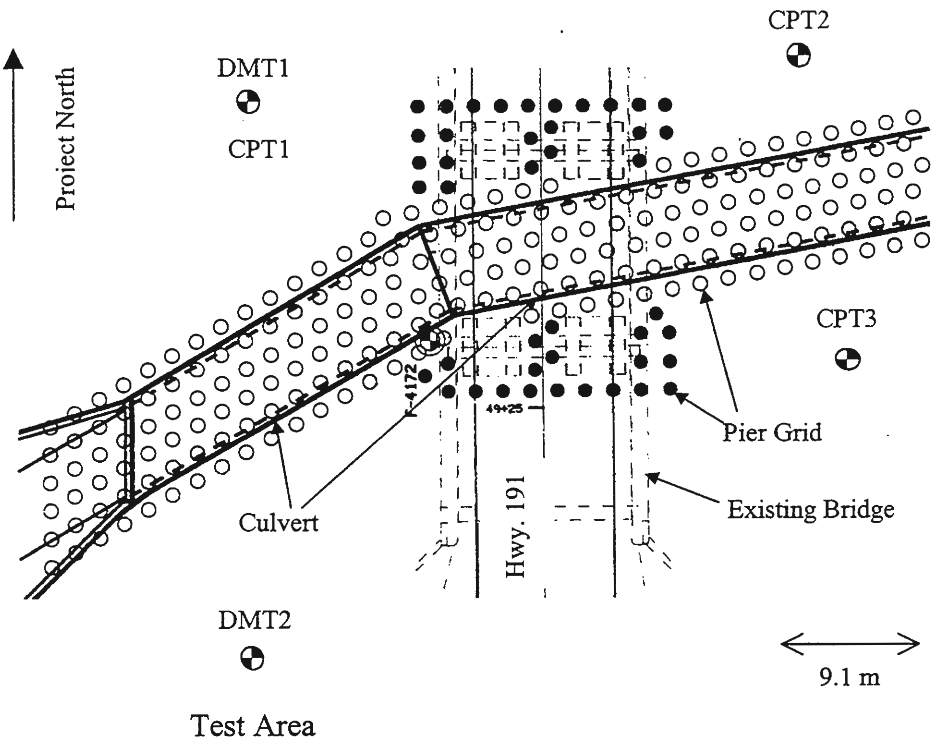

Figure 14. Plan view of project site with DMT and CPT sounding locations

alluvial formation and to identify the depth to a dense formation believed to be weathered shale bedrock. The CPT data was obtained using an electric subtraction cone with a pore pressure sensor near the tip. The cone was pushed hydraulically while data was collected at 5 cm intervals. An average 25 cm depth interval was used to report data. Geotechnical Services Incorporated (GSI) of Omaha, Ne., was subcontracted to conduct and analyze the CPT data. The CPT report is provided in Appendix A.

The Piezocone data for CPT1 is represented graphically in Figure 15. The profiles for CPT2 and CPT3 can be found in Appendix A. The parameters displayed in each of the graphs are defined as q_T for corrected tip resistance, f_s for sleeve friction, R_f for friction ratio (f_s/q_c x 100%), μ the pore water pressure, Q the normalized net tip resistance, F the

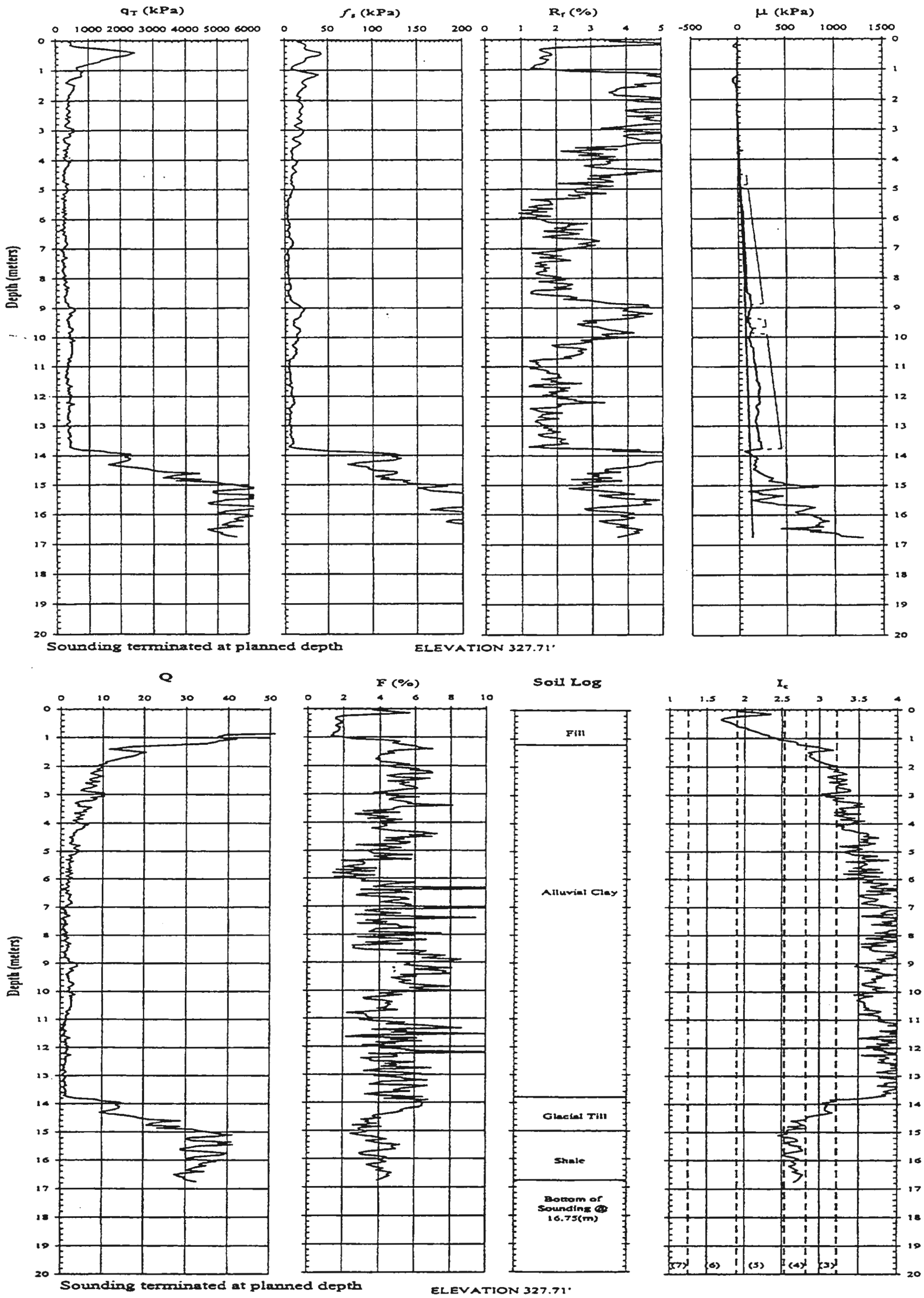

Figure 15. CPT1 data showing sleeve and tip resistance, and soil profile

normalized friction ratio, and I_c the soil behavior and classification index. Figure 15 also provides a soil log identifying the classifications of each soil layer. The soil classification is based on the Simplified Soil Classification Chart for Standard Electronic Friction Cone by Robertson and Campanella (1986). The correlation is founded on a relation between the magnitude of tip resistance, friction ratio and soil type.

Appendix A includes a tabular list of all CPT data including empirical correlations to drained friction angle (ϕ) and D_r (relative density). The drained friction angle was determined using a correlation proposed by Kulhawy and Mayne (1990). The relative density was determined using a correlation proposed by Jamiolkowski et al. (1985).

CPT1 and 2 indicate a thick natural alluvial clay layer underlain by glacial till and weathered shale bedrock. CPT3 indicates the same alluvial clay layer but was aborted due to rod refusal at an elevation of 312.6 m. This elevation corresponds to that of the glacial till layer in each of the other soundings and probably indicates a very dense till. The profile indicates a layer of fill averaging 1.2 m in thickness underlain by alluvial clay with an average thickness of 12.5 m underlain by a glacial till roughly 2 m in thickness overlying weathered shale bedrock.

The alluvial clay is of primary interest in this project. The graphs of tip resistance give sufficient reason for this concern, very soft and compressible clay. The tabulated cone data indicates an average drained friction angle of 22° for this layer. The unconfined compressive strength (q_u) was estimated using a relationship proposed by Robertson and Campanella (1986). Figure 16 is a representation of the correlation to q_u for data obtained in CPT1. The data is presented in Appendix A. The result is an average unconfined compressive strength of 17 +/- 5 kPa for the clay layer. This classifies as very soft

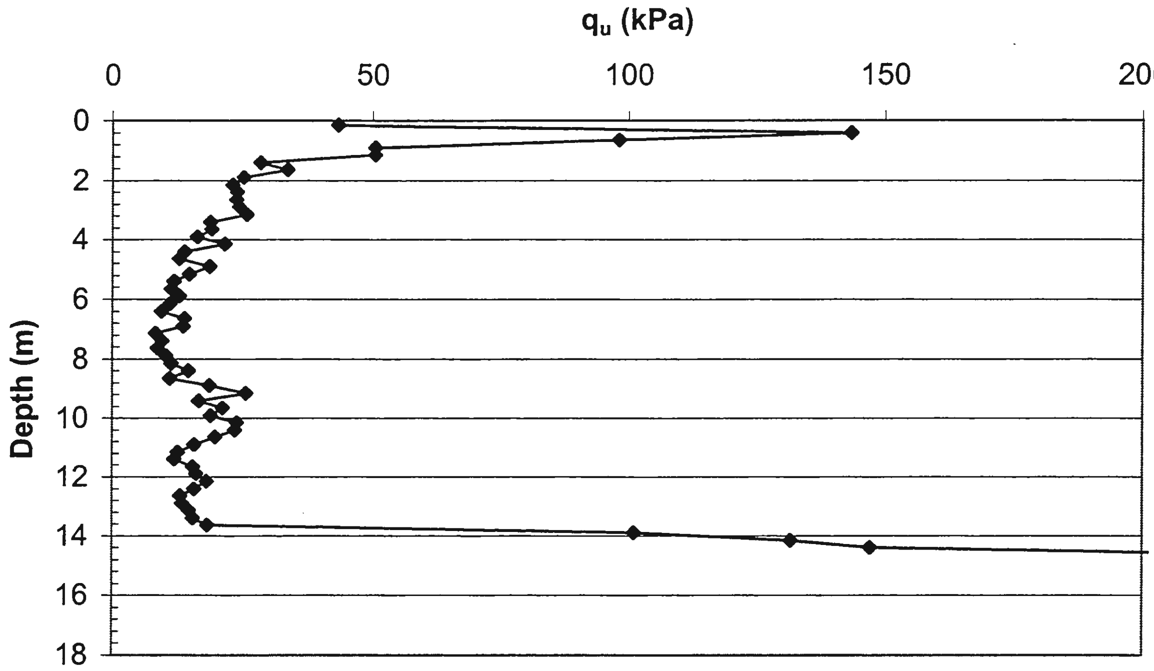

Figure 16. q_u at CPT1 using Robertson and Campanella (1986)

clay according to Terzaghi and Peck (1967). With a high water table it is apparent that bearing capacity and settlement will be controlling factors in the design of the soft soil reinforcement for the project embankment.

DMT data

The Flat Dilatometer Test (DMT) was implemented on the site for subsurface profiling. The DMT was pushed hydraulically by the Iowa State University Mobile B-40, truck mounted drill rig. Two soundings were performed. The first, DMT1, was performed at CPT1 and the second, DMT2, was performed in the center of the load testing area. Procedures described by Marchetti (1980) were used to carry out the testing and reduce the data. Readings were taken at 0.3 m intervals.

The first step in data reduction for the DMT is to produce the three primary dilatometer variables at each data point: Material Index (I_d), Horizontal Stress Index (K_d), and Dilatometer Modulus (E_d). These were calculated using the procedures outlined by Marchetti (1980). Subsequent correlations are based on an identification of the soil type obtained through the Material Index. DMT1 and DMT2 classified the soft layer as silty clay (Marchetti, 1980). Furthermore, the Material Index combined with the Dilatometer modulus classified the clay layer as soft silty clay, very nearly mud (Marchetti, 1980). With the Material Index less than 1.2, Marchetti (1980) indicates that it is appropriate to correlate the undrained shear strength (s_u) and horizontal earth pressure (K_o) of the soil to the DMT data. Figure 17 shows the profile for the calculated undrained shear strength (s_u). The DMT1 data averages s_u at 0.10 bars (10 kPa), while the DMT2 data averages $s_u = 0.09$ bars (9 kPa). The CPT1 data gave a value of 17 kPa for the unconfined compressive strength, showing good agreement with the DMT data. K_o was averaged to be 0.39 for DMT1 and 2. With a plasticity index of 16 and the assumption that the clay is normally consolidated, Lambe and Whitman (1969) list a typical value for K_o as 0.49. This is in reasonably good agreement with the DMT correlation.

Graphical representations of the data are presented in Figure 17 for DMT1. Raw data and correlations are presented in Appendix B. Comparison of the CPT1 data with the DMT1 data shows good agreement. The dilatometer sounding indicates a moderately stiff zone for the first meter, which confirms the fill layer indicated by the CPT profile. The DMT data shows the fill underlain by a soft layer to a depth of 13.5 m. The soil begins to stiffen at 13.5 m as indicated by the Dilatometer modulus profile. This is in perfect agreement with the beginning of the glacial till layer indicated in the CPT1 profile. Rod refusal at a depth of 14 m disallowed the performance of any DMT soundings beyond that depth. Rod refusal was surmised to correlate with the beginning of the stiff glacial till layer indicated in the CPT data. Although little data was obtained for the glacial till, the profile for the clay layer is very consistent in readings throughout its depth. The DMT2 data produced profiles similar to that of DMT1.

PMT data

The Pressuremeter Tests (PMT) were conducted to determine modulus of the clay layer. Previous research has shown that soft clay conditions yield reliable data from the pressuremeter (Briaud, 1989). PMT testing was performed at CPT1 and CPT2. For simplicity data profiles are referred to as PMT1 and PMT2. The PMT was performed in a pre-bored hole after sampling by a standard 7.9 cm Shelby tube. The procedures used to carry out testing and data reduction were in general accordance with recommendations from Briaud (1989).

PMT1 was performed at 1.52 m intervals beginning at a depth of 4.5 m. The tests continued to a depth of 12.5 m. At 13.5 m hollow-stem augering was refused by the glacial till layer indicated in the CPT and DMT data. Individual tests were advanced on a constant pressure increment basis while observing volume change. Figure 18 presents the calculated pressuremeter modulus (E_{pmt}) for each depth at PMT1. The average E_{pmt} for the clay layer is 1320 +/- 461 kPa (+/- denotes one standard deviation herein). This classifies as very soft clay (Briaud, 1989). The data collected in PMT2 gives the same Pressuremeter modulus. The tabulated data and a graph of each PMT test are located in Appendix C.

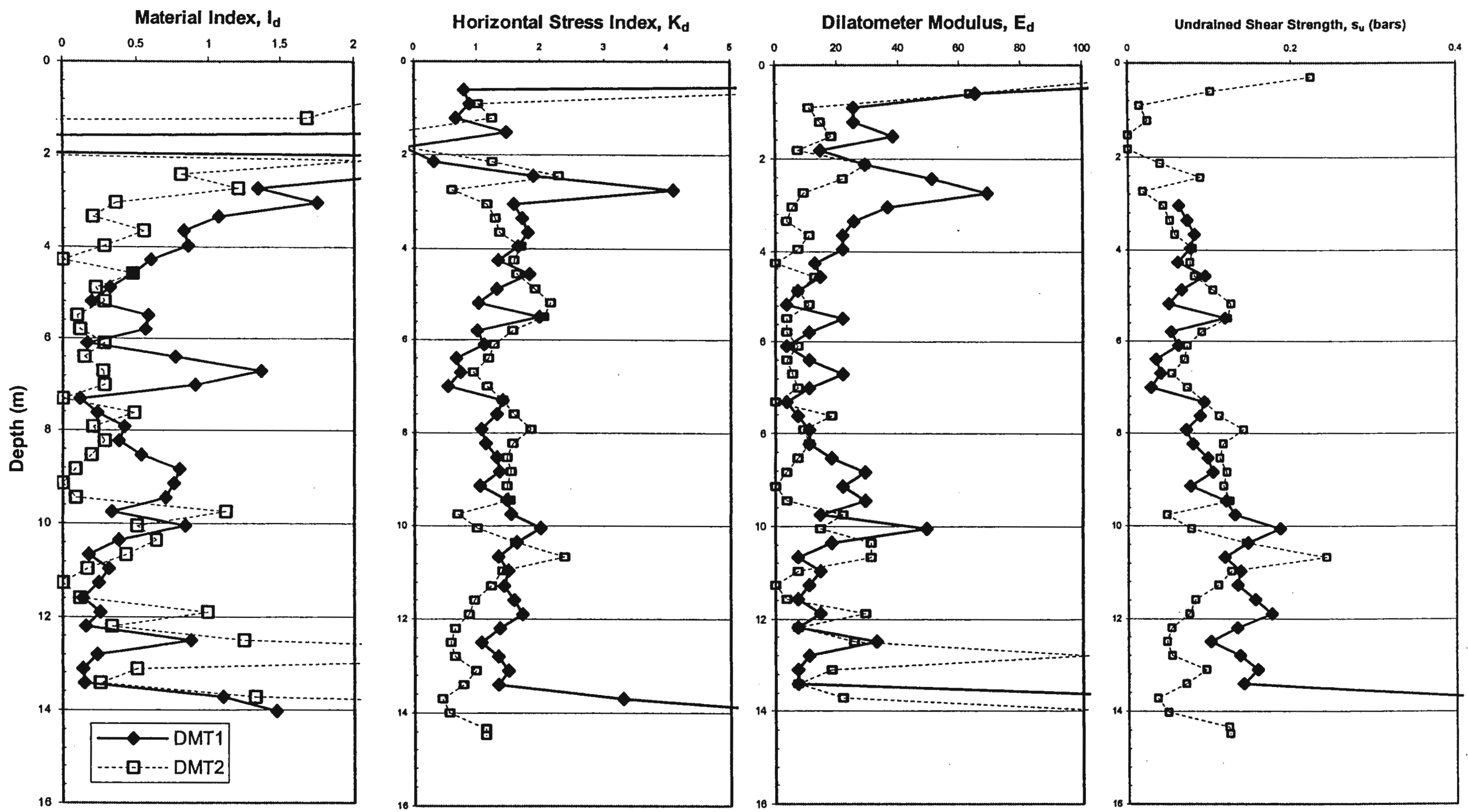

Figure 17. Profile of dilatometer indices at DMT 1 including dilatometer modulus and undrained shear strength

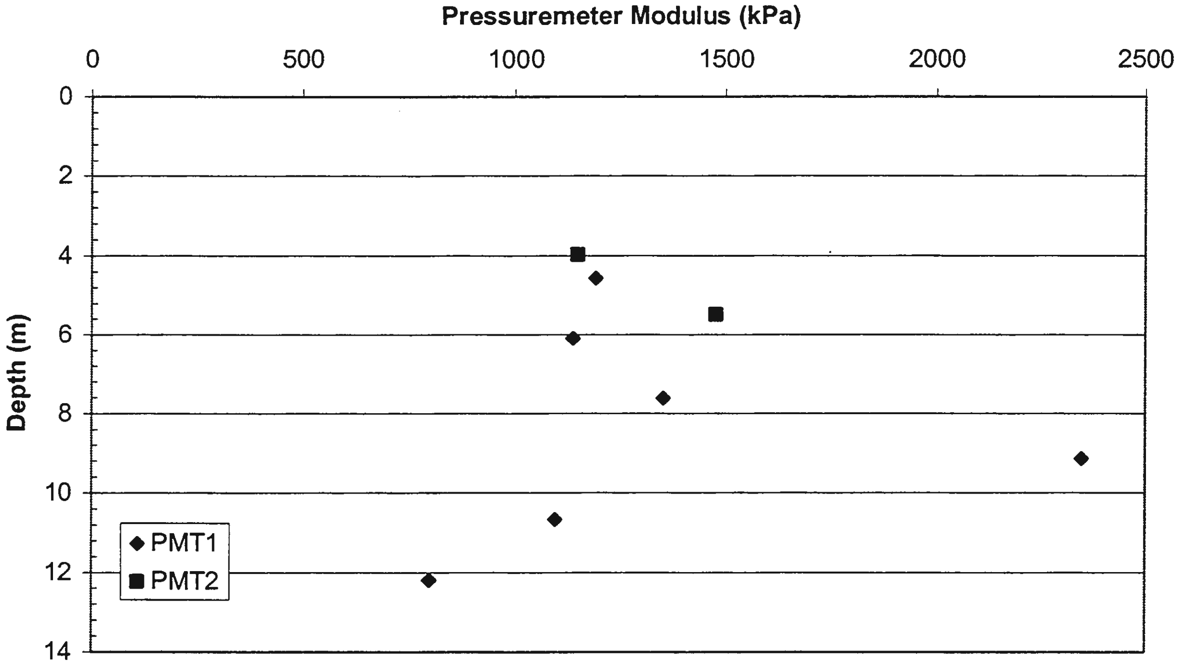

Figure 18. Calculated pressuremeter modulus at each depth using Briaud (1989)

Borehole Shear data

Two Borehole Shear tests (BST) were performed in the load test area to measure the drained friction angle and cohesion intercept of the alluvial clay layer. The test consists of lowering an expandable shear head into a borehole (created by a standard 7.9 cm Shelby tube), expanding the shear head against the walls under a constant normal stress, allowing the soil to consolidate (hence drain), and pulling vertically on the shear head measuring shear resistance. Several studies have compared the BST to CD and CU triaxial tests (Wineland, 1976; Schmertmann, 1976) and have supported a previous assessment that the BST is usually a drained test (Handy, 1976). Points are produced on the Mohr-Coulomb shear envelope by

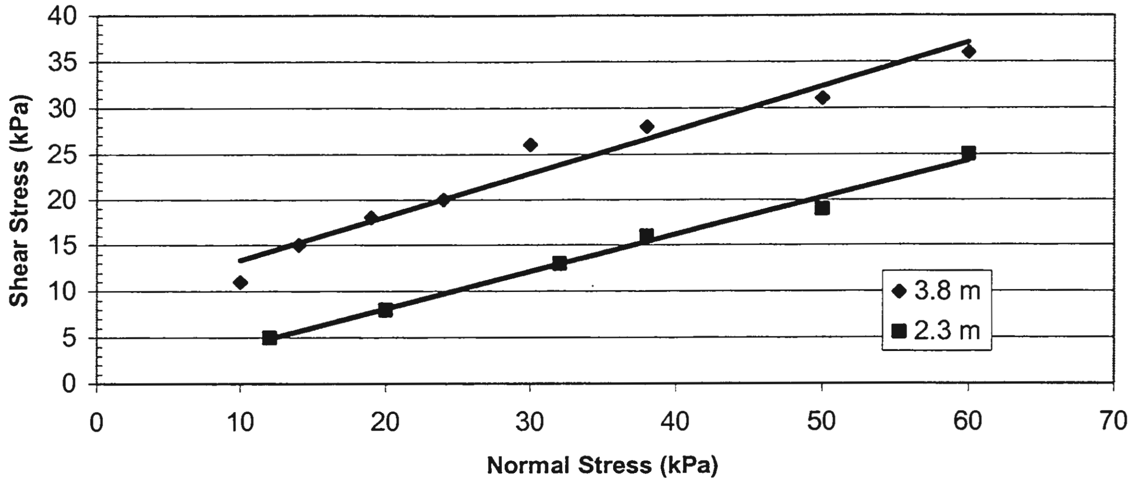

Figure 19. Borehole Shear test data at load test area

measuring the maximum shear resistance at successive increments of normal stress applied. Cohesion intercept (c) is given by a regression of the data.

Figure 19 presents a graph of each test. The test at a depth of 3.8 m indicates $\phi=22^\circ$ and $c\cong0$ kPa for the clay. A strong correlation for the test is indicated by an R^2 value of 0.99. The value of friction angle agrees closely with the data indicated by the CPT. The second test conducted at 2.3 m indicates $\phi=25^\circ$ and c=8 kPa. The tabulated data is presented in Appendix D for the BST.

Laboratory Testing Program

Consolidated drained (CD) triaxial compression tests, unconsolidated undrained (UU) triaxial compression tests, confined compression (oedometer) tests, particle size distribution, and Atterberg limit tests were performed on representative portions of undisturbed samples obtained by Shelby tube sampling procedures. Following is a description of the testing and results.

Consolidated drained (CD) triaxial compression test

A series of consolidated drained (CD) triaxial compression tests were conducted to determine the approximate shear strength of the soil in terms of effective stresses. Three CD tests were performed on alluvial clay extracted from a depth of 4.2 m at CPT2. Each Shelby tube extracted sample was prepared with a height to diameter ratio of 2.0. The three tests were conducted at confining pressures (σ_3) of 21, 41, and 62 kPa.

The stress-strain behavior for the series of CD triaxial tests is shown in Figure 20. Initial assessment of the test results reveals the typical increase in peak strength with higher consolidation stress. Volume decreased (contraction) during loading, indicative of normally consolidated soils (Lambe and Whitman, 1969). The stress paths for the CD tests are shown in the p'-q diagram in Figure 21. Volume change is shown in Figure 22. A linear regression of the peak p' and q values generates the K_f-line. Evaluation of the generated K_f-line produces $\phi' = 16°$ and $c' = 12$ kPa. The tabulated data can be found in Appendix E.

Unconsolidated undrained (UU) triaxial compression test

A series of unconsolidated undrained (UU) triaxial compression tests were performed to determine the shear strength of the soil in terms of total stresses. Three UU tests were conducted on the alluvial clay extracted from a depth of 5.8 m at CPT2. Each Shelby tube extracted sample was prepared with a height to diameter ratio of 2.0. The three tests were conducted at confining pressures (σ_3) of 62, 83, and 103 kPa.

The UU test results were analyzed by plotting the stress path of each specimen to

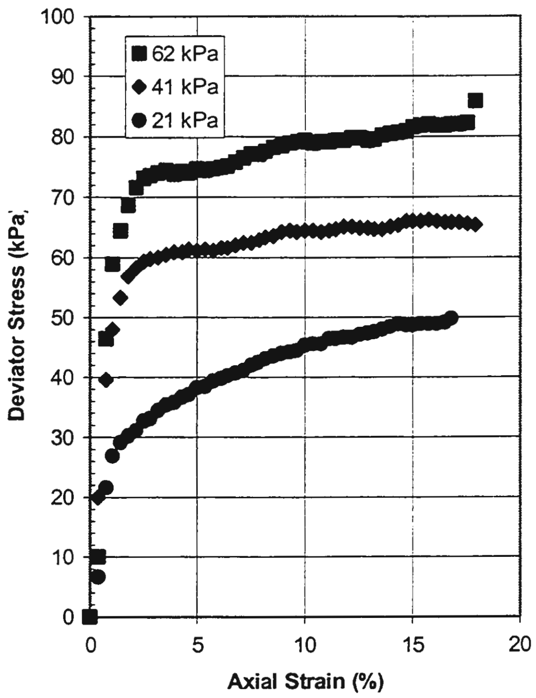

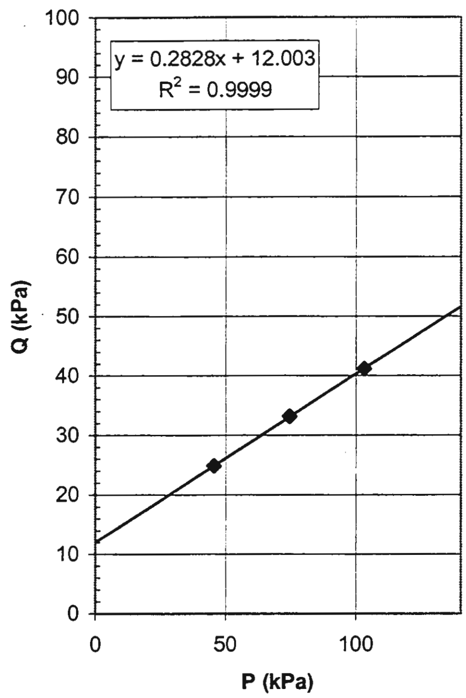

Figures 20. Stress-strain behavior for CD testing

Figure 21. P-Q diagram for CD testing

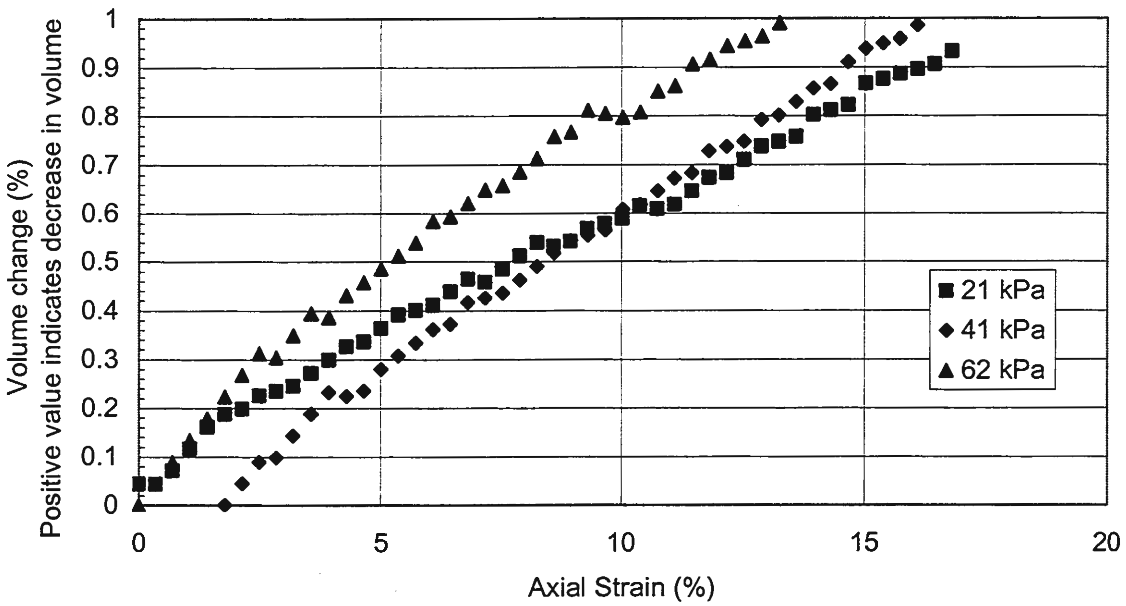

Figure 22. Volume change behavior during CD testing

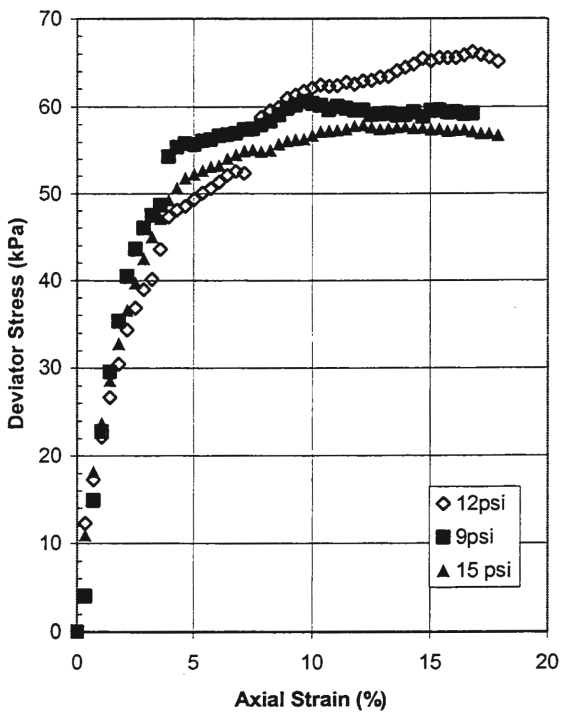

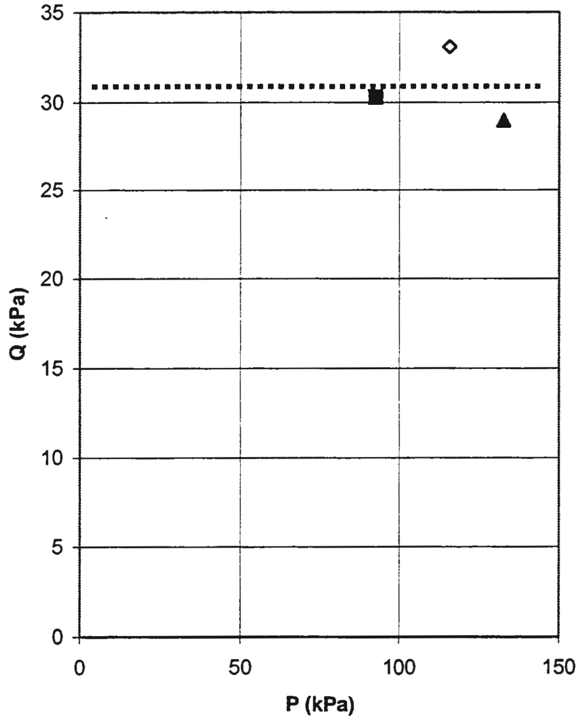

Figures 23. Stress-strain behavior for UU testing

Figure 24. P-Q diagram for UU testing

failure. By evaluating the stress conditions at failure, the soil's strength parameter of undrained shear strength (s_u) was determined in terms of total stresses.

The stress-strain behavior for the series of UU triaxial tests is shown in Figure 23. Initial assessment of the results reveals the "$\phi = 0$ concept" illustrated by the horizontal K_f-line in Figure 24. This concept states specimens of like material subjected to equivalent effective stresses prior to loading will result in equivalent shear failure strengths (Lambe and Whitman, 1969). The resulting s_u of 31 kPa for the soil is read as the intercept of the K_f-line with the q axis, shown in Figure 10. The tabulated data can be found in Appendix F.

Confined compression (oedometer) test

Four one-dimensional confined compression tests were conducted to determine the compressibility of the alluvial clay layer. Consolidation parameters are used to provide primary consolidation settlement and rate of settlement estimates. Tests were performed on Shelby tube samples obtained from depths of 3.9 m and 5.8m, and are assumed to be representative of the entire layer.

The test was performed on samples prepared with a height to diameter ratio of 0.4, and then restrained laterally and loaded axially. Each stress increment was maintained until excess pore pressures were dissipated (time = t_{100}). During the consolidation process the change in specimen height was recorded as a function of time. The tabulated data is displayed in Appendix G.

For rate of settlement analysis the square root of time compression curves (compression vs. $\sqrt{\text{time}}$) were plotted for several pressure increments. By applying the square root of time method, the coefficient of consolidation, c_v, was calculated and time-settlement relationships were established. The square root of time compression curves are shown in Appendix G. Table 2 lists a summary of c_v values. The average c_v value from the four tests over the expected pressure range was 0.07 +/- 0.03 m^2/day. This was used to establish predicted time-settlement relationships.

The consolidation test results were also analyzed by plotting void ratio, e, versus the logarithm of pressure applied to the sample, commonly referred to as the e-log-p curve. The data plot for each test is shown in Figure 25. The linear relationship of the e-log-p curve denotes virgin compression, further reinforcing the observation that the alluvial clay is

Table 2. Calculated c_v (m^2/day) values for different pressure increments and tests

Pressure	Test Number					
(kPa)	1	2	3	4	Avg.	Stan. Dev.
25	0.164	**	0.066	0.066	0.099	0.057
50	0.126	0.045	0.064	0.051	0.071	0.037
98	0.036	0.084	0.069	0.029	0.054	0.026
196	0.027	0.058	0.046	**	0.044	0.016
392	0.025	0.052	0.019	0.019	0.029	0.016
783	**	0.024	0.010	0.028	0.021	0.010

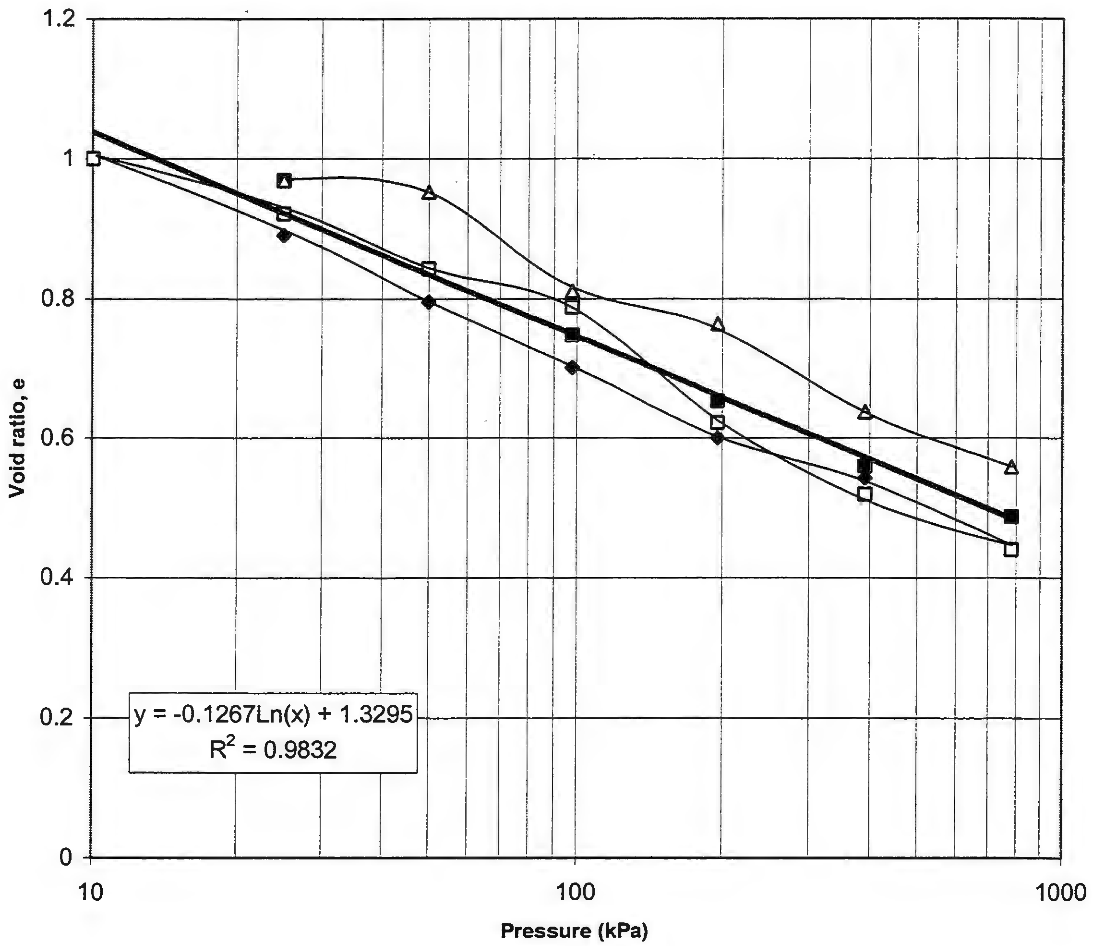

Figure 25. Data points and e-log(p) curve for combined data from each oedometer test

normally consolidated. The slope of this line, referred to as the compression index, C_c, averages 0.28 using the regression. The results of each test appear similar with respect to change in void ratio, e. This made it reasonable to regress all the data together to create the "average" e-log-p curve. The linear regression was used in the prediction of total settlement for the box culvert.

Atterberg limits

Atterberg limit testing was performed on samples obtained at CPT 1 and 2. The depth of samples ranges from 3.5 to 5.5 m. Figure 26 presents the plastic limit, moisture content, and liquid limit determined at each depth. The average liquid limit is 39% and the average plasticity index is 16. In-situ moisture content was fairly constant at 36%. It should be noted that this moisture content is near the liquid limit, resulting in a liquidity index of 0.81. The plasticity index of 16 classifies the silty-clay as CL according to the Unified Soil Classification System, designating it as inorganic clay possessing low to medium plasticity. This designation is typical of the silty-clay mixture indicated by in-situ testing.

Particle size distribution

Further classification of the clay layer at the site was provided by hydrometer and sieve analysis. Figure 27 shows the particle size distribution. Inspection reveals 26% of clay size particles dominated by a silt content of 74%, resulting in the overall distribution being classified as clay. This confirms the data gathered by in-situ testing.

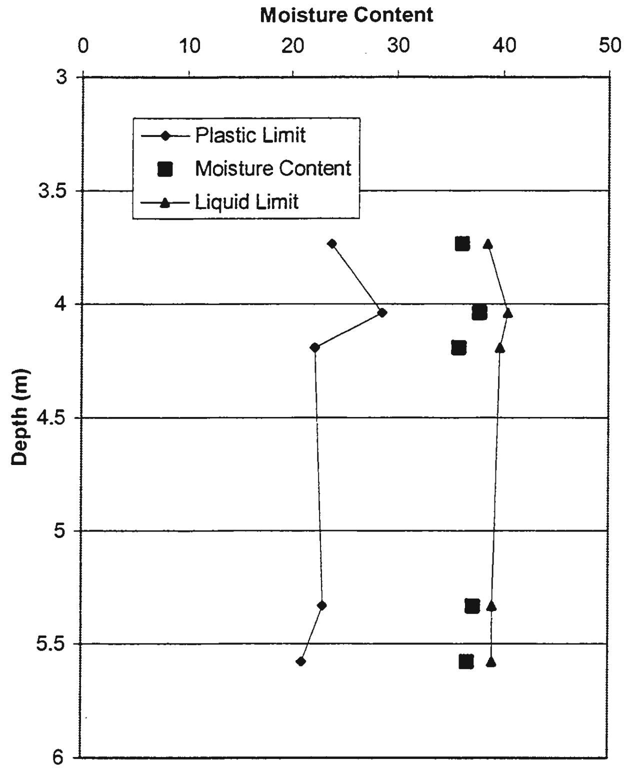

Figure 26. Atterberg limits and moisture content for clay layer

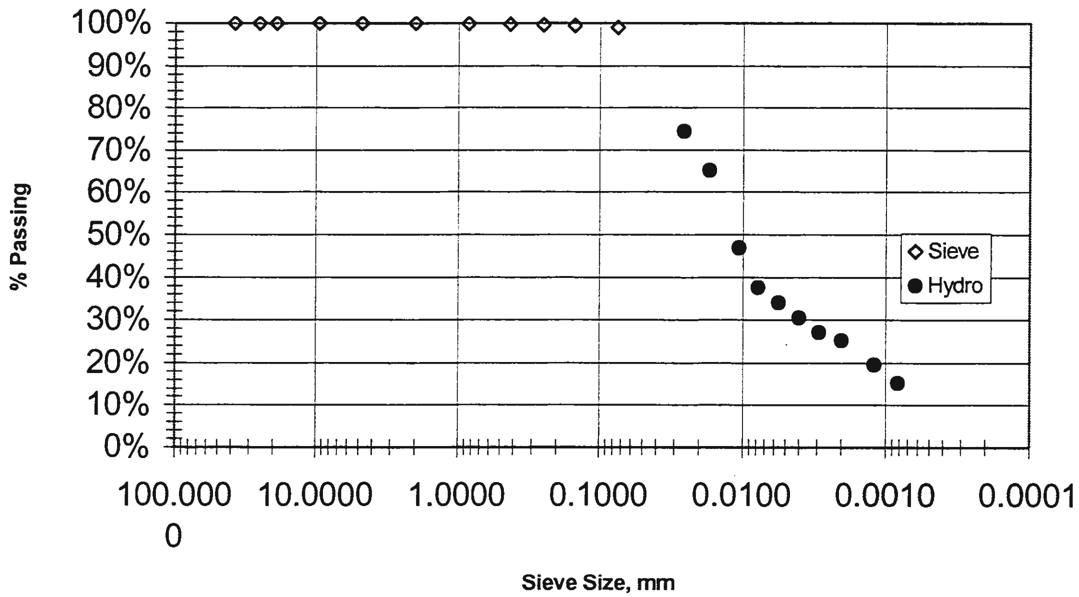

Figure 27. Particle size distribution for clay layer sample

LOAD TESTING DATA

An extensive load testing program was designed and carried at the southwest corner of the production site. Vertical load tests were performed on full scale constructed piers. Three tests were performed on individual piers while two tests were performed on pier groups of four each. The four piers in each group test were capped by a reinforced concrete footing covering both the piers and the matrix soil. This test program intended to compare and contrast the behavior of the individual pier element with a group of piers acting within a grid of pier installations. A grid of piers in a triangular or rectangular installation pattern beneath a footing is the usual granular pile installation. The group tests are designed to test the behavior of a unit cell of this grid pattern, represented by a full-scale footing over four piers.

To further investigate the behavior of pier and matrix soil under vertical load, various instrumentation measurements were recorded during loading. Manual dial-gauge readings were used to monitor top of pier settlement, and bottom of pier settlement. Stress cells were installed in one of the individual pier tests and also one of the group pier tests. The stress cells were placed strategically within piers and also between piers on the matrix soil. The intent was to monitor stress distribution vertically through the pier during loading and stress concentration at the top of piers and matrix soil. Inclinometer casings were installed near one of the individual load test piers, and one of the group test piers. The inclinometer is a device consisting of two accelerometers capable of quantifying tilt-angle of the instrument in reference to two perpendicular axes. The device is pulled through the inclinometer casing to develop a profile, allowing the monitoring of casing deflection installed adjacent to a pier.

This measurement can reveal horizontal movement in the soil profile, indicating pier bulging during loading.

Individual Load Testing Data

Load testing was performed on three individual piers of 0.76 m diameter. The installations were located in the test area on the southwest corner of the project site. Pier No. 1 was installed to a depth of 2.97 m and included stress cell and inclinometer instrumentation. Pier No. 2 was installed to a depth of 2.74 m with a tell-tale as the only instrumentation. Pier No. 3 was installed to a depth of 5.05 m also with a tell-tale as the only instrumentation. Piers 1 and 2 were spaced 3.05 m and piers two and three were spaced 4.57 m apart to minimize any interaction effects.

Individual load test #1

Individual pier No. 1 was installed to a depth of 2.97 m. The pier was fitted with four stress cells, one tell-tale, and two inclinometer casings. Figure 28 shows the locations of the instrumentation.

Figure 29 shows the settlement of the top of pier and tell-tale throughout loading. Testing of the pier was discontinued at 878 kPa. At completion the top of pier had settled 21 mm and the tell-tale had settled 4.5 mm. This difference indicates pier bulging.

Figure 30 displays the stiffness of the pier calculated throughout loading. The stiffness of the pier ranged 87 to 41 kPa/mm from 81 to 878 kPa. A slowing in the decay of stiffness can be noted from 158 to 718 kPa. This coincided with a slowing in tell-tale settlement indicated in Figure 29. The stress cells were installed as shown in Figure 28. Figure 31 shows the change in cell stress with increasing load on the pier. The stresses are graduated from top to bottom, as more of the load is transferred to the soil through shear. At test completion the stress increase was 76% of the total pier stress load at the 0.66 m cell and 22% at the 2.3 m cell. Figure 28 shows the two inclinometer casings installed adjacent to pier one.

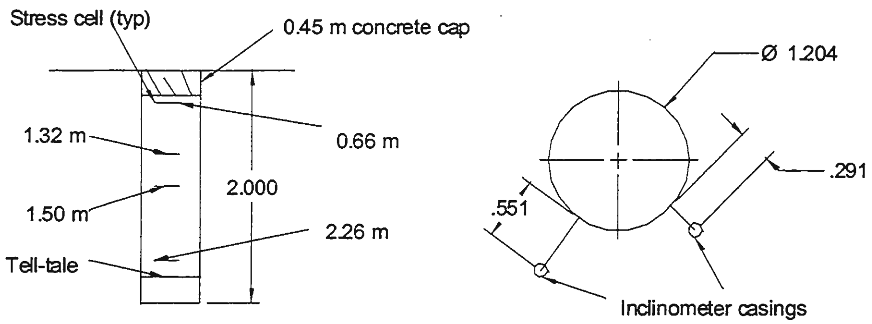

Figure 28. Plan and profile of individual pier one with instrumentation locations

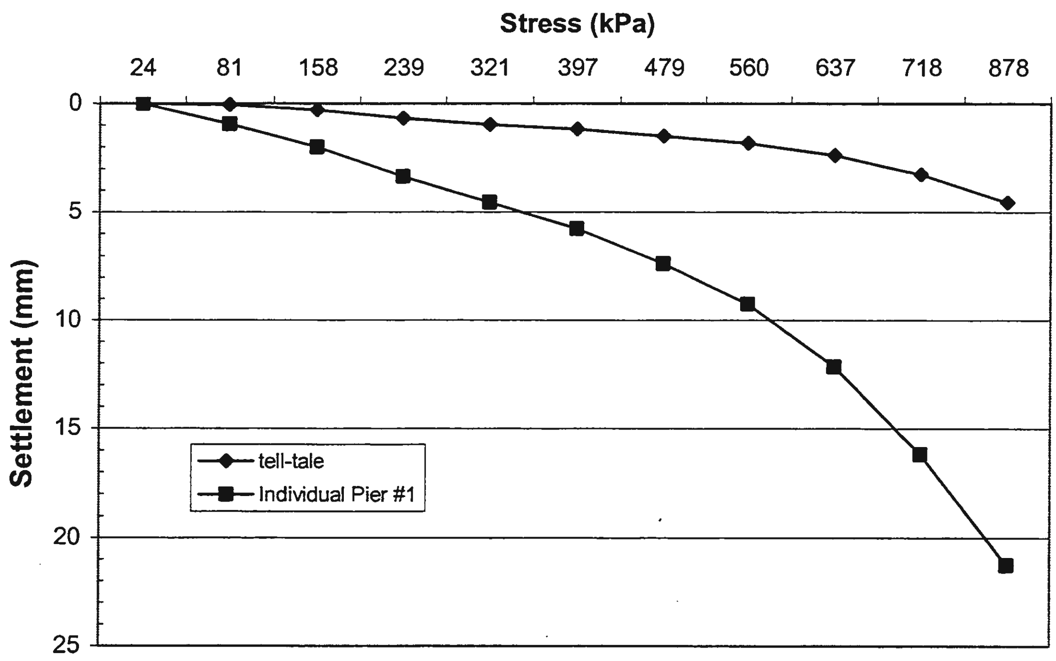

Figure 29. Settlement of individual load test one with advancing stress

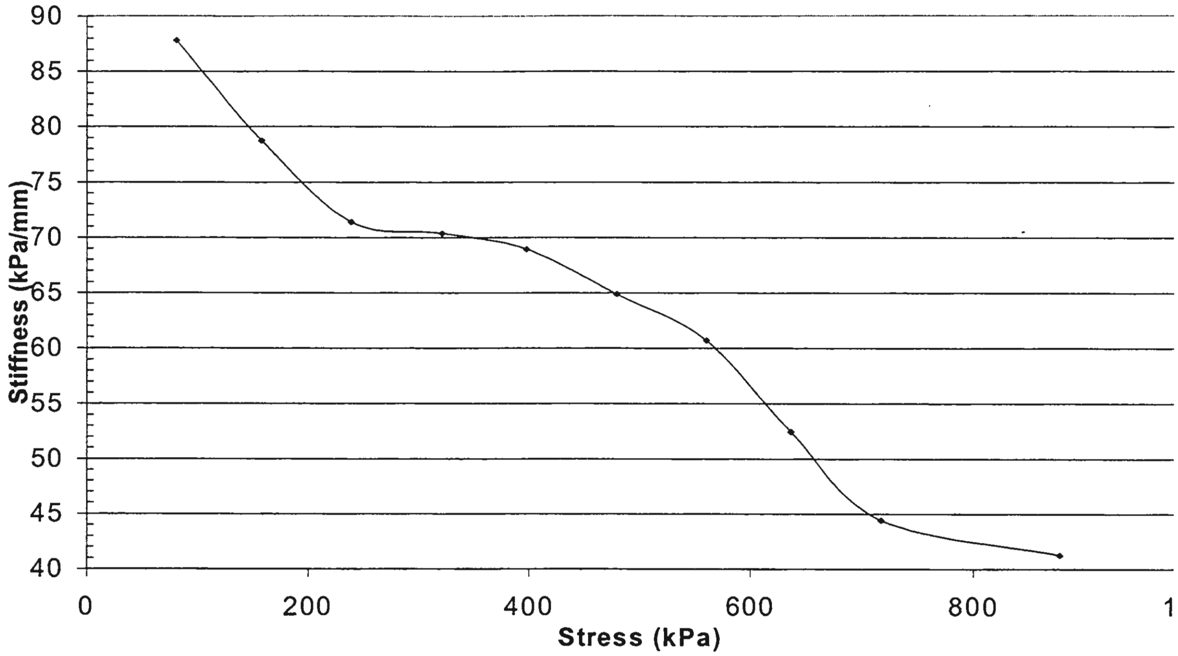

Figure 30. Stiffness of individual load test one with advancing stress

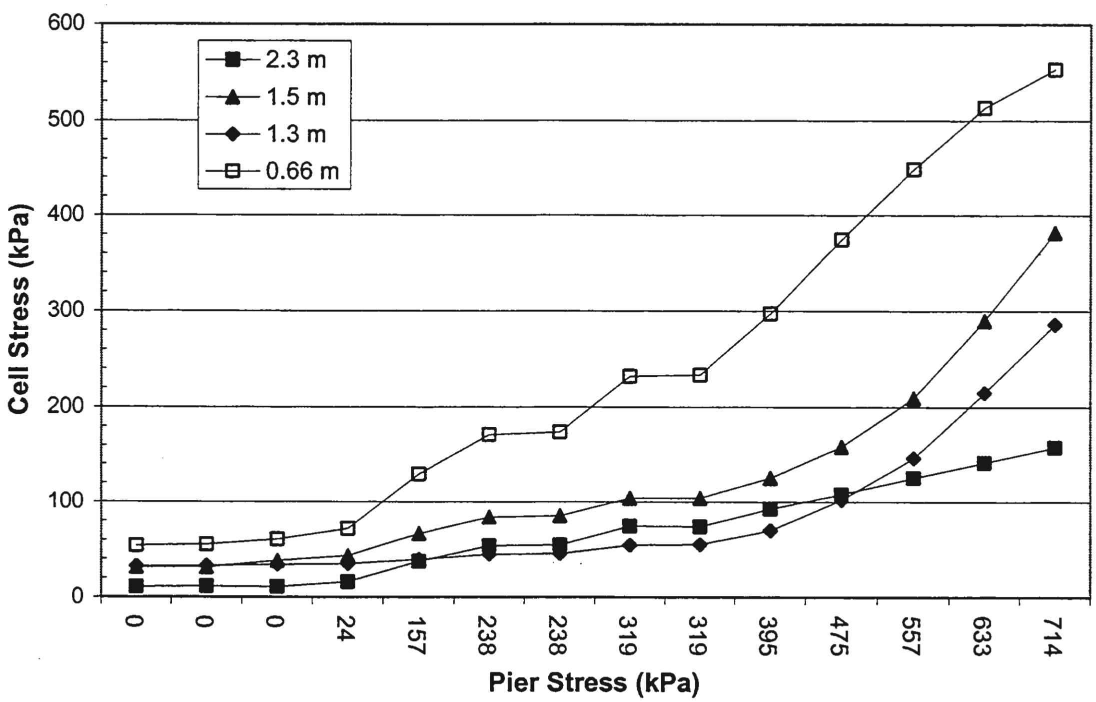

Figure 31. Stress cell readings within individual pier test one during loading

Inclinometer one is located at 0.15 m from the pier and two is 0.3 m from the pier. Figure 32 and 33 show the profile of the casings immediately after pier installation. Both figures indicate deflection of the casing as a result of pier ramming during installation. A maximum deflection of 14 mm is indicated at a depth of 3.2 m for the casing 0.15 m from the pier. This bulge is associated with a length of casing that is bowing from 2 to 5 m in the soil profile, a volume adjacent to the bottom bulb of the pier located at 2.7 m. Figure 34 and 35 display the profile at successive loadings for each casing relative to the profile of the casing after pier installation. In this manner the graph shows only the deflection associated with loading

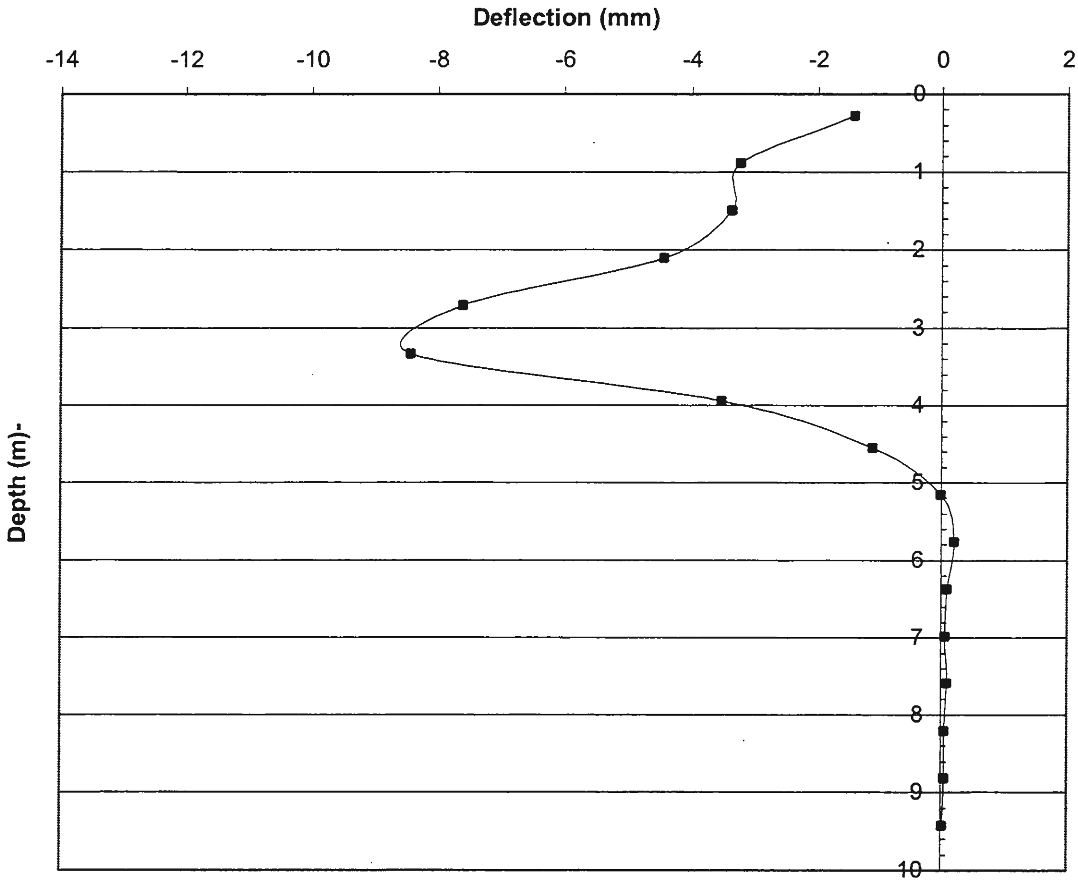

Figure 32. Inclinometer profile (0.15 m); after pier install, individual load test one

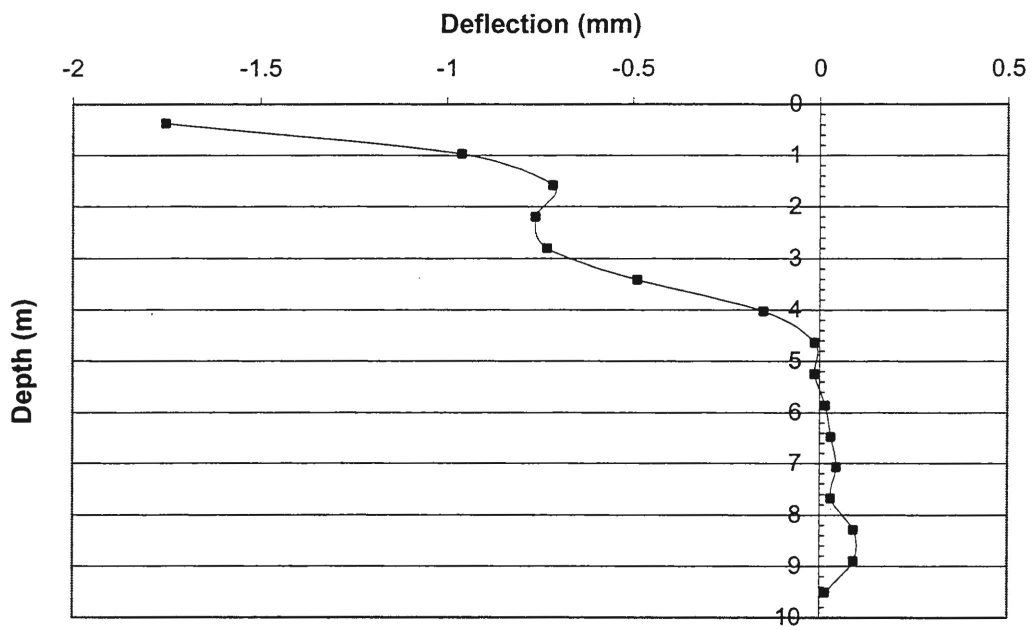

Figure 33. Inclinometer profile (0.3 m); after pier install, individual load test one

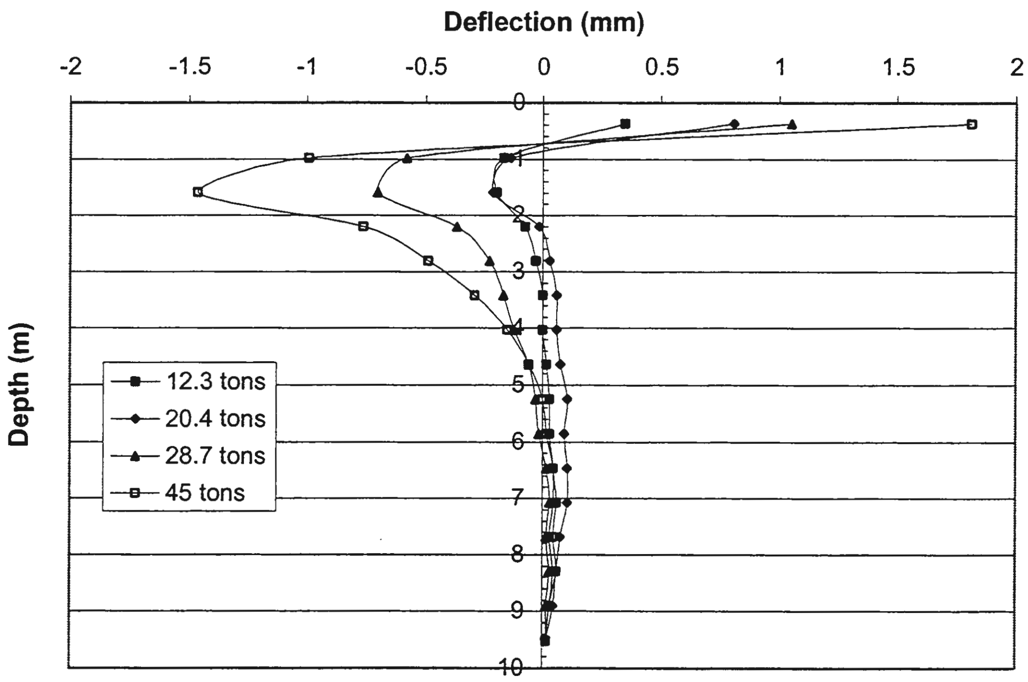

Figure 34. Inclinometer profile 0.3 m from pier; individual load test one

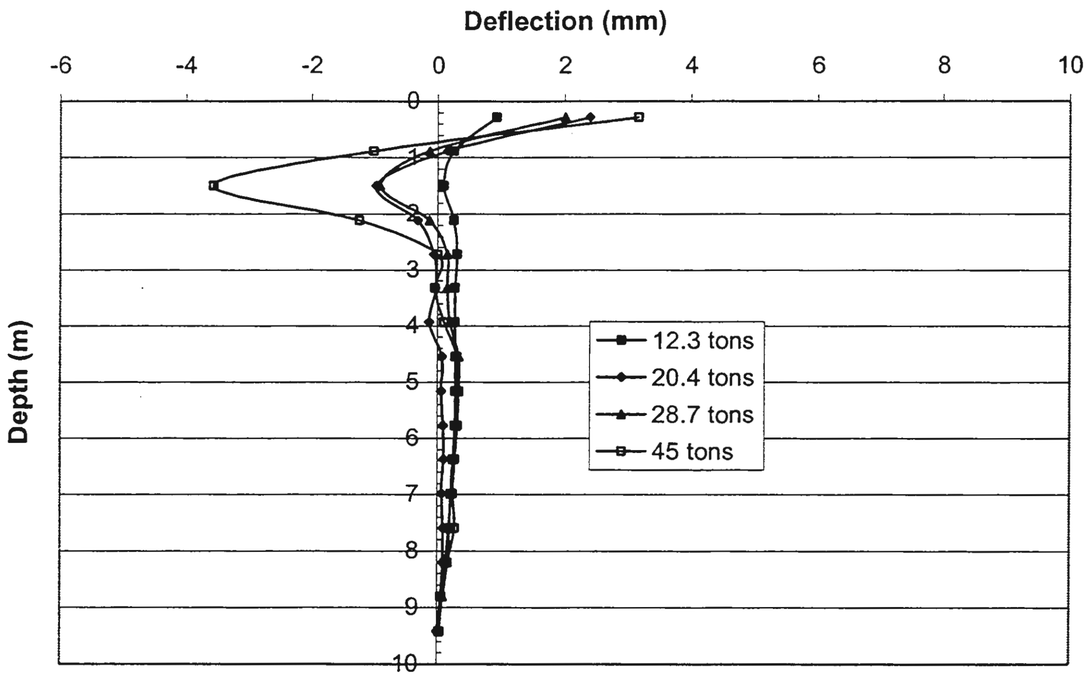

Figure 35. Inclinometer profile 0.15 m from pier; individual load test one

of the pier. Each casing shows an area of deflection extending from 1 to 3 m in the soil profile, with a maximum of 6 mm at a depth of 1.5 m. This indicates bulging associated with the mid-depth of the pier. Please reference Appendix H for tabulated data concerning individual load test one.

Individual load test #2

Pier two was drilled to a depth of 2.74 m. A tell-tale was installed above the bottom bulb. No other instrumentation was installed in the pier.

Figures 36 and 37 display the settlement and stiffness characteristics of the pier. Figure 36 indicates the test was aborted at a stress of 560 kPa due to failure. The top of pier had settled 74 mm at this point while the tell-tale had settled 45 mm. The difference in settlement indicates pile type failure with some bulging.

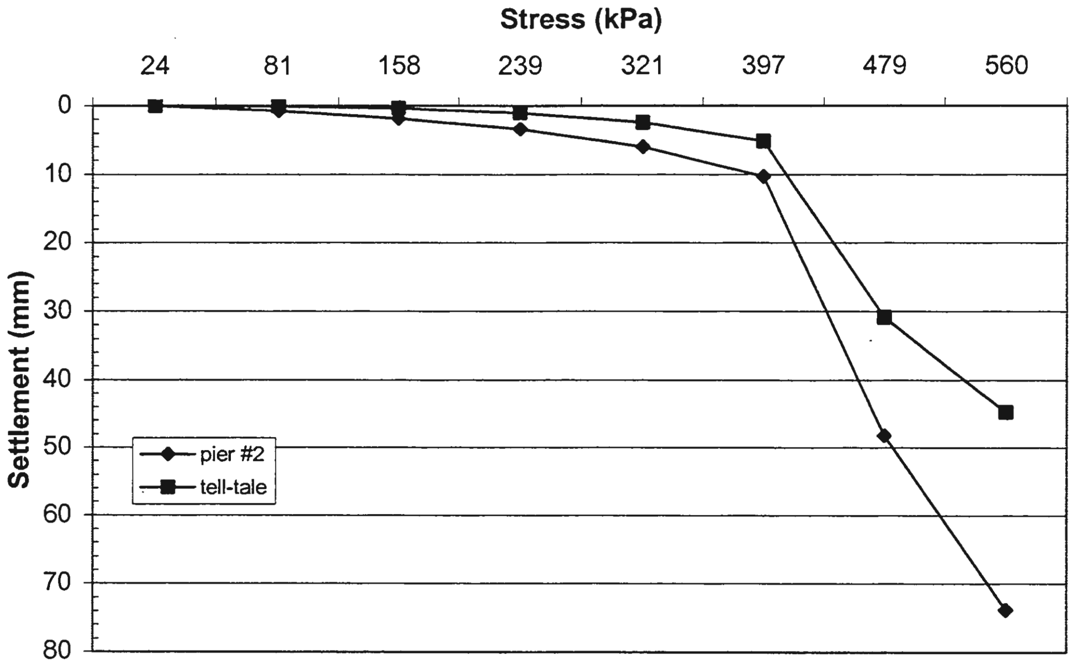

Figure 36. Settlement of individual load test two with advancing stress

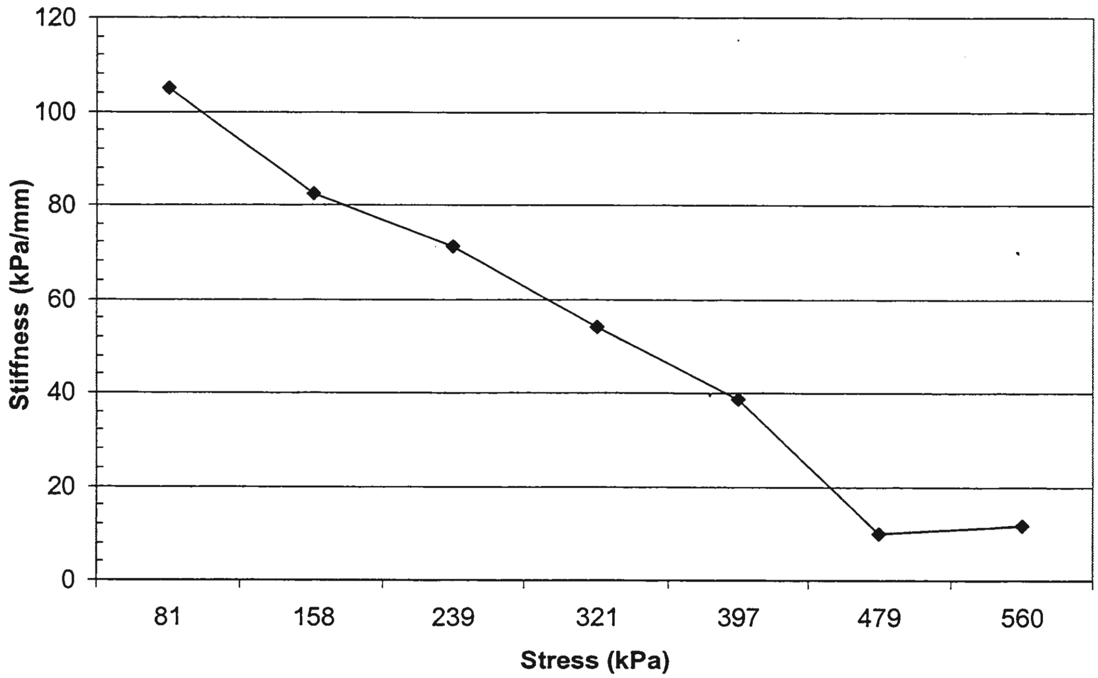

Figure 37. Stiffness of individual load test two with advancing stress

Figure 37 indicates a stiffness ranging from 81 to 479 kPa. Comparison with pier one indicates the ultimate strength and stiffness of pier two are measurably lower. Reference Appendix H for tabulated data associated with individual load test two.

Individual load test #3

Pier #3 was installed to a depth of 5.05 m. A tell-tale was installed prior to construction of the bottom bulb. No additional instrumentation was installed in the pier.

Figures 38 and 39 display the settlement and stiffness characteristics of the pier. Figure 33 indicates the test was aborted at a stress of 637 kPa due to failure. The top of pier had settled 22 mm at this point while the tell-tale had settled 1.4 mm. The difference in settlement indicates pier bulging.

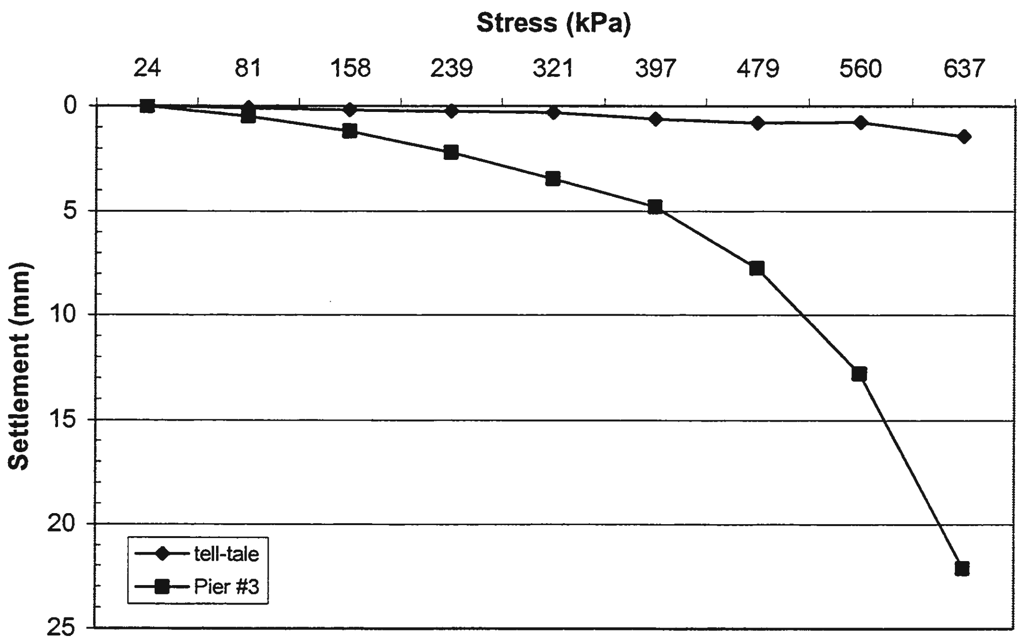

Figure 38. Settlement of individual load test three with advancing stress

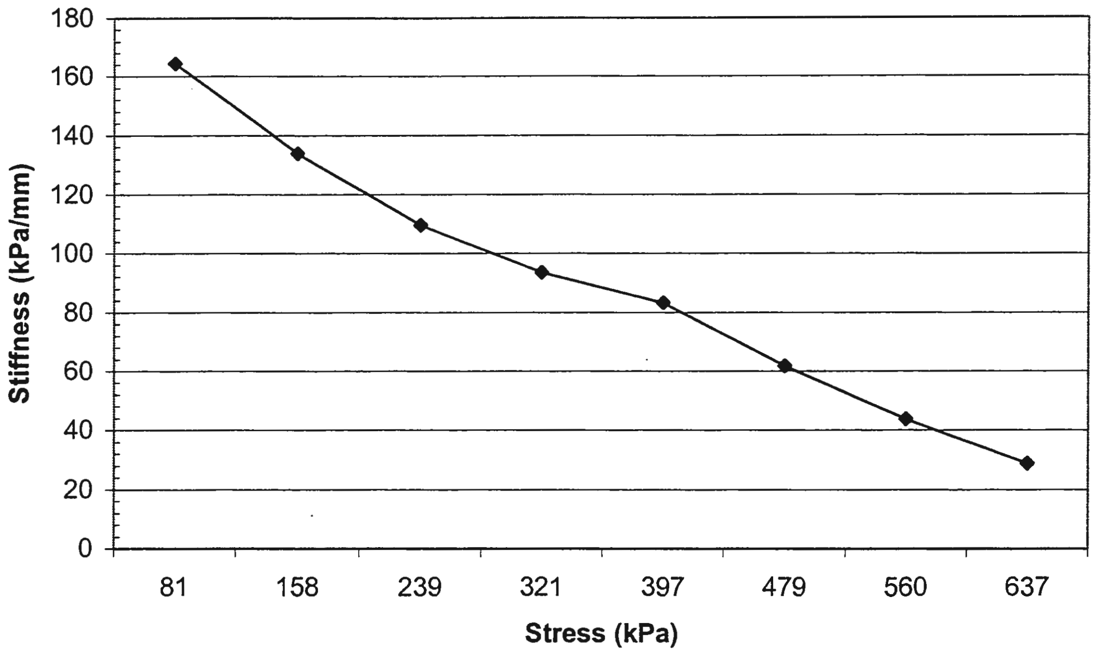

Figure 39. Stiffness of individual load test two with advancing stress

Figure 39 indicates a stiffness ranging from 164 to 28 kPa/mm from 81 to 637 kPa. Comparison with pier one indicates the ultimate strength and stiffness of pier three are measurably lower. Please reference Appendix H for tabulated data associated with individual load test three.

Group Load Testing Data

Two group tests were performed. Each consisted of a group of four 0.76 m diameter piers installed in a square pattern with 1.07 m spacing and a 0.46 m depth slab (reinforced) poured over them. Figures 40 and 41 show a plan and profile view of the installation. The stress cell and inclinometer instrumentation indicated in the schematics was included in the first group test only. Tell-tales were installed in two of the piers for each load test.

With the foundation and pier design complete, it was necessary to design a loading system capable of stressing the element to failure. Previous load testing has only been performed on individual piers, necessitating the design of a loading and reaction frame system. The hydraulic jack capacity required was estimated using preliminary figures on strength of the four-pier system. Four 100-ton capacity jacks were specified to load the foundation. Each jack was placed on the concrete foundation over the center underlying piers. The reaction frame was designed using the capacity of the jacks, and is based on the standard setup used in individual Geopier™ load tests. Anchoring was provided by helical anchors screwed to weathered shale. Figure 42 shows the constructed group load test apparatus.

Group load test #1

Figure 43 displays the settlement vs. stress applied to the raft. Figures 44 and 45 display the load test results regarding settlement and stiffness characteristics. Because there are four sets of data, one for each pier, a representative set of data was compiled by averaging the settlements of all piers and tell-tales. Figures 44 and 45 are based on this average set of data. The stress displayed in each graph represents the stress each pier would react to if the pier were an individual one acted upon only by the jack above it. This convention, coupled with the averaging of the four piers, describes the group as an individual element and is for purposes of comparison with the individual load tests. As can be seen in Figure 44, the testing was aborted at a stress of 718 kPa. This point was determined to be failure as load could not be increased.

The stiffness numbers indicated in Figure 45 are comparable to modulus of subgrade reaction, a figure quantifying the ratio of stress and displacement for a material. The

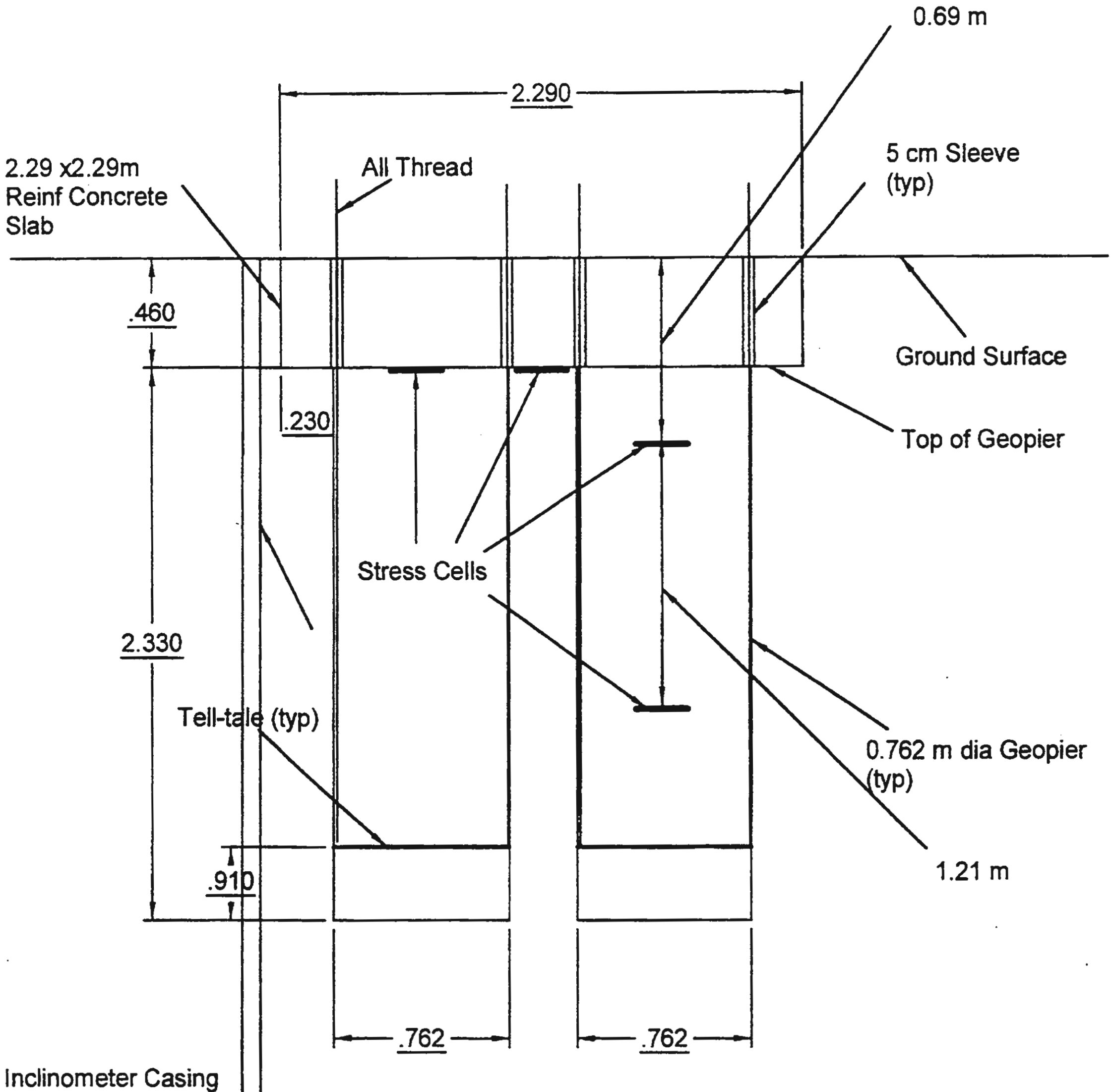

Cell ID	Pier#	Depth	Cell ID	Pier#	Depth
440	2	1.89 m	657	mid	0.46 m
439	2	0.69 m	661	mid	0.46 m
438	3	1.91 m	666	mid	0.46 m
436	3	0.69 m	662	1	0.46 m

Figure 40. Group load test one profile view showing instrumentation locations

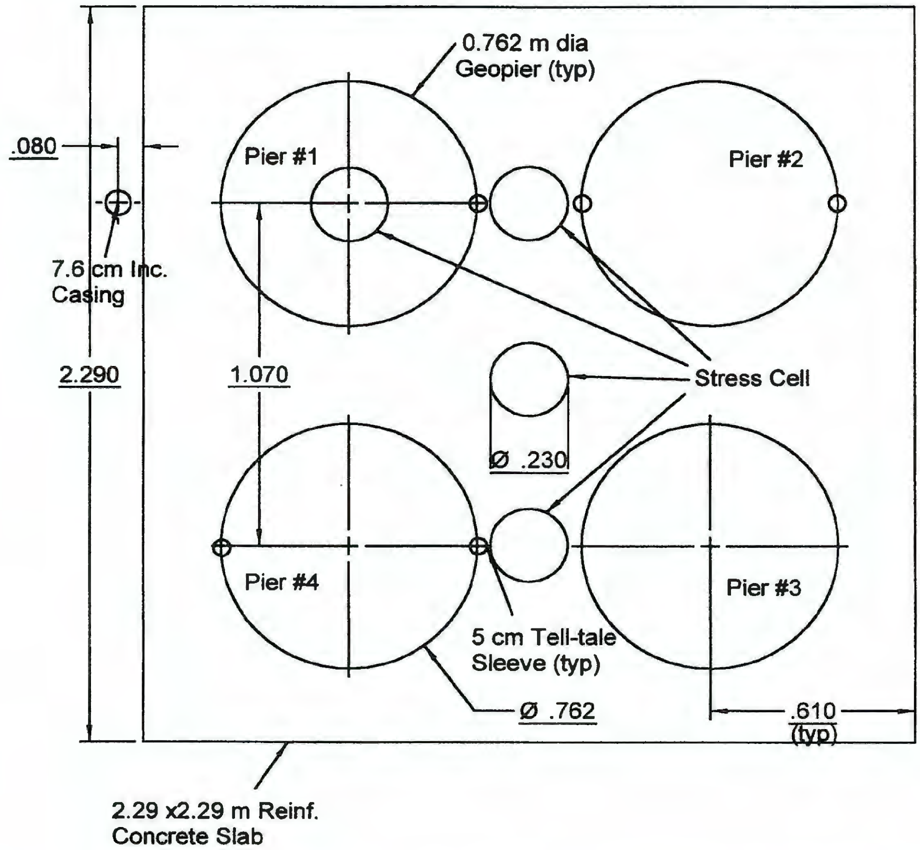

Figure 41. Group load test one plan view with instrumentation and pier numbers

Figure 42. Group load test reaction frame, note individual setup in background

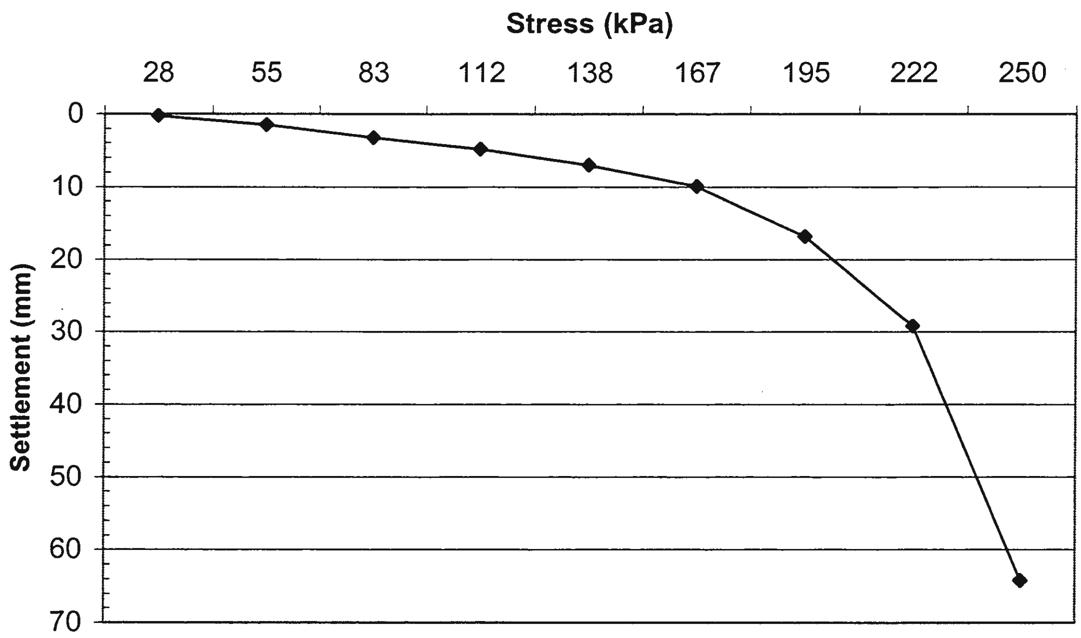

Figure 43. Settlement with stress applied to the raft foundation

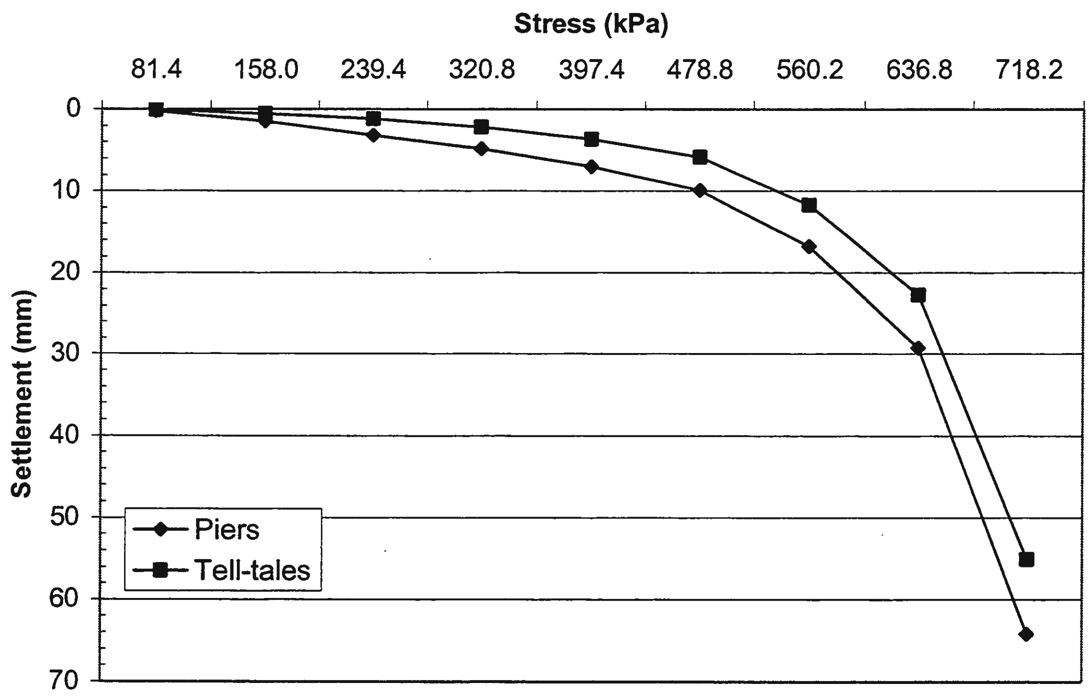

Figure 44. Settlement of group load test one with advancing stress

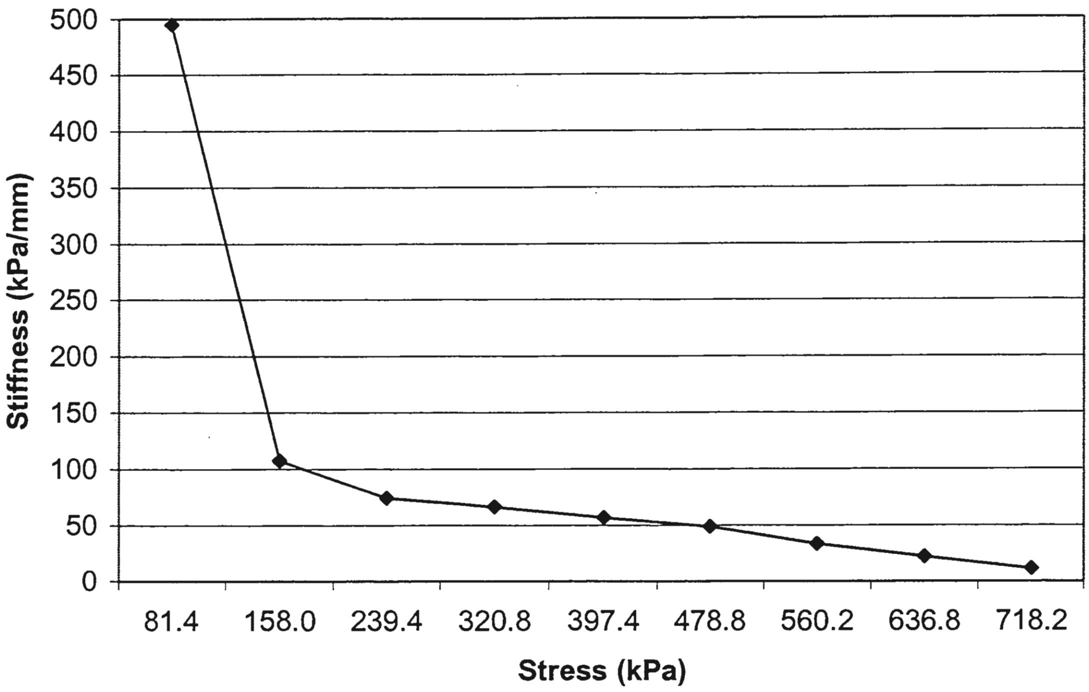

Figure 45. Stiffness of group load test one with advancing stress

stiffness (kPa/mm) in this case is calculated as the stress, according to the individual pier convention described above, divided by the total settlement at that point.

The high initial stiffness at low stress is related to mobilization of shear strength associated with initial loading. Therefore, the stiffness throughout the loading stress range should be considered in comparisons. The stiffness for group test #1 ranged from 107 to 34 kPa/mm at a stress of 81 to 560 kPa, respectively.

Inspection of Figure 44 reveals that both the top of piers and tell-tales settled about 60 mm during the test. This does not indicate pier bulging. Again, the tell-tales were positioned at 1.9 m below top of footing as shown in Figure 40.

This group test also implemented the use of 8 total stress cells. These were utilized to monitor stress distribution vertically through the pier, on top of the pier, and on top of the matrix soil between piers. Figure 40 lists the location of each stress cell and shows a schematic of their location. Four stress cells were placed within piers, one on top of a pier, and three on the matrix soil just beneath the footing. Figure 46 shows the stress increase recorded by each stress cell as load was increased. It is known that a greater portion of the bearing load is transferred to the stiff elements of the rammed aggregate piers, rather than the softer matrix soil (Fox and Lawton, 1994). It should also be noted that this stress concentration ratio increases with time as consolidation proceeds (Fox and Lawton, 1994). The stress cells allow an instant, real-time measurement of this stress concentration ratio of pier to matrix soil. The data in Figure 46 show stress increases ranging from 69 to 400 kPa. Indeed, it can be seen that stress cells located within piers carried a greater amount of stress than those placed on the matrix soil. Stress cell 50662, located on top of pier 1, carried the greatest stress increase of 400 kPa.

Figure 47 shows stress concentration ratio at each load increment. The ratio is calculated as the stress reading at the top of pier 1 (cell 662) divided by the average matrix soil reading given by cells 657, 661 and 666.

Inclinometer data was first recorded before and then after pier installation. Inclinometer data was then recorded at zero and then three subsequent loadings. Figure 48 is a graphical representation of the shape of the inclinometer casing profile during loading, showing lateral deflection. The direction of deflection is in the plane of a line drawn from the center of pier 1 to the center of the inclinometer casing. Reference Figure 40 for the location of the inclinometer casing and pier 1. Figure 48 shows deflection of up to 5.3 mm at a load of 32.4 tons for pier 1, or 4x(32.4) = 129.6 tons for the group. The zone of bulging

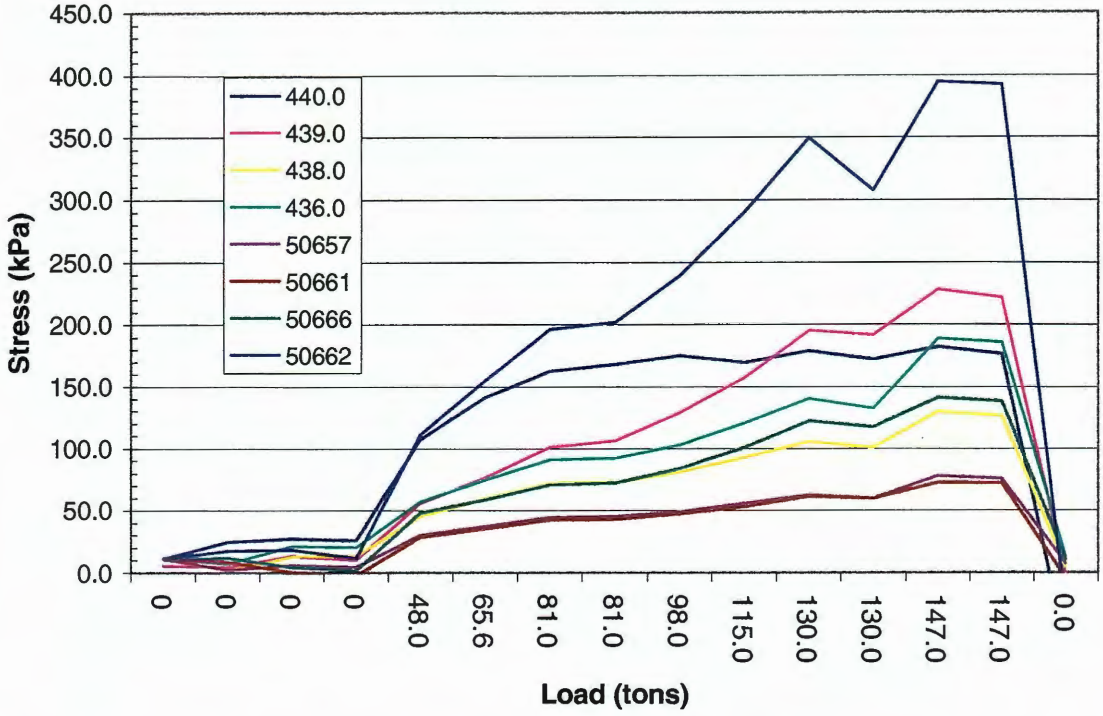

Figure 46. Stress cell response during loading of group test one

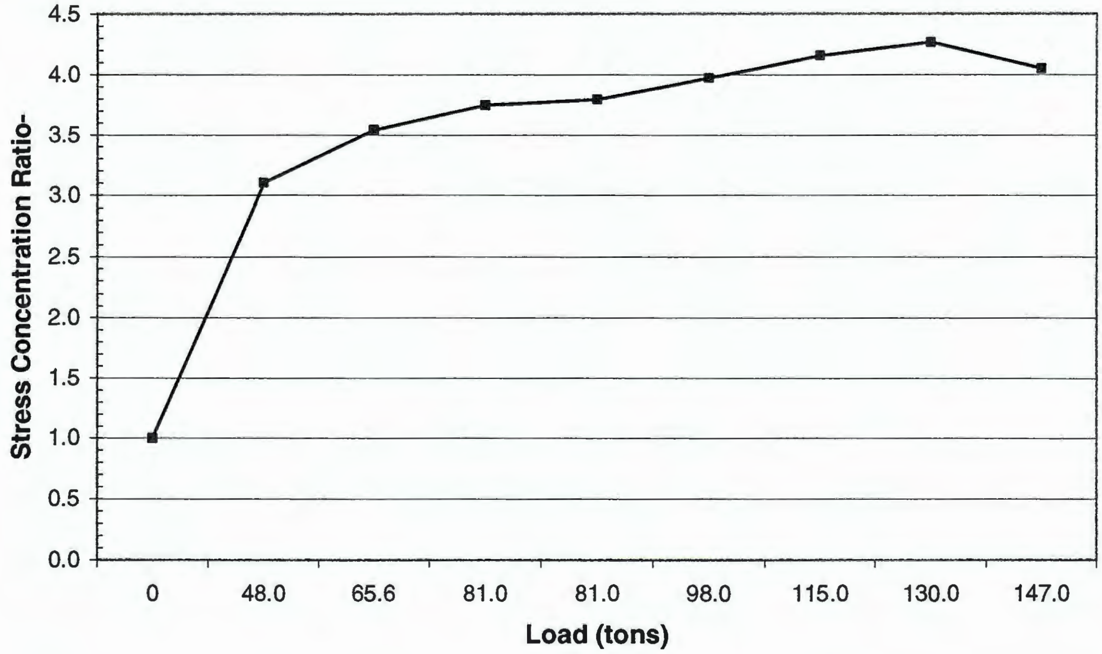

Figure 47. Stress concentration ratio from stress cells in group test one

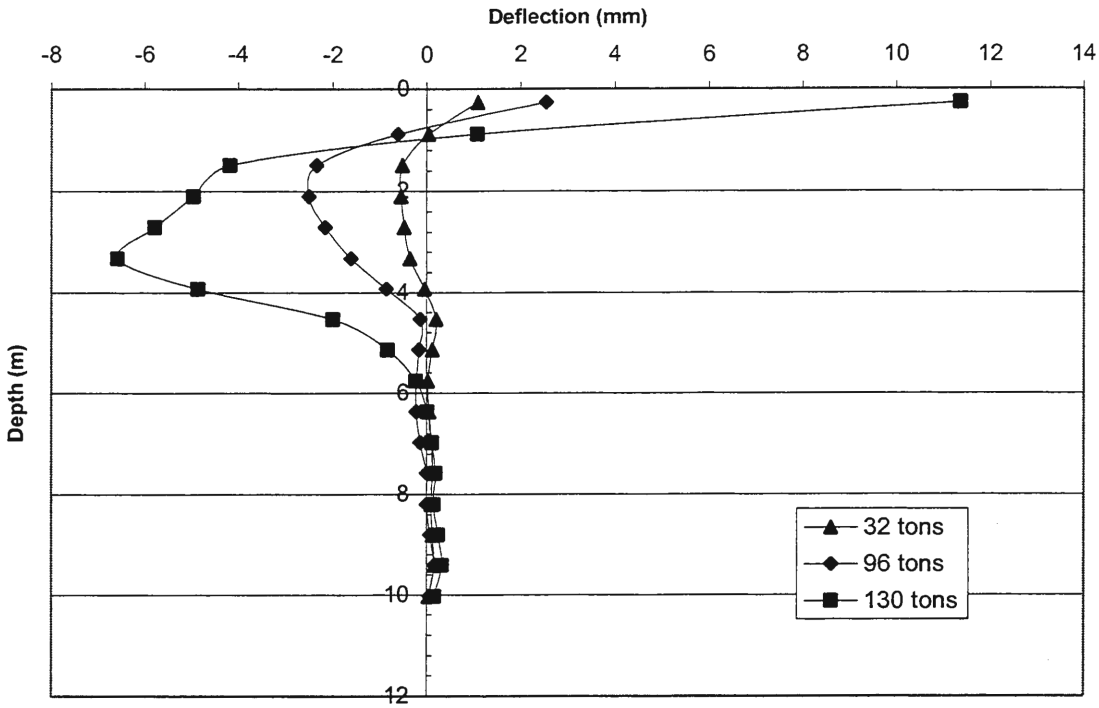

Figure 48. Inclinometer profile for group load test one during loading (0.15 m)

soil extends from 1.5 m to 6.0 m below grade. Note that the depth of each pier is 2.7 m below grade. Reference Appendix I for tabulated data concerning group load test one.

Group load test #2

Another group load test was performed with a setup similar to the previous group load test, excluding inclinometer and stress cell instrumentation. Also, the piers were installed to a depth of 5.13, 5.46, 5.03 and 5.08 m, double that of the previous test. The testing was located in the same southwest corner of the project site. The installation was placed 9 m away from the first group load test to avert any soil disturbance effects.

Figures 49 and 50 display the load test results regarding settlement and stiffness characteristics. Once again, the stress on the abscissa axis is based on the individual pier

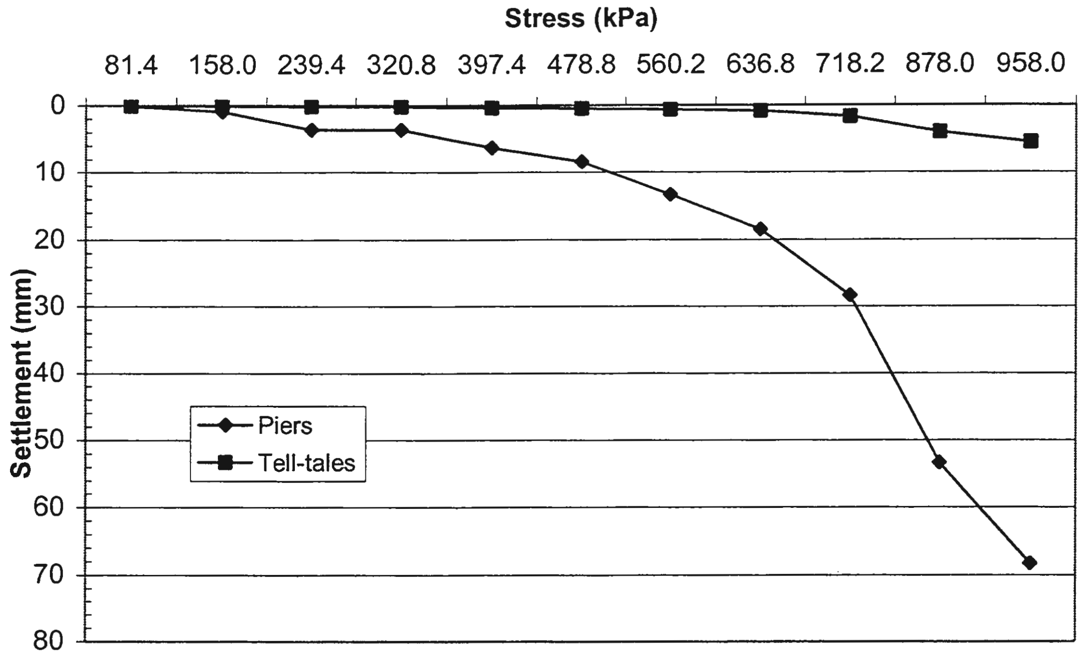

Figure 49. Settlement of group load test two with advancing stress

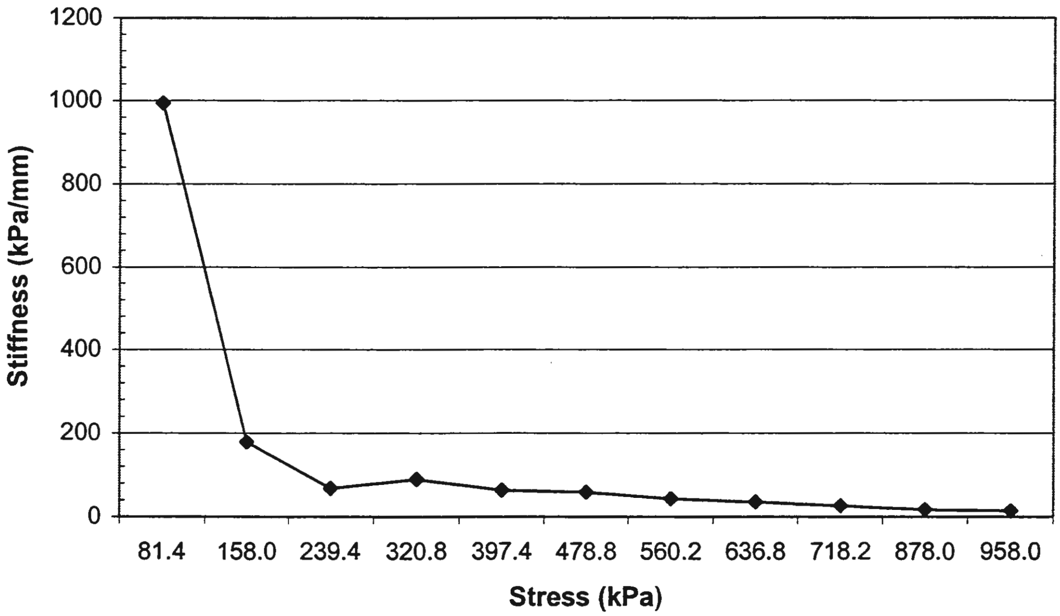

Figure 50. Stiffness of group load test two with advancing stress

convention. Testing was aborted at a stress of 958 kPa representing 200% of design capacity. This point was determined to be failure, defined as the point at which the system cannot support increased load, resulting in a condition of settlement with no increased resistance. The top of pier settled 69 mm at this point, while the tell-tale located at the bottom of pier settled 5.5 mm. It should be noted that the tell-tale acted independently of top of pier settlement in this load test, indicating pier bulging.

Stiffness, as read from Figure 50, ranged from 178 to 14 kPa/mm from 158 to 958 kPa. It can be noted that both the failure strength and the stiffness of group load test two are measurably higher than that of group load test one. Reference Appendix I for tabulated data on group load test two.

PERFORMANCE

The determination of success from a design perspective rests upon the fulfillment of the original design criteria. Total settlement, differential settlement, and the remaining serviceability of the bridge were all considered as design criteria. To the extent that these goals are met, the design would be considered a success. Each of these criteria relies on the performance of the soft soil reinforcement. To measure success in this area, only the settlement log need be consulted. But how do we quantify the success of the rammed aggregate piers from a soil reinforcement perspective?

The performance of the soil reinforcement is quantified as improvement over the original conditions. In other words, what would have been the result of placing the embankment on unimproved soil? Estimations of total settlement and rate of settlement for the unimproved condition can be compared with the observed behavior of the embankment. The oedometer data gathered on the soft clay layer was used to approximate this unimproved condition. Data gathered from the stress cell instrumentation was also incorporated into these calculations to estimate actual stress increase in the clay layer. In addition, rate of settlement and total settlement were estimated for the reinforced condition. Data on performance of the embankment is presented in the instrumentation program described herein.

Instrumentation Program Data

A comprehensive set of geotechnical instrumentation was installed before construction of the embankment. Vibrating wire total stress cells, settlement cells and piezometers were included to measure changes within the embankment during and after construction. An instrumentation console consisting of a data logging device, memory storage, battery and solar panel, was placed at the site to provide automatic logging of data on a scheduled basis. A plan view schematic of the instrumentation installation positions is shown in Figure 51. The instrumentation is intended to monitor the embankment for a period of 3 to 5 years.

In addition to instrumentation, eleven pins were installed at equidistant intervals along the floor of the culvert. These pins were surveyed on a regular basis before and after construction, serving as the primary indicators of settlement.

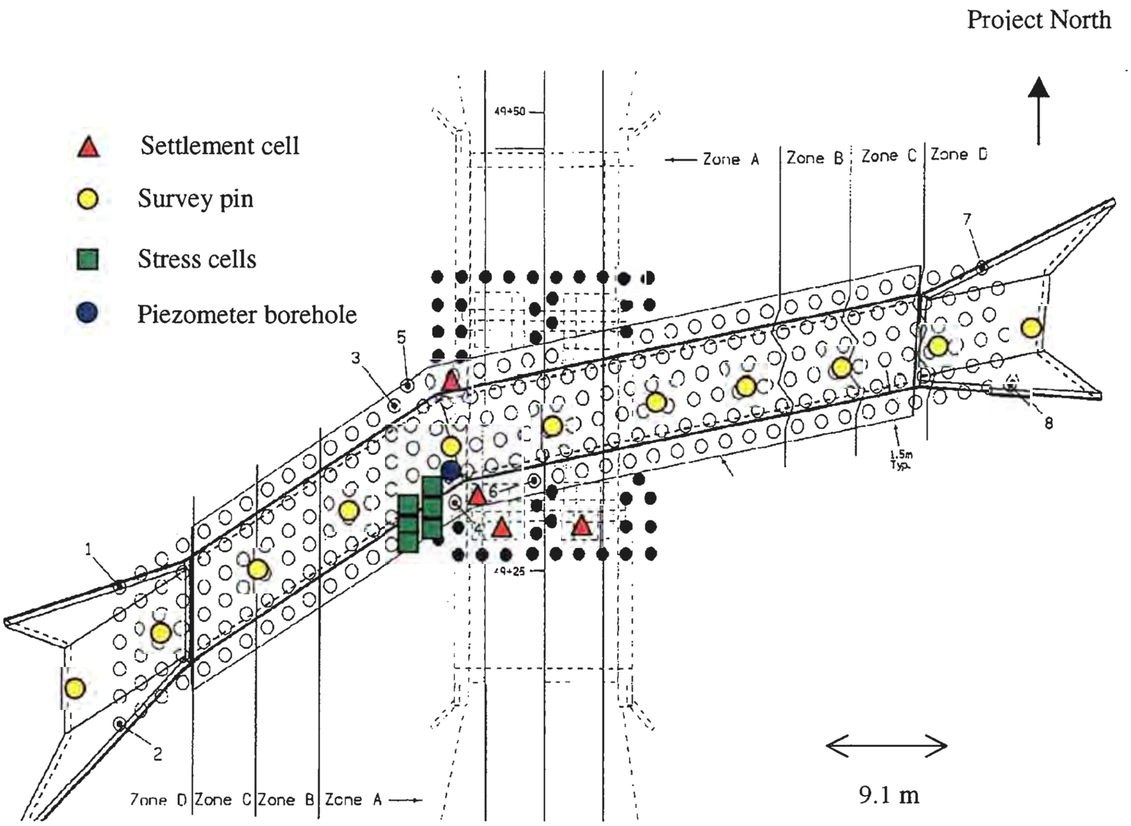

Figure 51. Locations of instrumentation and pier installation zones

Short-term monitoring

Piezometers

A test was performed using the four vibrating wire piezometers installed in a borehole before construction of the embankment. The piezometers were installed in the alluvial clay layer to measure pore pressure changes within the layer during and after construction. The piezometers are located at depths of 0.6 m, 2.1 m, 4.7 m, and 5.9 m below top of pier elevation. The borehole was located in the center of three piers drilled on a triangular grid pattern. Reference Figure 51 for the location of the borehole. After installation, the piezometers were given one week to stabilize before pier installations. The test was then performed while the three piers adjacent to the borehole were being drilled and rammed.

The data-logger was programmed to register piezometer readings at four-second intervals during pier installation. A log was taken simultaneously documenting the activities being performed during specific time intervals.

Long-term monitoring

Equipment installed within the embankment included six total stress cells, four settlement cells, and four piezometers. The piezometers are the same as those used in the short-term monitoring test. The plan view locations of the instrumentation are shown in Figure 51. The stress cells were placed at top of pier elevation while the piezometers were placed as discussed in the short-term monitoring section. Two of the settlement cells were located on top of the culvert, while the other two were located on the southern span bridge pier. All of the instrumentation was installed and connected to the data logger one week prior to the start of fill operations. This allowed the instrumentation to equilibrate and reach a baseline reading.

Stress cells

The stress cells were installed in groups of three. Two on piers with one located on matrix soil between them. The location of individual cells is labeled in Figure 51. Elevation of each cell is top of pier. The stress cells were located to measure stress increase under the largest part of the embankment and also to measure stress concentration ratios between the pier and matrix soil. Each measures 0.23 m in diameter.

Settlement cells

The locations of the settlement cells are shown in Figure 51. The settlement cells on the culvert will be used for long-term monitoring of the center of the culvert without requiring survey techniques. Their location on either side of the culvert will also indicate if there is differential settlement laterally along the culvert. This condition could indicate rotation of the culvert.

The other two settlement cells are located on a pier cap spanning the two piers of the southern bridge span. These cells are intended to monitor bridge settlement. The project included a design criterion stating that the bridge was not to settle concurrently with the embankment settlement. The stipulation of this criterion is based on the bridge being installed in 1927 using timber piles of unknown depth. It was not known whether the piles penetrated to the stiff glacial till layer. If not, it is possible that the settlement of the embankment could drag down the bridge piles. The settlement cells located on the piers are therefore intended to monitor this condition long-term.

Piezometers

The piezometers were located to measure pore pressure increase in the alluvial clay layer during embankment construction, and subsequent decrease during settlement resulting from pore pressure dissipation. The locations are specified in the short-term monitoring section and also on Figure 51.

Monitoring results

Piezometers (short-term)

Testing consisted of real time piezometer readings taken while the three piers surrounding the borehole were drilled and rammed. The data are presented in Figure 52. To accomplish the real time monitoring, the data-logging device was temporarily programmed to log readings at four-second intervals. The time and duration of installation activities were noted simultaneously as the test progressed. The superposition of pore pressure activity with installation activity is intended for data interpretation, and is shown on Figure 52.

The data indicate relatively large pore pressure decreases associated with drilling of the piers. It was observed during drilling that penetration of a sand layer below the clay layer was associated with rapid water infiltration into the drilled hole. This confirmed the presence of the sand layer indicated by the DOT boring logs, but not shown by the DMT or CPT. This occurrence correlated to the large decreases in pore pressure shown in Figure 52.

Pore pressure increases of high frequency can be seen correlating to times of pier ramming. In fact, individual pore pressure spikes were associated with individual lifts being rammed for piers 122 and 143. It is instructive to note that larger spikes in pore pressure relative to each piezometer are associated with the ramming taking place near individual piezometers. This is evidenced in the ramming of pier 122. Confirmation of pore pressure increases strengthens the contention that ramming causes remolding of soil fabric in the immediate vicinity of the pier (White et al., 2000). This is discussed further in the

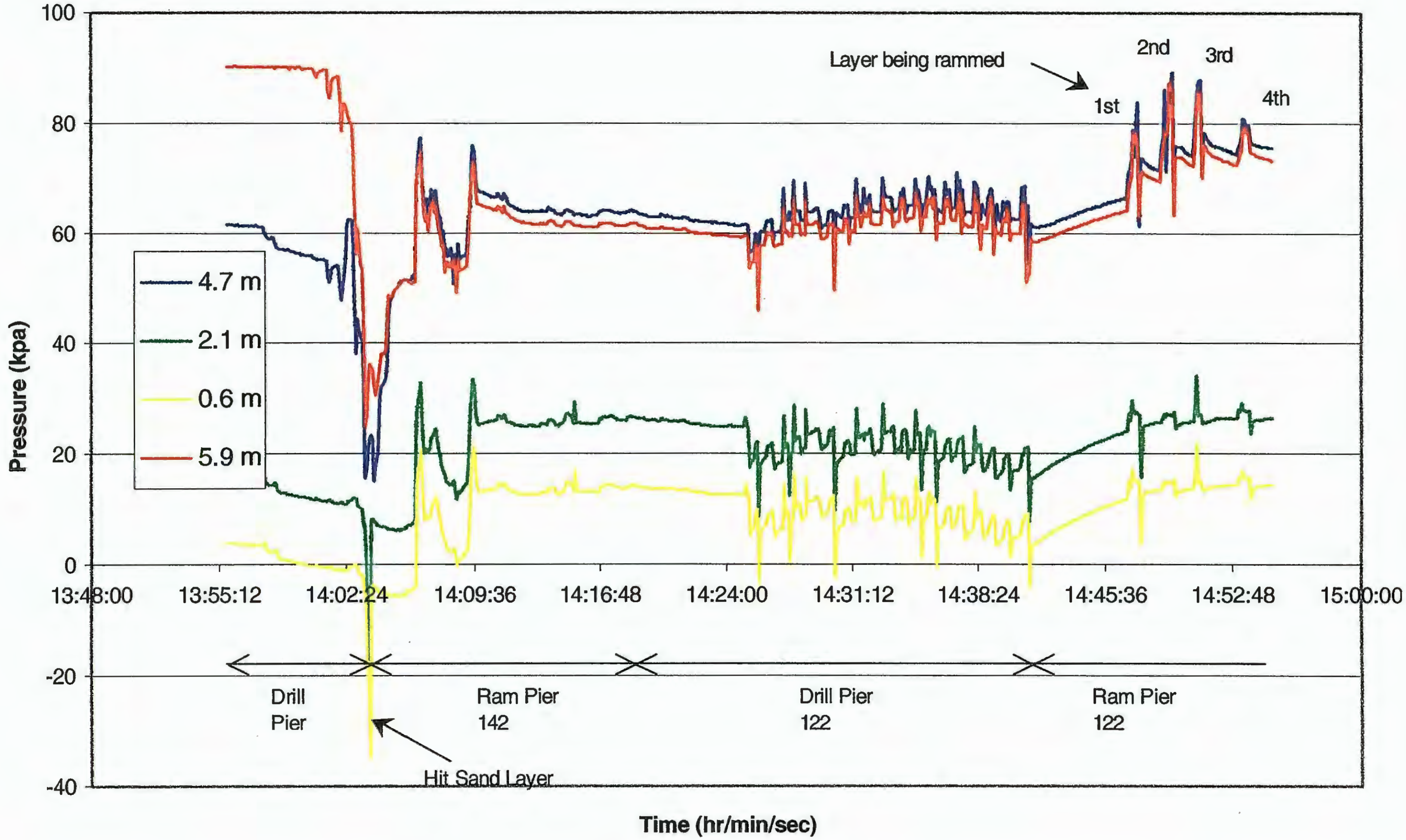

Figure 52. Piezometer readings for first half of dynamic pore pressure test

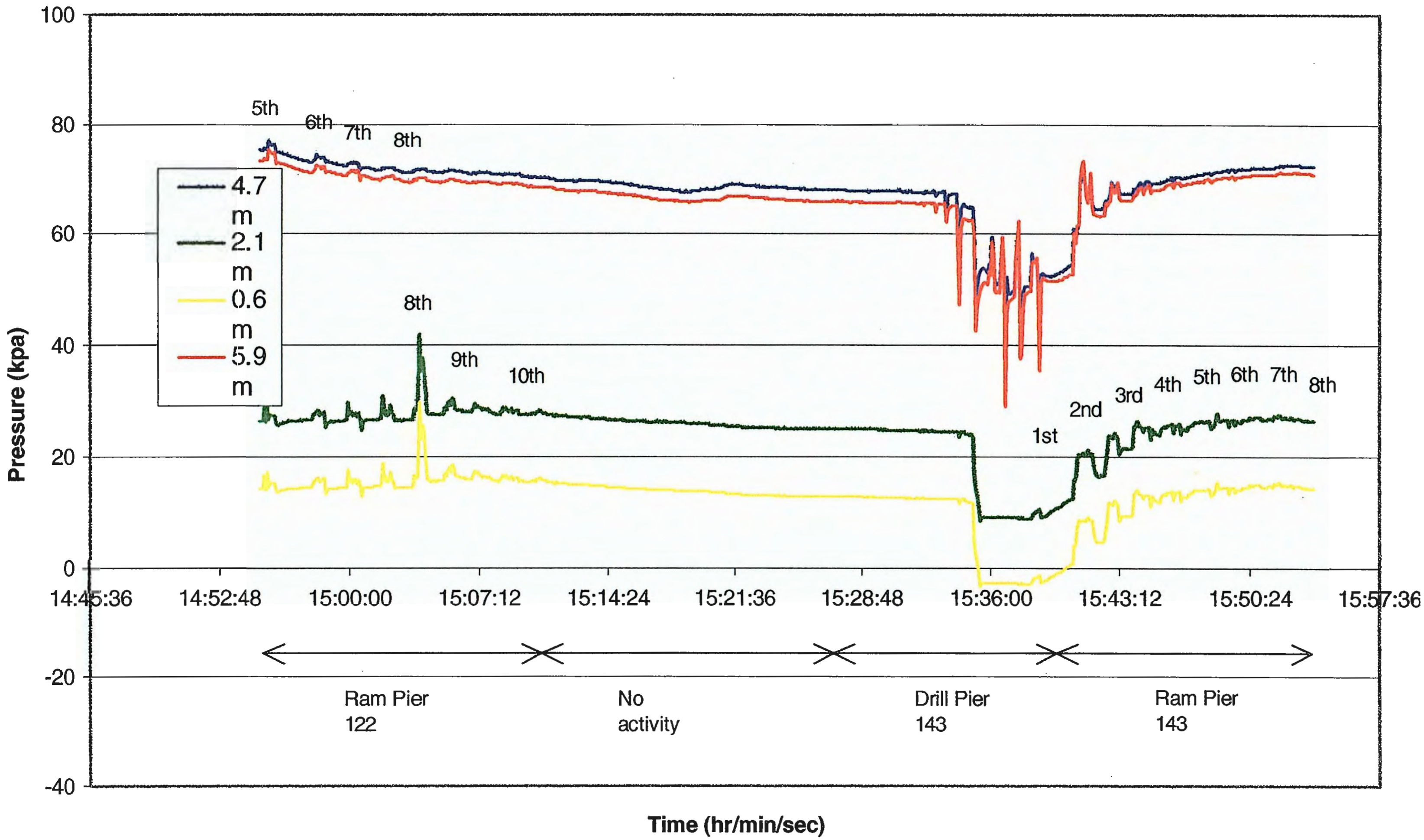

Figure 52(continued). Piezometer readings for second half of dynamic pore pressure test

conclusions section at the end of the report.

Piezometers (long-term)

Pressure readings before and after embankment construction are shown in Figure 53. It was intended for the piezometers to measure pore pressure increase associated with embankment fill and also reveal its dissipation. Figure 53 shows that no significant pore pressure increase resulted within the piezometer borehole during filling operations. It has been surmised that operations during pier installation disturbed the confinement of the piezometer borehole by opening it to the sand layer below. This is evidenced by the overlap of readings seen for the 4.7 and 5.9 m piezometers at the end of the dynamic pore

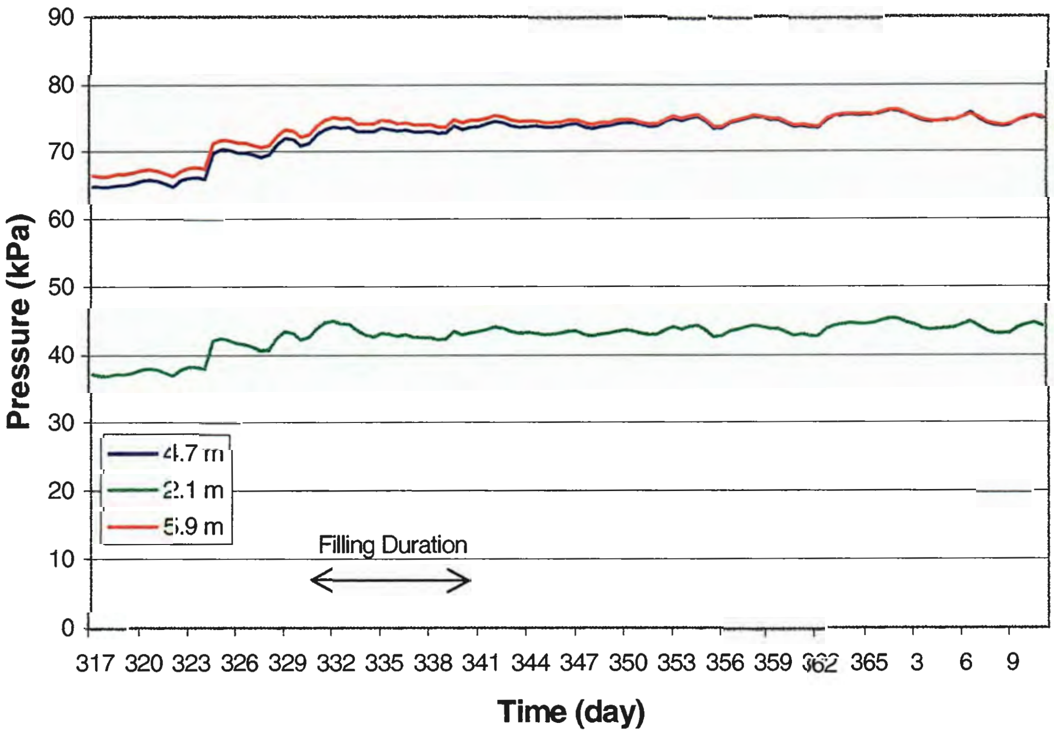

Figure 53. Piezometer readings before, during, and after embankment construction

pressure test and also subsequent readings shown in Figure 53. This would place the piezometers in a drainage path that would not register pore pressure increase. Regardless, the piezometers will remain a useful tool for analyzing variations in the height of the water table throughout monitoring.

Stress cells

Figure 54 shows the stress cell readings starting one-week prior and ending five-weeks after embankment construction. Stress increases range from 60 to 110 kPa. Four of the stress cell readings range from 100 to 117 kPa. The readings agree fairly well with the theoretical vertical stress increase of 125 kPa calculated using the density of the embankment fill and a height of 7.5 m for that fill.

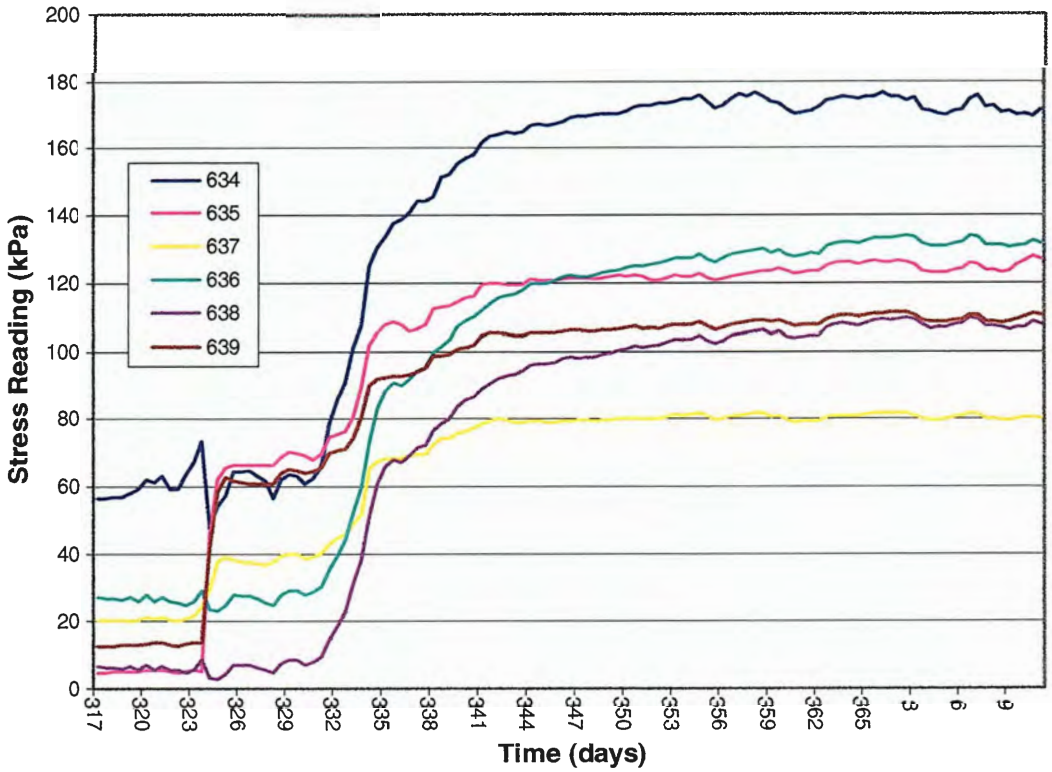

Figure 54. Stress cell readings before and after embankment construction

Further inspection does not reveal the stress concentration on the piers as expected. This is likely explained by the conditions of installation. A 0.5 m aggregate working blanket was installed for machinery due to the soft and wet soil conditions. Additional aggregate was added as needed to maintain mobility of equipment, so that the blanket became thicker than 0.5 m in certain areas. Although the individual cells were placed in sand, the blanket resulted in the entire group being placed in the aggregate. This is in contrast to the expected situation of pier cells on aggregate and those in-between placed on matrix soil. Longer term monitoring will assess any change in stress states for the stress cells.

Settlement cells

The settlement cells were placed as previously described and shown in Figure 51. Figure 55 displays the readings before and after construction. The graph shows

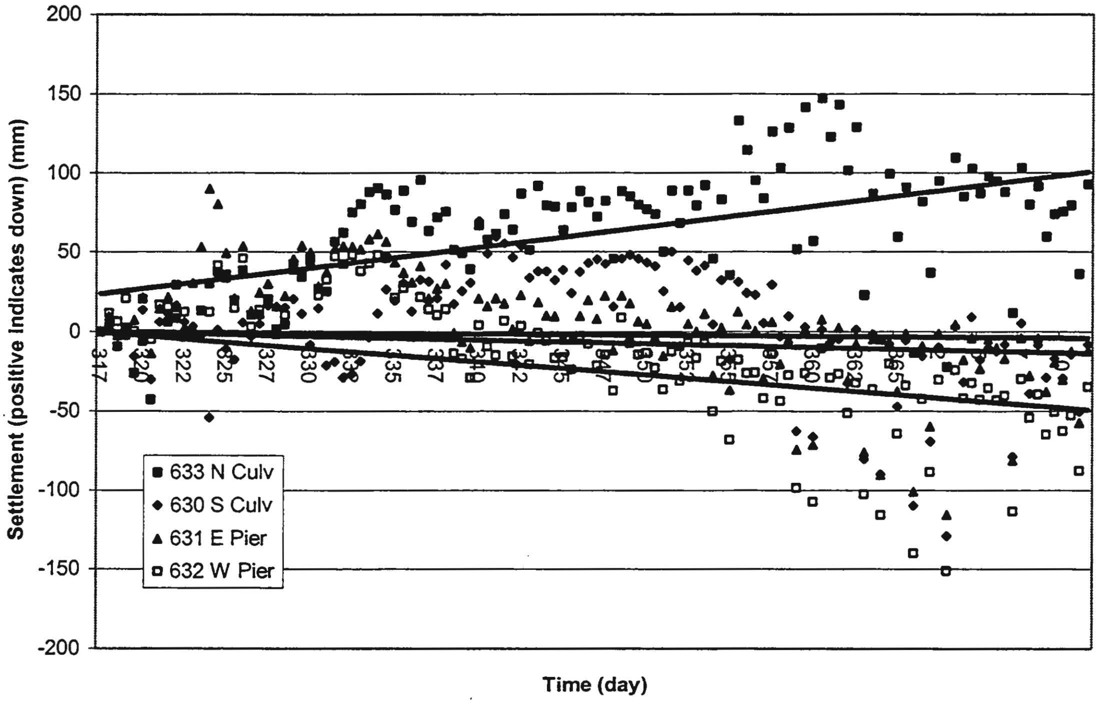

Figure 55. Settlement cell readings prior to and post embankment construction

considerable scatter, but does indicate trends revealing settlements commensurate with those found by manual surveying techniques. Cell 633 indicates that the culvert has settled around 12.5 cm, near the 11.5 cm indicated by surveys. The trend for the cells placed on the piers indicates that the piers are not settling. This indicates that the bridge is acting independent of the embankment settlement. Long-term monitoring of the settlement cells will reveal the magnitude of any secondary settlement for the culvert or bridge.

Performance Results

Predicted settlement

Unreinforced condition

Data from the four one-dimensional consolidation tests was used to establish pertinent settlement variables. The square root of time compression curves were used to calculate a coefficient of consolidation, c_v, of 0.07 +/- 0.03 m^2/day. This is assumed to represent the entire clay layer. Refer to the subsurface investigation section on oedometer testing for a calculation description and Table 1 for the tabulated data. A compression index, C_c, of 0.28 was calculated as the slope of the e-log p regression produced by the four one-dimensional consolidation tests. Additionally, an empirical value for C_c of 0.26 was calculated for verification using a relationship proposed by Skempton (1944). The relationship is presented in equation 1:

$$C_c = 0.009\,(LL - 10) \tag{1}$$

where LL represents the liquid limit. $C_c = 0.28$ was therefore accepted as a reasonable value for the compression index. Refer to Figure 25 for a graphical representation of C_c.

A total settlement of 63 cm has been estimated for the culvert in the unreinforced condition using Terzaghi's consolidation theory and Boussinesq's theory on distribution of stress beneath a rectangular solid. An inverted wedge represents a vertical section of the actual embankment, however, this situation was approximated assuming a rectangular solid of equal volume. A stress increase of 125 kPa at the mid-height of the clay layer was calculated incorporating the influence factors associated with Boussinesq theory. This value was verified using the total stress cell measurements indicating an average stress increase of 105 kPa after embankment construction. Local disturbance around the cells can account for this deviation from 125 kPa, however, the value is in good agreement with the theoretical stress increase. Figure 54 shows the stress cell readings. Details of this settlement estimate are provided in Appendix J.

A period of 170 days was estimated for 90% consolidation of the clay layer in the unreinforced condition. The calculation was based on Terzaghi's consolidation equation and is show in Appendix J. Double drainage was considered using the sand indicated in the pre-construction boring logs as the underlying drain and the absence of an overlying layer sufficient to prevent drainage. This resulted in a drainage distance equal to half the thickness of the clay layer or 3.75 m.

Reinforced condition

A period of 7 days was estimated for 90% consolidation of the clay layer in the reinforced condition. The difference results from a decrease in maximum drainage distance from 3.75 m to 0.75 m. The 0.75 m represents half the distance between any two piers (center to center). In a cohesive soil reinforced with granular piles, pore water moves toward the pile in a curved path having both vertical and radial components of flow (Bergado et al., 1996). In this manner, double drainage is considered with the piers acting as the draining elements. Compared with the unreinforced condition at 170 days, 7 days represents just 4% of the time it would normally take for consolidation. In fact, previous studies have shown that granular piles can accelerate the consolidation process in the same manner as sand drains (Bergado et al., 1996). This is an inherent benefit of the rammed aggregate pier. The calculation for this settlement time is once again directly based on Terzaghi's consolidation theory, with details provided in Appendix J.

Post-construction observation

Settlement

The rammed aggregate pier reinforcement was designed for a maximum 15 cm (6 in) of total settlement and 10 cm (4 in) of differential settlement. Figure 56 (in feet) and Table 3 (in mm) show the surveying log, indicating a maximum settlement of 11.5 cm (4.5 in) at pin number 5 and a maximum differential settlement of 7.9 cm (3.1in) between pin numbers 5 and 11. This indicates compliance with design criteria. From this settlement data, the settlement ratio is 0.18 $\left(SR = \frac{S_r}{S_u}\right)$ and the improvement factor is 5.5 $\left(IF = \frac{1}{SR}\right)$, i.e., rammed aggregate piers reduced settlement by a factor 5.5 times that of the unreinforced foundation.

Figure 57 shows the settlement of pin 5 with the advancement of fill height. This graph indicates that the culvert had settled 1 cm before backfilling began. It has been surmised that this was due to the considerable size of the culvert, seating upon the relatively disturbed surface of the rammed aggregate pier grid. Backfilling began on 11/27/01 and was completed by 12/6/01, a ten-day period. Figure 58 shows the settlement of the culvert at pin

5 with respect to time. This figure shows that primary consolidation began on 11/27/01 and was 90% complete by 12/13/01. Thus 90% primary consolidation was complete within 16 days from the start of filling, and within 7 days of embankment completion. The time of 7 days for 90% consolidation, while seemingly aggressive, is in fact confirmed by actual behavior of the culvert.

The final design criterion to be met is serviceability of the bridge. It was not originally known whether the piles supporting the existing bridge extended to the firm layer underlying the clay layer. Therefore settlement of the embankment could conceivably cause the bridge piles to settle along with the embankment fill and clay layer. Two vibrating wire

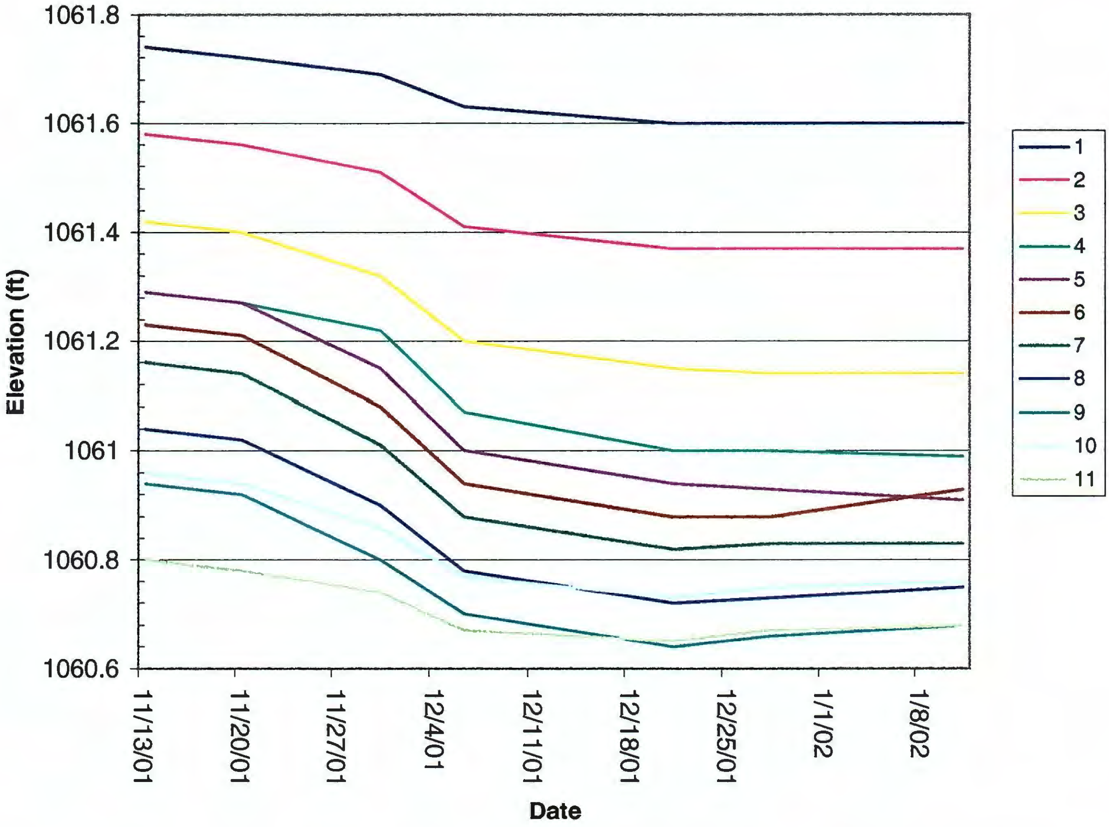

Figure 56. Settlement of culvert survey pins showing primary consolidation as a result of embankment construction (pin 1 west to pin 11 east)

Table 3. Absolute settlement of each surveying pin one week prior and five weeks post embankment construction

Date	Pin Number										
	1	2	3	4	5	6	7	8	9	10	11
	Absolute Settlement (mm)										
11/20/01	6	6	6	6	6	6	6	6	6	6	6
11/30/01	15	21	30	21	43	46	46	43	43	30	18
12/6/01	34	52	67	67	88	88	85	79	73	58	40
12/21/01	43	64	82	88	107	107	104	98	91	70	46
12/28/01	43	64	85	88	110	107	101	94	85	64	40
1/11/02	43	64	85	91	116	109	101	96	85	64	40

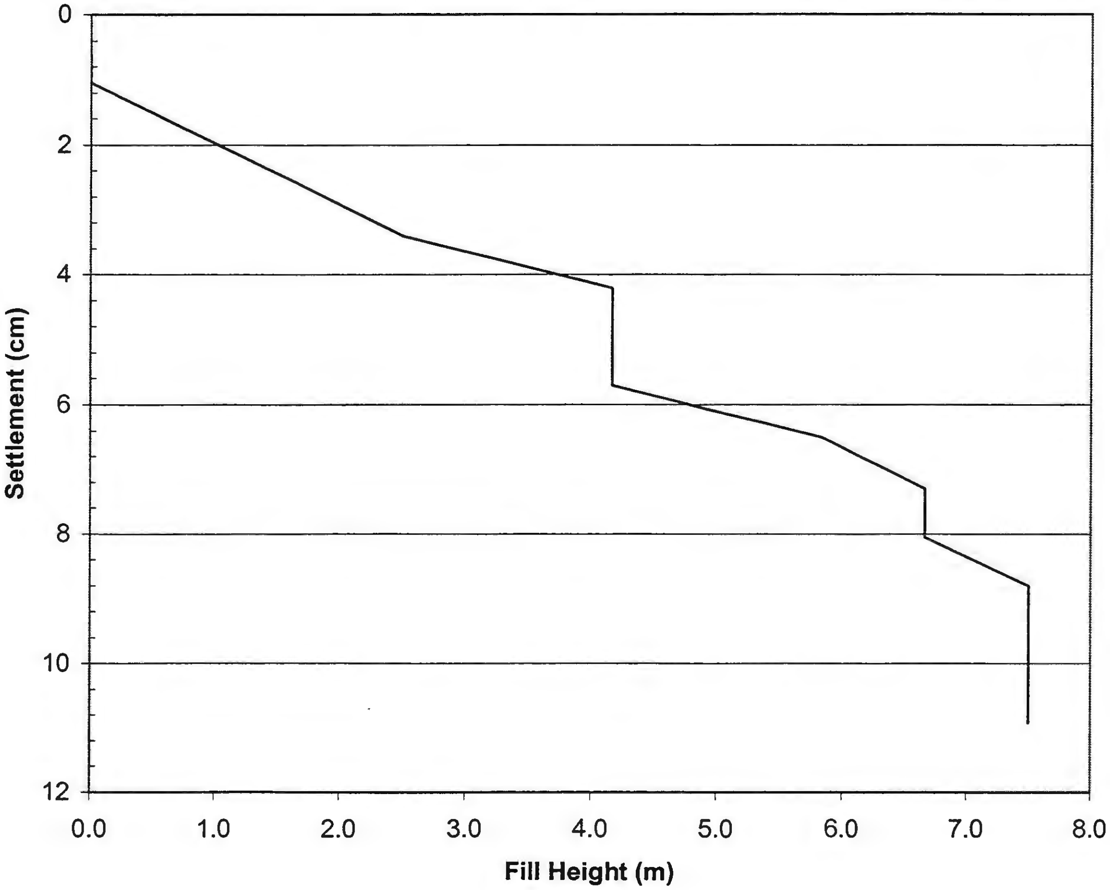

Figure 57. Settlement of pin 5 with the advancement of fill height

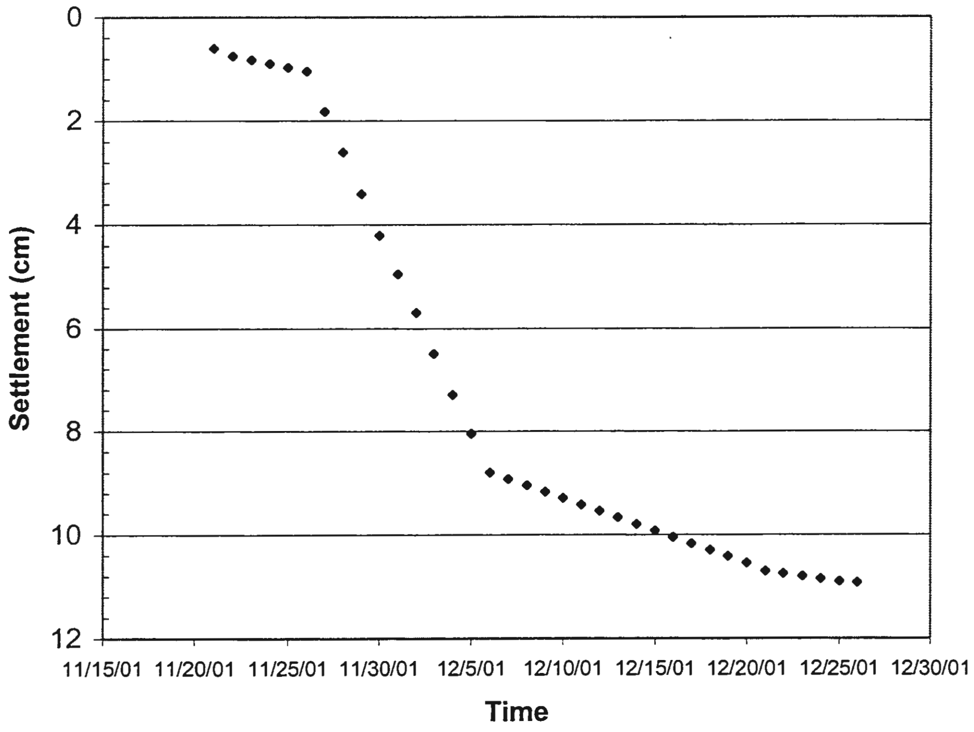

Figure 58. Settlement of pin 5 approximating settlement rate

settlement cells were installed on the two piers of the south bridge span to monitor movement of the piers within the embankment. Figure 55 shows the settlement readings for the east and west piers. There is considerable scatter in the data, however, the trend clearly shows no settlement of the piers. In fact, there is a slight rise indicated at the end of the data that can be accounted for by settlement of the vibrating wire instrument panel. This causes a shortening of the vertical liquid column from the instrument panel to the settlement cell, resulting in an apparent rise of the settlement cell. The settlement cells will be used in long-term monitoring to confirm no movement of the bridge.

Differential Settlement

Review of as-built documents

Although the project met the criterion for differential settlement, it has been proposed that the constructed length of piers may have had an adverse effect on the amount of differential settlement. The construction documents list four zones of pier installation assigned by pier depth. Varying the pier heights was intended to compensate for the non-uniform fill height that is placed over the culvert, i.e., shorter piers where there is less overburden. Figure 51 denotes the pier zones and Table 4 lists pier depths associated with each zone. Review of the pier installation inspection documents reveals that piers in zones A, B, and C were drilled as specified in the original design documents. However, zone D piers were specified in the construction documents as 2.3 m, but were specified in the original engineering design documents as 0.9 m. A review of the original design specifications and predictions can be compared to the actual settlement at points within pier zone D. Then a prediction can be made by the same methods for the actual installed piers of 2.3 m length. A determination is then made as to whether the increased length of piers in zone D had an adverse effect on differential settlement.

The original design documents specified pier lengths and also gave estimated settlements for each pier zone. The settlement estimates are based on Geopier™ design methods using soil modulus, pier modulus, and the estimated increase in bearing pressure. Table 4 provides estimated settlements using the original designed pier lengths. This indicates zone D was originally designed to settle 10.6 cm (4.18 in). Zone A was originally designed to settle 12.7 cm (4.99 in). This represents a total designed differential settlement of only 2.1 cm (0.83 in). Inspection of Table 3 indicates 4.3 cm (1.70 in) and 3.7 cm (1.45 in) of settlement for zone D survey pins 1 and 11, respectively, an average of 4 cm

Table 4. Settlement calculations from original design

Design Section (zone)	Shaft Length m (ft)	Bearing Pressure kPa (psf)	Upper Zone Settlement cm (in)	Lower Zone Settlement cm (in)	Total Settlement cm (in)
A	6.71 (22)	163 (3410)	1.4 (0.57)	10.3 (4.42)	12.7 (4.99)
B	5.79 (19)	123 (2560)	1.1 (0.43)	12.0 (4.71)	13.0 (5.13)
C	4.27 (14)	82 (1710)	0.7 (0.28)	11.9 (4.68)	12.6 (4.97)
D	0.91 (3)	41 (850)	0.4 (0.14)	10.3 (4.04)	10.6 (4.18)

(1.57 in). Table 3 also indicates that zone A settled 11.6 cm (4.57 in), 9.1 cm (3.58 in), and 10.1 cm (3.98 in) for survey pins 5, 6, and 7, respectively, an average of 10.26 cm (4.04 in). This results in an actual average differential settlement of 6.26 cm (2.46 in), well above the intended 2.1 cm (0.83 in). Although the settlement of zone A was about 2.54 cm (1.0 in) less than estimated, representing a 20% error, zone D was 6.6 cm (2.60 in) less than estimated, a 62% error. This indicates that the zone D settlement accounted for roughly three times more of the final differential settlement relative to zone A.

The settlement for the constructed pier length was then calculated using the same method devised by Geopier™. This predicted a settlement of 8.86 cm (3.49 in) for zone D using the constructed pier length of 2.3 m. This is a reduction in predicted settlement for zone D of 1.75 cm (0.69 in), changing the predicted total settlement to 8.85 cm (3.48 in). This would have increased the predicted differential settlement to 3.85 cm (1.52 in), but accounts for little of the total settlement error in zone D of 6.6 cm (2.60 in) resulting in a 46% total settlement error.

The data supports the fact that zone D was responsible for a disproportionate amount of the differential settlement. However, Geopier™ design calculations did not predict the settlement of either pier length accurately, indicating a larger settlement amount for each than was actually observed. To summarize, the constructed pier length did have a small effect on the amount of differential settlement observed, but was not as significant to differential settlement error as the calculations. A failure to predict the actual settlement in zone D is the largest cause of differential settlement error in this case.

Further investigation of zones B and C indicates significant error in estimated total settlement as well. Approximately 8 cm (3.15 in) was realized while roughly 12.8 cm (5.03 in) was predicted. This is an error of 37.5%. This progression of increasing error from zone A at 20% to zone D at 62% indicates a more general failure to accurately predict settlement. The piers in zones A, B, and C were constructed as designed, so pier length is no longer a reasonable cause. The conservative design calculations are a possible culprit, being conservative in a consistent fashion. Assuming the figures for modulus of pier and soil are correct, the only other variable remaining in the design calculations is bearing pressure. Figure 54 indicates a stress increase in zone A of 105 kPa. Table 4 indicates that a maximum bearing pressure of 163 kPa was assumed in zone A. This reduced linearly (by zone) to the minimum of 41 kPa in zone D. It was deduced that an overestimation in bearing pressure, indicated by the total stress cell, could be the cause of the increasing error in settlement estimation from zone A to zone D. This led to an estimation of settlements using decreased bearing pressures, but allowing them to decrease linearly at the same rate originally specified. The results are listed in Table 5.

The results listed in Table 5 support the theory that overestimated bearing pressures caused most of the predicted settlement error. This is confirmed by the accurate estimation of not only total settlement (error remained between 7 and 20%), but also differential

Table 5. Settlement calculations with adjusted bearing pressures and pier length

Design Section (zone)	Shaft Length m (ft)	Bearing Pressure kPa (psf)	Upper Zone Settlement cm (in)	Lower Zone Settlement cm (in)	Total Settlement cm (in)
A	6.71 (22)	140 (2924)	1.63 (0.64)	9.63 (3.79)	11.26 (4.43)
B	5.79 (19)	100 (2089)	0.89 (0.35)	9.75 (3.84)	10.64 (4.19)
C	4.27 (14)	60 (1253)	0.53 (0.21)	8.74 (3.44)	9.27 (3.65)
D	2.29 (7.5)	20 (417)	0.18 (0.07)	4.14 (1.63)	4.32 (1.70)

settlement. The decrease in bearing pressure increased the predicted differential settlement to 6.93 cm (2.73 in) in comparison to the actual differential settlement of 6.25 cm (2.46 in). The increased accuracy in the prediction of total settlement and differential settlement make overestimated bearing pressure a likely scenario in the underestimation of differential settlement. It is possible that the lower actual bearing pressure on the culvert is a result of arching within the embankment. Further investigation would be required to confirm this.

DATA ANALYSIS

Data from each of the load tests will be used to analyze strength, stiffness, and stress distribution characteristics for piers. In addition, inclinometer readings will be used to approximate failure conditions and also describe bulging of the piers during installation and loading. The group load tests afford the first opportunity to analyze a group of rammed aggregate piers loaded under a rigid footing. These tests also present the opportunity to compare the behavior of individual piers to groups of piers. Methods covered in the literature review will be used for data interpretation. Although the rammed aggregate pier is not designed in the same manner as a stone column, the intent here is to demonstrate the value of the concepts discussed in the literature review in characterizing rammed aggregate piers.

Individual Load Test Analysis

Bearing capacity

All three of the individual load test piers were installed with a 0.76 m diameter. Hughes and Withers (1974) was used to calculate a theoretical ultimate bearing capacity of the piers. Using ϕ_s=47° (a typical value for a rammed aggregate pier), s_u=10 kPa, and σ_{ro}=8 kPa, this results in a vertical capacity in the pier of 309 kPa (15.75 tons). Failure in the pier load tests was defined as the point that the pier could not resist increased load. This corresponded to a load of 878 kPa (45 tons), 560 kPa (28.7 tons), and 637 kPa (32 tons) for piers 1, 2 and 3, respectively. It should be noted that Pier No. 1 contained a significant amount of sand and four stress cells that could have altered behavior under load. The strengths are two and three times the predicted capacity. To resolve this, consideration needs to be taken of the soil profile.

The profile indicated by the CPT and DMT reveals stiff clay comprising the upper 1 m. Reference the subsurface investigation section for CPT and DMT profiles. This causes an increase in shear capacity and passive resistance in the upper 1 m. The effect is two-fold; first, the pier dissipates more vertical load through shear resistance in the upper 1 m resulting in a decrease in vertical load realized below 1 m where the soft alluvial clay resides. Second, bulging is not likely to occur in the upper 1 m due to the large increase in passive resistance, resulting in the appropriate stress increase required for bulging at a depth of at least 1 m. In fact, Figure 34 shows that bulging began to occur at 1 m depth in pier 1 as predicted. However, the first 0.46 m is a concrete cap where no shear resistance is developed, so the increase in resistance is actually only realized from 0.46 m to 0.92 m depth. This may account for some increase in bearing capacity, but likely not the two to three times shown by load testing. Bergado and Lam (1987) and Bergado et al. (1989) conducted 21 full scale load tests on compacted granular piles that each fell within 30% of the predicted ultimate capacity given by Hughes and Withers (1974). Bergado and Lam (1987) includes a stiff upper 2 m similar to the conditions at this site. This indicates that the rammed aggregate Pier No. 1 possesses significantly increased ultimate capacity.

The load-settlement curves in Figures 29 and 38 indicate bulging failures in piers 1 and 3 as the tell-tale located at the bottom of the pier moved insignificantly in relation to top of pier settlement. Bulging failure is also indicated by Figure 34, which shows the inclinometer profile of pier 1. This indicates that piers 1 and 3 exceeded their critical length in accordance with the concepts discussed in the literature review. The critical length is then around 2.74 m, the installed depth of Pier No. 2. Calculations using Hughes and Withers (1974) and Madhav and Vitkar (1978) predict a critical length of 5.39 and 7.73 m, respectively. This shows that the rammed aggregate pier is able to develop the shear resistance required to initiate bulging in two times less depth than required for the granular pile.

Although the ultimate bearing capacity of the individual piles varied, their load-settlement curves each reveal elastic settlement to a maximum of 397 kPa (20 tons), i.e., linearly increasing settlement with load to that point. This suggests that the shear capacity of the critical depth, the elastic settlement region, is in fact the same for each pier. The difference in capacity is then dictated by the passive resistance of the soil to bulging. It is instructive to note that the increased installation depth of Pier No. 3 at 5.05 m did not result in an increase in ultimate capacity as compared with piers 1 and 2. This is in agreement with the assumption that the ultimate capacity of a granular pile is determined by critical length and passive resistance, not length (assuming the critical length is exceeded).

The data suggest that the rammed aggregate piers behave in the same manner as the granular pile, but possess strength two to three times higher than can be predicted by empirical correlation or previous granular pile load testing. The design methodologies employed in the design of rammed aggregate piers are a result of significant research specifically tooled to better characterize their unique differences in pier-soil interaction.

Settlement

Several methods for settlement prediction of an individual pile were discussed in the literature review. Data gained in the Pier No. 1 load test coupled with pressuremeter data afforded the unique opportunity to re-evaluate the method proposed by Hughes et al. (1975).

Stress cell instrumentation within Pier No. 1 allows the plot of actual vertical stress distribution within the pier. This constitutes a significant advantage over the data contained in their paper as a result of not using an idealization of shear stress distribution. Another option used in their paper that did not compensate for shear resistance decreasing vertical load should not be considered, as this is clearly not the case. Figure 59 displays the vertical stress distribution within pier 1 as load increases. Note that vertical stress does not decrease in the first 0.46 m as a result of the concrete cap. The stress cell at 1.3 m was not included in the regression due to malfunction. Figure 60 shows the pressuremeter curve interpolated

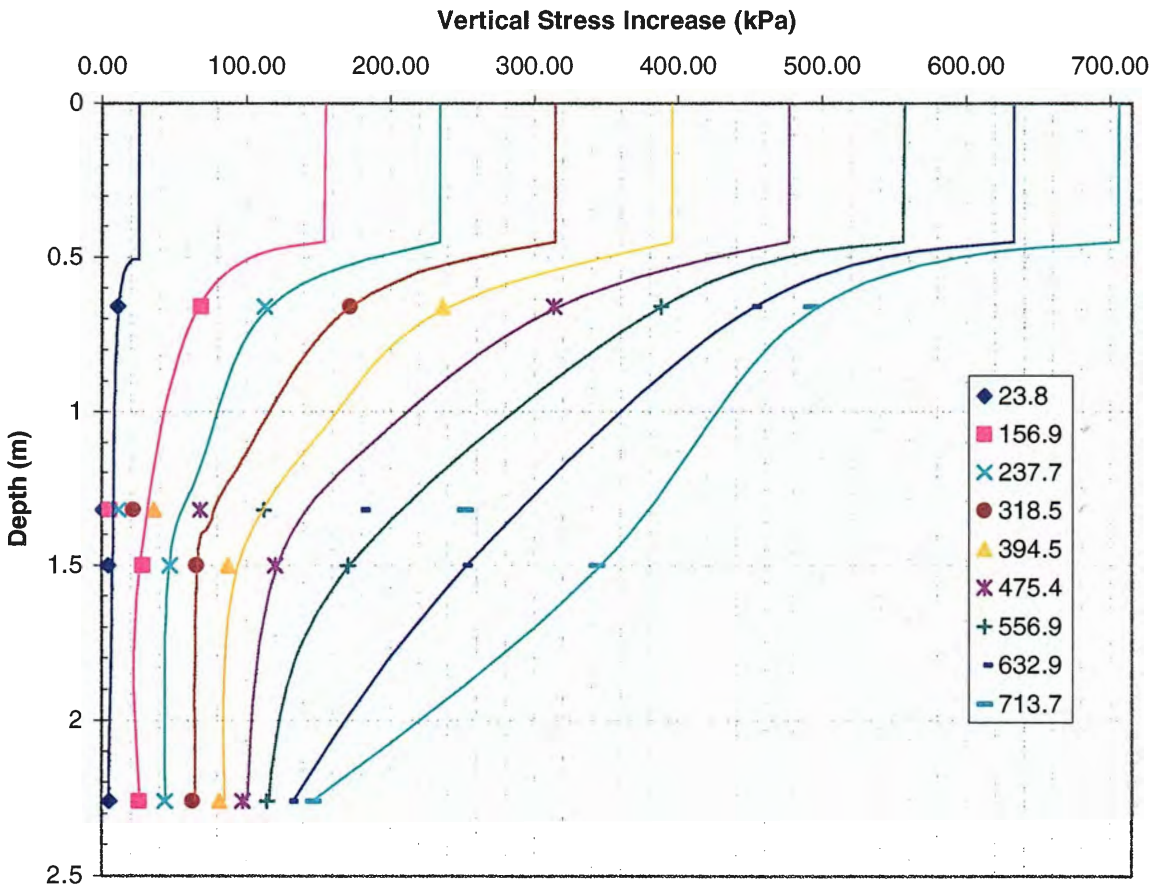

Figure 59. Vertical stress distribution in pier 1 using stress cell data at load increments

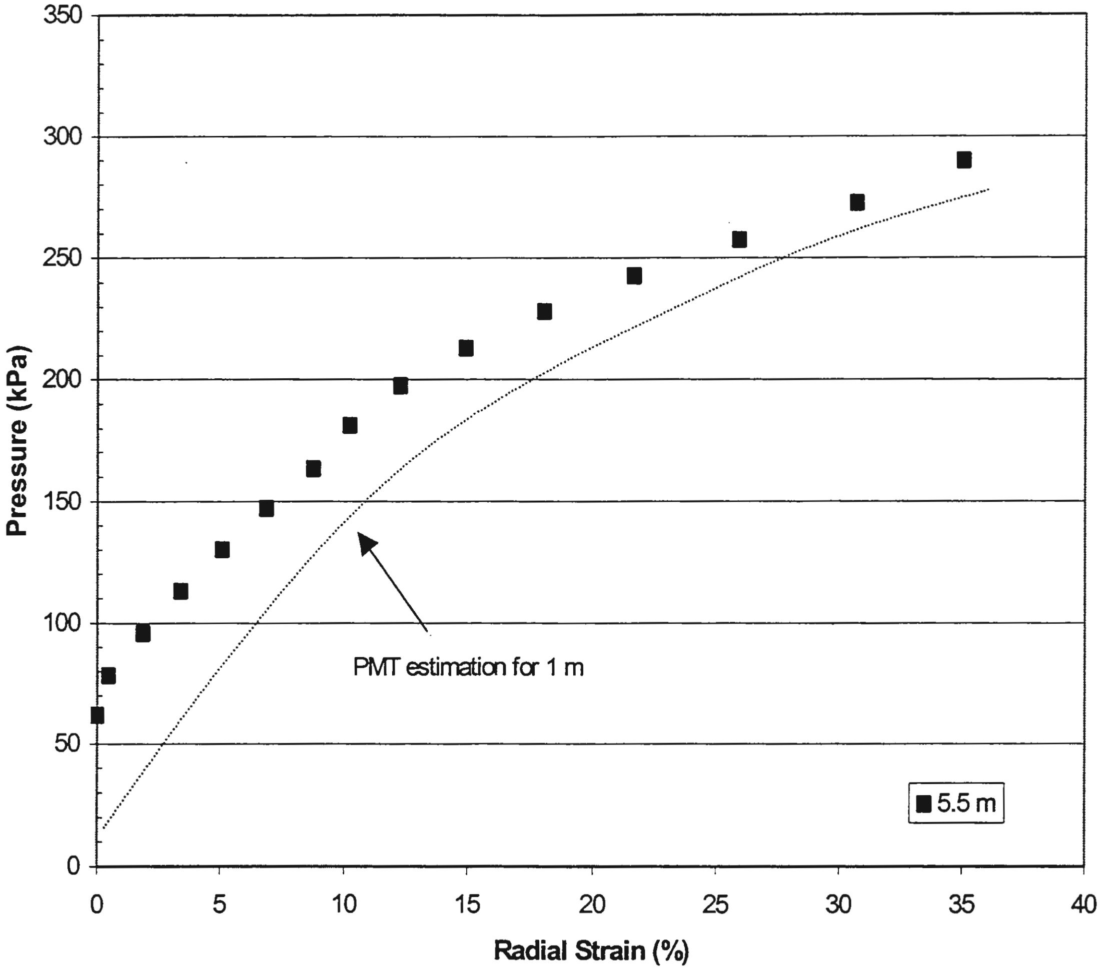

Figure 60. PMT curve approximation at 1.0 m depth with radial strain %

from the limit pressures of all the tests performed and the in-situ lateral stress present at 1 m depth. The knowledge of bulge location given by the inclinometer data of pier load test 1 also offers an advantage. Knowing that radial strain does not occur until this point is taken into account when dividing the pier into layers and summing settlements.

Knowledge of the vertical stress distribution allows the direct calculation of the horizontal stress distribution using the passive coefficient of the pier. This distribution was then used directly with the pressuremeter curve to estimate radial strain of each layer with

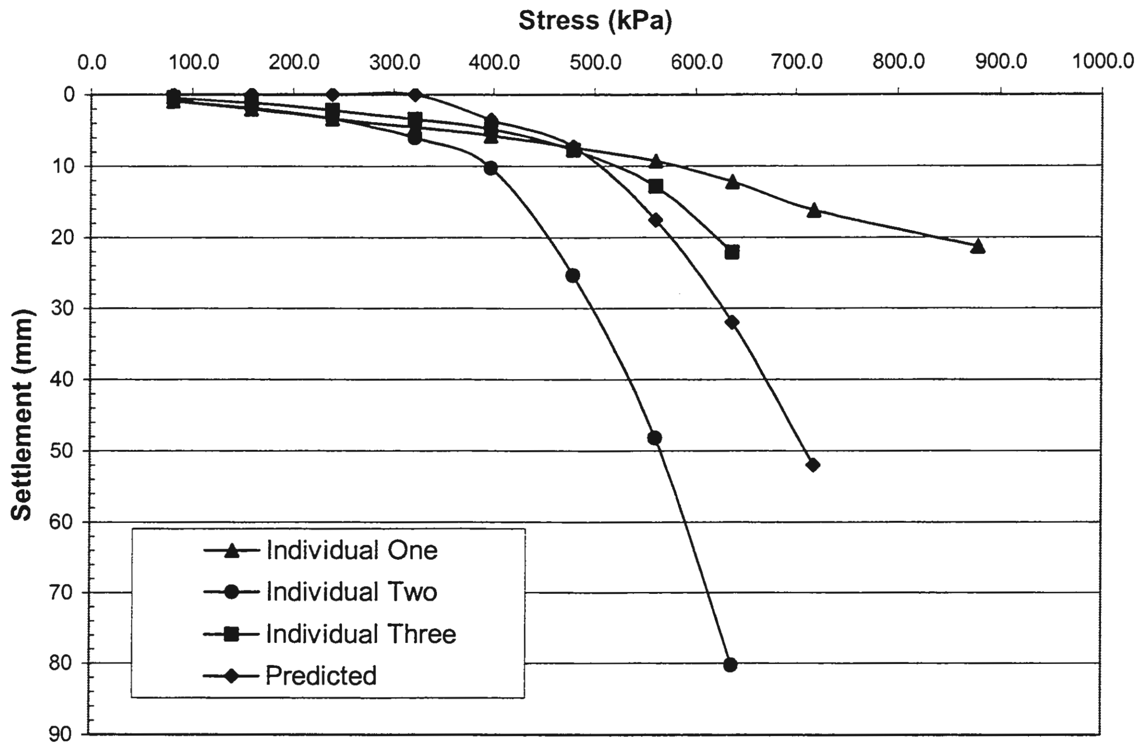

Figure 61. Settlement prediction for an individual pile using Hughes and Withers (1975)

increasing load. Figure 61 shows the settlement prediction results superimposed with the load-settlement curves from Piers 1, 2 and 3. Reference Appendix K for data tabulated on the settlement prediction. It is seen that the predicted settlement curve falls within the ranges of the pier load tests, nearly representing an average of the three curves. It is logical that the pier 2 settlement curve fell below the predicted curve as it had a punching type failure, i.e., pier 2 did not mobilize enough shear resistance for a bulging failure which would have resulted in increased strength.

Perhaps most instructive is an additional note that supports the theoretical basis of this method. Inspection of the vertical stress distribution reveals that the ultimate vertical capacity of 309 kPa is reached at a depth of 1 m just after the 560 kPa load increment. Evaluation of the corresponding load-settlement curve for pier 1 indicates that non-linear settlement is instigated just after the 560 kPa load. This supports both the assertion of bulging failure occurring at a prescribed vertical stress and reinforces the observation that bulging does not begin until a depth of 1 m.

Inspection of Figure 59 indicates that vertical stress increases at the bottom of the pier even as bulging failure progresses above it. This situation conflicts with plastic theory, which would suggest that resistance cannot increase in the pier as plastic failure (bulging) progresses. A list of theoretical reasons for the continued vertical stress increase below the bulging failure are:

1. The internal friction angle of the soil increases as shearing failure progresses due to dilation, thus increasing the resistance to bulging.
2. An increase in the confinement of the pier, caused by stress dissipation into the soil through soil-pier friction, results in an increased vertical stress within lower portions of the pier.
3. Bulging is not truly plastic, rather an elasto-plastic behavior.

The method offered by Hughes and Withers (1975) is surprisingly accurate. Some research has proven it the most accurate method available within several papers including Bergado et. al (1978), Bergado and Lam (1987) and Bergado et al. (1989). The key advantages to the method are the direct use of the radial stress-strain properties of the soil as measured by the pressuremeter, ability to account for the presence of a stiff upper layer and increased strength of the pier due to a higher internal friction angle.

Group Pile Load Test Analysis

Bearing capacity

The load tests performed on groups of four piers capped by a reinforced concrete raft constitute the first full-scale load tests on a group of four rammed aggregate piers. Individual load tests are often performed, and sometimes specified, on individual piers as a component in the project installation. The two group tests present the opportunity to collect data in a manner that is more representative of the field implementation. Although rammed aggregate pier grids are often designed with a method dependent upon area replacement ratio, the ultimate bearing capacity of smaller groups of piers can become important when used to support concentrated loads beneath mid-rise structures. The primary objective is thus to compare and contrast the data gained in the group load tests with that of the individuals.

The soil conditions are the same as the individual load tests, 1 m of stiff clay underlain by the soft alluvial clay. Barksdale and Bachus (1983) then suggest that the bearing capacity of the group is based on the capacity of a single pile within a group, multiplied by the number of piles. This is similar to the better known efficiency coefficient that is applied to the bearing capacity of driven piles located in a group. Under this assumption, the capacity of a pile in a group is less than that of an isolated pile. The data for an isolated pile within a group is not available, leaving the capacity of the individual tests to be used. This should be a rather liberal estimate and results in predicted bearing capacities of 180 tons, 115 tons and 128 tons. Group test one resulted in an ultimate capacity, load at which resistance cannot be increased, of 147.3 tons and group test two resulted in 196 tons. Inspection of the failure modes is helpful in evaluating these capacities.

The load-settlement curve for group load test one, Figure 44, indicates clearly that the tell-tale located at the bottom of the pier moved in unison with top of pier settlement. This indicates a punching type failure, precluding any bulging resistance. The inclinometer casing indicates lateral displacement at 1.5 m, Figure 48, extending to a depth of 5.75 m. This bulging peaked at a depth of 3.5 m, below the bottom of the pier. This indicates that soil is being pushed down and out as a result of the pile type "punching" failure. The stress transfer to the soil is what causes the down and out movement of the soil. Based upon the theory discussed in the literature review, it can be concluded that the pier installation depths at roughly 2.79 m did not exceed the critical depth in this case. This implies that the capacity of group test one is dependent upon the pile-soil shear resistance, rather than bulging. It is likely that the additional confinement of the matrix soil provided by the concrete raft, and the adjacent piers, resulted in an increased tendency to inhibit bulging. This is supported by data in Bergado et al. (1989) where increased loading plate size resulted in increased confinement of the pile. This would therefore effectively increase the critical depth of the pier, without changing the diameter of the pier itself, by increasing the shear resistance of the pile.

It can be seen that the capacity of group test one is well above that predicted by the capacity of either Pier No. 1 or 2. Pier No. 2 should be a more appropriate estimate as it failed in the same mode, punching. This suggests that a reduced capacity for a rammed aggregate pier within a group is not appropriate. The group efficiency in relation to pier two would be 1.28, relative to ultimate capacity. The data indicate, for groups of piers installed less than critical depth, that an acceptable approximation of bearing capacity is a multiplication of the number of piers and the capacity of an individual load test. The individual load test is one installed near the critical depth as indicated by this comparison. The application is limited to soft cohesive soils.

Group load test two was installed with an average of 5.10 m piers. The load-settlement curve indicates pier bulging as the tell-tale settled independently of top of pier settlement. The piers in this test therefore exceeded their critical length. The test resulted in an ultimate capacity of 196 tons. This exceeds the predicted capacity, utilizing the previous convention, by 9%, 71%, and 53% according to piers 1, 2 and 3, respectively. The data suggest that when a group failure mode is defined by bulging, the capacity is to a significant degree higher than that predicted by single pier capacity. The group efficiency factor in comparison to pier one and two is 1.09 and 1.53, respectively, relative to ultimate capacity. It is apparent that many more data are required to pose a reasonable increase.

The elastic portions of each group test settlement curve indicate further evidence of

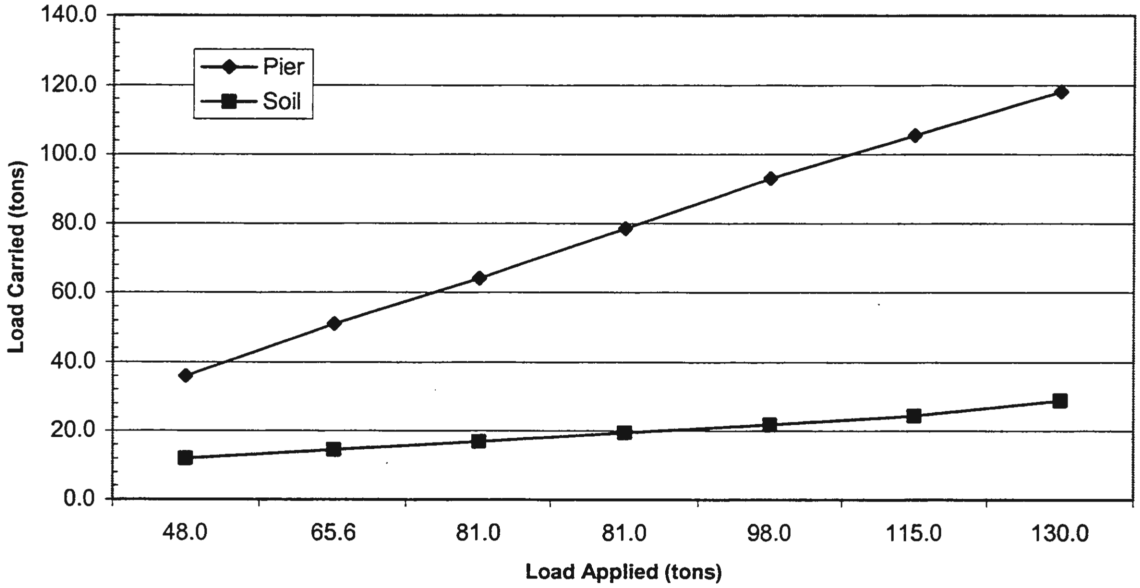

Figure 62. Load carried by pier and soil proportioned using stress concentration from stress cells

the relation between installed depth of pier and critical length. Each group test had an elastic response up to 479 kPa although their lengths varied from 2.79 m to 5 m.

Knowledge of the stress on the pier and soil afforded the calculation of stress concentration during group test one. Stress concentration increased with load, and reached a maximum of 4.3 at the ultimate capacity of the group. The portion of total load, according to stress concentration, carried by the soil and piers is plotted against load step in Figure 62. It has been posed that the stress concentration should increase with time as consolidation of the soil proceeds. The ratio of 4.3 is at the upper end of the 2 to 5 range suggested by Barksdale and Bachus (1983) for stone columns.

Reinforcement Performance Analysis

Settlement rate

Calculations in the performance section predicted a period of 7 days to attain 90% consolidation in the soft clay layer. The calculation was based on the Terzaghi one-dimensional consolidation equation considering only radial consolidation. The calculation was also based on only the vertical coefficient of consolidation found using oedometer testing. The actual time required for 90% consolidation was found to be somewhere between 7 and 14 days. Recent research has attempted to analyze settlement calculations in granular pile situations using both vertical and radial components of consolidation. Han and Ye (2001) have posed a simplified method that attempts to better characterize the consolidation acceleration resulting from the installation of a granular pile grid. Their method was discussed in the literature review, and was implemented to make a comparison with the actual consolidation rate.

Analysis by Han and Ye (2001) requires knowledge of both vertical and horizontal coefficients of consolidation. CPT pore pressure dissipation data was used to estimate the horizontal coefficient of consolidation, c_h. A dissipation was performed at both CPT2 and CPT3. Figure 63 displays the plot required to calculate c_h. From the plot c_h was determined to be $1.2x10^{-2}cm^2/s$. A stress concentration ratio between pier and soil is required to calculate the modified coefficients of consolidation. Stress cell information from group test one, Figure 47, was used to estimate a stress concentration of 3.25 in the stress range of 125 kPa corresponding to the overburden of the embankment. This resulted in modified coefficients of $c'_v=1.39x10^{-2}m^2/s$ and $c'_r=3.13x10^{-2}m^2/s$.

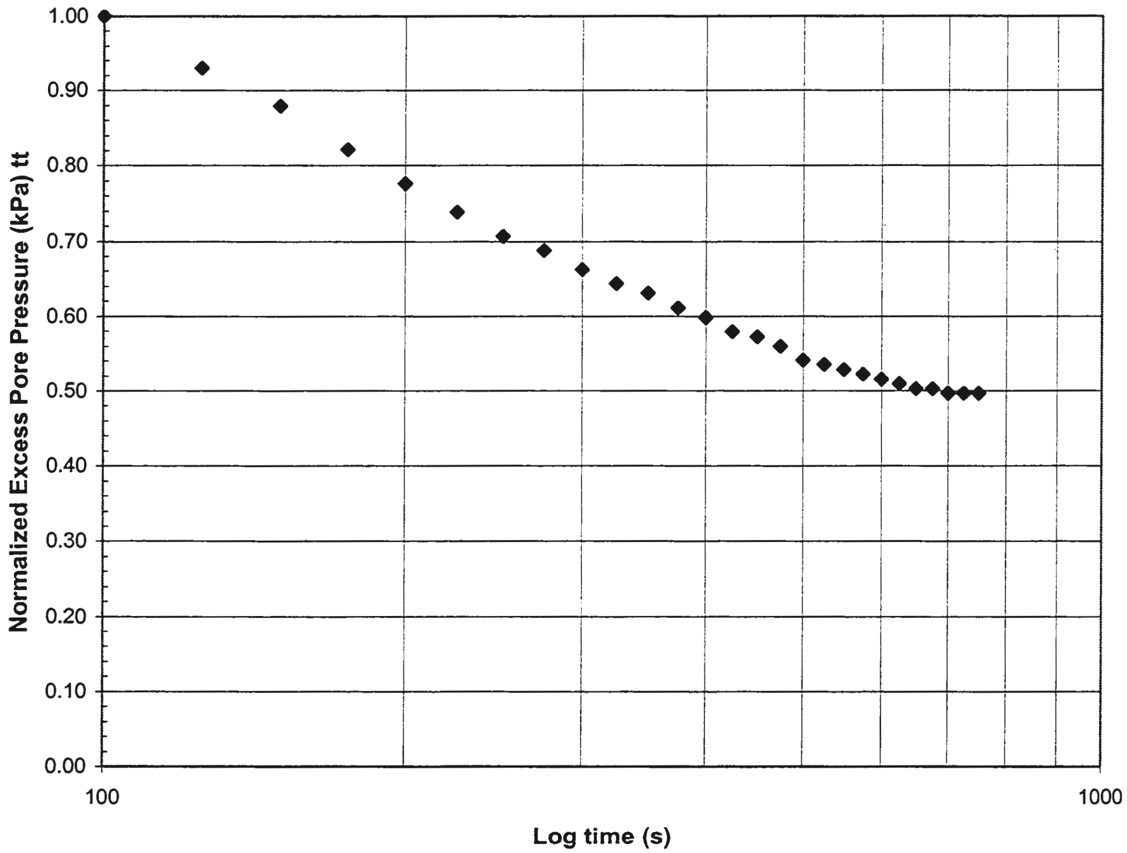

Figure 63. Pore pressure dissipation data at CPT2, used to calculate c'_r

Initial calculations resulted in a period of 1 day for 90% consolidation. It was then decided that c'_r may have been estimated too high using the CPT data. The value for c'_v from the oedometer was substituted for the horizontal coefficient. This resulted in a period of 2.2 days for 90% consolidation. With the calculations remaining low, Lambe and Whitman (1969) was consulted for typical values of c_v. $3.67 \times 10^{-3} m^2/s$ was listed as a typical value for a soil with a liquid limit of 40. Re-iterating this results in a period of 5.5 days for 90% consolidation using the coefficient from Lambe and Whitman (1969). The value was then substituted in the conventional Terzaghi 1-d equation resulting in an estimated 15 days.

Although the consolidation periods using the simplified method seem low, overestimation of the permeability of the clay greatly affects the results. It is likely that the CPT dissipation data overestimated the horizontal coefficient of consolidation. Use of the CPT coefficient resulted in unreasonably low consolidation times. Consideration should also be taken of the discontinuous placement of backfill. The calculations are based on the assumption that the overburden is placed in one operation. Actual backfilling took place over a period of 9 days. It is likely that placement of the backfill in one operation would result in an actual period of consolidation that is shorter than the 7 to 14 days realized from the actual data. The short duration returned by any of these methods should also be treated as they are intended, an estimate. Precision of just a few days in this short of a consolidation period is not reasonable to expect.

The results indicate that the simplified method from Han and Ye (2001) returned a consolidation period 2 to 3 times faster then the conventional Terzaghi 1-d method. This is in agreement with example results in Han and Ye (2001) that calculated consolidation periods 2.3 times faster than classical solutions. The staged placement of backfill and short period of consolidation in this project do not allow a comparison of any actual increased accuracy given by the new simplified method relative to the classical Terzaghi solution.

Total settlement

It is desirable to compare the settlement reduction ratio of the actual project to that of the predictions provided by Figure 8 in the literature review. The project ended with 12 cm of settlement compared to the 63 cm predicted for a settlement reduction ratio of roughly 0.19 . The area replacement ratio for the project, a_s, was calculated at roughly 0.25. The plot of these two values results in a settlement reduction ratio that is two to three times smaller than the predictions offered by any other method using the same area replacement ratio.

It is believed that both increased friction angle of the pier and increased stiffness result in the lowered settlement reduction ratio. It is known that friction angles of rammed aggregate piers are usually 45 to 50° (Lawton and Fox, 1994). A typical value could then assumed to be 47°. This is about 7 to 12° higher than that offered by typical stone columns (Barksdale and Bachus, 1983). The effect of increased stiffness of the pier is an increase in the modular ratio. To estimate this modular ratio it is necessary to know the modulus of the pier and also the matrix soil.

Load settlement curves for the individual load tests were used to calculate an average modulus of 1.05×10^5 kPa with a standard deviation of 4800 kPa for the piers using the slope of the initial portion of the curve and strain in relation to total pier length. The modulus of the soil is a more elusive quantity and was estimated using several methods to gain confidence in assigning a quantity. The methods used and associated values are listed in Table 6. The triaxial value was estimated from the consolidated drained stress-strain curves shown in Figure 20. The results have an average modulus value of 2500 kPa with a standard deviation of 800 kPa. The modulus values result in a pier to soil modular ratio of 42. This is above the upper value of 40 recommended for stone columns (Barksdale and Bachus, 1983). The data suggest that the increased friction angle and modular ratio of the rammed aggregate pier result in a settlement ratio two to three times smaller than those predicted by stone column correlations.

The data indicating smaller settlement ratios for rammed aggregate piers are supported by experimental values and several case histories. These are listed in Table 7.

Table 6. Modulus values of alluvial clay using several methods

Method	Average Value (kPa)	Reference	Equation
Cone Penetrometer	2050	Bowles, 1996	$5 \times q_c$
Pressuremeter	2100	Briaud, 1989	E_p / (2/3)
Dilatometer	2200	Marchetti, 1981	$R_m \times E_d$; Rm = 0.14+2.36xlogK_d
Triaxial data	3700	N/A	Tangent stress-strain curve

Table 7. Summary of settlement ratios for stone columns and rammed aggregate piers

Foundation Type	SR	IF	Prediction	Comparison	Reference
Stone Columns	0.50	2.0	Unreinf. Load Tests	Reinf. Load Tests	Buggy et al., 1994
Stone Columns	0.60	1.7	Lab Models	Lab Models	Stewart and Fahey, 1984
Stone Columns	0.40	2.5	Finite Element	Finite Element	Balaam and Booker, 1985
Stone Columns	0.70	1.4	Finite Element	Finite Element	Balaam and Booker, 1985
Stone Columns	0.80	1.3	1-D Consolidation	Observed Case	Van Imp, 1989
Geopier	0.17	5.9	CPT& 1-D Consol.	Observed Case	Lawton and Fox, 1994
Geopier	0.10	10.0	CPT& 1-D Consol.	Observed Case	Lawton and Fox, 1994
Geopier	0.17	5.9	CPT& 1-D Consol.	Observed Case	Lawton and Fox, 1994
Geopier	0.28	3.6	CPT& 1-D Consol.	Observed Case	Gaul, 2001
Geopier	0.20	5.0	1-D Consolidation	Observed Case	This study

SUMMARY AND CONCLUSIONS

The following conclusions have been made based on the information gathered throughout the course of this investigation.

1. The installed culvert settled 12 cm relative to the predicted unreinforced settlement of 63 cm resulting in a settlement ratio, SR, of 0.19. This results in an improvement factor, IF, of 5.3, meaning the rammed aggregate piers reduced settlement by 5.3 times over the unreinforced condition. Additionally, the settlement ratio is two to three times lower than stone column correlations using an area replacement ratio of 0.25.
2. The project met the criteria of 15.2 cm of total settlement and 11.4 cm of differential settlement.
3. The increase in construction length, as opposed to original design length, of the piers in Zone "D" likely resulted in an additional 1.75 cm of differential settlement. Although this contributed to the error in predicting differential settlement, it is probable that an overestimated bearing pressure in the clay layer resulted in the most error in differential settlement prediction.
4. Comparison of rammed aggregate pier load test data with empirical correlations and load test data for stone columns indicates that individual rammed aggregate piers are two to three times stiffer with an identical diameter and similar soil conditions.
5. Critical lengths for 0.762 m diameter individual rammed aggregate piers have been estimated at 2.74 m using data from individual load testing and site soil conditions. This length is two to three times smaller than estimates provided by stone column correlations indicating that rammed aggregate piers develop pile-soil shear resistance

capacity two to three times faster than stone columns. This would suggest that rammed aggregate piers can attain capacities of stone columns which are two to three times longer.

6. Calculation of the settlement of an individual pier using Hughes and Withers (1975) results in a load-settlement curve close to those observed in load testing. Knowledge of the vertical stress distribution in the pier is a significant advantage when applying this method.
7. The vertical stress distribution within individual pier one indicates that the ultimate vertical stress predicted by Hughes and Withers (1974) accurately locates the point at which bulging failure occurs. This suggests that the relationship is in fact quite accurate in estimating the conditions required for bulging failure.
8. The presence of a stiff layer above the soft layer to be reinforced results in significantly increased capacity of the rammed aggregate pier. The capacity increase is due to the dissipation of vertical stress through pile-soil shear resistance in the stiff upper layer, and also the increased passive resistance of the stiff layer that does not allow bulging at the surface.
9. Group load tests of rammed aggregate piers indicate that the ultimate capacity of groups of four piers loaded beneath a rigid foundation is greater than the sum of individual capacities. Punching failure results in a group efficiency of slightly greater than one, while bulging failure results in an efficiency significantly greater than one.
10. Critical lengths of piers installed below raft foundations increase due to confinement of the pier by matrix soil. Punching failure for groups is more likely at pier lengths close to the critical length for an individual pier.

11. Stress concentrations on the rammed aggregate piers during group load test one were measured at 4.3 relative to the matrix soil. It is likely that this concentration would increase as consolidation of the underlying matrix soil proceeds, resulting in a stress concentration factor above 5 for rammed aggregate piers.
12. Settlement rate within the clay layer increased by a factor of 17 over the unreinforced condition, resulting in a 90% consolidation period of between 7 and 14 days.
13. Settlement rates calculated from Han and Ye (2001) returned a consolidation period two to three times faster than the conventional Terzaghi one-dimensional method. This agrees with calculations made in Han and Ye (2001). The staged placement of backfill and short period of consolidation in this project do not allow a comparison of any increased accuracy given by the new simplified method.
14. Pore pressure increases adjacent to pier ramming were confirmed using real-time logging. This strengthens the contention that pier ramming can cause remolding of the soil fabric resulting in increased localized strength.

RECOMMENDATIONS FOR FURTHER STUDY

1. Perform more individual rammed aggregate pier load tests with stress cell instrumentation. Better characterization of the stress distribution in a pier is an important factor in predicting and understanding settlement behavior.
2. Perform more group load tests designed for bulging failure. Better knowledge of the capacity of rammed aggregate pier rafts could result in significant design efficiencies.
3. Perform more group load tests with inclinometer instrumentation. Knowledge of the bulging profile will aid in better characterizing failure mechanisms.
4. Study another rammed aggregate pier case history involving different lengths of piers to control differential settlement. Install stress cells throughout the project with the intent of measuring the stress distribution beneath different overburdens. This information would be invaluable to a better understanding of varying pier length in design.
5. Install a piezometer borehole in a rammed aggregate pier grid to measure pore pressure variation during loading and consolidation. This information could be used to confirm different methods of settlement rate prediction and coefficient of consolidation measurement.

APPENDIX A

PIEZOCONE PENETRATION DATA

Geotechnical Services Inc.

November 17, 2000

Iowa State University
394 Town Engineering
Ames, Iowa 50011

Attn: Mr. David White

RE: **ELECTRONIC PIEZOCONE SOUNDINGS FOR THE IOWA HWY. 191 BOX CULVERT, NEOLA, IOWA, GSI JOB #006051**

Dear Mr. White:

This letter presents cone penetration and pore pressure dissipation test data of OCTOBER December 26, 2000 made with the cone penetration equipment for the above referenced project. The work was authorized by Iowa Department of Transportation.

PENETRATION TEST DATA

The piezocone penetration test (CPTU) data were obtained using a Hogentogler Type 2, 10-ton electronic subtraction cone. The cone has a tip angle of 60 degrees, a tip area of 10 cm^2, a net area ratio correction factor of 0.8, and a friction sleeve area of 150 cm^2. The cone was pushed hydraulically by a 20-ton cone truck at a rate of about 1-inch per second. Data was collected at 5-cm intervals and is reported as an average over a 25-cm depth interval. The CPTU was made in substantial compliance with ASTM D 3441. The cone data were processed using procedures developed by Hogentogler & Co., and modified by GSI.

The CPTU data are presented in both tabular and graphical form on the enclosed tables and figures. The figures include the peizocone data collected and graphic logs containing our evaluation of the geologic materials from the piezocone data. The tabular data list the soil behavior type (soil classification) based on the Simplified Soil Classification Chart for Standard Electronic Friction Cone by Robertson and Campanella (1986) and Roberston, et al (1986). Although this interpretation provides a general indication of soil type based on tip resistance and friction ratio, the actual soil types may differ from those inferred. The relative density is determined using the correlation proposed by Jamiolkowski. The drained friction angle was determined using the correlation proposed by Kulhawy and Mayne (1990). The abbreviations used for the CPTU data are as follows:

q_c	Tip Resistance, Uncorrected	μ_o	Hydrostatic Pore Water Pressure
q_T	Tip Resistance, Corrected	σ'_{vo}	Effective Overburden Stress
f_s	Sleeve Friction	B_q	Pore Pressure Ratio
R_f	Friction Ratio	F	Normalized Friction Ratio
f_s/σ'_{vo}	Normalized Sleeve Friction	I_c	Soil Behavior and Classification
Q	Normalized Net Tip Resistance	Φ	Friction Angle
μ	Penetration Pore Water Pressure	D_r	Relative Density
σ_{vo}	Total Overburden Stress		

GEOTECHNICAL, MATERIALS ENGINEERING & ENVIRONMENTAL CONSULTANTS

7050 SOUTH 110TM STREET
OMAHA, NEBRASKA 68128-5716
(402) 339-6104 • FAX (402) 339-6297

OFFICES LOCATED THROUGHOUT IOWA, KANSAS, MISSOURI & NEBRASKA

The 3 piezocone penetration soundings were made at the locations shown on the attached site plan. The piezocone penetration soundings were located in the field by Iowa State University. The elevations shown were provided by Iowa State University.

DISSIPATION TEST DATA

The piezocone soundings were interrupted during the pushing process at depths of 4.65m, 8.15m, and 11.4m at CPTU-2 and 6.3m at CPTU-3 to record dissipation of the excess penetration pore pressure generated during the sounding. The depths and locations of the dissipation tests were determined in the field by Iowa State University personnel on site. The dissipation data was collected at 5 second intervals and is presented in graphical form. Horizontal drainage estimations were calculated for the dissipation tests at 11.4m from CPTU-2 and 6.3m from CPTU-3. The sounding data indicated overconsolidation of the clay at the dissipation depths. The results of the dissipation tests are considered representative for an overconsolidated material. The horizontal drainage calculations were corrected for normally consolidated conditions by dividing by a factor of 7.5. The data was processed using procedures developed by Conetec and modified by GSI.

INTERPRETATION OF DATA

The piezocone soundings were made to obtain subsurface information concerning the thickness of the natural alluvial formation and to identify the depth to a dense formation believed by Iowa State University and the Iowa DOT to be the shale bedrock. This information will be used to aid in the design of a box culvert to replace the existing bridge. Results of the cone penetration data from CPTU points 1-2, located east and west of the south abutment of the existing bridge, indicate natural alluvial clay and glacial till formations overlaying a dense formation believed to be shale bedrock at Elevation 312.7m and 312.4m respectively. CPTU-3 was located east side of the north abutment, and had a geological profile consisting of alluvial clay. The sounding was aborted due to rod refusal at Elevation 312.6. There was not enough data to determine if the dense layer encountered was the glacial till or shale bedrock. Based on information received from Iowa State University and Iowa DOT, CPTU points 1-3 appear to be underlain by fill extending to depths of 1 to 5 meters.

We look forward to working with you on other projects to apply this exploration technology. If you have any questions regarding this information or need further information, please contact our office.

Respectfully,
GEOTECHNICAL SERVICES, INC.

Jorge Santos
Senior Engineering Technician

Steven R. Saye, P.E.
Senior Engineer

Enclosures

cc: Iowa DOT Ames, Iowa
Attn: Andrew G. Barnes

GSI Des Moines, Iowa
Attn: Mike Lustig

TABLE OF REFERENCES

Robertson, P.K. and R.G. Campanella, "Guidelines fro Use, Interpretation, and Application of the CPT and CPTU", Hogentogler and Company, Inc., 3rd ed., November 1986

Robertson, P.K., R.G. Campanella, D. Gillespie, and J. Grieg, "Use of Piezometer Cone Data", Proceedings of In Situ 86, ASCE Specialty Conference, Blacksburg, Virginia, 1986

Jamiolkowski, M., G. Baldi, R. Bellotti, V. Ghionna, and E. Pasqualini, "Penetration Resistance and Liquefaction of Sand", Proceedings, 11th International Conference on Soil Mechanics and Foundation Engineering, Vol. 4, San Francisco, 1985, pp. 1891-1896.

Kulhawy, F.H. and P.W. Mayne, "Manual on Estimating Soil Properties for Foundation Design", August 1990, EL-6800 Electric Power Research Institute, Palo Alto, California.

Geotechnical Services Inc.
7050 South 110th Street• Omaha, NE 68128-5716
Phone: 402-339-6104• Fax: 402-339-6297

IDOT HIGHWAY 191
HIGHWAY 191
NEOLA, IOWA

CONE SOUNDING LOCATION PLAN

FIG # 1	REV. BY:
PROJ #: 006051	REV. DATE:
DATE: 11/16/2000	CHECKED BY:
DRAWN BY: DCD	CHK. DATE:
PROJECT MANAGER: JS	APPROVED BY:
	APP. DATE:

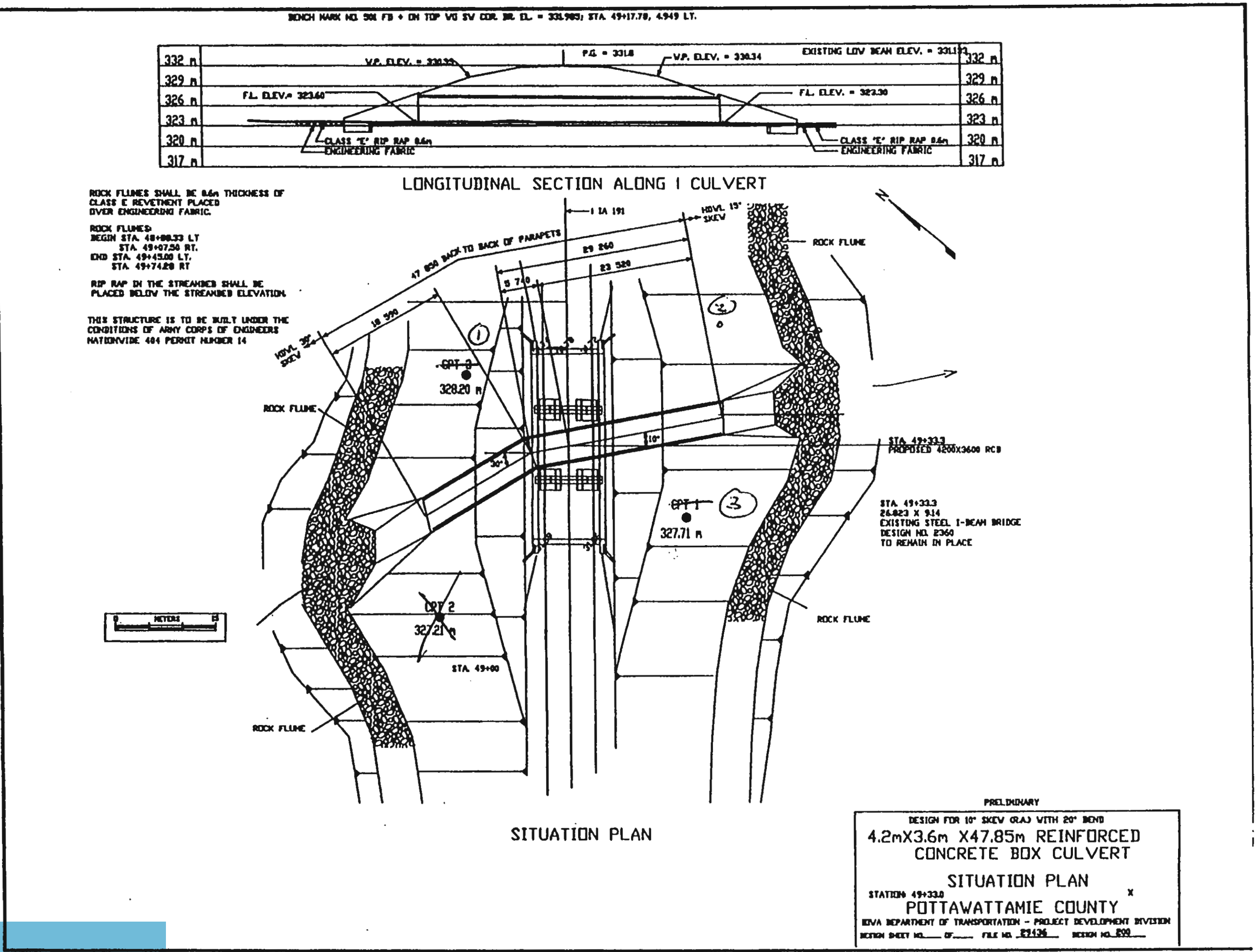

SOUNDING INFORMATION

						Depth (m)	Unit Weight (kN/m³)	Depth (m)	Unit Weight (m)	Water table depth used for σ'vo calculation	
PROJECT	DOT Highway 191 Box Culve	PROJECT LOCATION	Neola, Iowa								
CPT DESIGNATION	CPTU-1	PROJECT NUMBER	006051								
ELEVATION	327.71	DATE	10/26/2000			0	18.2	*	*	2.3	meters
STATION	*	SUPERVISOR	J. Santos	Water table Datum	measured value	*	*	*	*		
OFFSET	*	PUSHED BY	GSI	Water Depth ATD	2.3	*	*	*	*		
CONE USED	701	DRILLING EQUIPMENT	Cone Truck	Delayed Water Level	not measured	*	*	*	*		
CONE SIZE	10 Ton	NET AREA RATIO	0.8	Time of Delay	No reading taken						

Sounding terminated at planned depth

006051 CPTU-1 IDOT Highway 191 Box Culvert

Neola, Iowa

DEPTH (m)	q_T (kPa)	f_s (kPa)	R_f (%)	f_s/σ'_{vo}	Q	μ (kPa)	σ_{vo} (kPa)	μ_o (kPa)	σ'_{vo} (kPa)	B_q	F (%)	I_c	ϕ (Degrees)	D_r (%)
0.15	647	22.5	3.92	10.30	274.3	-15.3	2.73	0.0	2.73	-0.02	3.49	2.08	35.1	40.1
0.40	2138	36.8	1.71	5.07	297.6	2.9	7.28	0.0	7.28	0.00	1.73	1.77	38.5	60.3
0.65	1467	24.5	1.68	2.13	126.5	2.5	11.83	0.0	11.83	0.00	1.69	2.00	35.5	42.6
0.90	762	11.7	1.53	0.72	46.3	0.7	16.38	0.0	16.38	0.00	1.57	2.30	31.6	19.2
1.15	754	31.5	4.23	1.50	35.3	-1.7	20.93	0.0	20.93	0.00	4.30	2.67	31.0	15.3
1.40	440	23.1	5.39	0.91	16.2	-36.0	25.48	0.0	25.48	-0.09	5.57	2.99	27.9	-2.9
1.65	522	20.3	3.87	0.68	16.5	-9.4	30.03	0.0	30.03	-0.02	4.13	2.91	28.4	-0.4
1.90	398	16.6	4.19	0.48	10.5	-3.2	34.58	0.0	34.58	-0.01	4.56	3.09	26.7	-10.2
2.15	370	20.0	5.45	0.51	8.5	-1.9	39.13	0.0	39.13	-0.01	6.05	3.24	26.1	-14.0
2.40	385	18.4	4.84	0.43	8.0	-3.3	43.68	1.0	42.70	-0.01	5.38	3.22	26.1	-14.1
2.65	387	17.9	4.65	0.40	7.6	1.1	48.23	3.4	44.80	-0.01	5.28	3.24	26.0	-14.7
2.90	397	16.4	4.22	0.35	7.3	1.9	52.78	5.9	46.90	-0.01	4.76	3.22	26.0	-14.6
3.15	423	18.0	4.27	0.37	7.5	4.0	57.33	8.3	49.00	-0.01	4.92	3.22	26.2	-13.4
3.40	321	14.7	4.67	0.29	5.0	3.6	61.88	10.8	51.10	-0.03	5.70	3.40	24.8	-22.0
3.65	328	9.7	3.00	0.18	4.9	5.4	66.43	13.2	53.20	-0.03	3.70	3.30	24.8	-21.9
3.90	290	9.5	3.30	0.17	4.0	6.8	70.98	15.7	55.30	-0.04	4.34	3.42	24.1	-26.0
4.15	372	12.2	3.25	0.21	5.2	10.9	75.53	18.1	57.40	-0.02	4.10	3.31	25.2	-19.4
4.40	260	11.1	4.28	0.19	3.0	13.1	80.08	20.6	59.50	-0.04	6.17	3.60	23.4	-30.1
4.65	248	8.1	3.30	0.13	2.6	22.2	84.63	23.0	61.60	-0.01	4.99	3.60	23.1	-32.1
4.90	338	9.5	2.85	0.15	3.9	24.7	89.18	25.5	63.70	0.00	3.81	3.39	24.5	-23.6
5.15	283	7.6	2.71	0.12	2.9	25.9	93.73	27.9	65.80	-0.01	4.00	3.52	23.6	-29.2
5.40	243	4.5	1.92	0.07	2.1	31.3	98.28	30.4	67.90	0.01	3.11	3.58	22.8	-34.0
5.65	239	3.4	1.44	0.05	2.0	42.7	102.83	32.8	70.00	0.07	2.46	3.56	22.6	-34.9
5.90	263	3.4	1.32	0.05	2.2	48.7	107.38	35.3	72.10	0.09	2.16	3.50	23.0	-32.6
6.15	241	5.3	2.20	0.07	1.7	51.9	111.93	37.7	74.20	0.11	4.08	3.71	22.5	-35.5
6.40	220	4.9	2.28	0.06	1.4	55.7	116.48	40.2	76.30	0.15	4.72	3.84	22.0	-38.5
6.65	288	6.9	2.41	0.09	2.1	58.3	121.03	42.6	78.40	0.09	4.12	3.64	23.2	-31.2
6.90	287	7.9	2.75	0.10	2.0	61.2	125.58	45.1	80.50	0.10	4.92	3.70	23.2	-31.7
7.15	212	3.8	1.82	0.05	1.0	65.0	130.13	47.5	82.60	0.21	4.67	3.95	21.7	-40.7
7.40	233	4.1	1.81	0.05	1.2	67.2	134.68	50.0	84.70	0.18	4.20	3.87	22.0	-38.4

DEPTH (m)	q_T (kPa)	f_s (kPa)	R_f (%)	f_s/σ'_{vo}	Q	μ (kPa)	σ_{vo} (kPa)	μ_o (kPa)	σ'_{vo} (kPa)	B_q	F (%)	I_c	ϕ (Degrees)	D_r (%)
7.65	223	3.6	1.64	0.04	1.0	72.8	139.23	52.4	86.80	0.24	4.33	3.95	21.8	-39.9
7.90	251	4.3	1.72	0.05	1.2	74.7	143.78	54.9	88.90	0.18	4.00	3.85	22.3	-36.9
8.15	268	5.6	2.10	0.06	1.3	77.8	148.33	57.3	91.00	0.17	4.63	3.84	22.5	-35.4
8.40	319	5.3	1.65	0.06	1.8	84.0	152.88	59.8	93.10	0.15	3.16	3.65	23.3	-30.7
8.65	270	6.2	2.33	0.07	1.2	117.5	157.43	62.2	95.20	0.49	5.55	3.93	22.5	-35.9
8.90	386	15.3	3.96	0.16	2.3	127.6	161.98	64.7	97.30	0.28	6.85	3.73	24.1	-25.9
9.15	493	20.2	4.13	0.20	3.3	108.4	166.53	67.1	99.40	0.13	6.19	3.57	25.2	-19.2
9.40	361	13.1	3.61	0.13	1.9	96.4	171.08	69.6	101.50	0.14	6.90	3.80	23.7	-28.4
9.65	431	13.4	3.07	0.13	2.5	127.3	175.63	72.0	103.60	0.22	5.24	3.64	24.5	-23.6
9.90	401	14.9	3.74	0.14	2.1	119.1	180.18	74.5	105.70	0.20	6.76	3.76	24.1	-26.0
10.15	479	12.7	2.66	0.12	2.7	119.0	184.73	76.9	107.80	0.14	4.33	3.56	24.9	-21.2
10.40	476	12.1	2.54	0.11	2.6	150.4	189.28	79.4	109.90	0.25	4.20	3.57	24.8	-21.6
10.65	422	9.8	2.28	0.09	2.0	156.9	193.83	81.8	112.00	0.33	4.28	3.66	24.2	-25.3
10.90	366	5.2	1.42	0.05	1.5	171.1	198.38	84.3	114.10	0.52	3.08	3.72	23.5	-29.7
11.15	322	5.4	1.68	0.05	1.0	182.7	202.93	86.7	116.20	0.81	4.51	3.93	22.8	-33.6
11.40	316	5.9	1.90	0.05	0.9	193.3	207.48	89.2	118.30	0.96	5.45	4.01	22.7	-34.4
11.65	372	6.9	1.93	0.06	1.3	217.2	212.03	91.6	120.40	0.79	4.31	3.83	23.4	-30.0
11.90	383	7.6	2.00	0.06	1.4	211.3	216.58	94.1	122.50	0.70	4.54	3.83	23.5	-29.4
12.15	417	10.1	2.48	0.08	1.6	216.0	221.13	96.5	124.60	0.61	5.14	3.80	23.9	-27.2
12.40	385	6.4	1.67	0.05	1.3	193.7	225.68	99.0	126.70	0.59	4.02	3.83	23.5	-29.7
12.65	348	6.1	1.76	0.05	0.9	193.7	230.23	101.4	128.80	0.78	5.20	4.01	23.0	-32.9
12.90	357	5.5	1.54	0.04	0.9	185.3	234.78	103.9	130.90	0.67	4.47	3.97	23.0	-32.4
13.15	379	6.8	1.80	0.05	1.0	199.7	239.33	106.3	133.00	0.67	4.87	3.94	23.3	-30.9
13.40	393	7.3	1.86	0.05	1.1	208.8	243.88	108.8	135.10	0.67	4.87	3.92	23.4	-30.1
13.65	437	8.3	1.89	0.06	1.4	234.7	248.43	111.2	137.20	0.66	4.43	3.82	23.9	-27.3
13.90	1670	86.1	4.96	0.62	10.2	111.3	252.98	113.7	139.30	0.00	6.07	3.17	30.3	11.0
14.15	2128	112.9	5.28	0.80	13.2	180.9	257.53	116.1	141.40	0.03	6.04	3.09	31.4	17.7
14.40	2360	89.2	3.88	0.62	14.6	172.9	262.08	118.6	143.50	0.03	4.25	2.95	31.8	20.4
14.65	3658	118.6	3.27	0.82	23.3	276.4	266.63	121.0	145.60	0.05	3.50	2.74	33.9	32.8
14.90	4775	139.2	2.95	0.94	30.5	444.9	271.18	123.5	147.70	0.07	3.09	2.62	35.1	40.2
15.15	5545	168.6	3.09	1.13	35.2	376.9	275.73	125.9	149.80	0.05	3.20	2.58	35.8	44.3
15.40	5874	228.7	3.93	1.50	36.8	290.1	280.28	128.4	151.90	0.03	4.09	2.64	36.1	45.8
15.65	5331	217.3	4.14	1.41	32.8	498.1	284.83	130.8	154.00	0.07	4.31	2.69	35.6	42.8
15.90	5633	195.1	3.50	1.25	34.2	678.5	289.38	133.3	156.10	0.10	3.65	2.63	35.8	44.2
16.15	5727	210.6	3.67	1.33	34.3	855.4	293.93	135.7	158.20	0.13	3.88	2.65	35.8	44.4
16.40	5216	205.7	3.96	1.28	30.7	763.8	298.48	138.2	160.30	0.13	4.18	2.71	35.4	41.6
16.65	5201	209.0	4.03	1.29	30.2	1031.8	303.03	140.6	162.40	0.18	4.27	2.72	35.3	41.3

006051

IDOT Highway 191 Box Culvert

CPTU-1

Neola, Iowa

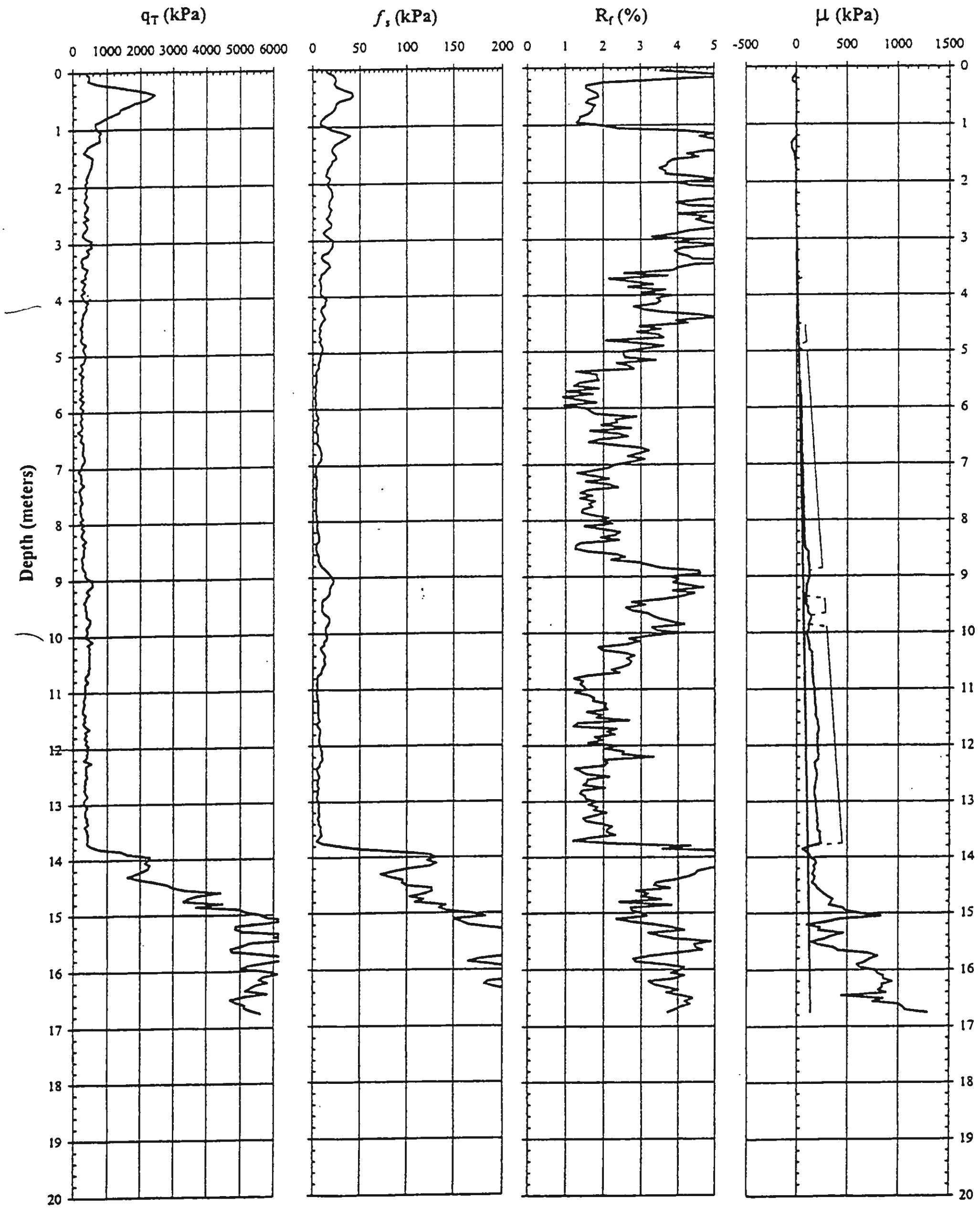

Sounding terminated at planned depth

ELEVATION 327.71'

11/16/2000 at 12:39 PM

006051

IDOT Highway 191 Box Culvert

CPTU-1

Neola, Iowa

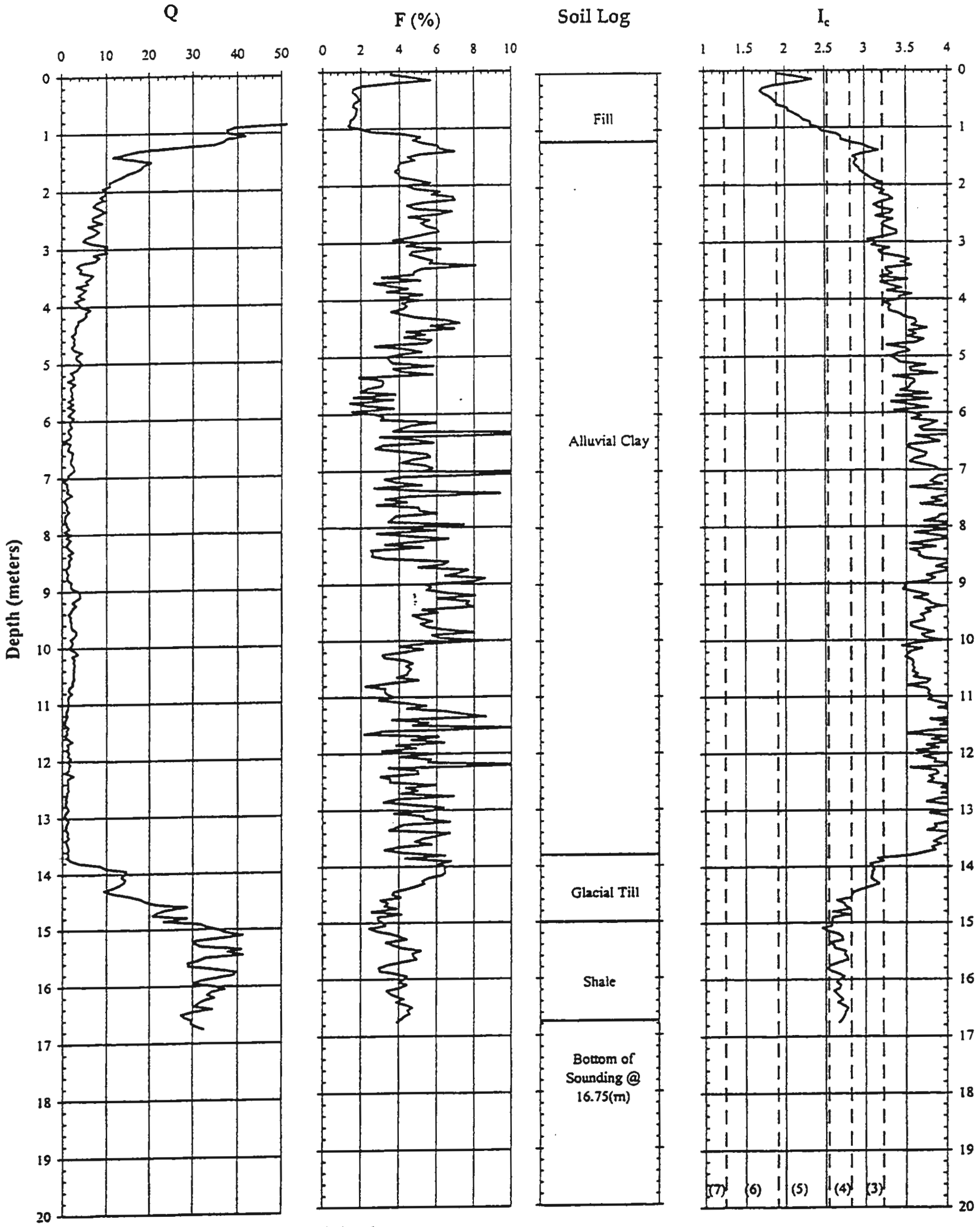

Sounding terminated at planned depth

ELEVATION 327.71'

11/16/2000 at 1:19 PM

SOUNDING INFORMATION

						Depth (m)	Unit Weight (kN/m³)	Depth (m)	Unit Weight (m)	Water table depth used for σ'_{vo} calculation	
PROJECT	DOT Highway 191 Box Culvei	PROJECT LOCATION	Neola, Iowa								
CPT DESIGNATION	CPTU-2	PROJECT NUMBER	006051								
ELEVATION	327.21	DATE	10/26/2000			0	18.2	•	•	2.1	meters
STATION	•	SUPERVISOR	J. Santos	Water table Datum	measured value	•	•	•	•		
OFFSET	•	PUSHED BY	GSI	Water Depth ATD	2.1	•	•	•	•		
CONE USED	701	DRILLING EQUIPMENT	Cone Truck	Delayed Water Level	not measured	•	•	•	•		
CONE SIZE	10 Ton	NET AREA RATIO	0.8	Time of Delay	No reading taken						

Sounding terminated at planned depth

006051 CPTU-2 IDOT Highway 191 Box Culvert

Neola, Iowa

DEPTH (m)	q_T (kPa)	f_s (kPa)	R_f (%)	f_s/σ'_{vo}	Q	μ (kPa)	σ_{vo} (kPa)	μ_o (kPa)	σ'_{vo} (kPa)	B_q	F (%)	I_c	ϕ (Degrees)	D_r (%)
0.15	755	29.4	4.14	12.75	300.6	-6.9	2.73	0.0	2.73	-0.01	3.91	2.08	35.9	44.6
0.40	885	38.7	4.39	5.39	122.2	-34.9	7.28	0.0	7.28	-0.04	4.41	2.32	34.3	35.0
0.65	1063	43.1	4.07	3.75	89.9	-30.3	11.83	0.0	11.83	-0.03	4.10	2.38	34.0	33.3
0.90	602	23.7	3.99	1.47	36.3	-18.1	16.38	0.0	16.38	-0.03	4.04	2.65	30.5	12.4
1.15	288	13.3	4.71	0.64	12.9	-17.4	20.93	0.0	20.93	-0.07	4.99	3.04	26.4	-12.3
1.40	180	9.9	5.58	0.39	6.1	-15.6	25.48	0.0	25.48	-0.10	6.39	3.37	23.7	-28.6
1.65	143	7.9	5.59	0.26	3.8	-8.7	30.03	0.0	30.03	-0.08	6.96	3.55	22.2	-37.5
1.90	164	6.9	4.22	0.20	3.7	-2.3	34.58	0.0	34.58	-0.02	5.32	3.49	22.5	-35.6
2.15	250	10.2	4.15	0.26	5.5	4.4	39.13	0.6	38.54	0.02	4.82	3.33	24.3	-25.1
2.40	193	8.1	4.44	0.20	3.7	14.2	43.68	2.9	40.74	0.08	5.44	3.50	22.9	-33.2
2.65	324	18.4	6.38	0.43	6.4	14.8	48.23	5.4	42.84	0.03	6.67	3.36	25.2	-19.2
2.90	413	22.9	5.70	0.51	8.0	-14.8	52.78	7.8	44.94	-0.06	6.36	3.27	26.3	-12.9
3.15	294	12.6	4.44	0.27	5.1	-1.0	57.33	10.3	47.04	-0.05	5.35	3.39	24.5	-23.3
3.40	174	6.0	3.55	0.12	2.3	4.6	61.88	12.7	49.14	-0.07	5.37	3.67	21.9	-38.9
3.65	200	6.7	3.54	0.13	2.6	16.1	66.43	15.2	51.24	0.01	5.04	3.61	22.5	-35.6
3.90	151	5.4	3.67	0.10	1.5	19.9	70.98	17.6	53.34	0.03	6.66	3.87	21.1	-44.1
4.15	165	5.0	3.07	0.09	1.6	25.9	75.53	20.1	55.44	0.07	5.56	3.81	21.4	-42.2
4.40	242	5.9	2.46	0.10	2.8	33.1	80.08	22.5	57.54	0.07	3.66	3.51	23.1	-31.7
4.65	347	16.4	4.63	0.27	4.4	43.4	84.63	25.0	59.64	0.07	6.25	3.47	24.8	-22.0
4.90	256	6.7	2.60	0.11	2.7	53.8	89.18	27.4	61.74	0.16	4.02	3.54	23.2	-31.2
5.15	221	5.6	2.53	0.09	2.0	57.6	93.73	29.9	63.84	0.22	4.36	3.67	22.5	-35.8
5.40	240	5.7	2.62	0.09	2.1	61.9	98.28	32.3	65.94	0.21	4.05	3.63	22.8	-33.9
5.65	232	4.6	2.07	0.07	1.9	65.5	102.83	34.8	68.04	0.24	3.55	3.65	22.5	-35.3
5.90	293	9.5	3.17	0.13	2.6	67.2	107.38	37.2	70.14	0.16	5.11	3.61	23.6	-29.1
6.15	432	16.0	3.70	0.22	4.4	72.0	111.93	39.7	72.24	0.10	5.00	3.41	25.4	-18.4
6.40	515	21.6	4.24	0.29	5.4	70.2	116.48	42.1	74.34	0.07	5.43	3.37	26.1	-13.8
6.65	402	16.4	4.12	0.21	3.7	68.4	121.03	44.6	76.44	0.08	5.82	3.52	24.9	-21.2
6.90	350	14.7	4.26	0.19	2.9	67.6	125.58	47.0	78.54	0.09	6.54	3.64	24.2	-25.7
7.15	305	8.7	2.86	0.11	2.2	69.0	130.13	49.5	80.64	0.11	4.99	3.67	23.4	-30.0
7.40	352	9.4	2.70	0.11	2.6	71.8	134.68	51.9	82.74	0.09	4.31	3.57	24.1	-26.2

11/15/20005:11 PM

DEPTH (m)	q_T (kPa)	f_s (kPa)	R_f (%)	f_s/σ'_{vo}	Q	μ (kPa)	σ_{vo} (kPa)	μ_o (kPa)	σ'_{vo} (kPa)	B_q	F (%)	I_c	ϕ (Degrees)	D_r (%)
7.65	240	5.4	2.33	0.06	1.2	73.5	139.23	54.4	84.84	0.19	5.34	3.91	22.2	-37.6
7.90	264	5.0	1.92	0.06	1.4	75.8	143.78	56.8	86.94	0.16	4.14	3.80	22.6	-35.2
8.15	313	11.9	3.91	0.13	1.8	104.1	148.33	59.3	89.04	0.27	7.22	3.82	23.3	-30.6
8.40	383	16.6	4.38	0.18	2.5	160.4	152.88	61.7	91.14	0.43	7.21	3.71	24.2	-25.2
8.65	413	14.2	3.41	0.15	2.7	143.1	157.43	64.2	93.24	0.31	5.55	3.61	24.5	-23.4
8.90	310	7.7	2.55	0.08	1.6	147.1	161.98	66.6	95.34	0.54	5.18	3.81	23.1	-31.9
9.15	358	11.9	3.33	0.12	2.0	156.2	166.53	69.1	97.44	0.46	6.21	3.76	23.8	-28.1
9.40	340	9.0	2.66	0.09	1.7	174.7	171.08	71.5	99.54	0.61	5.32	3.78	23.5	-29.8
9.65	506	16.2	3.20	0.16	3.3	199.1	175.63	74.0	101.64	0.38	4.90	3.52	25.3	-18.7
9.90	516	14.0	2.73	0.13	3.2	193.2	180.18	76.4	103.74	0.35	4.17	3.49	25.3	-18.5
10.15	401	9.4	2.40	0.09	2.0	194.7	184.73	78.9	105.84	0.54	4.34	3.67	24.1	-26.0
10.40	376	10.8	2.93	0.10	1.7	212.0	189.28	81.3	107.94	0.70	5.81	3.79	23.7	-28.2
10.65	383	8.7	2.28	0.08	1.7	226.6	193.83	83.8	110.04	0.75	4.60	3.74	23.8	-27.9
10.90	357	8.0	2.27	0.07	1.4	225.3	198.38	86.2	112.14	0.88	5.06	3.84	23.4	-30.1
11.15	460	9.8	2.19	0.09	2.2	219.5	202.93	88.7	114.24	0.51	3.81	3.60	24.6	-23.2
11.40	438	10.4	2.43	0.09	2.0	163.4	207.48	91.1	116.34	0.31	4.53	3.69	24.3	-24.8
11.65	456	8.0	1.81	0.07	2.1	134.3	212.03	93.6	118.44	0.17	3.30	3.60	24.4	-23.9
11.90	446	9.5	2.14	0.08	1.9	161.8	216.58	96.0	120.54	0.29	4.13	3.68	24.3	-24.8
12.15	416	8.2	2.02	0.07	1.6	175.3	221.13	98.5	122.64	0.39	4.22	3.75	23.9	-27.1
12.40	974	21.7	2.74	0.17	6.0	156.0	225.68	100.9	124.74	0.07	2.90	3.17	27.9	-2.9
12.65	648	23.5	3.61	0.18	3.3	206.0	230.23	103.4	126.84	0.25	5.61	3.55	26.0	-14.8
12.90	802	32.0	4.01	0.25	4.4	127.6	234.78	105.8	128.94	0.04	5.64	3.45	26.9	-9.0
13.15	1087	50.1	4.64	0.38	6.5	121.5	239.33	108.3	131.04	0.02	5.91	3.32	28.4	-0.5
13.40	2673	114.0	4.51	0.85	18.2	54.3	243.88	110.7	133.14	-0.02	4.69	2.91	32.6	25.1
13.65	2619	120.1	4.68	0.89	17.5	55.4	248.43	113.2	135.24	-0.02	5.07	2.94	32.5	24.3
13.90	2781	113.1	4.19	0.82	18.4	54.5	252.98	115.6	137.34	-0.02	4.47	2.89	32.7	25.8
14.15	4034	122.2	3.10	0.88	27.1	90.6	257.53	118.1	139.44	-0.01	3.24	2.67	34.5	36.2
14.40	3632	144.5	4.00	1.02	23.8	75.3	262.08	120.5	141.54	-0.01	4.29	2.80	33.9	33.0
14.65	3611	141.1	3.93	0.98	23.3	87.7	266.63	123.0	143.64	-0.01	4.22	2.80	33.9	32.6
14.90	5381	151.2	2.84	1.04	35.1	152.4	271.18	125.4	145.74	0.01	2.96	2.56	35.7	43.8
15.15	6271	253.3	4.10	1.71	40.5	281.5	275.73	127.9	147.84	0.03	4.22	2.62	36.4	48.0
15.40	5799	208.4	3.71	1.39	36.8	571.9	280.28	130.3	149.94	0.08	3.78	2.62	36.0	45.6

006051

IDOT Highway 191 Box Culvert

Neola, Iowa

CPTU-2

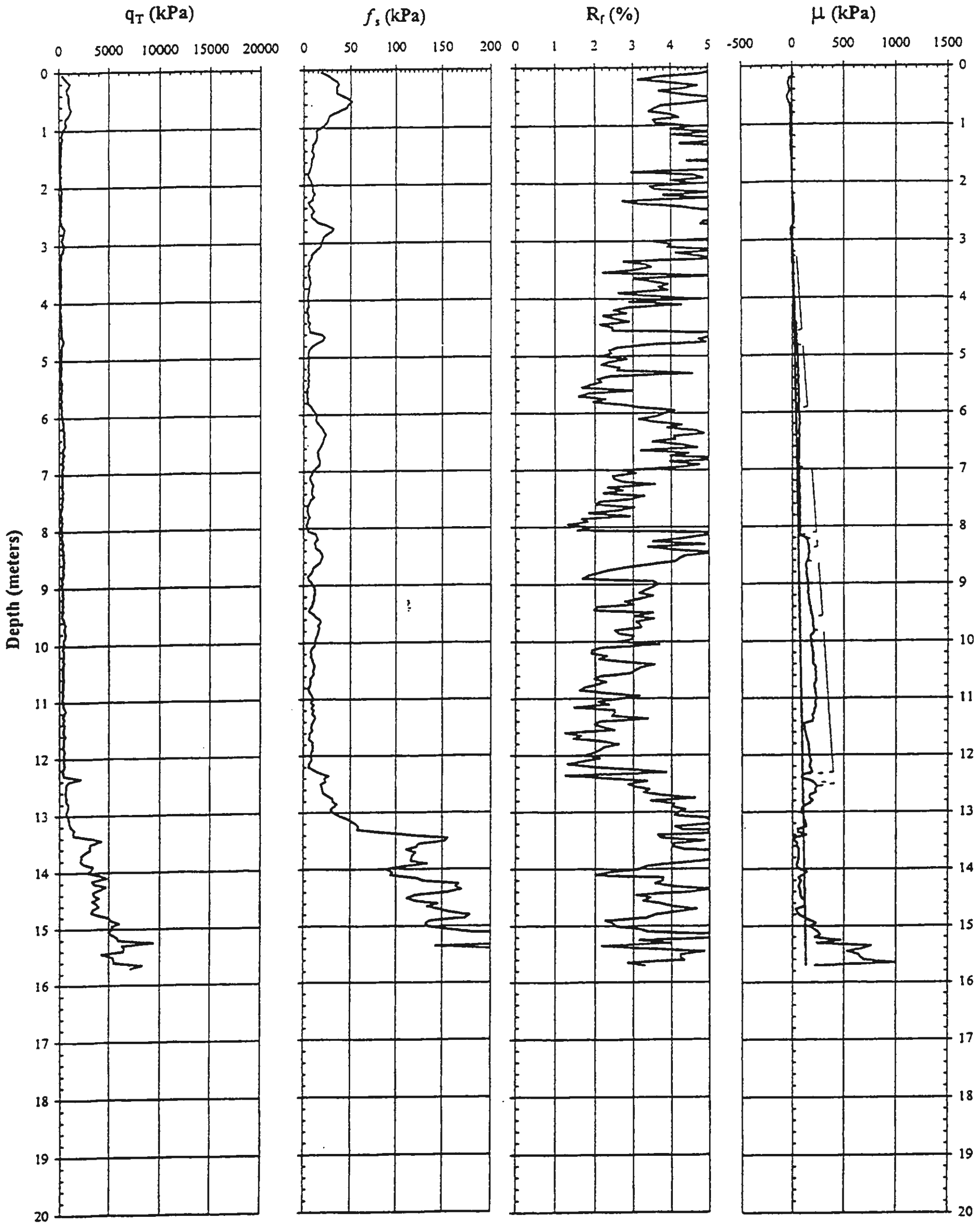

Sounding terminated at planned depth

ELEVATION 327.21'

11/16/2000 at 12:40 PM

006051

IDOT Highway 191 Box Culvert

Neola, Iowa

CPTU-2

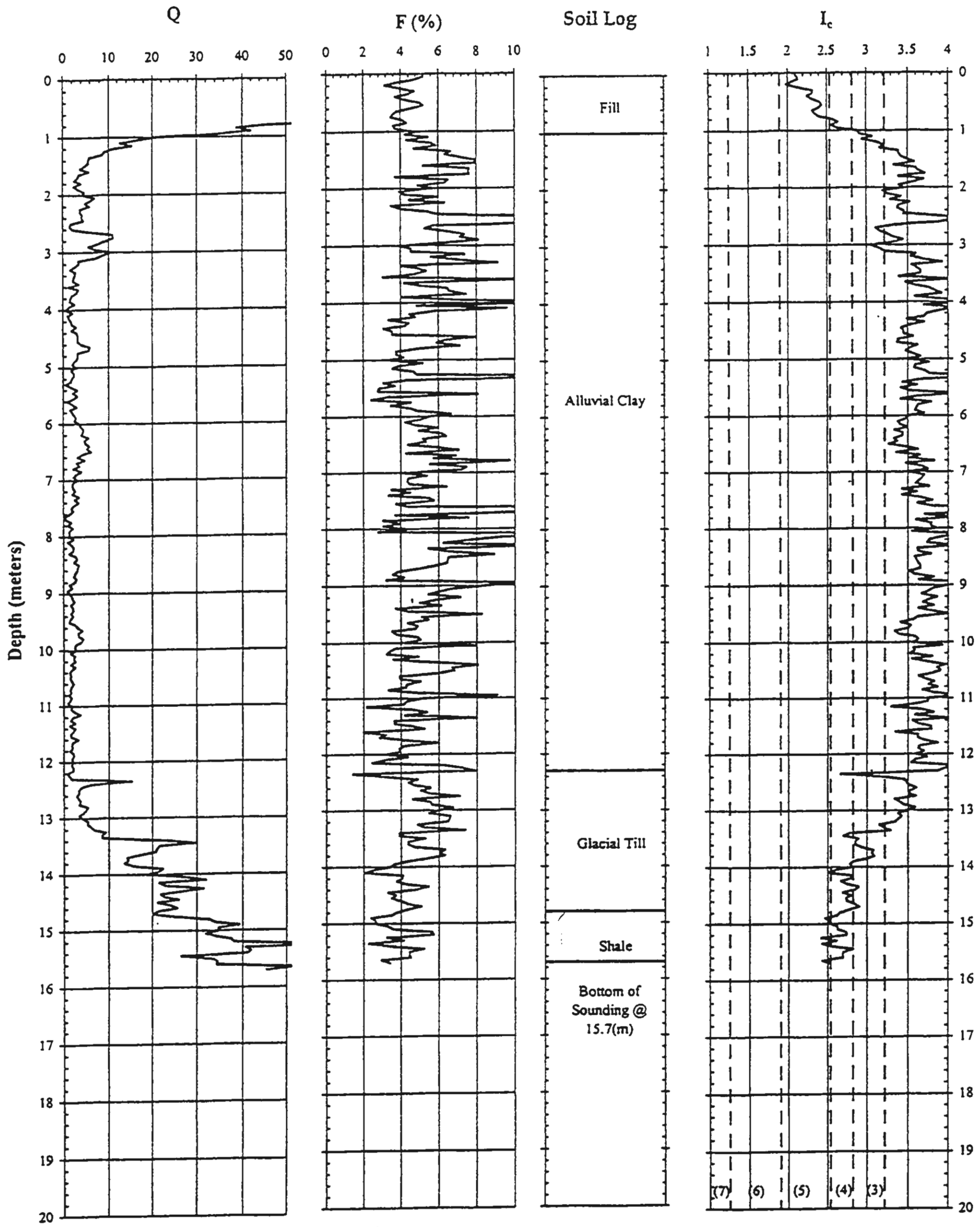

Sounding terminated at planned depth

ELEVATION 327.21'

11/16/2000 at 1:19 PM

006051

IDOT Highway 191 Box Culvert
Neola, Iowa

**CPTU-2
@
4.65 m**

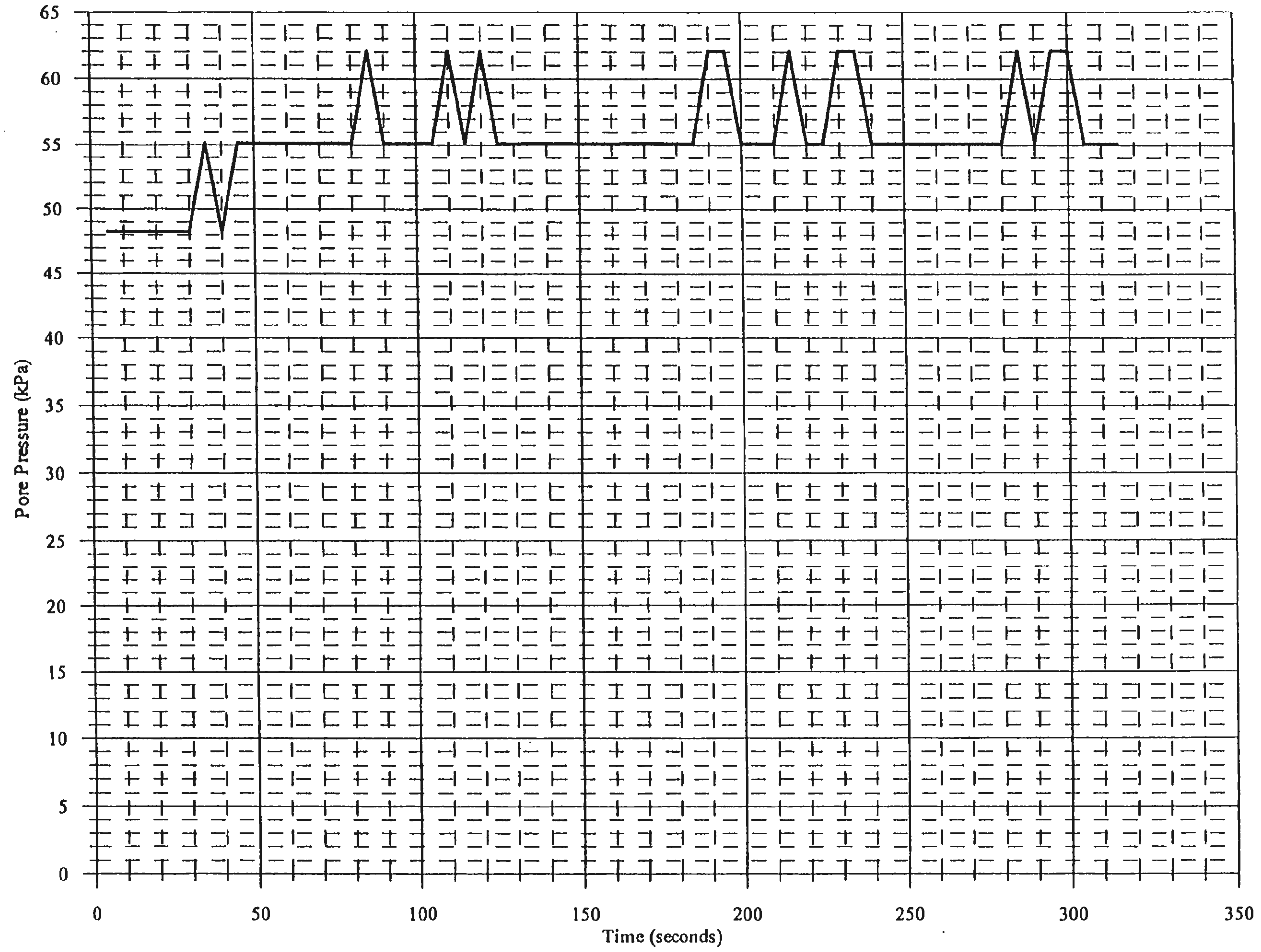

006051

IDOT Highway 191 Box Culvert
Neola, Iowa

CPTU-2
@
4.65 m

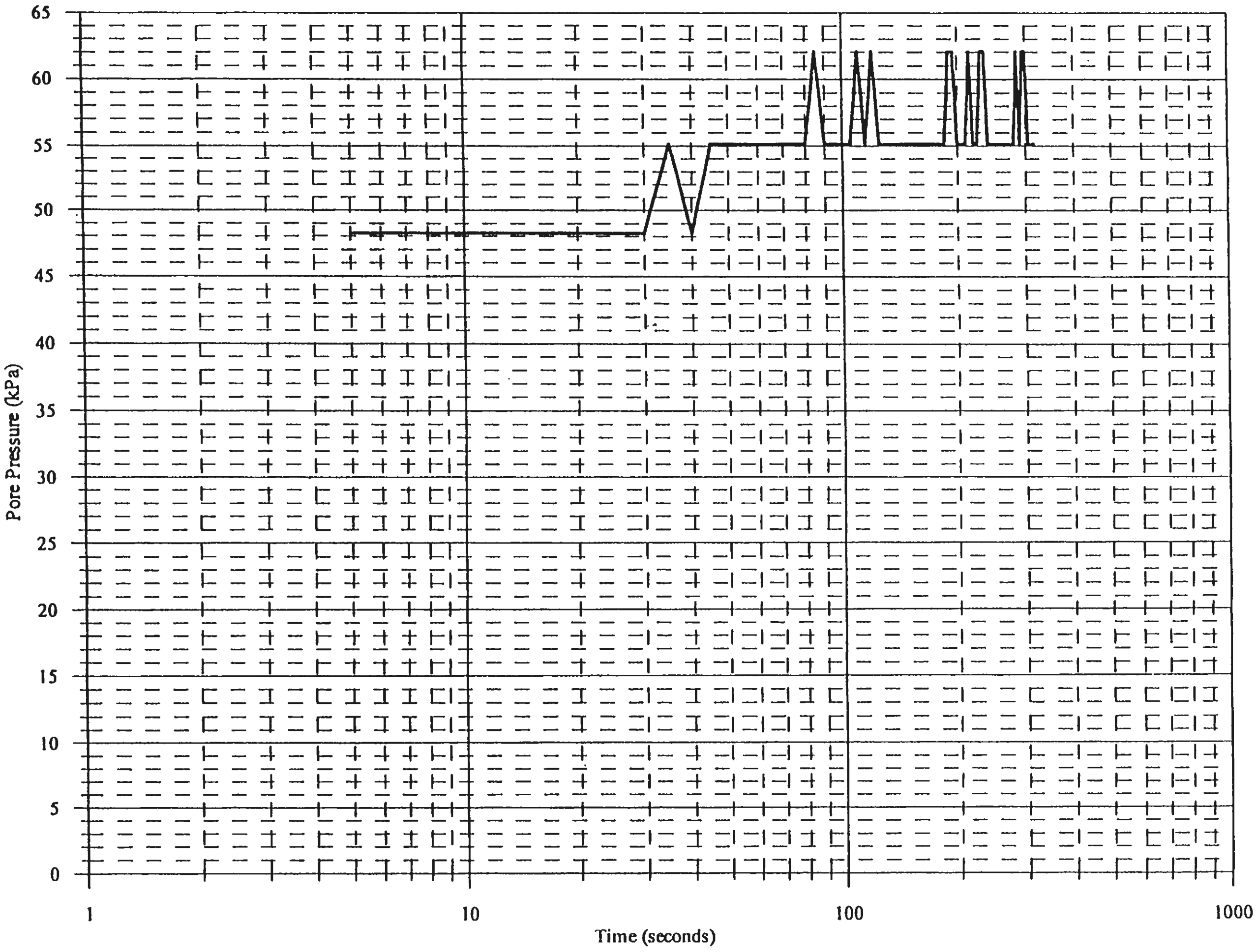

006051

CPTU-2
@
8.15 m

IDOT Highway 191 Box Culvert
Neola, Iowa

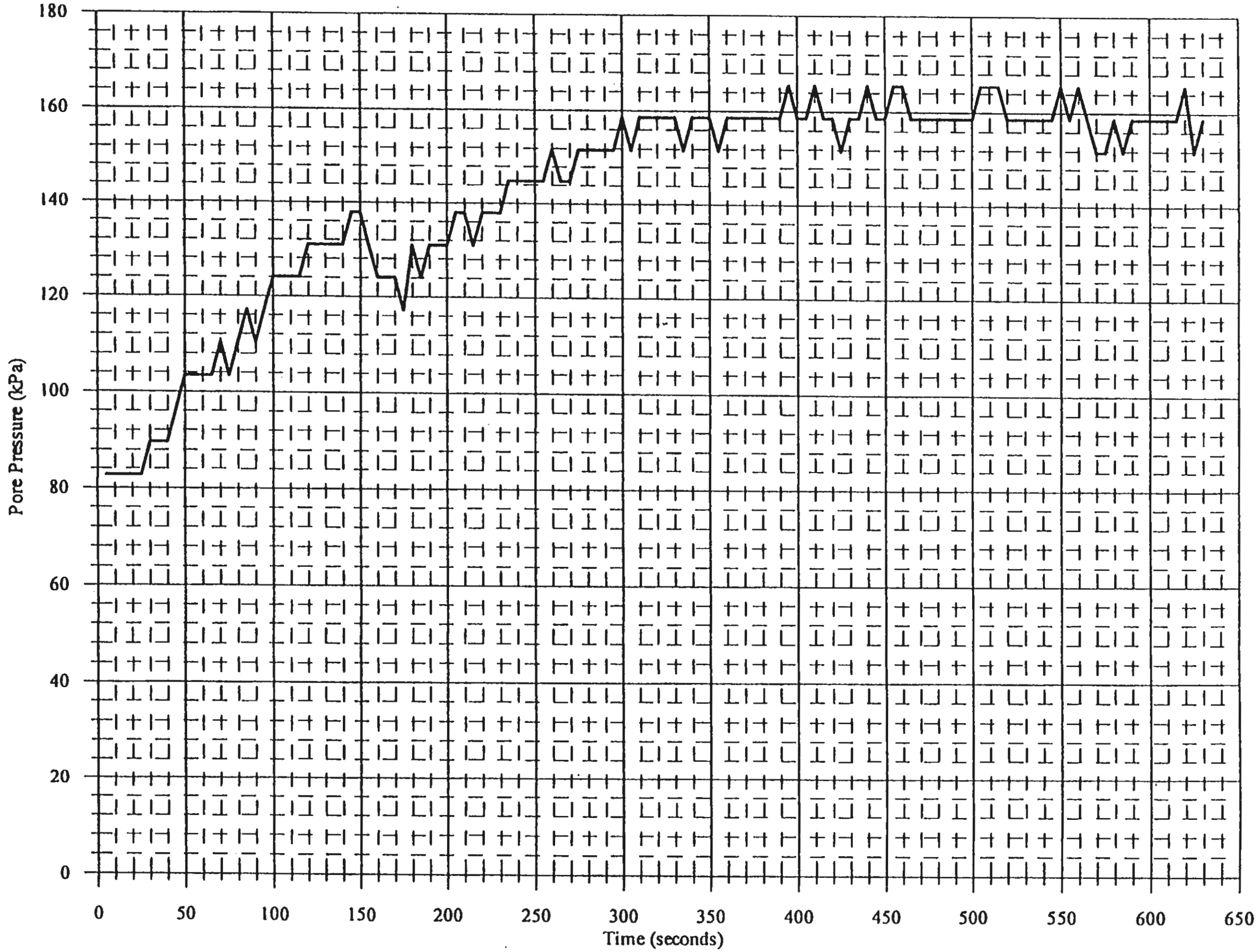

006051

CPTU-2
@
8.15 m

IDOT Highway 191 Box Culvert
Neola, Iowa

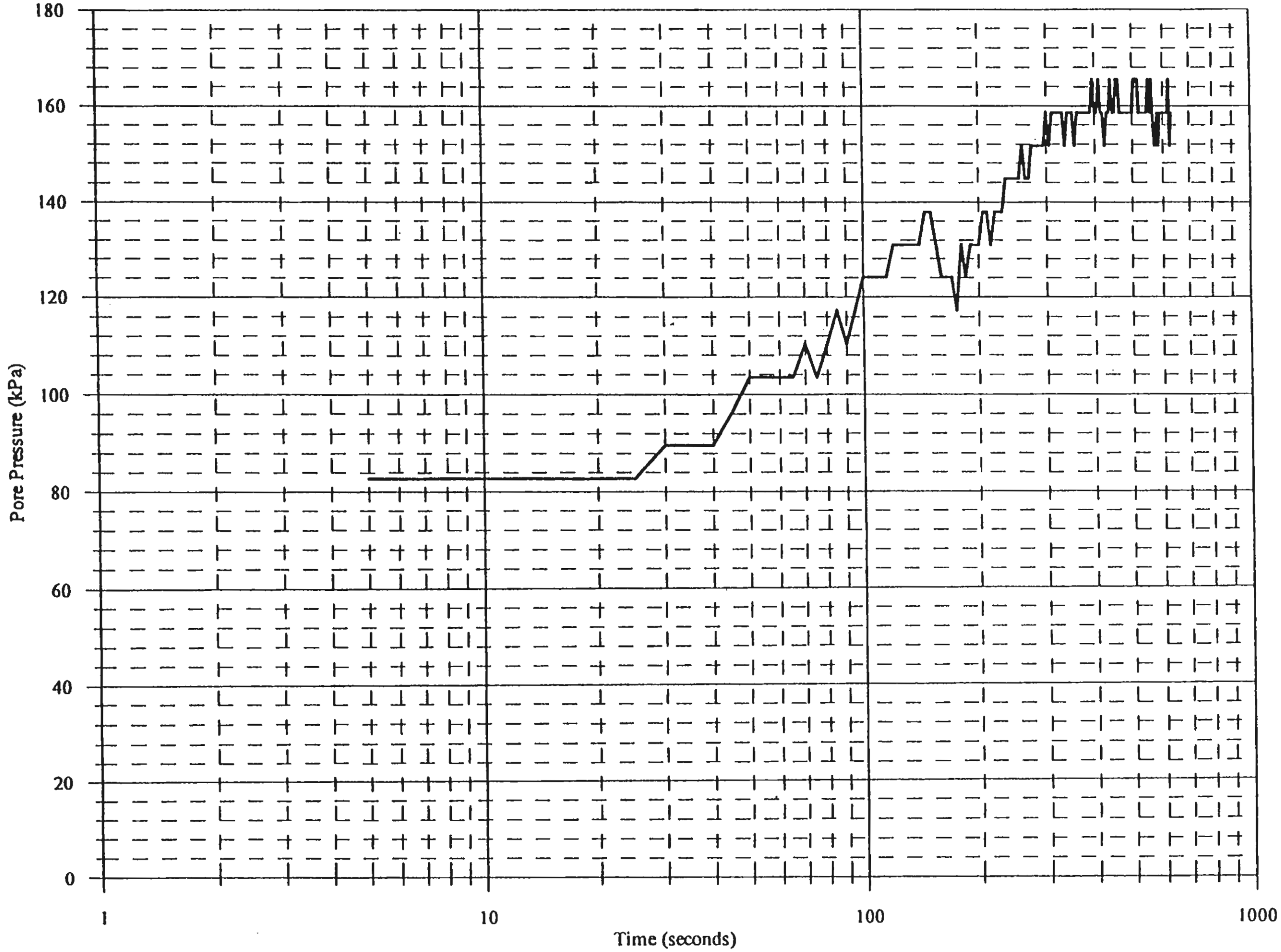

CPTU-2
@
11.4 m

IDOT Highway 191 Box Culvert
Neola, Iowa

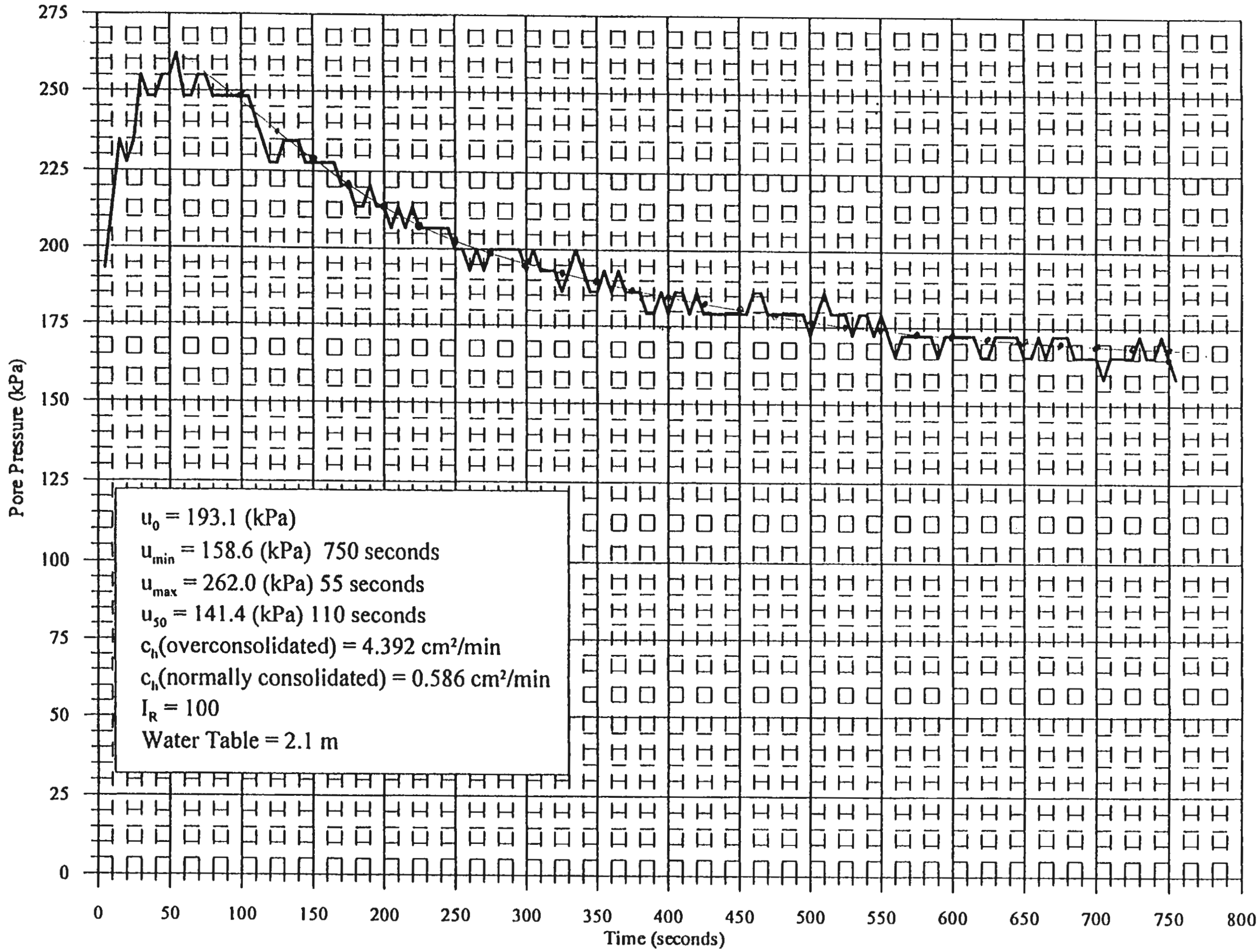

CPTU-2
@
11.4 m

IDOT Highway 191 Box Culvert
Neola, Iowa

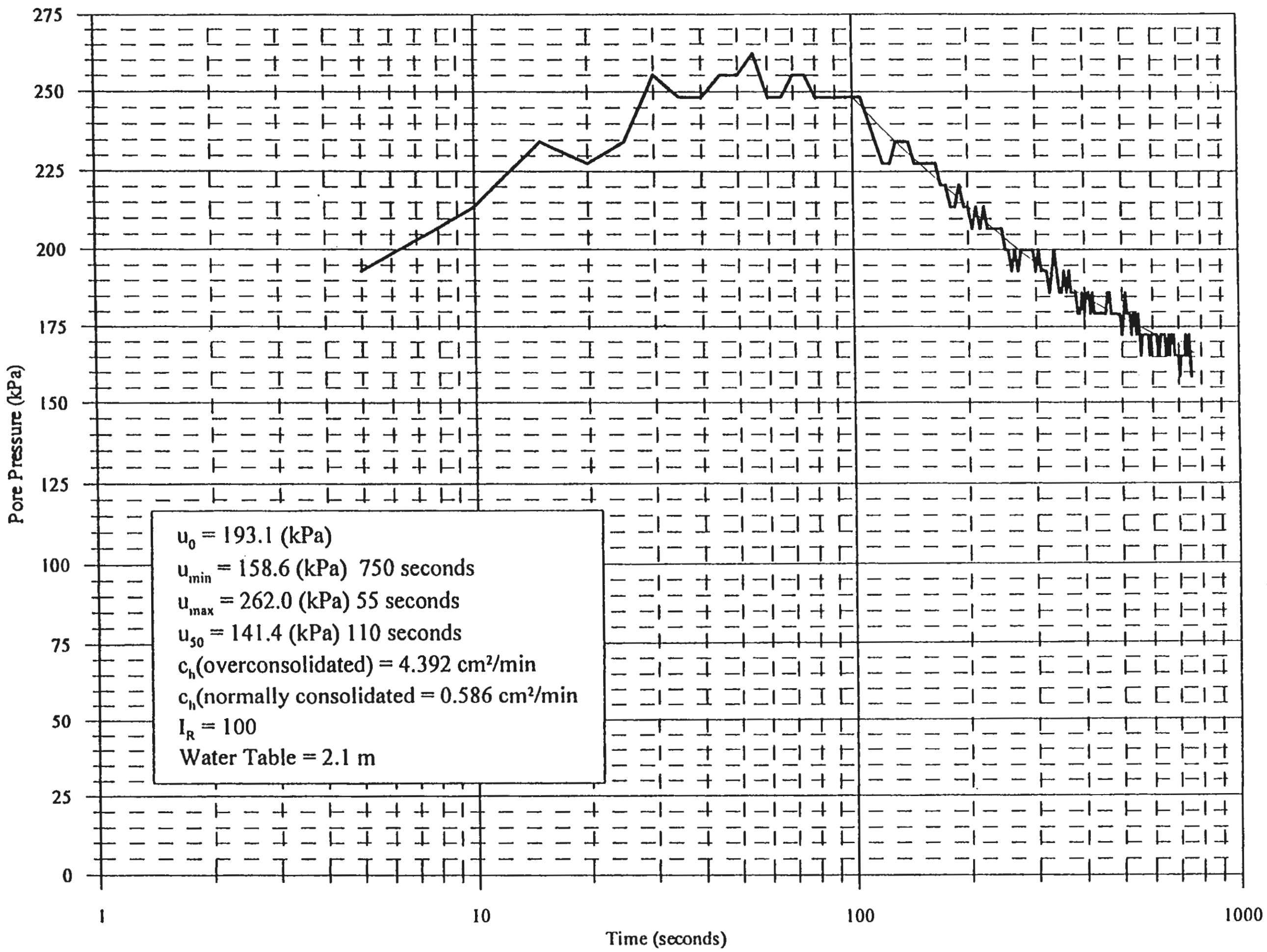

SOUNDING INFORMATION

							Depth (m)	Unit Weight (kN/m³)	Depth (m)	Unit Weight (m)	Water table depth used for σ'vo calculation	
PROJECT	)T Highway 191 Box Cul	PROJECT LOCATION	Neola, Iowa									
CPT DESIGNATION	CPTU-3	PROJECT NUMBER	006051									
ELEVATION	328.2	DATE	10/26/2000				0	18.2	•	•	3.2	meters
STATION	•	SUPERVISOR	J. Santos	Water table Datum	measured value		•	•	•	•		
OFFSET	•	PUSHED BY	GSI	Water Depth ATD	3.2		•	•	•	•		
CONE USED	701	DRILLING EQUIPMENT	Cone Truck	Delayed Water Level	not measured		•	•	•	•		
CONE SIZE	10 Ton	NET AREA RATIO	0.8	Time of Delay	No reading taken							

Sounding terminated at planned depth

006051 CPTU-3 IDOT Highway 191 Box Culvert

Neola, Iowa

DEPTH (m)	q_T (kPa)	f_s (kPa)	R_f (%)	f_s/σ'_{vo}	Q	μ (kPa)	σ_{vo} (kPa)	μ_o (kPa)	σ'_{vo} (kPa)	B_q	F (%)	I_c	ϕ (Degrees)	D_r (%)
0.15	549	20.5	3.87	9.85	301.6	-5.7	2.73	0.0	2.73	-0.01	3.75	2.14	34.3	35.4
0.40	1847	39.5	2.42	5.54	246.0	3.6	7.28	0.0	7.28	0.00	2.14	1.88	37.8	56.1
0.65	1101	21.6	2.01	1.92	96.2	9.7	11.83	0.0	11.83	0.01	1.99	2.14	34.2	34.4
0.90	1202	21.8	1.81	1.34	73.1	9.1	16.38	0.0	16.38	0.01	1.84	2.19	33.8	32.2
1.15	810	9.5	1.17	0.46	38.0	2.2	20.93	0.0	20.93	0.00	1.20	2.30	31.3	17.4
1.40	468	20.5	4.82	0.80	17.6	4.7	25.48	0.0	25.48	0.01	4.63	2.92	28.2	-1.2
1.65	434	21.8	5.04	0.73	13.5	-1.1	30.03	0.0	30.03	0.00	5.41	3.05	27.5	-5.7
1.90	362	21.5	5.98	0.62	9.5	-0.6	34.58	0.0	34.58	0.00	6.58	3.22	26.3	-12.9
2.15	212	12.2	5.83	0.31	4.4	-2.1	39.13	0.0	39.13	-0.01	7.03	3.50	23.4	-30.0
2.40	267	13.9	5.30	0.32	5.2	11.0	43.68	0.0	43.68	0.05	6.20	3.42	24.3	-24.9
2.65	253	11.7	4.65	0.24	4.3	16.0	48.23	0.0	48.23	0.08	5.70	3.46	23.8	-27.9
2.90	258	10.6	4.19	0.20	3.9	17.0	52.78	0.0	52.78	0.08	5.18	3.47	23.7	-28.7
3.15	135	6.0	4.99	0.11	1.4	21.5	57.33	0.1	57.23	0.27	7.72	3.94	20.4	-48.3
3.40	131	5.5	4.30	0.09	1.2	28.4	61.88	2.0	59.92	0.38	7.88	4.01	20.1	-49.9
3.65	117	5.2	4.39	0.08	0.8	31.4	66.43	4.4	62.02	0.53	10.15	4.20	19.5	-53.6
3.90	137	6.0	4.40	0.09	1.0	34.8	70.98	6.9	64.12	0.42	9.11	4.09	20.2	-49.6
4.15	105	4.8	4.59	0.07	0.4	36.5	75.53	9.3	66.22	0.92	16.26	4.53	18.8	-57.7
4.40	158	4.1	2.61	0.06	1.1	53.0	80.08	11.8	68.32	0.53	5.28	3.93	20.7	-46.4
4.65	200	5.1	2.54	0.07	1.6	62.2	84.63	14.2	70.42	0.42	4.39	3.75	21.8	-40.1
4.90	214	5.1	2.38	0.07	1.7	69.0	89.18	16.7	72.52	0.42	4.07	3.72	22.0	-38.6
5.15	184	4.0	2.20	0.05	1.2	75.7	93.73	19.1	74.62	0.63	4.47	3.87	21.2	-43.4
5.40	205	4.9	2.40	0.06	1.4	93.2	98.28	21.6	76.72	0.67	4.56	3.82	21.7	-40.6
5.65	209	4.1	2.15	0.05	1.3	105.5	102.83	24.0	78.82	0.77	3.89	3.80	21.7	-40.5
5.90	206	4.3	2.09	0.05	1.2	112.5	107.38	26.5	80.92	0.87	4.35	3.86	21.6	-41.2
6.15	220	6.3	2.85	0.08	1.3	120.5	111.93	28.9	83.02	0.84	5.83	3.90	21.8	-39.7
6.40	265	8.0	3.13	0.09	1.7	94.2	116.48	31.4	85.12	0.42	5.42	3.77	22.6	-34.8
6.65	231	3.4	1.46	0.04	1.3	94.0	121.03	33.8	87.22	0.55	3.04	3.77	21.9	-39.0
6.90	302	7.5	2.45	0.08	2.0	103.0	125.58	36.3	89.32	0.38	4.23	3.67	23.2	-31.7
7.15	330	11.7	3.58	0.13	2.2	111.4	130.13	38.7	91.42	0.36	5.85	3.71	23.5	-29.5

11/16/2000 12:42 PM

DEPTH (m)	q_T (kPa)	f_s (kPa)	R_f (%)	f_s/σ'_{vo}	Q	μ (kPa)	σ_{vo} (kPa)	μ_o (kPa)	σ'_{vo} (kPa)	B_q	F (%)	I_c	ϕ (Degrees)	D_r (%)
7.40	347	11.2	3.25	0.12	2.3	128.5	134.68	41.2	93.52	0.41	5.27	3.67	23.7	-28.3
7.65	310	11.3	3.65	0.12	1.8	138.6	139.23	43.6	95.62	0.56	6.61	3.81	23.1	-31.9
7.90	377	16.5	4.39	0.17	2.4	151.1	143.78	46.1	97.72	0.45	7.07	3.72	24.0	-26.6
8.15	483	19.9	4.16	0.20	3.3	163.8	148.33	48.5	99.82	0.34	5.95	3.56	25.1	-19.8
8.40	466	19.2	4.12	0.19	3.1	170.2	152.88	51.0	101.92	0.38	6.12	3.59	24.9	-21.2
8.65	433	18.7	4.31	0.18	2.6	180.4	157.43	53.4	104.02	0.46	6.79	3.67	24.5	-23.6
8.90	445	18.1	4.04	0.17	2.7	185.8	161.98	55.9	106.12	0.46	6.39	3.66	24.6	-23.1
9.15	726	30.7	4.26	0.28	5.2	201.3	166.53	58.3	108.22	0.26	5.50	3.38	26.9	-9.3
9.40	777	36.9	4.76	0.33	5.5	183.7	171.08	60.8	110.32	0.20	6.08	3.39	27.2	-7.6
9.65	435	14.8	3.34	0.13	2.3	163.1	175.63	63.2	112.42	0.39	5.73	3.68	24.3	-24.5
9.90	397	7.5	1.88	0.07	1.9	166.0	180.18	65.7	114.52	0.46	3.44	3.64	23.9	-27.4
10.15	447	16.7	3.71	0.14	2.2	178.9	184.73	68.1	116.62	0.42	6.36	3.72	24.4	-24.3
10.40	398	13.3	3.34	0.11	1.8	194.7	189.28	70.6	118.72	0.59	6.38	3.81	23.8	-27.9
10.65	424	14.7	3.46	0.12	1.9	206.3	193.83	73.0	120.82	0.58	6.36	3.78	24.1	-26.3
10.90	483	17.4	3.60	0.14	2.3	205.6	198.38	75.5	122.92	0.46	6.13	3.70	24.6	-22.8
11.15	383	10.6	2.77	0.09	1.4	200.1	202.93	77.9	125.02	0.68	5.91	3.86	23.5	-29.7
11.40	343	8.8	2.56	0.07	1.1	209.7	207.48	80.4	127.12	0.96	6.52	4.00	22.9	-33.1
11.65	307	5.2	1.67	0.04	0.7	220.4	212.03	82.8	129.22	1.44	5.42	4.10	22.4	-36.5
11.90	361	6.9	1.92	0.05	1.1	231.7	216.58	85.3	131.32	1.01	4.76	3.92	23.1	-32.1
12.15	393	6.5	1.67	0.05	1.3	241.0	221.13	87.7	133.42	0.89	3.79	3.81	23.4	-29.9
12.40	371	5.2	1.39	0.04	1.1	262.4	225.68	90.2	135.52	1.18	3.55	3.87	23.1	-31.7
12.65	409	5.8	1.44	0.04	1.3	267.5	230.23	92.6	137.62	0.98	3.27	3.78	23.6	-29.2
12.90	492	6.2	1.35	0.04	1.8	264.5	234.78	95.1	139.72	0.66	2.42	3.58	24.4	-24.1
13.15	405	7.3	1.82	0.05	1.2	270.3	239.33	97.5	141.82	1.05	4.41	3.88	23.4	-29.9
13.40	437	7.9	1.81	0.05	1.3	253.9	243.88	100.0	143.92	0.80	4.07	3.81	23.8	-28.0
13.65	521	8.2	1.59	0.06	1.9	262.6	248.43	102.4	146.02	0.59	3.02	3.62	24.6	-23.1
13.90	623	9.0	1.51	0.06	2.5	181.9	252.98	104.9	148.12	0.21	2.43	3.47	25.4	-18.2
14.15	610	11.6	2.04	0.08	2.3	173.9	257.53	107.3	150.22	0.19	3.28	3.55	25.3	-19.0
14.40	1158	12.7	1.09	0.08	5.9	74.1	262.08	109.8	152.32	-0.04	1.42	3.03	28.3	-0.8

006051

IDOT Highway 191 Box Culvert

Neola, Iowa

CPTU-3

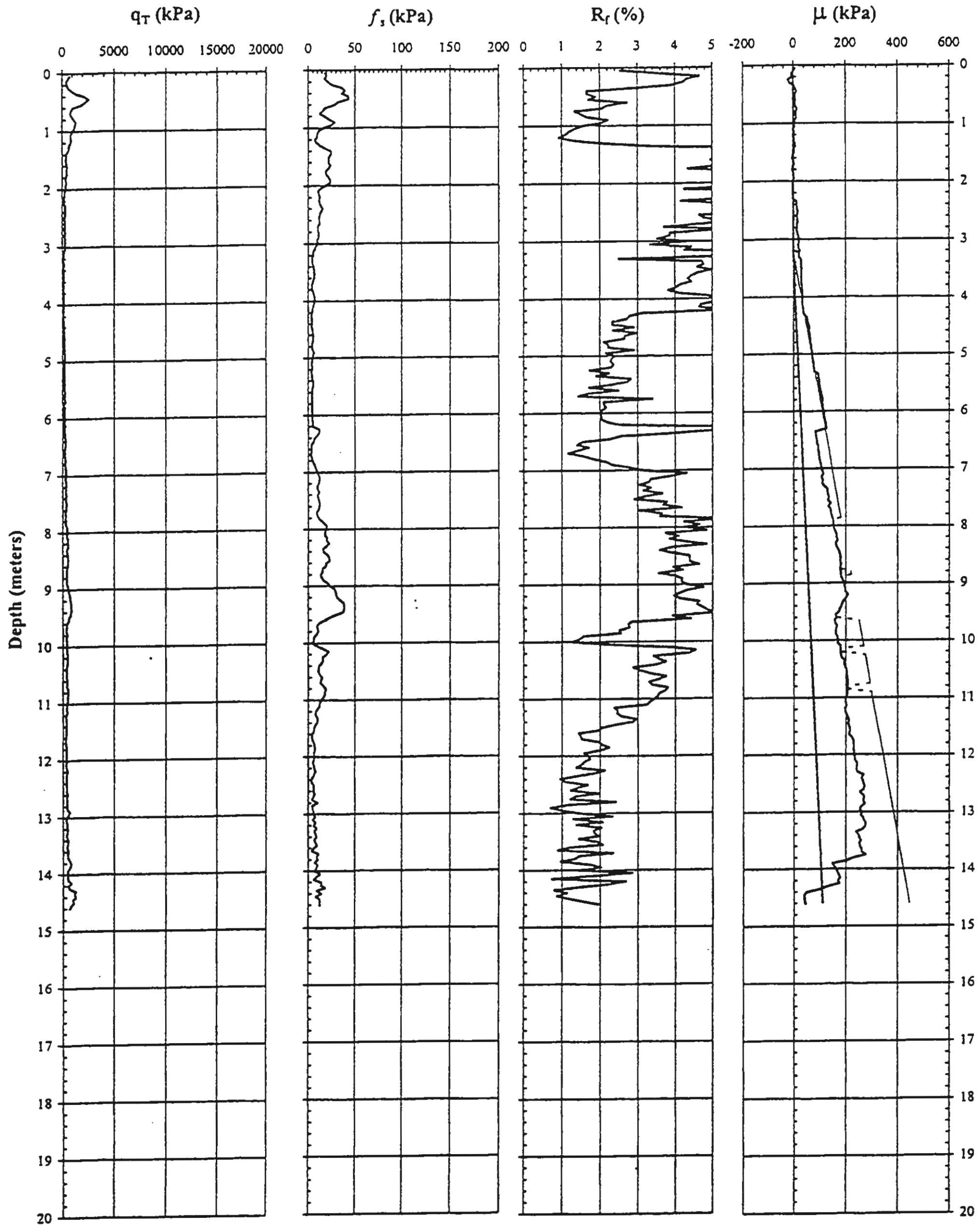

Sounding terminated at planned depth

ELEVATION 328.2'

11/16/2000 at 12:42 PM

006051

IDOT Highway 191 Box Culvert

Neola, Iowa

CPTU-3

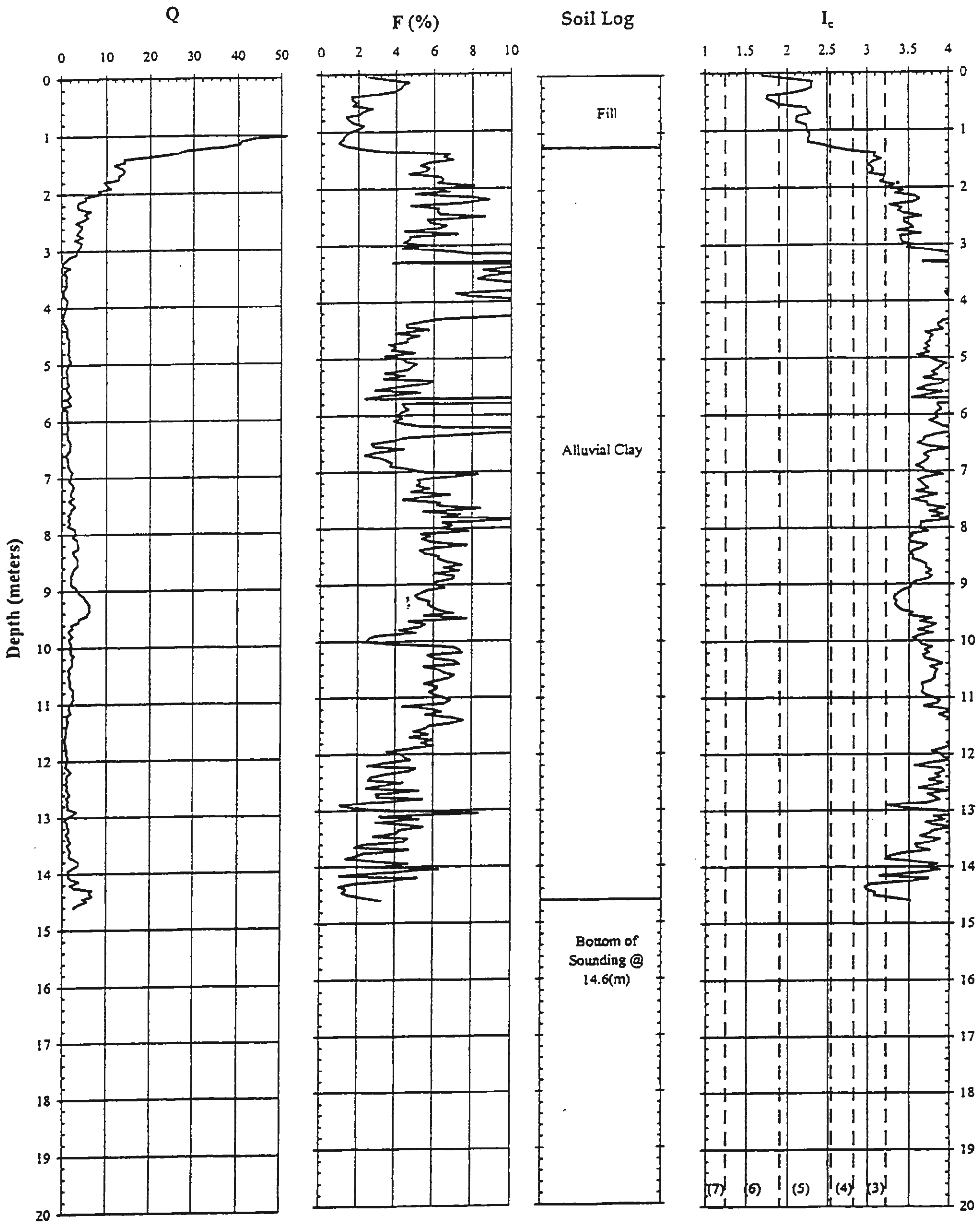

Sounding terminated at planned depth

ELEVATION 328.2'

11/16/2000 at 1:20 PM

CPTU-3
@
6.3 m

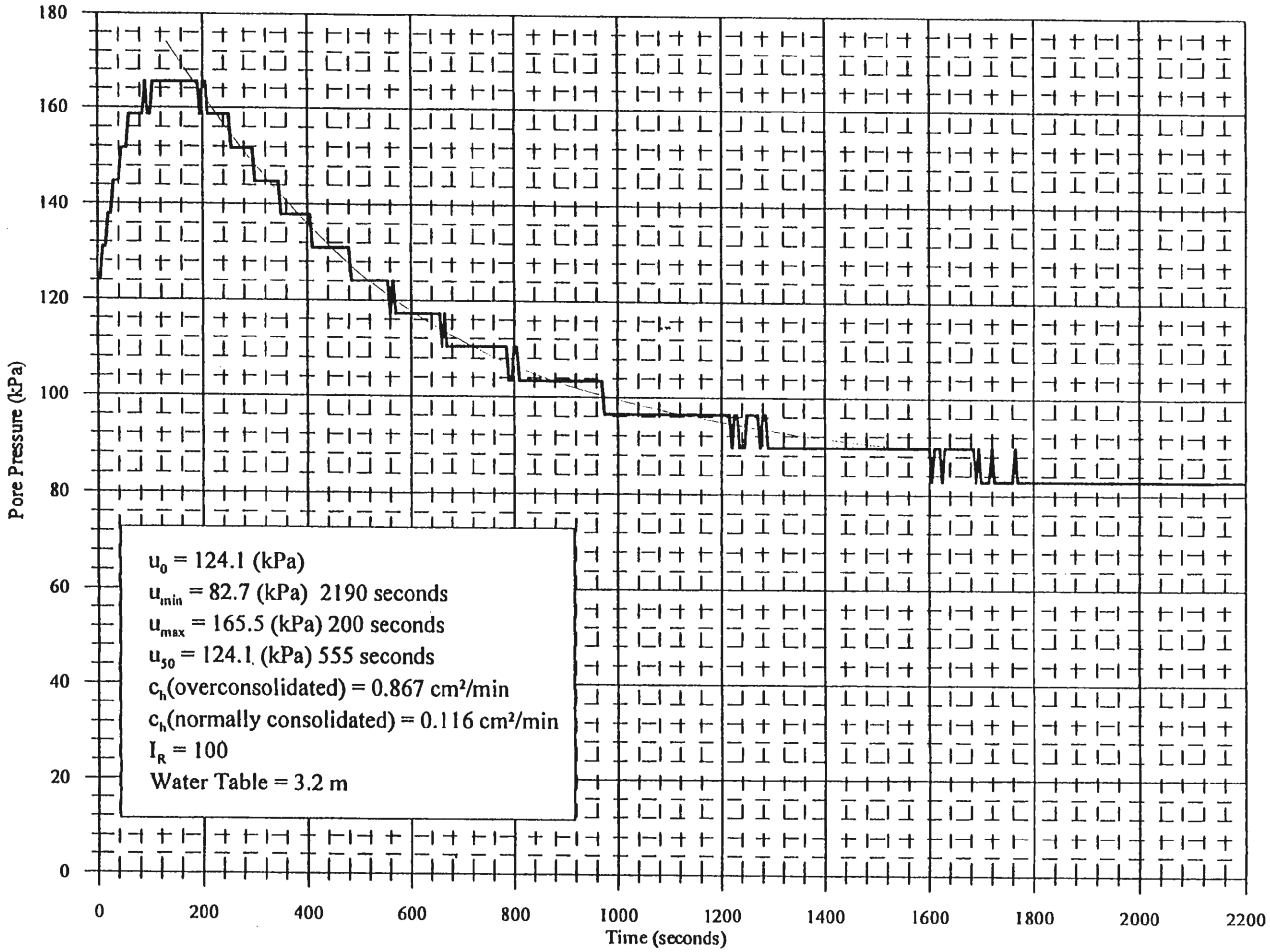
Pore Pressure (kPa)
0
20
40
60
80
100
120
140
160
180
0
200
400
600
800
1000
1200
1400
1600
1800
2000
2200
Time (seconds)
u0 = 124.1 (kPa)
umin = 82.7 (kPa) 2190 seconds
umax = 165.5 (kPa) 200 seconds
u50 = 124.1 (kPa) 555 seconds
ch(overconsolidated) = 0.867 cm²/min
ch(normally consolidated) = 0.116 cm²/min
IR = 100
Water Table = 3.2 m

006051

CPTU-3 @ 6.3 m

IDOT Highway 191 Box Culvert
Neola, Iowa

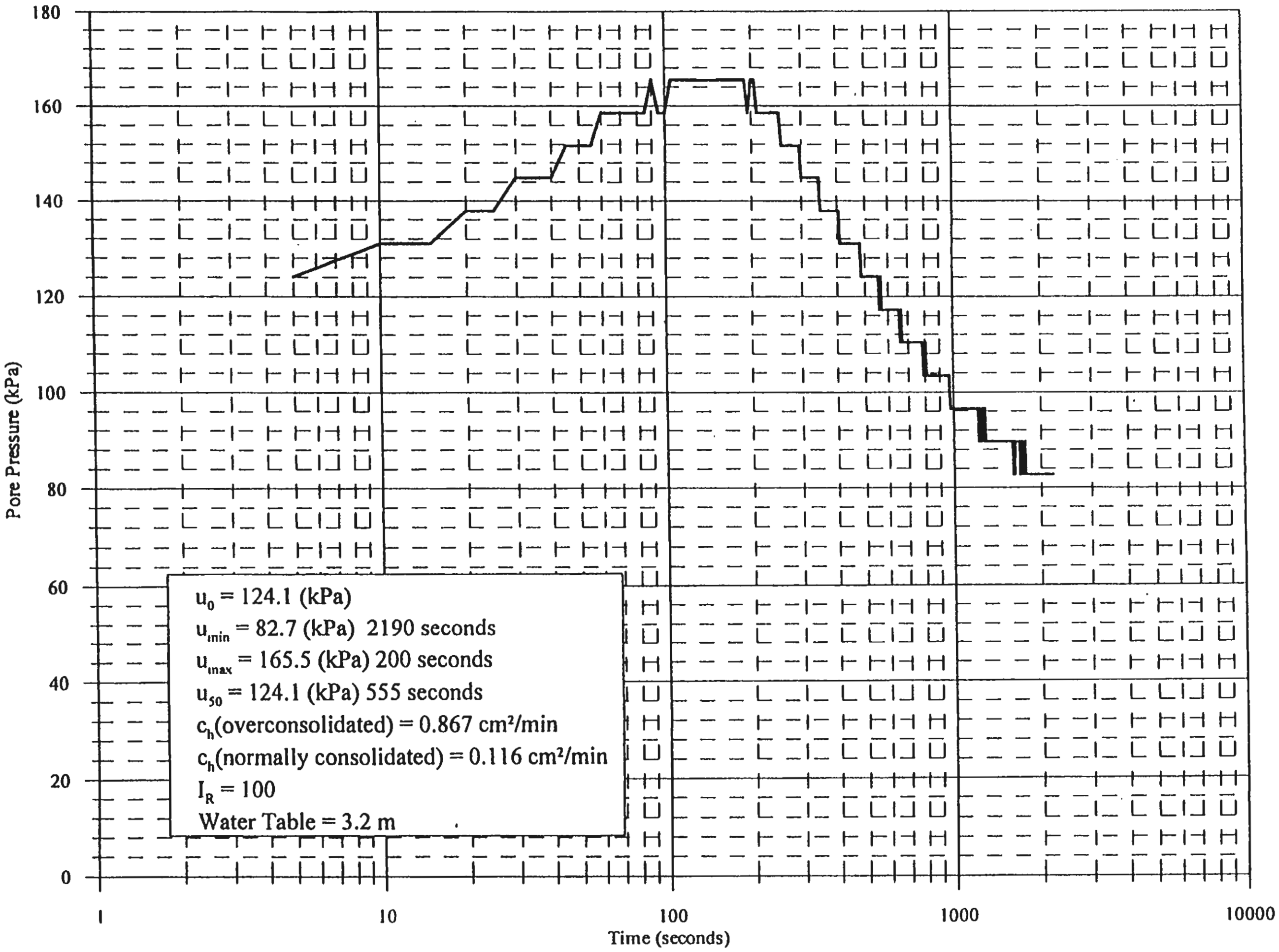

APPENDIX B

DILATOMETER SOUNDING DATA

Table B1. DMT1 data readings

m	ft	bar	var	bar	bar		bar	bar
Depth	Depth	A	B	po	p1	delta p	Vert Eff. Stress	uo
0.30	1	2.45	7.6	1.40	5.97	4.57	0.05	0.00
0.61	2	1	3.6	0.08	1.97	1.89	0.10	0.00
0.91	3	1	2.5	0.14	0.87	0.74	0.15	0.00
1.22	4	1	2.5	0.14	0.87	0.74	0.20	0.00
1.52	5	1.25	3.1	0.37	1.47	1.10	0.25	0.00
1.83	6	0.8	2	-0.05	0.37	0.42	0.30	0.00
2.13	7	1	2.6	0.13	0.97	0.84	0.32	0.03
2.44	8	1.6	3.8	0.70	2.17	1.47	0.34	0.06
2.74	9	2.5	5.2	1.58	3.57	2.00	0.36	0.09
3.05	10	1.6	3.4	0.72	1.77	1.05	0.38	0.12
3.35	11	1.7	3.2	0.84	1.57	0.74	0.40	0.15
3.66	12	1.8	3.2	0.94	1.57	0.63	0.42	0.18
3.96	13	1.8	3.2	0.94	1.57	0.63	0.44	0.21
4.27	14	1.7	2.85	0.85	1.22	0.37	0.46	0.24
4.57	15	2	3.2	1.15	1.57	0.42	0.49	0.27
4.88	16	1.8	2.8	0.96	1.17	0.21	0.51	0.30
5.18	17	1.7	2.6	0.87	0.97	0.11	0.53	0.33
5.49	18	2.3	3.7	1.44	2.07	0.63	0.55	0.36
5.79	19	1.8	2.9	0.96	1.27	0.32	0.57	0.39
6.10	20	1.9	2.8	1.07	1.17	0.11	0.59	0.42
6.40	21	1.7	2.8	0.86	1.17	0.32	0.61	0.45
6.71	22	1.8	3.2	0.94	1.57	0.63	0.63	0.48
7.01	23	1.7	2.8	0.86	1.17	0.32	0.65	0.51
7.32	24	2.3	3.2	1.47	1.57	0.11	0.67	0.54
7.62	25	2.3	3.3	1.46	1.67	0.21	0.69	0.57
7.92	26	2.2	3.3	1.36	1.67	0.32	0.71	0.60
8.23	27	2.3	3.4	1.46	1.77	0.32	0.73	0.63
8.53	28	2.5	3.8	1.65	2.17	0.53	0.75	0.66
8.84	29	2.6	4.2	1.73	2.57	0.84	0.77	0.69
9.14	30	2.4	3.8	1.54	2.17	0.63	0.79	0.72
9.45	31	2.8	4.4	1.93	2.77	0.84	0.81	0.75
9.75	32	2.9	4.1	2.05	2.47	0.42	0.83	0.78
10.06	33	3.4	5.55	2.50	3.92	1.42	0.85	0.81
10.36	34	3.1	4.4	2.25	2.77	0.53	0.87	0.84
10.67	35	2.9	3.9	2.06	2.27	0.21	0.89	0.87
10.97	36	3.1	4.3	2.25	2.67	0.42	0.91	0.90
11.28	37	3.1	4.2	2.26	2.57	0.32	0.93	0.93
11.58	38	3.3	4.3	2.46	2.67	0.21	0.95	0.96
11.89	39	3.5	4.7	2.65	3.07	0.42	0.97	0.99
12.19	40	3.2	4.2	2.36	2.57	0.21	1.00	1.02
12.50	41	3	4.7	2.13	3.07	0.95	1.02	1.05
12.80	42	3.3	4.4	2.46	2.77	0.32	1.04	1.08
13.11	43	3.5	4.5	2.66	2.87	0.21	1.06	1.11
13.41	44	3.4	4.4	2.56	2.77	0.21	1.08	1.14
13.72	45	5.8	10.4	4.78	8.77	3.99	1.10	1.17
14.02	46	9.6	20.3	8.28	18.67	10.40	1.12	1.20

Table B2. Reduced DMT1 data

Material Index	Classification	Horiz. Stress Index	Dilat. Modulus	Coeff Earth Press	Undrained Shear
I_d		K_d	E_d	Ko	C_u (bars)
3.26	sand	27.90	158.49	2.05	0.30
23.63	sand	0.80	65.58	0.30	0.01
5.44	sand	0.90	25.50	0.32	0.01
5.44	sand	0.67	25.50	0.27	0.01
3.00	silty sand	1.46	38.26	0.42	0.04
-8.40	n/a	-0.17	14.57	#NUM!	#NUM!
8.39	sand	0.31	29.15	0.18	0.01
2.30	silty sand	1.87	51.01	0.48	0.07
1.34	sandy silt	4.09	69.23	0.73	0.20
1.75	sandy silt	1.57	36.44	0.43	0.06
1.07	silt	1.70	25.50	0.45	0.07
0.83	clayey silt	1.79	21.86	0.47	0.08
0.86	clayey silt	1.64	21.86	0.44	0.08
0.60	silty clay	1.32	12.75	0.39	0.06
0.48	silty clay	1.82	14.57	0.47	0.09
0.32	clayey silt	1.31	7.29	0.39	0.07
0.20	clayey silt	1.02	3.64	0.34	0.05
0.58	silty clay	1.98	21.86	0.49	0.12
0.56	silty clay	1.00	10.93	0.34	0.05
0.16	clayey silt	1.10	3.64	0.36	0.06
0.77	clayey silt	0.67	10.93	0.27	0.03
1.36	sandy silt	0.74	21.86	0.29	0.04
0.91	clayey silt	0.54	10.93	0.24	0.03
0.11	clay	1.39	3.64	0.41	0.09
0.24	clay	1.29	7.29	0.39	0.09
0.42	silty clay	1.07	10.93	0.35	0.07
0.38	silty clay	1.13	10.93	0.36	0.08
0.53	silty clay	1.32	18.22	0.39	0.10
0.81	clayey silt	1.35	29.15	0.40	0.10
0.77	clayey silt	1.04	21.86	0.35	0.08
0.71	clayey silt	1.46	29.15	0.42	0.12
0.33	clay	1.53	14.57	0.43	0.13
0.84	clayey silt	1.99	49.19	0.49	0.19
0.37	silty clay	1.61	18.22	0.44	0.15
0.18	clay	1.34	7.29	0.40	0.12
0.31	clay	1.48	14.57	0.42	0.14
0.24	clay	1.42	10.93	0.41	0.13
0.14	clay	1.58	7.29	0.43	0.16
0.25	clay	1.71	14.57	0.45	0.18
0.16	clay	1.35	7.29	0.40	0.13
0.88	clayey silt	1.06	32.79	0.35	0.10
0.23	clay	1.33	10.93	0.40	0.14
0.14	clay	1.47	7.29	0.42	0.16
0.15	clay	1.32	7.29	0.40	0.14
1.10	silt	3.29	138.45	0.65	0.45
1.47	sandy silt	6.34	360.71	0.92	1.04

Table B3. DMT2 data readings

m	ft	bar	var	bar	bar		bar	bar
Depth	Depth	A	B	po	p1	delta p	Vert Eff. Stress	uo
0.30	1.00	2.10	6.00	1.12	4.37	3.26	0.05	0.00
0.61	2.00	1.60	4.15	0.68	2.52	1.84	0.10	0.00
0.91	3.00	1.00	2.10	0.16	0.47	0.32	0.15	0.00
1.22	4.00	1.10	2.30	0.25	0.67	0.42	0.20	0.00
1.52	5.00	0.80	2.10	-0.06	0.47	0.53	0.25	0.00
1.83	6.00	0.80	1.80	-0.04	0.17	0.21	0.30	0.00
2.13	7.00	1.30	2.90	0.43	1.27	0.84	0.32	0.03
2.44	8.00	1.70	3.10	0.84	1.47	0.63	0.34	0.06
2.74	9.00	1.15	2.20	0.31	0.57	0.26	0.36	0.09
3.05	10.00	1.40	2.35	0.56	0.72	0.16	0.38	0.12
3.35	11.00	1.50	2.40	0.67	0.77	0.11	0.40	0.15
3.66	12.00	1.60	2.70	0.76	1.07	0.32	0.42	0.18
3.96	13.00	1.80	2.80	0.96	1.17	0.21	0.44	0.21
4.27	14.00	1.80	2.60	0.97	0.97	0.00	0.46	0.24
4.57	15.00	1.90	3.05	1.05	1.42	0.37	0.49	0.27
4.88	16.00	2.10	3.10	1.26	1.47	0.21	0.51	0.30
5.18	17.00	2.30	3.40	1.46	1.77	0.32	0.53	0.33
5.49	18.00	2.30	3.20	1.47	1.57	0.11	0.55	0.36
5.79	19.00	2.10	3.00	1.27	1.37	0.11	0.57	0.39
6.10	20.00	2.00	3.00	1.16	1.37	0.21	0.59	0.42
6.40	21.00	2.00	2.90	1.17	1.27	0.11	0.61	0.45
6.71	22.00	1.90	2.85	1.06	1.22	0.16	0.63	0.48
7.01	23.00	2.10	3.10	1.26	1.47	0.21	0.65	0.51
7.32	24.00	2.30	3.10	1.47	1.47	0.00	0.67	0.54
7.62	25.00	2.50	3.80	1.65	2.17	0.53	0.69	0.57
7.92	26.00	2.75	3.80	1.91	2.17	0.26	0.71	0.60
8.23	27.00	2.60	3.70	1.76	2.07	0.32	0.73	0.63
8.53	28.00	2.60	3.60	1.76	1.97	0.21	0.75	0.66
8.84	29.00	2.70	3.60	1.87	1.97	0.11	0.77	0.69
9.14	30.00	2.70	3.50	1.87	1.87	0.00	0.79	0.72
9.45	31.00	2.80	3.70	1.97	2.07	0.11	0.81	0.75
9.75	32.00	2.20	3.60	1.34	1.97	0.63	0.83	0.78
10.06	33.00	2.50	3.70	1.65	2.07	0.42	0.85	0.81
10.36	34.00	3.10	4.75	2.23	3.12	0.89	0.87	0.84
10.67	35.00	3.85	5.50	2.98	3.87	0.89	0.89	0.87
10.97	36.00	3.00	4.00	2.16	2.37	0.21	0.91	0.90
11.28	37.00	2.90	3.70	2.07	2.07	0.00	0.93	0.93
11.58	38.00	2.70	3.60	1.87	1.97	0.11	0.95	0.96
11.89	39.00	2.70	4.30	1.83	2.67	0.84	0.97	0.99
12.19	40.00	2.50	3.50	1.66	1.87	0.21	1.00	1.02
12.50	41.00	2.50	4.00	1.64	2.37	0.74	1.02	1.05
12.80	42.00	2.70	6.30	1.73	4.67	2.94	1.04	1.08
13.11	43.00	3.00	4.30	2.15	2.67	0.53	1.06	1.11
13.41	44.00	2.80	3.80	1.96	2.17	0.21	1.08	1.14
13.72	45.00	2.50	3.90	1.64	2.27	0.63	1.10	1.17
14.02	46.00	2.80	6.80	1.81	5.17	3.36	1.12	1.20
14.33	47.00	3.50	7.30	2.52	5.67	3.15	1.14	1.22
14.48	47.50	3.80	13.10	2.55	11.47	8.93	1.15	1.24

Table B4. Reduced DMT2 data

Material Index	Classification	Horiz. Stress Index	Dilat. Modulus	Coeff Earth Press	Undrained Shear
Id		Kd	Ed	Ko	Cu (bars)
2.92	silty sand	22.18	112.95	1.81	0.22
2.69	silty sand	6.79	63.76	0.96	0.10
2.03	silty sand	1.03	10.93	0.35	0.01
1.68	silty sand	1.24	14.57	0.38	0.02
-9.55	n/a	-0.22	18.22	#NUM!	#NUM!
-5.25	n/a	-0.13	7.29	#NUM!	#NUM!
2.10	silty sand	1.24	29.15	0.38	0.04
0.81	silt	2.28	21.86	0.53	0.09
1.20	sandy silt	0.60	9.11	0.26	0.02
0.36	silty clay	1.16	5.47	0.37	0.04
0.20	silty clay	1.28	3.64	0.39	0.05
0.55	clayey silt	1.36	10.93	0.40	0.06
0.28	silty clay	1.69	7.29	0.45	0.08
0.00	clay	1.57	0.00	0.43	0.08
0.47	clayey silt	1.61	12.75	0.44	0.08
0.22	clay	1.90	7.29	0.48	0.10
0.28	silty clay	2.14	10.93	0.51	0.13
0.09	clay	2.02	3.64	0.50	0.12
0.12	clay	1.55	3.64	0.43	0.09
0.28	silty clay	1.26	7.29	0.39	0.07
0.15	clay	1.18	3.64	0.37	0.07
0.27	silty clay	0.93	5.47	0.33	0.05
0.28	silty clay	1.16	7.29	0.37	0.07
0.00	clay	1.39	0.00	0.41	0.09
0.49	silty clay	1.56	18.22	0.43	0.11
0.20	clay	1.85	9.11	0.47	0.14
0.28	clay	1.54	10.93	0.43	0.12
0.19	clay	1.47	7.29	0.42	0.11
0.09	clay	1.53	3.64	0.43	0.12
0.00	clay	1.46	0.00	0.42	0.12
0.09	clay	1.50	3.64	0.42	0.12
1.12	sandy silt	0.68	21.86	0.28	0.05
0.50	clayey silt	0.99	14.57	0.34	0.08
0.64	clayey silt	1.59	30.97	0.44	0.14
0.42	silty clay	2.36	30.97	0.54	0.24
0.17	clay	1.38	7.29	0.41	0.13
0.00	clay	1.22	0.00	0.38	0.11
0.12	clay	0.95	3.64	0.33	0.08
1.00	silt	0.87	29.15	0.31	0.08
0.33	silty clay	0.65	7.29	0.27	0.05
1.25	sandy silt	0.58	25.50	0.25	0.05
4.49	sand	0.63	102.02	0.27	0.05
0.51	clayey silt	0.98	18.22	0.34	0.10
0.25	silty clay	0.77	7.29	0.29	0.07
1.33	sandy silt	0.43	21.86	0.22	0.04
5.46	sand	0.55	116.59	0.25	0.05
2.43	silty sand	1.14	109.31	0.36	0.12
6.84	sand	1.14	309.70	0.36	0.12

APPENDIX C

PRESSUREMETER DATA

Table C1. PMT1 data at 4.57 m

Depth (m)	V30	V60	Volume (cm3)	Creep	Creep V (cm3)	P (psi)	P (kPa)
4.57	16.50	16.70	1338.84	0.00	0.00	5.00	34.47
4.57	17.70	17.90	1435.04	0.20	16.03	10.00	68.95
4.57	19.10	19.30	1547.28	0.20	16.03	15.00	103.42
4.57	20.30	20.40	1635.47	0.10	8.02	20.00	137.89
4.57	21.40	21.60	1731.67	0.20	16.03	25.00	172.37
4.57	22.80	23.00	1843.91	0.20	16.03	30.00	206.84
4.57	23.90	25.00	2004.25	1.10	88.19	35.00	241.31
4.57	27.20	28.00	2244.76	0.80	64.14	39.00	268.89

Membrane Resistance (kPa)	Head (kPa)	Final Corr P (kPa)	Compressibility (cm3)	Initial (cm3)	Final Corr. V (cm3)
19.09	44.52	59.91	0.00	1258.67	80.17
26.55	44.52	86.92	0.00	1258.67	176.37
34.46	44.52	113.48	0.00	1258.67	288.61
40.08	44.52	142.33	0.00	1258.67	376.80
45.62	44.52	171.27	0.00	1258.67	473.00
51.30	44.52	200.07	2.87	1258.67	582.37
57.94	44.52	227.90	6.38	1258.67	739.20
64.67	44.52	248.75	8.85	1258.67	977.24

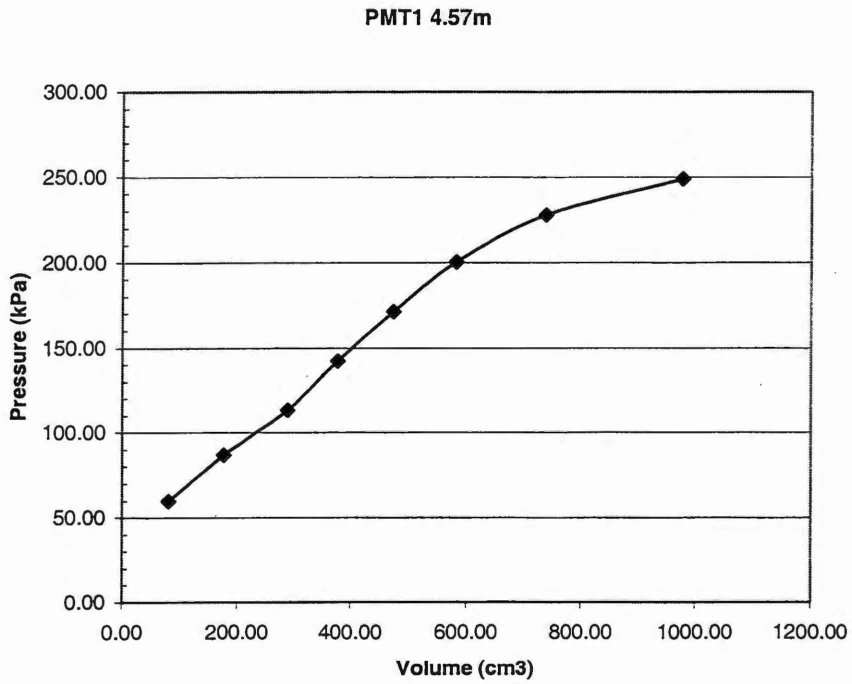

Figure C1. PMT1 curve at 4.57 m

Table C2. PMT1 data at 6.10 m

Depth (m)	V30	V60	Volume (cm3)	Creep	Creep V (cm3)	P (psi)	P (kPa)
6.10	17.1	17.7	1419.01	0.00	0.00	5.00	34.47
6.10	19.2	19.6	1571.33	0.40	32.07	10.00	68.95
6.10	20.8	21.2	1699.60	0.40	32.07	15.00	103.42
6.10	22.3	22.6	1811.84	0.30	24.05	20.00	137.89
6.10	23.7	24.1	1932.10	0.40	32.07	25.00	172.37
6.10	25.6	25.9	2076.40	0.30	24.05	30.00	206.84
6.10	27.5	28.1	2252.78	0.60	48.10	34.00	234.42
6.10	29.8	30.3	2429.15	0.50	40.09	37.00	255.10

Membrane Resistance (kPa)	Head (kPa)	Final Corr P (kPa)	Compressibility (cm3)	Initial (cm3)	Final Corr. V (cm3)
25.35	59.36	68.49	0.00	1202.55	216.46
36.04	59.36	92.27	0.00	1202.55	368.78
43.84	59.36	118.94	0.00	1202.55	497.05
49.76	59.36	147.50	0.00	1202.55	609.29
55.17	59.36	176.57	0.00	1202.55	729.55
60.37	59.36	205.84	2.87	1202.55	870.98
64.83	59.36	228.96	5.72	1202.55	1044.51
67.20	59.36	247.27	7.65	1202.55	1218.95

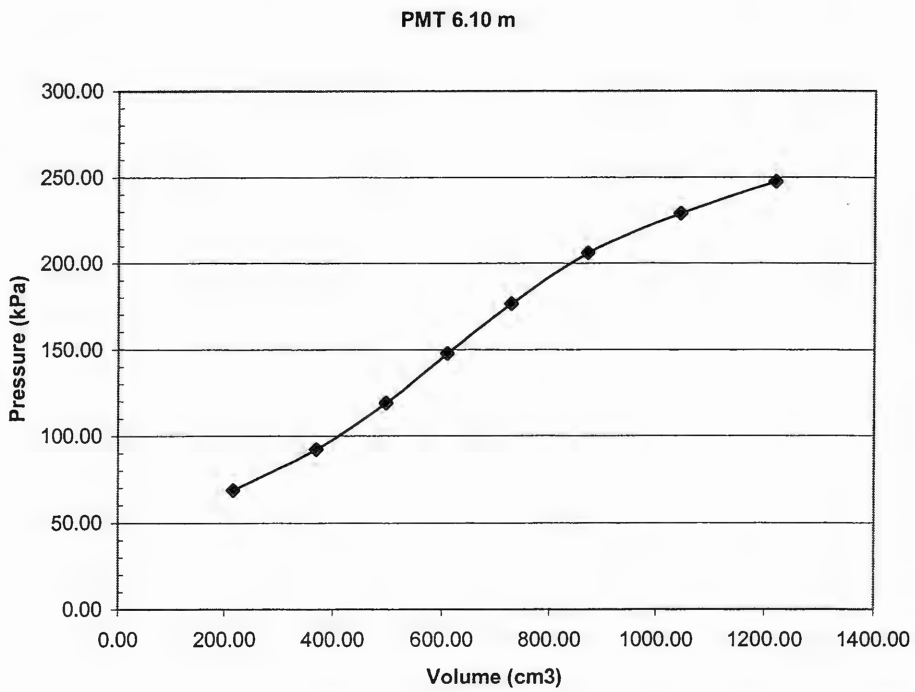

Figure C2. PMT1 curve at 6.10 m

Table C3. PMT data at 7.62 m

Depth (m)	V30	V60	Volume (cm3)	Creep	Creep V (cm3)	P (psi)	P (kPa)
7.62	16.2	16.3	1306.771	0	0	5	34.4735
7.62	17.8	18.2	1459.094	0.4	32.068	10	68.947
7.62	19.2	19.3	1547.281	0.1	8.017	15	103.421
7.62	20.3	20.5	1643.485	0.2	16.034	20	137.894
7.62	21.6	21.7	1739.689	0.1	8.017	25	172.368
7.62	23	23.3	1867.961	0.3	24.051	30	206.841
7.62	25.1	25.6	2052.352	0.5	40.085	35	241.315
7.62	27.6	27.9	2236.743	0.3	24.051	39	268.893
7.62	29.8	30.5	2445.185	0.7	56.119	44	303.367

Membrane Resistance (kPa)	Head (kPa)	Final Corr P (kPa)	Compressibility (cm3)	Initial (cm3)	Final Corr. V (cm3)
16.46842552	74.205701	92.21077531	0	1202.55	104.221
28.31360755	74.205701	114.8390933	0	1202.55	256.544
34.45931228	74.205701	143.1668886	0	1202.55	344.731
40.56819956	74.205701	171.5315013	0	1202.55	440.935
46.05567689	74.205701	200.5175239	0	1202.55	537.139
52.40567562	74.205701	228.6410252	2.868535548	1202.55	662.5424645
59.59836571	74.205701	255.9218351	6.381668813	1202.55	843.4203312
64.50823727	74.205701	278.5907636	8.852519495	1202.55	1025.340481
67.30965089	74.205701	310.2628499	11.6113447	1202.55	1231.023655

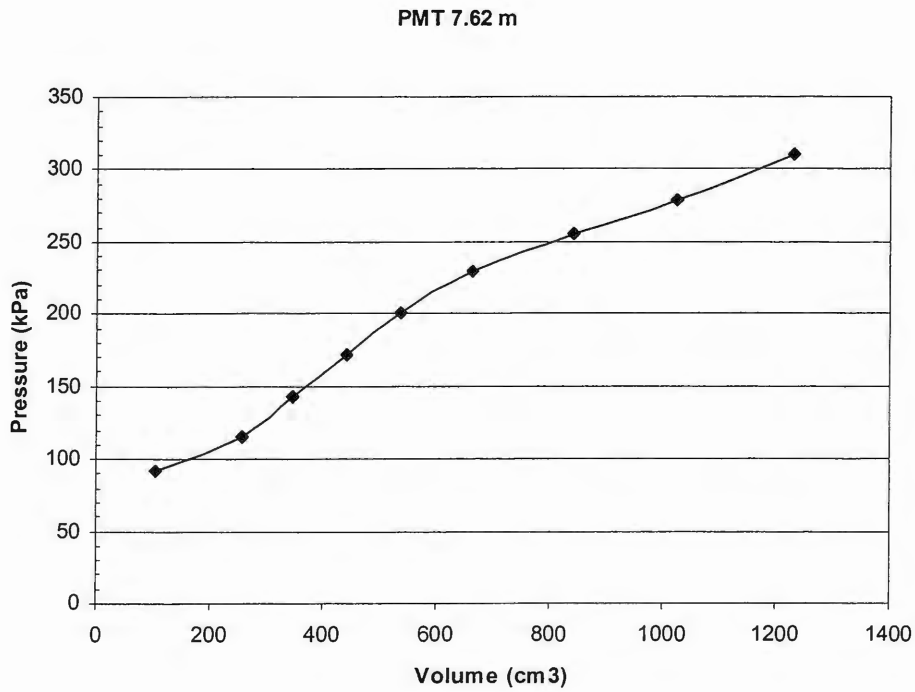

Figure C3. PMT1 curve at 7.62 m

Table C4. PMT data at 9.14 m

Depth (m)	V30	V60	Volume (cm3)	Creep	Creep V (cm3)	P (psi)	P (kPa)
9.14	16.2	16.3	1306.771	0	0	5	34.4735
9.14	17.6	17.7	1419.009	0.1	8.017	10	68.947
9.14	18.5	18.6	1491.162	0.1	8.017	15	103.421
9.14	19.2	19.3	1547.281	0.1	8.017	20	137.894
9.14	19.9	20	1603.4	0.1	8.017	25	172.368
9.14	20.7	20.9	1675.553	0.2	16.034	30	206.841
9.14	21.7	21.9	1755.723	0.2	16.034	35	241.315
9.14	23.1	23.2	1859.944	0.1	8.017	40	275.788
9.14	24.9	25.1	2012.267	0.2	16.034	45	310.262
9.14	27.1	27.6	2212.692	0.5	40.085	50	344.735
9.14	29.6	30	2405.1	0.4	32.068	54	372.314
9.14	31.5	32.1	2573.457	0.6	48.102	57	392.998

Membrane Resistance (kPa)	Head (kPa)	Final Corr P (kPa)	Compressibility (cm3)	Initial (cm3)	Final Corr V (cm3)
16.46842552	89.046841	107.0519155	0	1202.55	104.221
25.34749153	89.046841	132.6463495	0	1202.55	216.459
30.60882413	89.046841	161.8585169	0	1202.55	288.612
34.45931228	89.046841	192.4815287	0	1202.55	344.731
38.09834843	89.046841	223.3159926	0	1202.55	400.85
42.46640422	89.046841	253.4214368	2.868535548	1202.55	470.1344645
46.90984159	89.046841	283.4514994	6.381668813	1202.55	546.7913312
52.0411658	89.046841	312.7936752	9.431156057	1202.55	647.9628439
58.22892804	89.046841	341.079413	12.12583733	1202.55	797.5911627
63.99727965	89.046841	369.7845613	14.54016493	1202.55	995.6018351
66.99747322	89.046841	394.3631678	16.30602379	1202.55	1186.243976
67.58364117	89.046841	414.4610998	17.5477516	1202.55	1353.359248

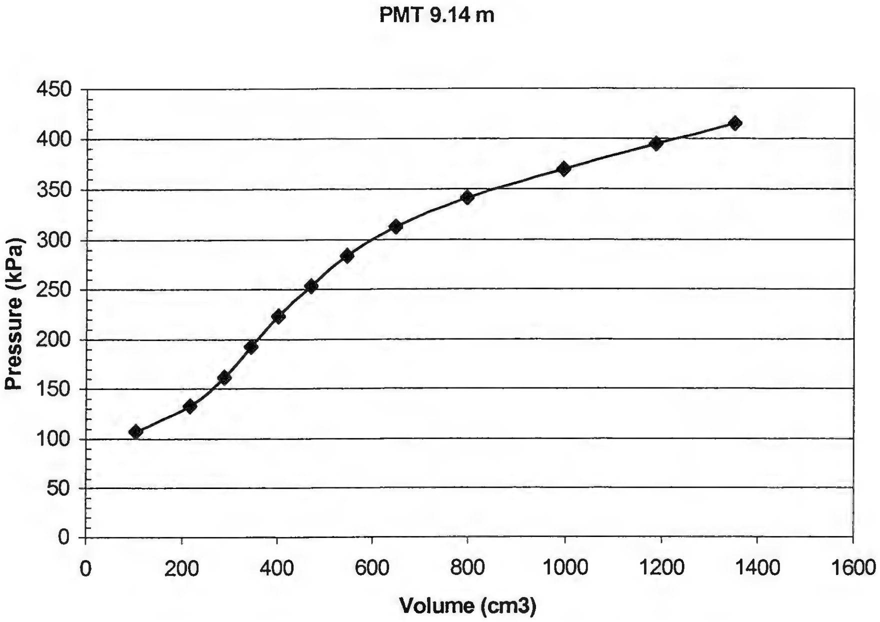

Figure C4. PMT1 curve at 9.14 m

Table C5. PMT data at 10.67 m

Depth (m)	V30	V60	Volume (cm3)	Creep	Creep V (cm3)	P (psi)	P (kPa)
10.67	16	16.1	1290.737	0	0	5	34.4735
10.67	17.4	17.7	1419.009	0.3	24.051	10	68.947
10.67	19.2	19.3	1547.281	0.1	8.017	15	103.421
10.67	20.6	20.8	1667.536	0.2	16.034	20	137.894
10.67	21.9	22.2	1779.774	0.3	24.051	25	172.368
10.67	23.7	23.9	1916.063	0.2	16.034	30	206.841
10.67	25.7	26.1	2092.437	0.4	32.068	35	241.315
10.67	28	28.4	2276.828	0.4	32.068	40	275.788
10.67	30.2	31	2485.27	0.8	64.136	45	310.262

Membrane Resistance (kPa)	Head (kPa)	Final Corr P (kPa)	Compressibility (cm3)	Initial (cm3)	Final Corr. V (cm3)
15.13094197	103.88798	123.2305392	0	1202.55	88.187
25.34749153	103.88798	147.4874896	0	1202.55	216.459
34.45931228	103.88798	172.8491689	0	1202.55	344.731
41.99832608	103.88798	199.7836551	0	1202.55	464.986
48.15872354	103.88798	228.0967576	0	1202.55	577.224
54.50211225	103.88798	256.2268689	2.868535548	1202.55	710.6444645
60.8599197	103.88798	284.3425615	6.381668813	1202.55	883.5053312
65.27352638	103.88798	314.4024548	9.431156057	1202.55	1064.846844
67.51394489	103.88798	346.6355363	12.12583733	1202.55	1270.594163

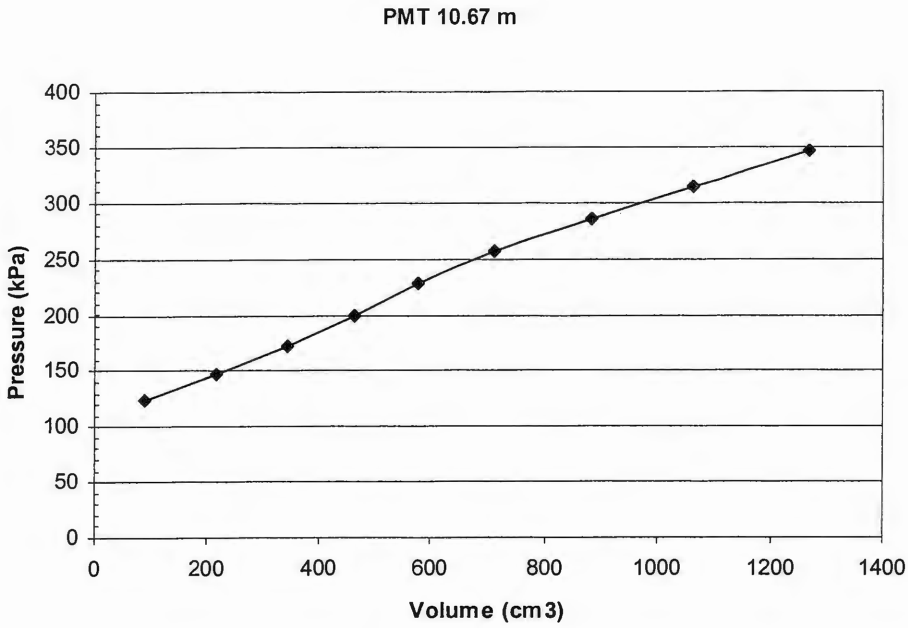

Figure C5. PMT1 curve at 10.67 m

Table C6. PMT2 data at 4.0 m

Depth (m)	V30	V60	Volume (cm3)	Creep	Creep V (cm3)	P (psi)	P (kPa)
4.00	1.38	1.38	110.63	0.00	0.00	4.00	27.58
4.00	2.48	2.60	208.44	0.12	9.62	10.00	68.95
4.00	3.70	3.80	304.65	0.10	8.02	15.00	103.42
4.00	4.90	5.05	404.86	0.15	12.03	20.00	137.89
4.00	6.40	6.65	533.13	0.25	20.04	25.00	172.37
4.00	8.25	8.70	697.48	0.45	36.08	30.00	206.84
4.00	10.75	11.70	937.99	0.95	76.16	35.00	241.31
4.00	14.20	15.70	1258.67	1.50	120.26	40.00	275.79

Membrane Resistance (kPa)	Head (kPa)	Final Corr P (kPa)	Compress (cm3)	Initial (cm3)	Final Corr V (cm3)
18.87	39.33	48.04	0.00	80.17	30.46
27.30	39.33	80.98	0.00	80.17	128.27
34.95	39.33	107.80	0.00	80.17	224.48
42.25	39.33	134.97	0.00	80.17	324.69
50.60	39.33	161.09	0.00	80.17	452.96
59.66	39.33	186.51	3.33	80.17	613.98
69.59	39.33	211.05	6.58	80.17	851.24
76.69	39.33	238.42	9.43	80.17	1169.07

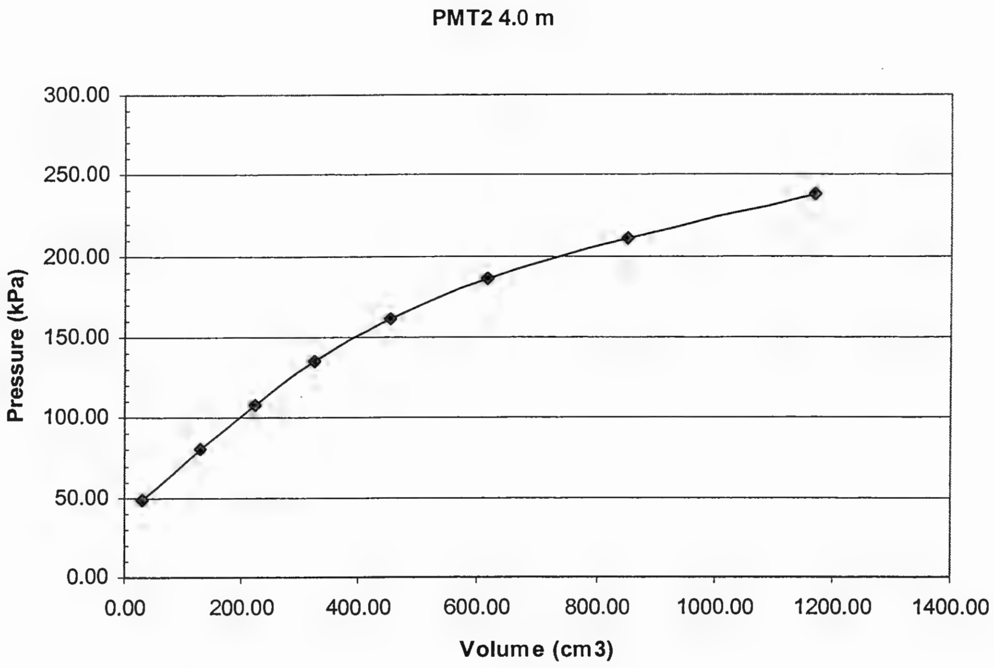

Figure C6. PMT2 curve at 4.0 m

Table C7. PMT2 data at 5.50 m

Depth (m)	V30	V60	Volume (cm3)	Creep	Creep V (cm3)	P (psi)	P (kPa)
5.50	0.6	0.6	48.102	0	0	3	20.6841
5.50	1.15	1.15	92.1955	0	0	6	41.3682
5.50	1.55	1.6	128.272	0.05	4.0085	9	62.0523
5.50	2.05	2.1	168.357	0.05	4.0085	12	82.7364
5.50	2.5	2.65	212.4505	0.15	12.0255	15	103.421
5.50	3.12	3.25	260.5525	0.13	10.4221	18	124.105
5.50	3.7	3.9	312.663	0.2	16.034	21	144.789
5.50	4.3	4.4	352.748	0.1	8.017	24	165.473
5.50	5	5.15	412.8755	0.15	12.0255	27	186.157
5.50	5.85	6.13	491.4421	0.28	22.4476	30	206.841
5.50	6.9	7.3	585.241	0.4	32.068	33	227.525
5.50	8.2	8.7	697.479	0.5	40.085	36	248.209
5.50	9.7	10.4	833.768	0.7	56.119	39	268.893
5.50	11.6	12.35	990.0995	0.75	60.1275	42	289.577
5.50	13.2	14.2	1138.414	1	80.17	45	310.262

Table C7 (continued). PMT2 data at 5.50 m

Membrane Resistance (kPa)	Head (kPa)	Final Corr P (kPa)	Compressibility (cm3)	Initial (cm3)	Final Corr. V (cm3)
13.13536801	54.170162	61.71889359	0	80.17	0
17.20450041	54.170162	78.3338612	0	80.17	12.0255
20.43515405	54.170162	95.78730756	0	80.17	48.102
23.9206529	54.170162	112.9859087	0	80.17	88.187
27.62811812	54.170162	129.9625435	0	80.17	132.2805
31.52138301	54.170162	146.7533786	0	80.17	180.3825
35.56099295	54.170162	163.3978687	0	80.17	232.493
38.54234968	54.170162	181.1006119	0	80.17	272.578
42.80889207	54.170162	197.5181695	1.122401813	80.17	331.5830982
48.0122223	54.170162	212.9989393	3.326498197	80.17	407.9456018
53.67298341	54.170162	228.0222782	5.334029704	80.17	499.7369703
59.65789009	54.170162	242.7214715	7.178186854	80.17	610.1308131
65.77013376	54.170162	257.2933279	8.884333998	80.17	744.713666
71.22113613	54.170162	272.5264255	10.47230102	80.17	899.457199
74.85167858	54.170162	289.579983	11.9578913	80.17	1046.286109

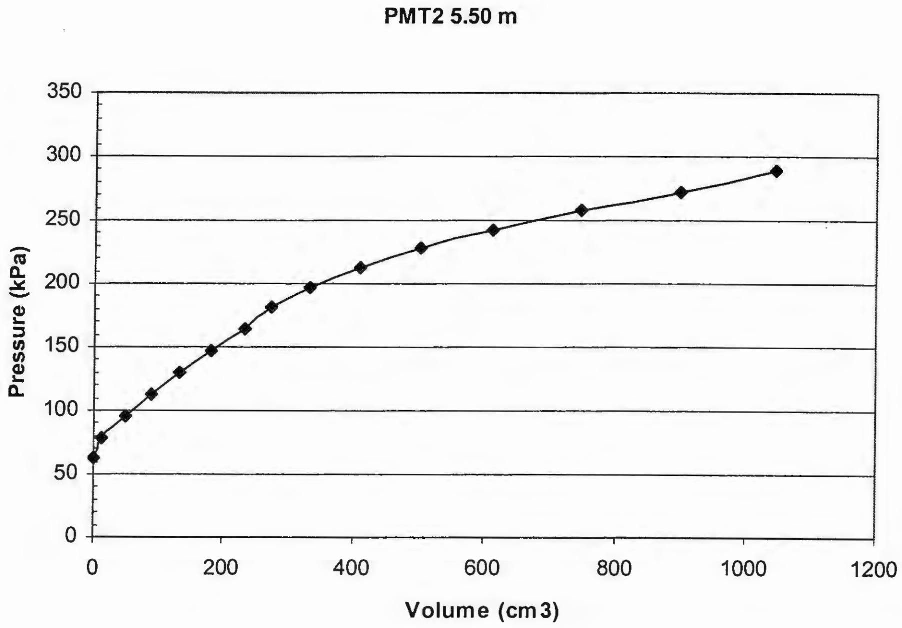

Figure C7. PMT2 curve at 5.50 m

APPENDIX D

BOREHOLE SHEAR TEST DATA

Table D1. Borehole shear test data at 4.19 m

Depth (m)	Normal Stress (kPa)	Shear Stress (kPa)
4.19	12	5
4.19	20	8
4.19	32	13
4.19	38	16
4.19	50	19
4.19	60	25
	phi (deg)	22
	c (kPa)	0.05

Table D2. Borehole shear test data at 2.29 m

Depth (m)	Normal Stress (kPa)	Shear Stress (kPa)
2.29	10	11
2.29	14	15
2.29	19	18
2.29	24	20
2.29	30	26
2.29	38	28
2.29	50	31
2.29	60	36
	phi (deg)	25.4
	c (kPa)	8.6

APPENDIX E

CONSOLIDATED DRAINED TRIAXIAL DATA

Table E1. Consolidated drained triaxial data for clay at 20.68 kPa confinement

Axial Deflection (in)	Axial Strain (%)	Volume Change (cm^3)	Corrected VC (cm^3)	Volume Change (%)	Corrected Area (cm^2)	Axial Load (lb)	Axial Stress (kPa)	σ 1 (kPa)	p (kPa)	q (kPa)
0	0	0	0	0.044604	40.583568	0	0	20.6843	20.68428	0
0.02	0.35781	-0.257	0.257	0.044604	40.711135	6.1	6.665042	27.3493	24.0168	3.33252
0.04	0.71562	-0.414	0.414	0.071852	40.846715	19.8	21.58949	42.2738	31.47902	10.7947
0.06	1.07343	-0.671	0.671	0.116456	40.976157	24.7	26.81883	47.5031	34.0937	13.4094
0.08	1.43124	-0.928	0.928	0.16106	41.106538	26.8	29.0441	49.7284	35.20633	14.522
0.1	1.78905	-1.085	1.085	0.188308	41.245041	28.1	30.26232	50.9466	35.81544	15.1312
0.12	2.14686	-1.142	1.142	0.198201	41.391755	29.0	31.13837	51.8226	36.25346	15.5692
0.14	2.50467	-1.299	1.299	0.225449	41.532321	30.5	32.6663	53.3506	37.01743	16.3331
0.16	2.86248	-1.356	1.356	0.235342	41.681175	31.1	33.20063	53.8849	37.28459	16.6003
0.18	3.22029	-1.413	1.413	0.245234	41.831128	32.3	34.37893	55.0632	37.87375	17.1895
0.2	3.5781	-1.57	1.57	0.272483	41.97489	33.2	35.23084	55.9151	38.2997	17.6154
0.22	3.93592	-1.727	1.727	0.299731	42.119723	33.9	35.75391	56.4382	38.56124	17.877
0.24	4.29373	-1.884	1.884	0.326979	42.265639	34.8	36.59346	57.2777	38.98101	18.2967
0.26	4.65154	-1.941	1.941	0.336872	42.420036	35.4	37.09993	57.7842	39.23424	18.55
0.28	5.00935	-2.098	2.098	0.36412	42.568183	36.6	38.24567	58.9299	39.80711	19.1228
0.3	5.36716	-2.255	2.255	0.391368	42.717449	36.9	38.42963	59.1139	39.89909	19.2148
0.32	5.72497	-2.312	2.312	0.401261	42.87532	37.8	39.23742	59.9217	40.30299	19.6187
0.34	6.08278	-2.369	2.369	0.411154	43.034394	38.4	39.7229	60.4072	40.54573	19.8615
0.36	6.44059	-2.526	2.526	0.438402	43.187156	39.0	40.21068	60.895	40.78962	20.1053
0.38	6.7984	-2.683	2.683	0.46565	43.341091	39.7	40.69393	61.3782	41.03124	20.347
0.4	7.15621	-2.64	2.64	0.458187	43.511385	40.3	41.15827	61.8426	41.26342	20.5791
0.42	7.51402	-2.797	2.797	0.485436	43.667765	41.2	41.94294	62.6272	41.65575	20.9715
0.44	7.87183	-2.954	2.954	0.512684	43.82536	41.8	42.41126	63.0955	41.88991	21.2056
0.46	8.22964	-3.111	3.111	0.539932	43.984185	42.7	43.18348	63.8678	42.27602	21.5917
0.48	8.58745	-3.068	3.068	0.532469	44.159662	43.3	43.62633	64.3106	42.49745	21.8132
0.5	8.94526	-3.125	3.125	0.542362	44.328784	43.9	44.072	64.7563	42.72028	22.036
0.52	9.30307	-3.282	3.282	0.56961	44.491474	44.2	44.21578	64.9001	42.79217	22.1079
0.54	9.66088	-3.339	3.339	0.579503	44.663249	44.5	44.34949	65.0338	42.85903	22.1747
0.56	10.0187	-3.396	3.396	0.589395	44.836391	45.8	45.38859	66.0729	43.37858	22.6943
0.58	10.3765	-3.553	3.553	0.616644	45.003056	46.1	45.52197	66.2062	43.44526	22.761
0.6	10.7343	-3.51	3.51	0.609181	45.186838	46.4	45.63707	66.3213	43.50281	22.8185
0.62	11.0921	-3.567	3.567	0.619074	45.364177	47.3	46.35587	67.0402	43.86222	23.1779
0.64	11.4499	-3.724	3.724	0.646322	45.534995	47.6	46.47992	67.1642	43.92424	23.24
0.66	11.8077	-3.881	3.881	0.67357	45.707199	47.9	46.60163	67.2859	43.9851	23.3008
0.68	12.1656	-3.938	3.938	0.683463	45.888825	48.2	46.71284	67.3971	44.0407	23.3564
0.7	12.5234	-4.095	4.095	0.710711	46.063885	48.8	47.12437	67.8086	44.24646	23.5622
0.72	12.8812	-4.252	4.252	0.737959	46.240383	49.1	47.2379	67.9222	44.30323	23.6189
0.74	13.239	-4.309	4.309	0.747852	46.426456	49.7	47.63303	68.3173	44.50079	23.8165
0.76	13.5968	-4.366	4.366	0.757745	46.614069	50.3	48.02341	68.7077	44.69599	24.0117
0.78	13.9546	-4.623	4.623	0.802348	46.786871	50.9	48.426	69.1103	44.89728	24.213
0.8	14.3124	-4.68	4.68	0.812241	46.977556	51.5	48.80703	69.4913	45.0878	24.4035
0.82	14.6702	-4.737	4.737	0.822134	47.16984	51.5	48.60807	69.2924	44.98832	24.304
0.84	15.028	-4.994	4.994	0.866738	47.347166	51.9	48.71257	69.3968	45.04056	24.3563
0.86	15.3859	-5.051	5.051	0.87663	47.542639	52.2	48.79765	69.4819	45.08311	24.3988
0.88	15.7437	-5.108	5.108	0.886523	47.739773	52.5	48.88034	69.5646	45.12445	24.4402
0.9	16.1015	-5.165	5.165	0.896416	47.938588	52.8	48.96063	69.6449	45.16459	24.4803
0.92	16.4593	-5.222	5.222	0.906308	48.139107	53.1	49.03852	69.7228	45.20354	24.5193
0.94	16.8171	-5.379	5.379	0.933557	48.332883	54.0	49.68401	70.3683	45.52629	24.842

Table E2. Consolidated drained triaxial data at 41.37 kPa confinement

Axial Deflection (in)	Axial Strain (%)	Volume Change (cm^3)	Corrected VC (cm^3)	Volume Change (%)	Corrected Area (cm^2)	Axial Load (lb)	Axial Stress (kPa)	σ 1 (kPa)	p (kPa)	q (kPa)
0	0	0	0	0	40.613373	0	0	41.3686	41.36856	0
0.02	0.35787	-0.257	0.257	0.044579	40.74107	18.3	19.98043	61.349	51.35878	9.99022
0.04	0.71575	-0.514	0.514	0.089158	40.869687	36.295	39.50315	80.8717	61.12014	19.7516
0.06	1.07362	-0.571	0.571	0.099045	41.013478	44.225	47.96534	89.3339	65.35123	23.9827
0.08	1.4315	-0.828	0.828	0.143624	41.144018	49.41	53.41883	94.7874	68.07798	26.7094
0.1	1.78937	-1.085	1.085	0.188204	41.27551	52.765	56.86431	98.2329	69.80071	28.4322
0.12	2.14725	-1.342	1.342	0.232783	41.407963	54.29	58.32063	99.6892	70.52888	29.1603
0.14	2.50512	-1.299	1.299	0.225324	41.563067	55.51	59.40868	100.777	71.0729	29.7043
0.16	2.863	-1.356	1.356	0.235211	41.71206	56.12	59.84699	101.216	71.29205	29.9235
0.18	3.22087	-1.613	1.613	0.27979	41.847598	56.425	59.97735	101.346	71.35724	29.9887
0.2	3.57875	-1.77	1.77	0.307023	41.991447	57.035	60.41807	101.787	71.5776	30.209
0.22	3.93662	-1.927	1.927	0.334256	42.136369	57.645	60.85423	102.223	71.79568	30.4271
0.24	4.29449	-2.084	2.084	0.36149	42.282374	57.95	60.96497	102.334	71.85104	30.4825
0.26	4.65237	-2.141	2.141	0.371377	42.436864	58.56	61.38243	102.751	72.05977	30.6912
0.28	5.01024	-2.398	2.398	0.415956	42.577685	58.56	61.17941	102.548	71.95827	30.5897
0.3	5.36812	-2.455	2.455	0.425843	42.73446	58.865	61.27244	102.641	72.00478	30.6362
0.32	5.72599	-2.512	2.512	0.43573	42.892425	58.865	61.04679	102.415	71.89195	30.5234
0.34	6.08387	-2.669	2.669	0.462963	43.044093	59.475	61.46206	102.831	72.09959	30.731
0.36	6.44174	-2.826	2.826	0.490196	43.196921	59.78	61.55869	102.927	72.14791	30.7793
0.38	6.79962	-2.983	2.983	0.51743	43.350923	60.39	61.96592	103.334	72.35152	30.983
0.4	7.15749	-3.14	3.14	0.544663	43.506113	61	62.36857	103.737	72.55285	31.1843
0.42	7.51536	-3.197	3.197	0.55455	43.67012	61.305	62.44501	103.814	72.59107	31.2225
0.44	7.87324	-3.254	3.254	0.564437	43.835402	61.915	62.82857	104.197	72.78284	31.4143
0.46	8.23111	-3.511	3.511	0.609016	43.98662	62.525	63.22945	104.598	72.98328	31.6147
0.48	8.58899	-3.568	3.568	0.618903	44.154435	63.135	63.60366	104.972	73.17039	31.8018
0.5	8.94686	-3.725	3.725	0.646136	44.315832	64.05	64.29045	105.659	73.51379	32.1452
0.52	9.30474	-3.882	3.882	0.67337	44.478503	64.355	64.36035	105.729	73.54873	32.1802
0.54	9.66261	-3.939	3.939	0.683257	44.650261	64.355	64.11277	105.481	73.42495	32.0564
0.56	10.0205	-4.196	4.196	0.727836	44.807726	64.965	64.49303	105.862	73.61508	32.2465
0.58	10.3784	-4.253	4.253	0.737723	44.982171	65.27	64.54453	105.913	73.64083	32.2723
0.6	10.7362	-4.31	4.31	0.74761	45.158014	65.27	64.2932	105.662	73.51516	32.1466
0.62	11.0941	-4.567	4.567	0.792189	45.319425	65.575	64.36358	105.732	73.55035	32.1818
0.64	11.452	-4.624	4.624	0.802077	45.498052	66.185	64.70726	106.076	73.72219	32.3536
0.66	11.8099	-4.781	4.781	0.82931	45.670141	66.795	65.05757	106.426	73.89735	32.5288
0.68	12.1677	-4.938	4.938	0.856543	45.843633	67.1	65.10731	106.476	73.92221	32.5537
0.7	12.5256	-4.995	4.995	0.86643	46.026598	67.1	64.8485	106.217	73.79281	32.4242
0.72	12.8835	-5.252	5.252	0.911009	46.194892	67.405	64.90594	106.274	73.82153	32.453
0.74	13.2414	-5.409	5.409	0.938242	46.372695	67.405	64.65707	106.026	73.6971	32.3285
0.76	13.5992	-5.466	5.466	0.948129	46.560125	67.71	64.68818	106.057	73.71265	32.3441
0.78	13.9571	-5.523	5.523	0.958017	46.749113	68.32	65.00709	106.376	73.87211	32.5035
0.8	14.315	-5.68	5.68	0.98525	46.931459	68.93	65.33268	106.701	74.0349	32.6663
0.82	14.6729	-5.937	5.937	1.029829	47.107078	69.845	65.95313	107.322	74.34513	32.9766
0.84	15.0307	-5.994	5.994	1.039716	47.300758	70.15	65.9699	107.338	74.35351	32.985
0.86	15.3886	-6.051	6.051	1.049603	47.496077	70.455	65.98426	107.353	74.36069	32.9921
0.88	15.7465	-6.108	6.108	1.05949	47.693055	71.065	66.28067	107.649	74.50889	33.1403
0.9	16.1044	-6.265	6.265	1.086724	47.883316	71.065	66.01731	107.386	74.37721	33.0087
0.92	16.4622	-6.322	6.322	1.096611	48.083641	71.065	65.74227	107.111	74.23969	32.8711
0.94	16.8201	-6.579	6.579	1.14119	48.26875	71.37	65.77122	107.14	74.25417	32.8856
0.96	17.178	-6.636	6.636	1.151077	48.472471	71.675	65.77469	107.143	74.2559	32.8873
0.98	17.5359	-6.793	6.793	1.17831	48.669418	71.675	65.50852	106.877	74.12282	32.7543
1	17.8937	-6.95	6.95	1.205543	48.868081	71.675	65.24221	106.611	73.98967	32.6211

Table E3. Consolidated drained triaxial data at 62.05 kPa confinement

Axial Deflection (in)	Axial Strain (%)	Volume Change (cm^3)	Corrected VC (cm^3)	Volume Change (%)	Corrected Area (cm^2)	Axial Load (lb)	Axial Stress (kPa)	σ 1 (kPa)	p (kPa)	q (kPa)
0	0	0	0	0	40.599503	0.00	0	62.0528	62.05284	0
0.02	0.35794	-0.257	0.257	0.044602	40.727173	9.15	9.993626	72.0465	67.04965	4.99681
0.04	0.71588	-0.514	0.514	0.089205	40.855764	42.70	46.49013	108.543	85.29791	23.2451
0.06	1.07382	-0.771	0.771	0.133807	40.985285	54.29	58.92209	120.975	91.51388	29.461
0.08	1.43175	-1.028	1.028	0.178409	41.115747	59.48	64.34466	126.398	94.22517	32.1723
0.1	1.78969	-1.285	1.285	0.223011	41.247159	63.75	68.74456	130.797	96.42512	34.3723
0.12	2.14763	-1.542	1.542	0.267614	41.379533	66.49	71.47547	133.528	97.79057	35.7377
0.14	2.50557	-1.799	1.799	0.312216	41.512879	68.32	73.20677	135.26	98.65623	36.6034
0.16	2.86351	-1.756	1.756	0.304753	41.668969	68.93	73.58373	135.637	98.8447	36.7919
0.18	3.22145	-2.013	2.013	0.349356	41.804372	69.54	73.99447	136.047	99.05007	36.9972
0.2	3.57939	-2.27	2.27	0.393958	41.940781	70.15	74.40077	136.454	99.25322	37.2004
0.22	3.93732	-2.227	2.227	0.386495	42.10021	69.85	73.79676	135.85	98.95122	36.8984
0.24	4.29526	-2.484	2.484	0.431098	42.238745	70.46	74.19712	136.25	99.1514	37.0986
0.26	4.6532	-2.641	2.641	0.458345	42.38571	70.46	73.93986	135.993	99.02277	36.9699
0.28	5.01114	-2.798	2.798	0.485592	42.533783	71.37	74.63937	136.692	99.37252	37.3197
0.3	5.36908	-2.955	2.955	0.51284	42.682975	71.37	74.37847	136.431	99.24208	37.1892
0.32	5.72702	-3.112	3.112	0.540087	42.833301	71.98	74.75092	136.804	99.4283	37.3755
0.34	6.08496	-3.369	3.369	0.584689	42.97727	72.29	74.8162	136.869	99.46094	37.4081
0.36	6.44289	-3.426	3.426	0.594582	43.137403	72.90	75.16748	137.22	99.63658	37.5837
0.38	6.80083	-3.583	3.583	0.621829	43.291206	73.81	75.8406	137.893	99.97314	37.9203
0.4	7.15877	-3.74	3.74	0.649076	43.446195	74.73	76.50687	138.56	100.3063	38.2534
0.42	7.51671	-3.797	3.797	0.658968	43.610003	75.64	77.1528	139.206	100.6292	38.5764
0.44	7.87465	-3.954	3.954	0.686216	43.767435	75.95	77.18526	139.238	100.6455	38.5926
0.46	8.23259	-4.111	4.111	0.713463	43.926095	76.56	77.52419	139.577	100.8149	38.7621
0.48	8.59053	-4.368	4.368	0.758065	44.078289	77.47	78.1799	140.233	101.1428	39.0899
0.5	8.94846	-4.425	4.425	0.767958	44.247157	78.08	78.49476	140.548	101.3002	39.2474
0.52	9.3064	-4.682	4.682	0.81256	44.40182	78.69	78.83245	140.885	101.4691	39.4162
0.54	9.66434	-4.639	4.639	0.805097	44.581108	79.30	79.12406	141.177	101.6149	39.562
0.56	10.0223	-4.596	4.596	0.797635	44.761823	79.91	79.41081	141.464	101.7582	39.7054
0.58	10.3802	-4.653	4.653	0.807527	44.936118	79.61	78.80088	140.854	101.4533	39.4004
0.6	10.7382	-4.91	4.91	0.852129	45.096025	80.22	79.12315	141.176	101.6144	39.5616
0.62	11.0961	-4.967	4.967	0.862022	45.27307	80.52	79.11341	141.166	101.6095	39.5567
0.64	11.454	-5.224	5.224	0.906624	45.435631	81.13	79.42755	141.48	101.7666	39.7138
0.66	11.812	-5.281	5.281	0.916516	45.615491	81.44	79.41179	141.465	101.7587	39.7059
0.68	12.1699	-5.438	5.438	0.943764	45.788796	82.05	79.70382	141.757	101.9048	39.8519
0.7	12.5278	-5.495	5.495	0.953656	45.971573	82.35	79.68205	141.735	101.8939	39.841
0.72	12.8858	-5.552	5.552	0.963548	46.155853	82.35	79.36391	141.417	101.7348	39.682
0.74	13.2437	-5.709	5.709	0.990796	46.333531	82.96	79.6452	141.698	101.8754	39.8226
0.76	13.6017	-5.966	5.966	1.035398	46.504527	83.88	80.22756	142.28	102.1666	40.1138
0.78	13.9596	-6.023	6.023	1.04529	46.693324	84.49	80.48428	142.537	102.295	40.2421
0.8	14.3175	-6.28	6.28	1.089893	46.867251	85.10	80.76456	142.817	102.4351	40.3823
0.82	14.6755	-6.237	6.237	1.08243	47.067411	85.71	80.99759	143.05	102.5516	40.4988
0.84	15.0334	-6.394	6.394	1.109677	47.252672	86.62	81.54138	143.594	102.8235	40.7707
0.86	15.3914	-6.451	6.451	1.11957	47.447829	87.23	81.77787	143.831	102.9418	40.8889
0.88	15.7493	-6.608	6.608	1.146817	47.63628	87.84	82.02396	144.077	103.0648	41.012
0.9	16.1072	-6.765	6.765	1.174064	47.82634	87.84	81.698	143.751	102.9018	40.849
0.92	16.4652	-7.022	7.022	1.218667	48.009594	88.15	81.66875	143.722	102.8872	40.8344
0.94	16.8231	-7.079	7.079	1.228559	48.211367	88.76	81.88977	143.943	102.9977	40.9449
0.96	17.1811	-7.036	7.036	1.221096	48.423392	89.37	82.09156	144.144	103.0986	41.0458
0.98	17.539	-7.093	7.093	1.230989	48.628713	89.98	82.30294	144.356	103.2043	41.1515
1	17.8969	-7.25	7.25	1.258236	48.827242	94.25	85.85832	147.911	104.982	42.9292

APPENDIX F

UNCONSOLIDATED UNDRAINED TRIAXIAL DATA

Table F1. Unconsolidated undrained data for clay at 62.05 kPa confinement

Axial Deflection (in)	Axial Strain (%)	Volume Change (cm^3)	Corrected VC (cm^3)	Volume Change (%)	Corrected Area (cm^2)	Axial Load (lb)	Axial Stress (kPa)	σ 1 (kPa)	p (kPa)	q (kPa)
0	0	0	0	0	40.715041	0	0	62.0528	62.05284	0
0.02	0.35775	-0.257	0.257	0.044452	40.843057	3.7	3.986108	66.0389	64.04589	1.99305
0.04	0.71549	-0.314	0.314	0.054311	40.986181	13.7	14.89571	76.9485	69.50069	7.44785
0.06	1.07324	-0.471	0.471	0.081466	41.123222	21.0	22.76397	84.8168	73.43483	11.382
0.08	1.43099	-0.728	0.728	0.125918	41.254114	27.5	29.59793	91.6508	76.85181	14.799
0.1	1.78873	-0.385	0.385	0.066591	41.428982	32.9	35.3676	97.4204	79.73664	17.6838
0.12	2.14648	-0.442	0.442	0.07645	41.576341	37.8	40.46332	102.516	82.2845	20.2317
0.14	2.50423	-0.799	0.799	0.138199	41.703113	40.9	43.59357	105.646	83.84962	21.7968
0.16	2.86197	-1.056	1.056	0.18265	41.838068	43.3	46.04716	108.1	85.07642	23.0236
0.18	3.21972	-1.313	1.313	0.227102	41.974021	44.8	47.51414	109.567	85.80991	23.7571
0.2	3.57746	-1.57	1.57	0.271554	42.110983	46.1	48.6483	110.701	86.37699	24.3241
0.22	3.93521	-2.027	2.027	0.350599	42.234303	51.5	54.28845	116.341	89.19707	27.1442
0.24	4.29296	-2.384	2.384	0.412347	42.365904	52.8	55.40076	117.454	89.75322	27.7004
0.26	4.6507	-2.641	2.641	0.456799	42.505878	53.4	55.85669	117.91	89.98118	27.9283
0.28	5.00845	-2.898	2.898	0.501251	42.646906	53.4	55.67197	117.725	89.88883	27.836
0.3	5.3662	-3.255	3.255	0.562999	42.781558	54.0	56.131	118.184	90.11834	28.0655
0.32	5.72394	-3.612	3.612	0.624747	42.917233	54.3	56.26967	118.323	90.18768	28.1348
0.34	6.08169	-3.869	3.869	0.669199	43.061439	54.9	56.71136	118.764	90.40852	28.3557
0.36	6.43944	-4.126	4.126	0.713651	43.206749	55.2	56.83464	118.887	90.47016	28.4173
0.38	6.79718	-4.483	4.483	0.7754	43.345618	55.5	56.96555	119.018	90.53561	28.4828
0.4	7.15493	-4.74	4.74	0.819851	43.493142	56.1	57.3962	119.449	90.75094	28.6981
0.42	7.51268	-5.097	5.097	0.8816	43.634193	56.4	57.52159	119.574	90.81363	28.7608
0.44	7.87042	-5.354	5.354	0.926052	43.783983	57.0	57.94453	119.997	91.0251	28.9723
0.46	8.22817	-5.611	5.611	0.970503	43.934941	57.6	58.36303	120.416	91.23436	29.1815
0.48	8.58592	-5.968	5.968	1.032252	44.079377	58.6	59.09516	121.148	91.60042	29.5476
0.5	8.94366	-6.325	6.325	1.094	44.224948	59.5	59.82096	121.874	91.96332	29.9105
0.52	9.30141	-6.582	6.582	1.138452	44.379432	60.1	60.22414	122.277	92.16491	30.1121
0.54	9.65915	-6.939	6.939	1.2002	44.527344	60.7	60.63346	122.686	92.36957	30.3167
0.56	10.0169	-7.096	7.096	1.227356	44.692085	60.7	60.40996	122.463	92.25782	30.205
0.58	10.3746	-7.253	7.253	1.254511	44.85814	60.7	60.18634	122.239	92.14601	30.0932
0.6	10.7324	-7.41	7.41	1.281666	45.025527	60.4	59.66127	121.714	91.88347	29.8306
0.62	11.0901	-7.567	7.567	1.308822	45.194261	61.0	60.03891	122.092	92.0723	30.0195
0.64	11.4479	-7.724	7.724	1.335977	45.364358	61.0	59.81379	121.867	91.95974	29.9069
0.66	11.8056	-7.881	7.881	1.363133	45.535835	61.0	59.58855	121.641	91.84711	29.7943
0.68	12.1634	-8.038	8.038	1.390288	45.708708	61.3	59.65999	121.713	91.88284	29.83
0.7	12.5211	-8.295	8.295	1.43474	45.874946	61.0	59.14806	121.201	91.62687	29.574
0.72	12.8789	-8.452	8.452	1.461895	46.050632	61.3	59.21702	121.27	91.66135	29.6085
0.74	13.2366	-8.609	8.609	1.489051	46.227767	61.6	59.2836	121.336	91.69464	29.6418
0.76	13.5944	-8.666	8.666	1.49891	46.414519	61.6	59.04507	121.098	91.57537	29.5225
0.78	13.9521	-8.723	8.723	1.508769	46.602823	61.9	59.09761	121.15	91.60164	29.5488
0.8	14.3099	-8.78	8.78	1.518628	46.7927	62.5	59.43768	121.491	91.77168	29.7188
0.82	14.6676	-8.937	8.937	1.545783	46.975917	62.2	58.91705	120.97	91.51137	29.4585
0.84	15.0254	-9.094	9.094	1.572938	47.160676	63.1	59.54927	121.602	91.82747	29.7746
0.86	15.3831	-9.251	9.251	1.600094	47.346997	63.4	59.60147	121.654	91.85358	29.8007
0.88	15.7408	-9.508	9.508	1.644546	47.526543	63.4	59.37631	121.429	91.741	29.6882
0.9	16.0986	-9.665	9.665	1.671701	47.716013	63.7	59.42487	121.478	91.76527	29.7124
0.92	16.4563	-9.822	9.822	1.698857	47.907106	63.7	59.18783	121.241	91.64676	29.5939
0.94	16.8141	-9.979	9.979	1.726012	48.099842	64.1	59.23273	121.286	91.6692	29.6164
0.96	17.1718	-10.136	10.136	1.753167	48.294244	63.7	58.71337	120.766	91.40953	29.3567
0.98	17.5296	-10.293	10.293	1.780323	48.490332	64.1	58.75573	120.809	91.43071	29.3779
1	17.8873	-10.45	10.45	1.807478	48.688129	64.1	58.51703	120.57	91.31136	29.2585

Table F2. Unconsolidated undrained triaxial data at 82.73 kPa confinement

Axial Deflection (in)	Axial Strain (%)	Volume Change (cm^3)	Corrected VC (cm^3)	Volume Change (%)	Corrected Area (cm^2)	Axial Load (lb)	Axial Stress (kPa)	σ 1 (kPa)	p (kPa)	q (kPa)
0	0	0	0	0	40.715041	0	0	82.7371	82.73712	0
0.02	0.35775	-0.257	0.257	0.044452	40.843057	11.285	12.2905	95.0276	88.88237	6.14525
0.04	0.71549	-0.414	0.414	0.071607	40.979088	15.86	17.2158	99.9529	91.34502	8.6079
0.06	1.07324	-0.671	0.671	0.116059	41.108985	20.435	22.1118	104.849	93.79302	11.0559
0.08	1.43099	-0.828	0.828	0.143215	41.246969	24.705	26.64275	109.38	96.0585	13.3214
0.1	1.78873	-1.085	1.085	0.187666	41.378788	28.365	30.49238	113.229	97.98331	15.2462
0.12	2.14648	-1.242	1.242	0.214822	41.518768	32.025	34.31081	117.048	99.89252	17.1554
0.14	2.50423	-1.499	1.499	0.259274	41.652551	34.465	36.80637	119.543	101.1403	18.4032
0.16	2.86197	-1.756	1.756	0.303726	41.78732	36.6	38.96035	121.697	102.2173	19.4802
0.18	3.21972	-1.913	1.913	0.330881	41.930362	37.82	40.12169	122.859	102.798	20.0608
0.2	3.57746	-2.07	2.07	0.358036	42.074465	41.175	43.53126	126.268	104.5028	21.7656
0.22	3.93521	-2.327	2.327	0.402488	42.212311	44.835	47.24592	129.983	106.3601	23.623
0.24	4.29296	-2.484	2.484	0.429644	42.358546	45.75	48.04369	130.781	106.759	24.0218
0.26	4.6507	-2.641	2.641	0.456799	42.505878	46.36	48.51552	131.253	106.9949	24.2578
0.28	5.00845	-2.898	2.898	0.501251	42.646906	47.275	49.30946	132.047	107.3919	24.6547
0.3	5.3662	-3.055	3.055	0.528406	42.796441	48.19	50.08821	132.825	107.7812	25.0441
0.32	5.72394	-3.312	3.312	0.572858	42.939642	48.8	50.55308	133.29	108.0137	25.2765
0.34	6.08169	-3.469	3.469	0.600014	43.091432	49.715	51.31954	134.057	108.3969	25.6598
0.36	6.43944	-3.726	3.726	0.644465	43.236856	50.63	52.08829	134.825	108.7813	26.0441
0.38	6.79718	-3.883	3.883	0.671621	43.390953	51.24	52.52864	135.266	109.0014	26.2643
0.4	7.15493	-4.14	4.14	0.716073	43.538651	51.24	52.35045	135.088	108.9123	26.1752
0.42	7.51268	-4.397	4.397	0.760525	43.687493	56.425	57.45141	140.189	111.4628	28.7257
0.44	7.87042	-4.654	4.654	0.804976	43.83749	57.95	58.80226	141.539	112.1383	29.4011
0.46	8.22817	-4.811	4.811	0.832132	43.99633	58.865	59.51507	142.252	112.4947	29.7575
0.48	8.58592	-5.068	5.068	0.876584	44.14871	59.475	59.92426	142.661	112.6993	29.9621
0.5	8.94366	-5.225	5.225	0.903739	44.310022	60.695	60.93085	143.668	113.2025	30.4654
0.52	9.30141	-5.482	5.482	0.948191	44.464841	61.305	61.32893	144.066	113.4016	30.6645
0.54	9.65915	-5.839	5.839	1.009939	44.613091	61.915	61.73335	144.47	113.6038	30.8667
0.56	10.0169	-6.096	6.096	1.054391	44.770346	62.525	62.12258	144.86	113.7984	31.0613
0.58	10.3746	-6.353	6.353	1.098843	44.928857	63.135	62.50735	145.244	113.9908	31.2537
0.6	10.7324	-6.71	6.71	1.160591	45.080749	63.135	62.29674	145.034	113.8855	31.1484
0.62	11.0901	-7.067	7.067	1.22234	45.233864	63.44	62.3858	145.123	113.93	31.1929
0.64	11.4479	-7.424	7.424	1.284088	45.388216	64.05	62.77147	145.509	114.1229	31.3857
0.66	11.8056	-7.681	7.681	1.32854	45.551805	64.05	62.54604	145.283	114.0101	31.273
0.68	12.1634	-8.038	8.038	1.390288	45.708708	64.66	62.92497	145.662	114.1996	31.4625
0.7	12.5211	-8.395	8.395	1.452036	45.866896	64.965	63.00374	145.741	114.239	31.5019
0.72	12.8789	-8.752	8.752	1.513785	46.026382	65.575	63.37496	146.112	114.4246	31.6875
0.74	13.2366	-9.009	9.009	1.558236	46.1953	65.88	63.43691	146.174	114.4556	31.7185
0.76	13.5944	-9.466	9.466	1.637281	46.349317	66.795	64.10426	146.841	114.7892	32.0521
0.78	13.9521	-9.823	9.823	1.69903	46.512798	67.405	64.46232	147.199	114.9683	32.2312
0.8	14.3099	-10.18	10.18	1.760778	46.677645	68.015	64.81597	147.553	115.1451	32.408
0.82	14.6676	-10.437	10.437	1.80523	46.852126	68.93	65.44331	148.18	115.4588	32.7217
0.84	15.0254	-10.694	10.694	1.849682	47.028076	68.93	65.19846	147.936	115.3363	32.5992
0.86	15.3831	-10.951	10.951	1.894133	47.205514	69.54	65.5282	148.265	115.5012	32.7641
0.88	15.7408	-11.008	11.008	1.903992	47.401175	69.845	65.54393	148.281	115.5091	32.772
0.9	16.0986	-11.065	11.065	1.913851	47.598504	70.15	65.55724	148.294	115.5157	32.7786
0.92	16.4563	-11.222	11.222	1.941007	47.789094	70.76	65.86357	148.601	115.6689	32.9318
0.94	16.8141	-11.379	11.379	1.968162	47.981323	71.37	66.16522	148.902	115.8197	33.0826
0.96	17.1718	-11.536	11.536	1.995318	48.175212	71.37	65.89892	148.636	115.6866	32.9495
0.98	17.5296	-11.693	11.693	2.022473	48.370784	71.37	65.63248	148.37	115.5534	32.8162
1	17.8873	-11.75	11.75	2.032332	48.576636	71.065	65.07506	147.812	115.2747	32.5375

Table F3. Unconsolidated undrained data at 103.42 kPa confinement

Axial Deflection (in)	Axial Strain (%)	Volume Change (cm^3)	Corrected VC (cm^3)	Volume Change (%)	Corrected Area (cm^2)	Axial Load (lb)	Axial Stress (kPa)	σ 1 (kPa)	p (kPa)	q (kPa)
0	0	0	0	0	40.71504	0	0	103.4214	103.4214	0
0.02	0.3577	-0.257	0.257	0.04445	40.84306	10.065	10.9618	114.3832	108.9023	5.4808991
0.04	0.7155	-0.514	0.514	0.0889	40.972	16.775	18.21217	121.6336	112.5275	9.1060845
0.06	1.0732	-0.771	0.771	0.13336	41.10187	21.96	23.76605	127.1875	115.3044	11.883026
0.08	1.431	-1.028	1.028	0.17781	41.23268	26.535	28.62621	132.0476	117.7345	14.313103
0.1	1.7887	-1.285	1.285	0.22226	41.36445	30.5	32.79887	136.2203	119.8208	16.399435
0.12	2.1465	-1.542	1.542	0.26671	41.49718	34.16	36.61724	140.0386	121.73	18.308618
0.14	2.5042	-1.799	1.799	0.31116	41.63088	37.21	39.75853	143.1799	123.3007	19.879265
0.16	2.862	-2.056	2.056	0.35561	41.76557	39.955	42.55386	145.9753	124.6983	21.276931
0.18	3.2197	-2.313	2.313	0.40007	41.90126	42.395	45.00636	148.4278	125.9246	22.503178
0.2	3.5775	-2.57	2.57	0.44452	42.03795	44.53	47.11915	150.5406	126.981	23.559575
0.22	3.9352	-2.827	2.827	0.48897	42.17566	46.665	49.21706	152.6385	128.0299	24.60853
0.24	4.293	-3.084	3.084	0.53342	42.3144	48.19	50.65882	154.0802	128.7508	25.329408
0.26	4.6507	-3.341	3.341	0.57787	42.45418	49.41	51.7703	155.1917	129.3066	25.88515
0.28	5.0085	-3.598	3.598	0.62233	42.59501	50.02	52.23616	155.6576	129.5395	26.118078
0.3	5.3662	-3.855	3.855	0.66678	42.73691	50.63	52.69763	156.119	129.7702	26.348815
0.32	5.7239	-4.112	4.112	0.71123	42.87988	51.24	53.15471	156.5761	129.9988	26.577357
0.34	6.0817	-4.369	4.369	0.75568	43.02395	51.545	53.29206	156.7135	130.0674	26.646032
0.36	6.4394	-4.626	4.626	0.80013	43.16911	52.46	54.05569	157.4771	130.4492	27.027845
0.38	6.7972	-4.883	4.883	0.84459	43.31539	53.07	54.49957	157.921	130.6712	27.249785
0.4	7.1549	-5.14	5.14	0.88904	43.4628	53.68	54.93904	158.3604	130.8909	27.469519
0.42	7.5127	-5.397	5.397	0.93349	43.61135	53.985	55.063	158.4844	130.9529	27.531498
0.44	7.8704	-5.654	5.654	0.97794	43.76105	53.985	54.87463	158.296	130.8587	27.437316
0.46	8.2282	-5.911	5.911	1.02239	43.91192	54.29	54.99506	158.4165	130.9189	27.497529
0.48	8.5859	-6.168	6.168	1.06684	44.06397	55.205	55.72897	159.1504	131.2859	27.864487
0.5	8.9437	-6.425	6.425	1.1113	44.21721	55.815	56.14949	159.5709	131.4961	28.074745
0.52	9.3014	-6.682	6.682	1.15575	44.37167	56.12	56.2598	159.6812	131.5513	28.129899
0.54	9.6592	-6.939	6.939	1.2002	44.52734	56.425	56.36779	159.7892	131.6053	28.183897
0.56	10.017	-7.196	7.196	1.24465	44.68426	57.035	56.77709	160.1985	131.8099	28.388546
0.58	10.375	-7.453	7.453	1.2891	44.84243	57.645	57.18193	160.6033	132.0124	28.590965
0.6	10.732	-7.71	7.71	1.33356	45.00186	57.95	57.28082	160.7022	132.0618	28.64041
0.62	11.09	-7.967	7.967	1.37801	45.16258	58.255	57.37738	160.7988	132.1101	28.688692
0.64	11.448	-8.224	8.224	1.42246	45.32459	58.56	57.47161	160.893	132.1572	28.735807
0.66	11.806	-8.481	8.481	1.46691	45.48793	59.17	57.86177	161.2832	132.3523	28.930884
0.68	12.163	-8.738	8.738	1.51136	45.65259	59.475	57.95025	161.3717	132.3965	28.975126
0.7	12.521	-8.995	8.995	1.55581	45.81859	59.475	57.74029	161.1617	132.2915	28.870144
0.72	12.879	-9.252	9.252	1.60027	45.98597	59.475	57.53014	160.9515	132.1865	28.765068
0.74	13.237	-9.509	9.509	1.64472	46.15472	59.78	57.61374	161.0351	132.2283	28.80687
0.76	13.594	-9.766	9.766	1.68917	46.32487	60.085	57.695	161.1164	132.2689	28.847498
0.78	13.952	-10.023	10.023	1.73362	46.49643	60.39	57.7739	161.1953	132.3083	28.88695
0.8	14.31	-10.28	10.28	1.77807	46.66943	60.39	57.55974	160.9811	132.2013	28.77987
0.82	14.668	-10.537	10.537	1.82253	46.84387	60.695	57.63501	161.0564	132.2389	28.817505
0.84	15.025	-10.794	10.794	1.86698	47.01979	60.695	57.41938	160.8408	132.1311	28.70969
0.86	15.383	-11.051	11.051	1.91143	47.19719	61	57.49101	160.9124	132.1669	28.745505
0.88	15.741	-11.308	11.308	1.95588	47.3761	61	57.2739	160.6953	132.0584	28.636951
0.9	16.099	-11.565	11.565	2.00033	47.55654	61.305	57.34188	160.7633	132.0923	28.67094
0.92	16.456	-11.822	11.822	2.04479	47.73852	61.61	57.40749	160.8289	132.1251	28.703744
0.94	16.814	-12.079	12.079	2.08924	47.92206	61.61	57.18761	160.609	132.0152	28.593806
0.96	17.172	-12.336	12.336	2.13369	48.10719	61.61	56.96754	160.3889	131.9052	28.483768
0.98	17.53	-12.593	12.593	2.17814	48.29393	61.915	57.02819	160.4496	131.9355	28.514094
1	17.887	-12.85	12.85	2.22259	48.4823	61.915	56.80662	160.228	131.8247	28.40331

APPENDIX G

OEDOMETER DATA

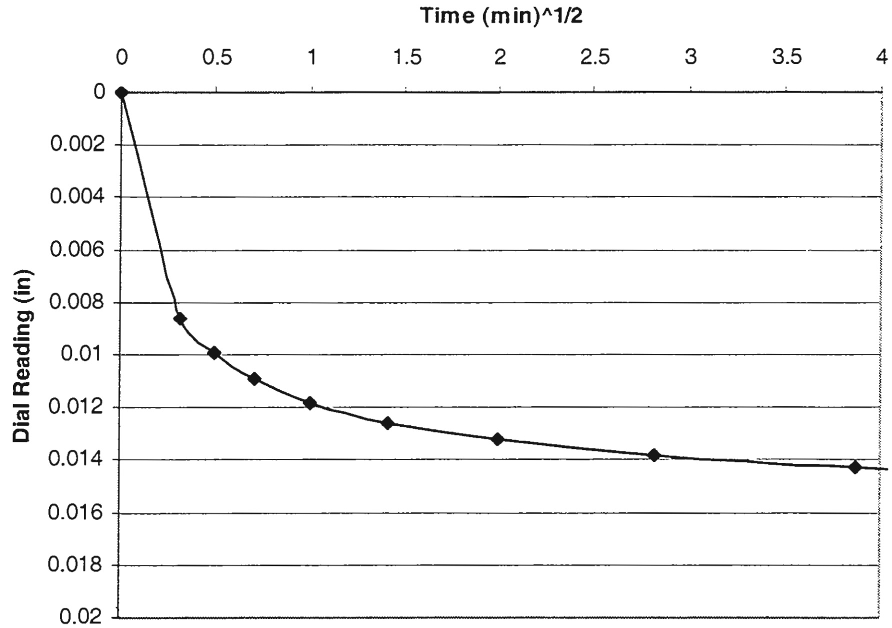

Figure G1. Oedometer data for test one, 50 kPa load increment

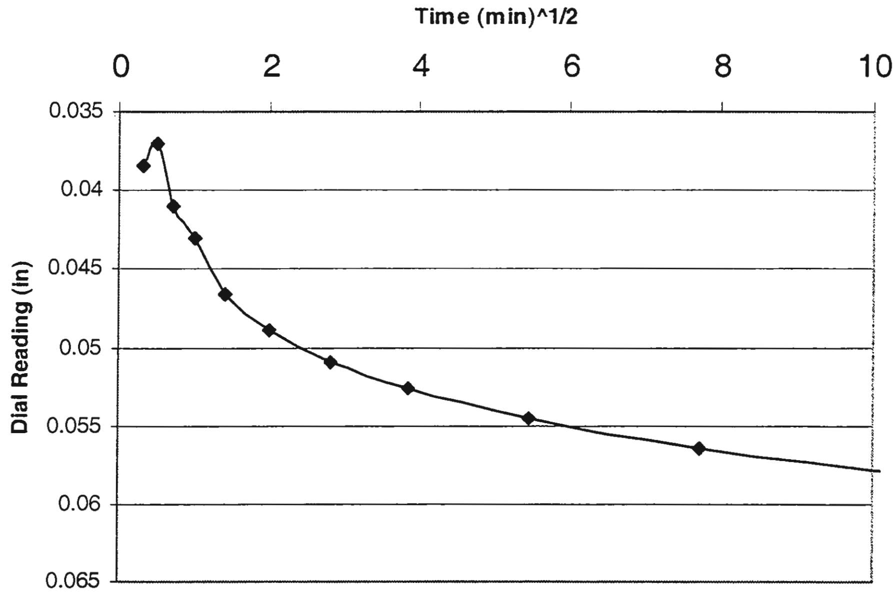

Figure G2. Oedometer data for test one, 99 kPa load increment

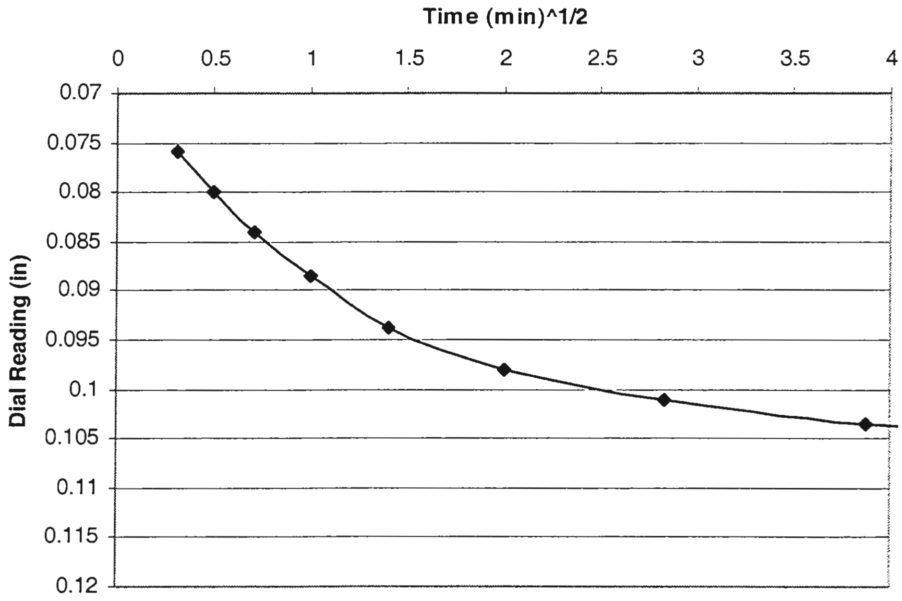

Figure G3. Oedometer data for test one, 196 kPa load increment

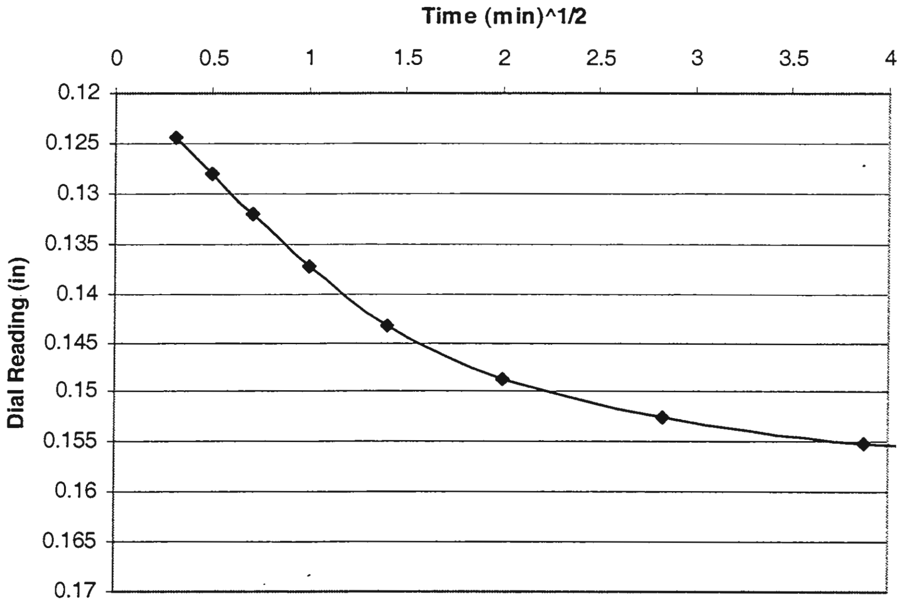

Figure G4. Oedometer data for test one, 392 kPa load increment

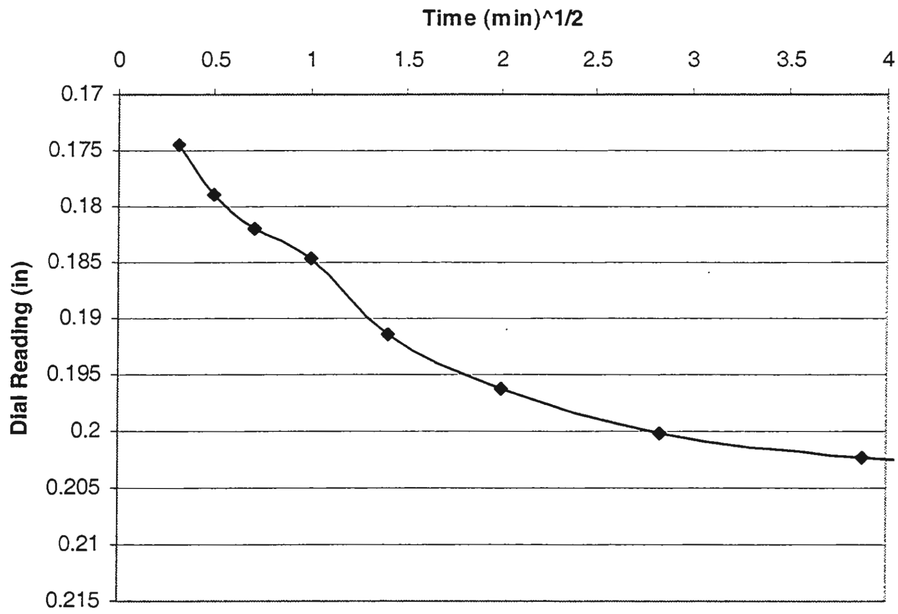

Figure G5. Oedometer data for test one, 783 kPa load increment

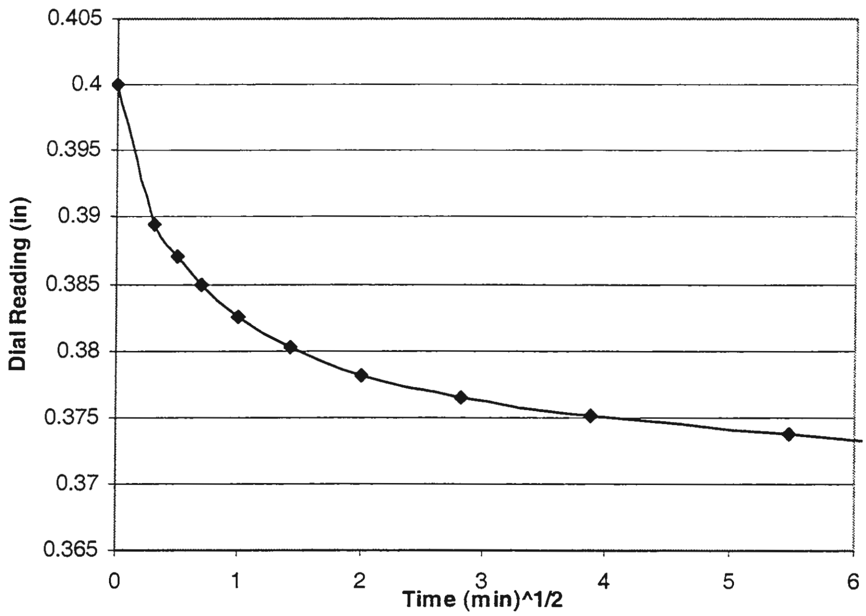

Figure G6. Oedometer data for test two, 50 kPa load increment

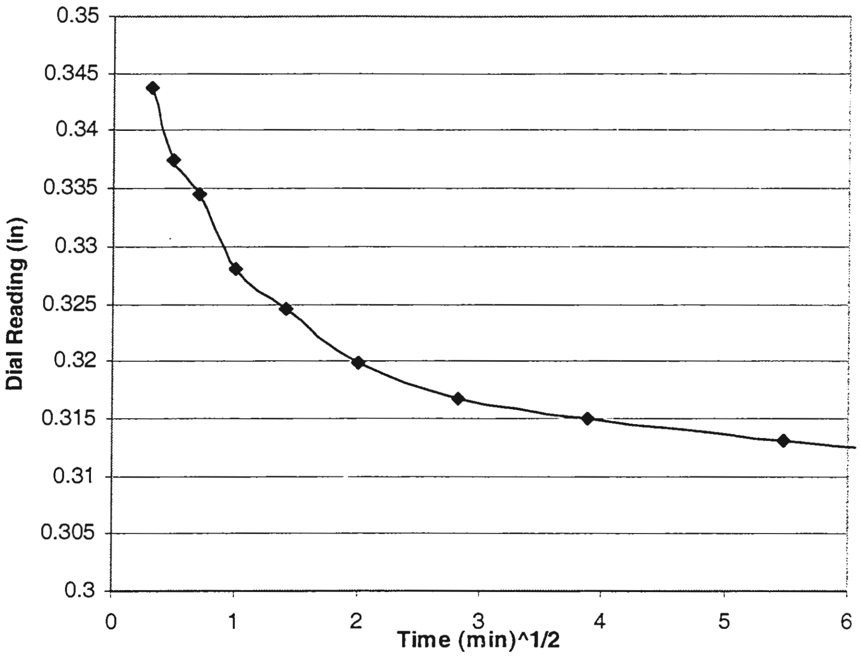

Figure G7. Oedometer data for test two, 99 kPa load increment

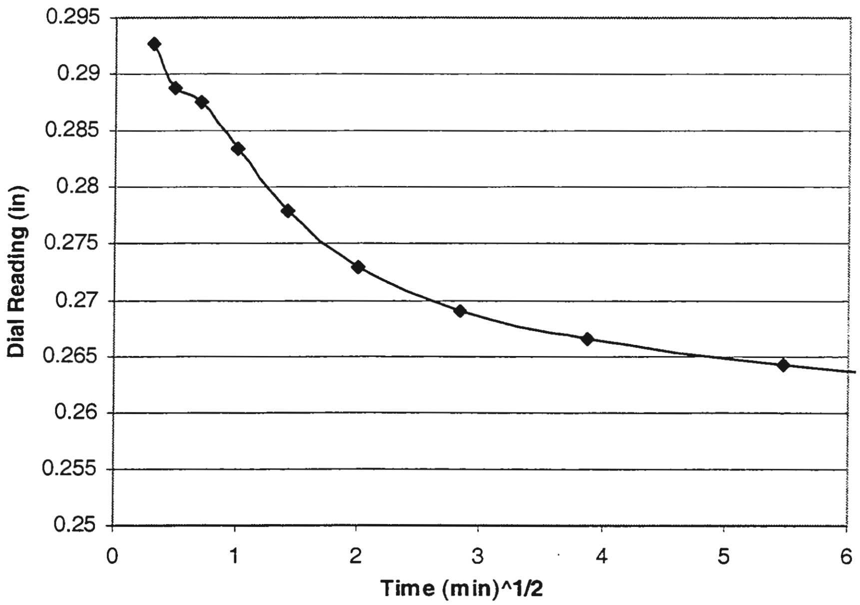

Figure G8. Oedometer data for test two, 196 kPa load increment

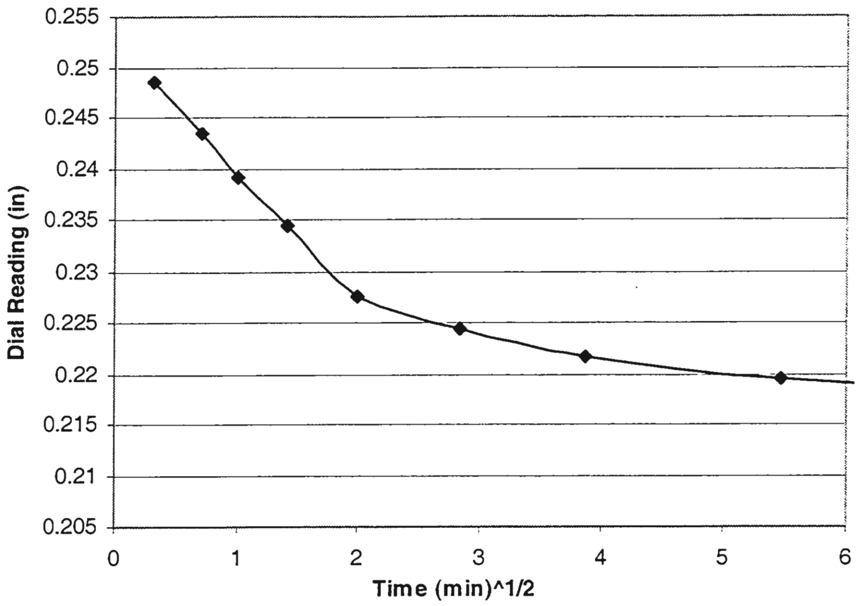

Figure G9. Oedometer data for test two, 392 kPa load increment

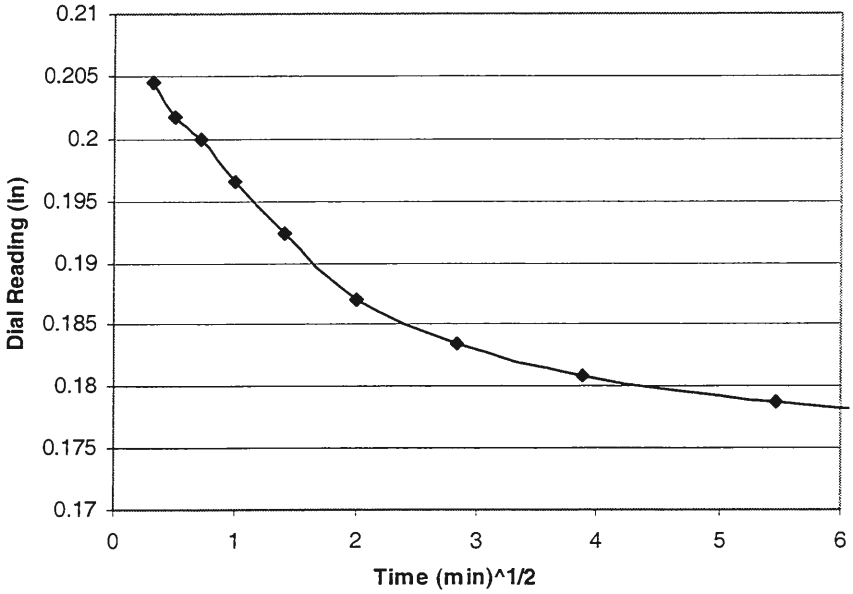

Figure G10. Oedometer data for test two, 783 kPa load increment

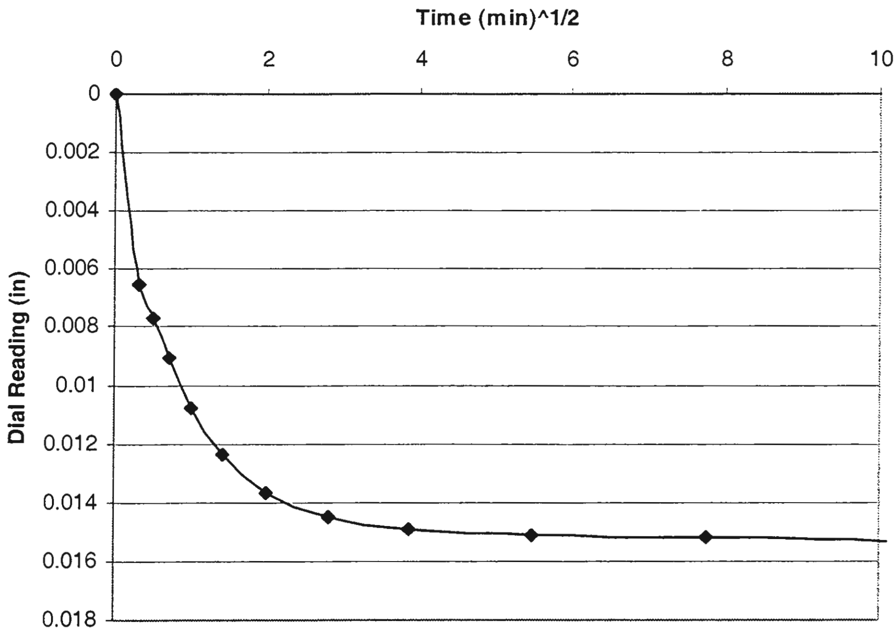

Figure G11. Oedometer data for test three, 50 kPa load increment

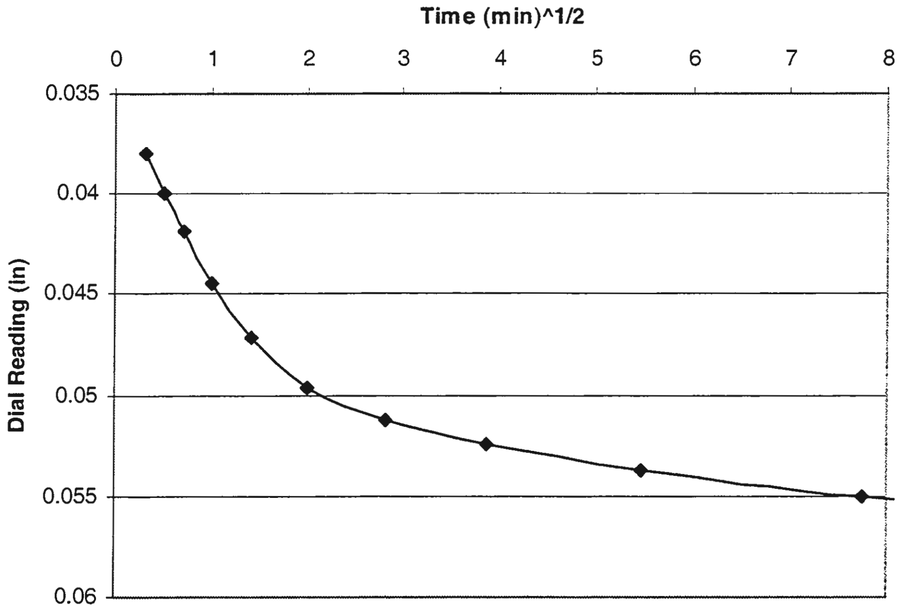

Figure G12. Oedometer data for test three, 99 kPa load increment

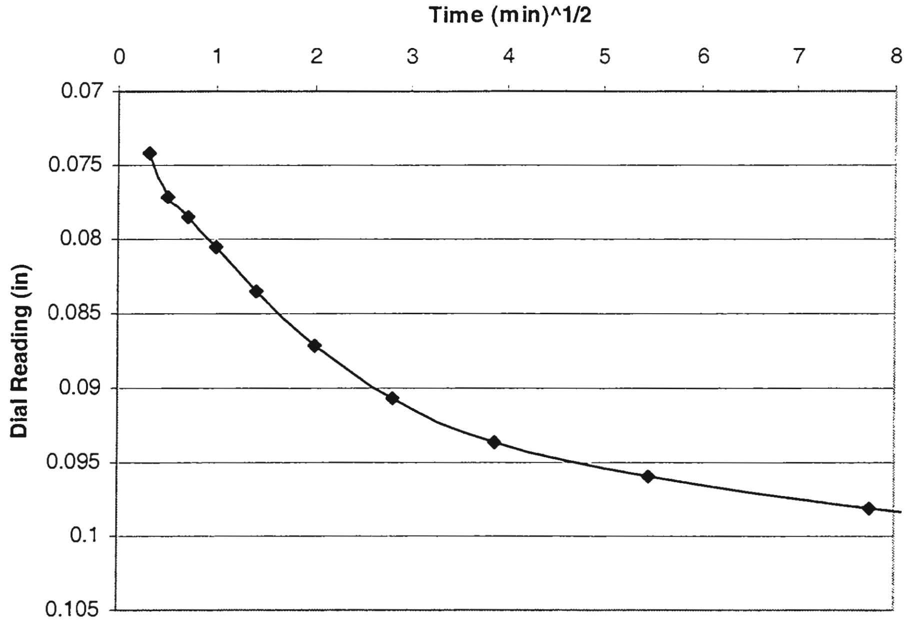

Figure G13. Oedometer data for test three, 196 kPa load increment

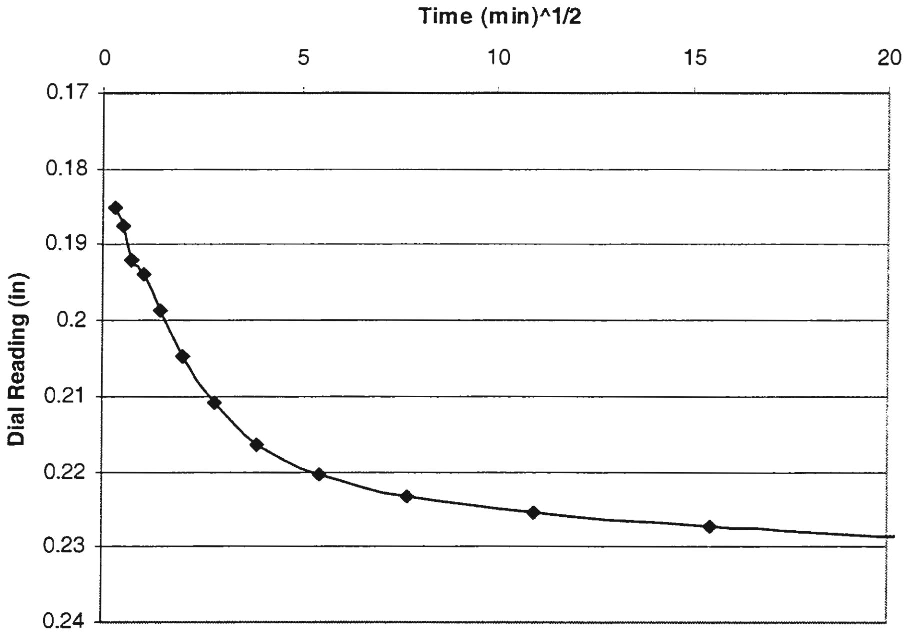

Figure G14. Oedometer data for test three, 783 kPa load increment

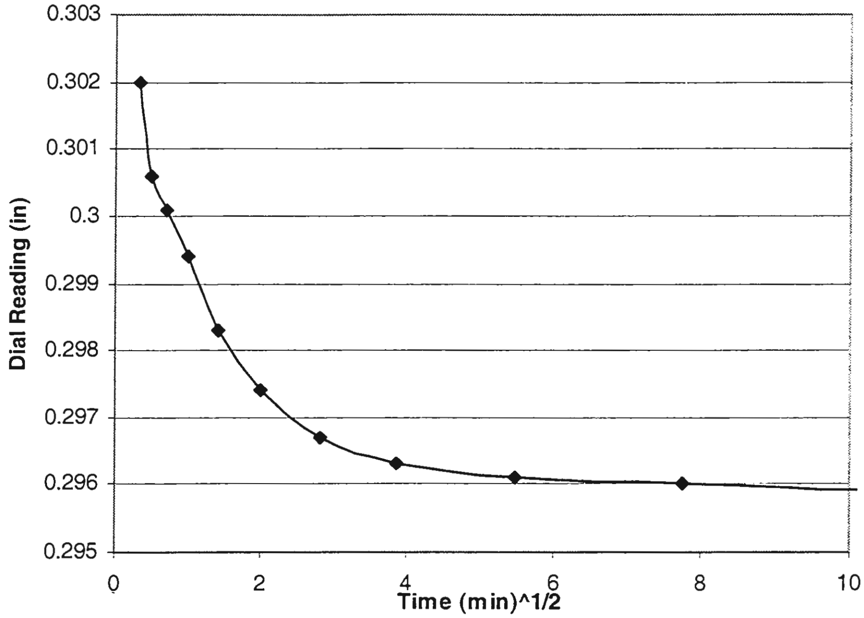

Figure G15. Oedometer data for test four, 50 kPa load increment

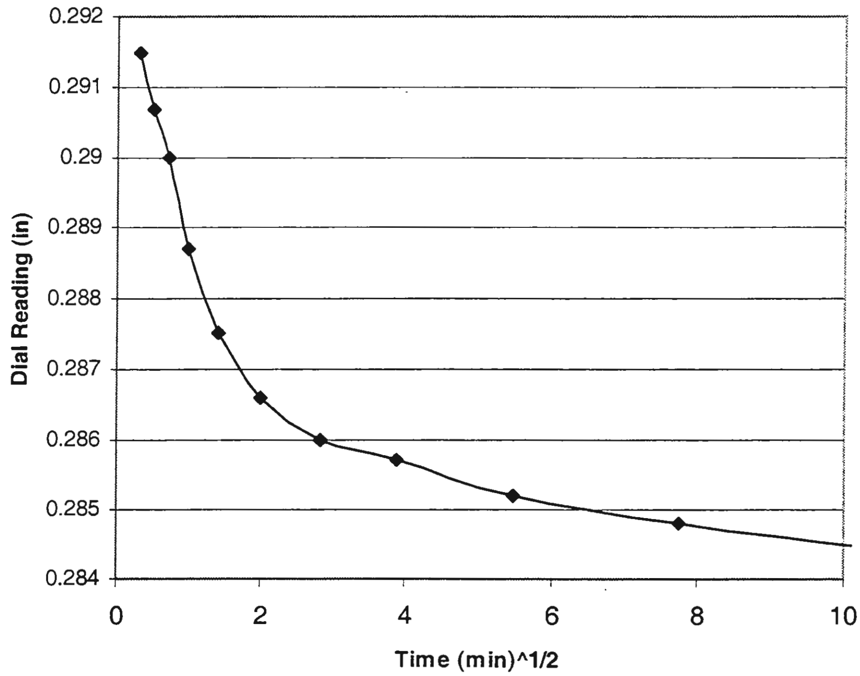

Figure G16. Oedometer data for test four, 99 kPa load increment

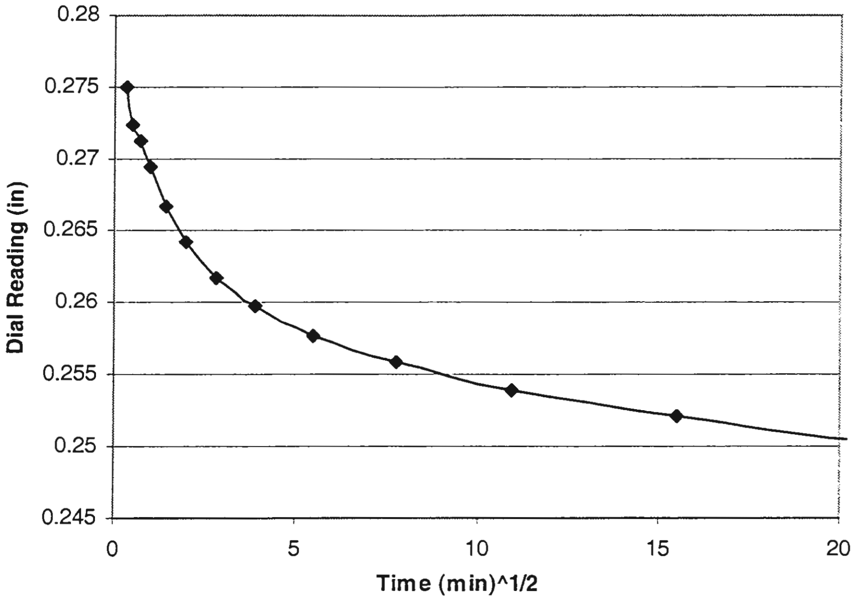

Figure G17. Oedometer data for test four, 196 kPa load increment

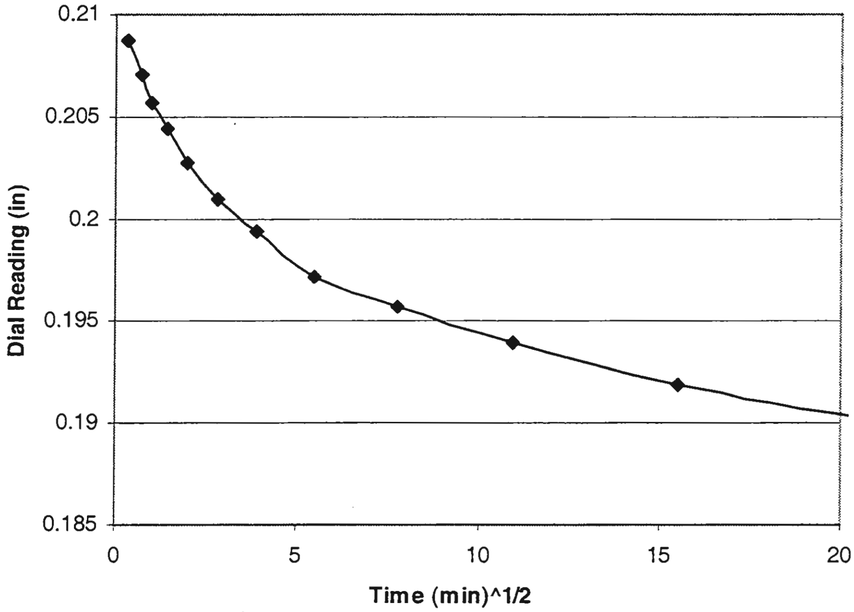

Figure G18. Oedometer data for test four, 392 kPa load increment

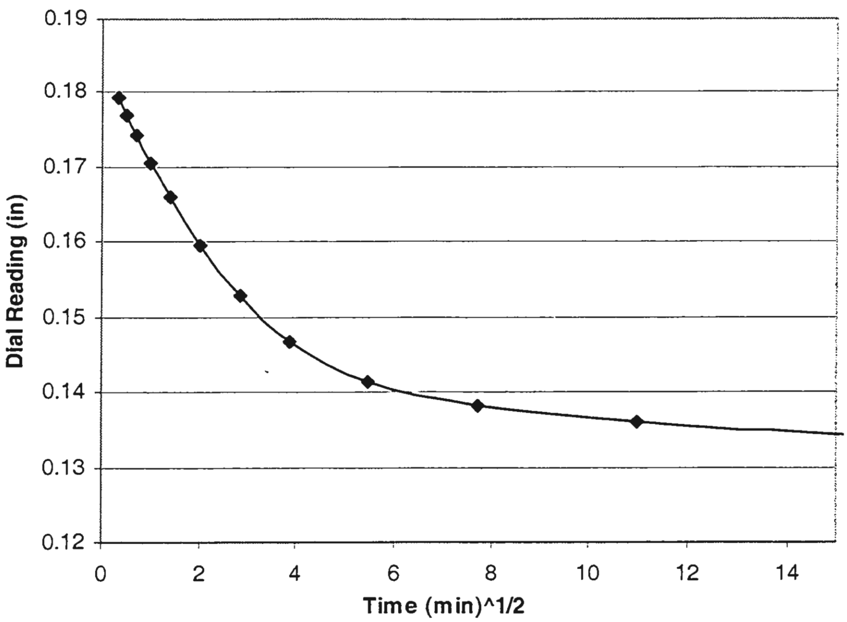

Figure G19. Oedometer data for test four, 783 kPa load increment

APPENDIX H

INDIVIDUAL LOAD TEST DATA

Table H1. Load test data for individual pier one

Stress		Gauge Pressure (psi)			Dial Reading (in)			Tell-Tale Reading (in)			Remarks
(kPa)	Load (tons)	planned	actual	time hr:min	#1	#2	Avg.	#1	#2	Avg.	
24	1.23	130	500	2:20	1.895	1.981	1.938	1.824	1.66	1.742	
81	4.17	440	500	3:39	1.854	1.949	1.9015	1.82	1.659	1.7395	
158	8.1	850	800	4:16	1.797	1.921	1.859	1.811	1.651	1.731	
239	12.27	1290	1200	4:48	1.739	1.873	1.806	1.795	1.637	1.716	
321	16.44	1720	1640	5:57	1.697	1.82	1.7585	1.781	1.626	1.7035	
397	20.37	2130	2100	7:16	1.644	1.778	1.711	1.774	1.617	1.6955	
479	24.54	2560	2450	8:30	1.581	1.714	1.6475	1.763	1.603	1.683	
560	28.72	2990	2900	9:56	1.513	1.636	1.5745	1.751	1.589	1.67	
637	32.64	3400	3250	11:01	1.4	1.52	1.46	1.733	1.565	1.649	
718	36.82	3800	3700	12:51	1.239	1.364	1.3015	1.703	1.524	1.6135	
878	45	4200	4500	12:56	1.044	1.156	1.1	1.665	1.462	1.5635	
718	36.82	3500	3500		1.058	1.17	1.114	1.66	1.465	1.5625	unload
479	24.54				1.109	1.222	1.1655	1.684	1.499	1.5915	
239	12.27				1.146	1.253	1.1995	1.692	1.563	1.6275	
81	4.17				1.229	1.326	1.2775	1.704	1.517	1.6105	
0	0				1.418	1.483	1.4505	1.719	1.536	1.6275	

Table H2. Inclinometer data 0.38 m from pier one, 0 load increment

Depth (ft)	A+	A-	Diff
34	492	-530	1022
32	511	-509	1020
30	473	-474	947
28	450	-446	896
26	457	-458	915
24	442	-439	881
22	451	-452	903
20	479	-479	958
18	491	-490	981
16	486	-485	971
14	439	-439	878
12	404	-403	807
10	406	-406	812
8	406	-406	812
6	365	-366	731
4	411	-415	826
2	417	-421	838

Table H3. Inclinometer data 0.38 m from pier one, 12.3 ton load increment

Depth (ft)	A+	A-	Diff
34	493	-530	1023
32	511	-510	1021
30	474	-474	948
28	449	-446	895
26	458	-458	916
24	442	-439	881
22	450	-452	902
20	479	-479	958
18	490	-490	980
16	486	-484	970
14	438	-440	878
12	403	-402	805
10	404	-405	809
8	402	-402	804
6	367	-366	733
4	428	-432	860
2	458	-474	932

Table H4. Inclinometer data 0.38 m from pier one, 20.37 ton load increment

Depth (ft)	A+	A-	Diff
34	493	-530	1023
32	511	-511	1022
30	474	-474	948
28	449	-448	897
26	458	-459	917
24	441	-440	881
22	450	-452	902
20	479	-480	959
18	490	-489	979
16	485	-485	970
14	438	-440	878
12	403	-402	805
10	404	-405	809
8	400	-399	799
6	368	-368	736
4	442	-446	888
2	461	-473	934

Table H5. Inclinometer data 0.38 m from pier one, 28.72 ton load increment

Depth (ft)	A+	A-	Diff
34	493	-530	1023
32	511	-509	1020
30	475	-473	948
28	449	-446	895
26	458	-458	916
24	441	-439	880
22	450	-451	901
20	479	-478	957
18	490	-489	979
16	485	-482	967
14	437	-438	875
12	402	-401	803
10	401	-402	803
8	395	-395	790
6	370	-369	739
4	465	-468	933
2	452	-460	912

Table H6. Inclinometer data 0.38 m from pier one, 45 ton load increment

Depth (ft)	A+	A-	Diff
34	493	-530	1023
32	511	-510	1021
30	474	-475	949
28	448	-447	895
26	457	-459	916
24	441	-439	880
22	450	-451	901
20	478	-479	957
18	488	-489	977
16	483	-482	965
14	433	-436	869
12	397	-397	794
10	396	-398	794
8	383	-383	766
6	382	-380	762
4	503	-507	1010
2	504	-506	1010

Table H7. Inclinometer data 0.165 m from pier one, 0 ton load increment

Depth (ft)	A+	A-	Diff
34	22	-66	88
32	45	-45	90
30	-5	6	-11
28	-61	63	-124
26	-63	63	-126
24	-40	41	-81
22	-47	46	-93
20	-49	48	-97
18	-72	69	-141
16	-136	130	-266
14	-172	177	-349
12	-2	0	-2
10	56	-56	112
8	-27	25	-52
6	-50	54	-104
4	92	-99	191
2	108	-112	220

Table H8. Inclinometer data 0.165 m from pier one, 12.3 ton load increment

Depth (ft)	A+	A-	Diff
34	23	-67	90
32	45	-47	92
30	-3	3	-6
28	-60	61	-121
26	-62	62	-124
24	-39	40	-79
22	-46	45	-91
20	-48	48	-96
18	-72	69	-141
16	-137	130	-267
14	-172	177	-349
12	0	0	0
10	55	-54	109
8	-32	31	-63
6	-44	49	-93
4	114	-121	235
2	124	-130	254

Table H9. Inclinometer data 0.165 m from pier one, 20.37 ton load increment

Depth (ft)	A+	A-	Diff
34	22	-66	88
32	46	-46	92
30	-4	5	-9
28	-61	62	-123
26	-63	63	-126
24	-40	40	-80
22	-47	46	-93
20	-49	49	-98
18	-72	69	-141
16	-139	134	-273
14	-172	177	-349
12	-2	1	-3
10	52	-51	103
8	-40	38	-78
6	-39	41	-80
4	134	-143	277
2	139	-150	289

Table H10. Inclinometer data 0.165 m from pier one, 28.72 ton load increment

Depth (ft)	A+	A-	Diff
34	24	-67	91
32	46	-47	93
30	-3	3	-6
28	-61	61	-122
26	-63	62	-125
24	-40	38	-78
22	-46	44	-90
20	-48	47	-95
18	-72	69	-141
16	-140	135	-275
14	-174	178	-352
12	-2	0	-2
10	46	-47	93
8	-53	50	-103
6	-25	28	-53
4	163	-169	332
2	132	-137	269

Table H11. Inclinometer data 0.165 m from pier one, 45 ton load increment

Depth (ft)	A+	A-	Diff
34	37	-54	91
32	60	-32	92
30	12	17	-5
28	-42	75	-117
26	-50	78	-128
24	-26	53	-79
22	-32	58	-90
20	-34	62	-96
18	-58	85	-143
16	-128	151	-279
14	-164	195	-359
12	13	12	1
10	28	-2	30
8	-90	114	-204
6	45	-18	63
4	243	-224	467
2	237	-215	452

Table H12. Inclinometer data 0.165 m from pier one after pier installation

depth (ft)	initial	diff	change	change	deflection (in)
34	88	89	1	1	0.0006
32	89	91	2	3	0.0018
30	-11	-11	0	3	0.0018
28	-123	-120	3	6	0.0036
26	-122	-124	-2	4	0.0024
24	-80	-78	2	6	0.0036
22	-99	-92	7	13	0.0078
20	-89	-103	-14	-1	-0.0006
18	-75	-146	-71	-72	-0.0432
16	-85	-244	-159	-231	-0.1386
14	-34	-357	-323	-554	-0.3324
12	-55	0	55	-499	-0.2994
10	-97	111	208	-291	-0.1746
8	-127	-57	70	-221	-0.1326
6	-117	-108	9	-212	-0.1272
4	33	153	120	-92	-0.0552
2	-88	37	125	33	0.0198

Table H13. Inclinometer data 0.38 m from pier one after pier installation

depth	initial	diff	change	change	deflection (in)
34	1015	1016	1	1	0.0006
32	1015	1020	5	6	0.0036
30	948	948	0	6	0.0036
28	898	894	-4	2	0.0012
26	915	916	1	3	0.0018
24	878	877	-1	2	0.0012
22	903	902	-1	1	0.0006
20	956	954	-2	-1	-0.0006
18	983	983	0	-1	-0.0006
16	985	976	-9	-10	-0.006
14	893	871	-22	-32	-0.0192
12	820	804	-16	-48	-0.0288
10	813	811	-2	-50	-0.03
8	807	810	3	-47	-0.0282
6	746	730	-16	-63	-0.0378
4	875	823	-52	-115	-0.069
2	873	822	-51	-166	-0.0996

Table H14. Stress cell readings from pier one at each load increment

	Stress Cell Number			
Stress (kPa)	444	443	442	441
53.45	10.78	31.68	32.31	53.80
54.96	11.24	31.48	33.05	55.32
60.73	10.92	38.33	33.88	61.13
71.94	16.32	43.17	34.81	72.41
129.02	37.13	66.95	39.70	129.87
170.16	54.26	84.08	44.97	171.28
172.81	54.72	85.49	45.62	173.95
230.13	74.96	104.04	54.95	231.64
231.86	74.04	104.44	55.78	233.38
295.18	92.66	125.80	70.47	297.12
372.60	108.53	158.45	102.16	375.05
446.20	125.54	209.04	146.15	449.13
509.98	141.87	289.86	214.43	513.34
549.39	157.96	382.16	285.76	553.00

Table H15. Load test data for individual pier number two

Stress	Load	Gauge Pressure (psi)			Dial Reading (in)			Tell-Tale Reading (in)			Remarks
(kPa)	(tons)	planned	actual	time hr:min	#1	#2	Avg.	#1	#2	Avg.	
24	1.23	130	500	2:20	1.958	1.872	1.915	1.856	1.756	1.806	
81	4.17	440	500	3:39	1.929	1.84	1.8845	1.856	1.752	1.804	
158	8.1	850	800	4:16	1.888	1.791	1.8395	1.843	1.739	1.791	
239	12.27	1290	1200	4:48	1.829	1.736	1.7825	1.821	1.713	1.767	
321	16.44	1720	1640	5:57	1.729	1.632	1.6805	1.765	1.655	1.71	
397	20.37	2130	2100	7:16	1.553	1.466	1.5095	1.662	1.543	1.6025	
479	24.54	2560	2450	8:30	0.94	0.891	0.9155	1.367	1.218	1.2925	
					0.02	0.014	0.017	0.678	0.508	0.593	
479					1.852	1.754	1.803	1.868	1.714	1.791	
560	28.72	2990	2900	9:56	0.8	0.791	0.7955	1.33	1.156	1.243	
560	28.72	3400	3250	11:01	0.541	0.542	0.5415	1.19	1.011	1.1005	unload
321	36.82	3800	3700	12:51	0.561	0.575	0.568	1.205	1.023	1.114	
158	45	4200	4500	12:56	0.618	0.631	0.6245	1.247	1.058	1.1525	
	0	3500	3500		0.685	0.7	0.6925	1.285	1.108	1.1965	
					0.89	0.88	0.885	1.358	1.187	1.2725	

Table H16. Load test data for individual pier number three

Stress	Load	Gauge Pressure (psi)		Time	Dial Reading (in)			Tell-Tale Reading (in)			Remarks
(kPa)	(tons)	planned	actual	hr:min	#1	#2	Avg.	#1	#2	Avg.	
24	1.23	215	225	2:20	1.7	1.4	1.55	1.7	1.7	1.7	
81	4.17	511	510	3:39	1.686	1.375	1.5305	1.7	1.694	1.697	
158	8.1	905	900	4:16	1.66	1.347	1.5035	1.7	1.686	1.693	
239	12.27	1324	1325	4:48	1.62	1.308	1.464	1.7	1.681	1.6905	
321	16.44	1743	1750	5:57	1.572	1.258	1.415	1.7	1.675	1.6875	
397	20.37	2137	2150	7:16	1.52	1.204	1.362	1.695	1.656	1.6755	
479	24.54	2556	2550	8:30	1.404	1.086	1.245	1.686	1.652	1.669	
560	28.72	2975	2975	9:56	1.205	0.887	1.046	1.68	1.659	1.6695	
637	32.64	3389	3400	11:01	0.839	0.52	0.6795	1.656	1.632	1.644	
479		2571	2600		0.804	0.483	0.6435	1.658	1.641	1.6495	unload
321		1728	1728		0.814	0.502	0.658	1.671	1.653	1.662	
158		1000	1000		0.86	0.547	0.7035	1.675	1.679	1.677	
0		110	110		1.002	0.714	0.858	1.682	1.699	1.6905	

APPENDIX I

GROUP LOAD TEST DATA

Table I1. Load test data for group load test one, pier one

Stress	Load	Gauge Pressure (psi)			Dial Reading (in)			Remarks
(kPa)	(tons)	planned	actual	time hr:min	#1	#2	Avg.	
24	1.23	121.5	120	3:19	1.671	1.849	1.76	
81	4.17	412	400	3:39	1.661	1.835	1.748	
158	8.1	800.4	800	4:16	1.61	1.793	1.7015	
239	12.27	1212.4	1200	4:48	1.548	1.747	1.6475	
321	16.44	1624.5	1625	5:57	1.49	1.676	1.583	
397	20.37	2050	2050	7:16	1.402	1.595	1.4985	
479	24.54	2450	2450	8:30	1.287	1.487	1.387	
560	28.72	2900	2900	9:56	1.018	1.235	1.1265	
637	32.64	3250	3250	11:01	0.536	0.789	0.6625	
					1.457	1.815	1.636	
718	36.82	3700	3700	12:51	0.072	0.474	0.273	
	24.54	2450	2450	12:56	0.06	0.46	0.26	unload
				1:02	0.182	0.564	0.373	
	4.17	412	400	1:08	0.358	0.717	0.5375	
	0	0	0		0.514	0.869	0.6915	

Table I2. Load test data for group load test one, pier two

Stress	Load	Gauge Pressure (psi)		time	Dial Reading (in)			Tell-Tale Reading (in)			Remarks
(kPa)	(tons)	planned	actual	hr:min	#1	#2	Avg.	#1	#2	Avg.	
23.9	1.23	121.5	120	3:19	1.864	1.762	1.813	1.761	1.687	1.724	
81.4	4.17	412	400	3:39	1.863	1.756	1.8095	1.761	1.686	1.7235	
158.0	8.1	800.4	800	4:16	1.806	1.713	1.7595	1.747	1.668	1.7075	
239.4	12.27	1212.4	1200	4:48	1.713	1.623	1.668	1.718	1.639	1.6785	
320.8	16.44	1624.5	1625	5:57	1.648	1.561	1.6045	1.674	1.61	1.642	
397.4	20.37	2050	2050	7:16	1.557	1.47	1.5135	1.612	1.55	1.581	
478.8	24.54	2450	2450	8:30	1.434	1.337	1.3855	1.519	1.463	1.491	
560.2	28.72	2900	2900	9:56	1.139	1.02	1.0795	1.275	1.225	1.25	
636.8	32.64	3250	3250	11:01	0.594	0.436	0.515	0.803	0.765	0.784	
636.8	32.64	3250	3250		1.674	1.672	1.673				
718.2	36.82	3700	3700	12:51	0.245	0.2	0.2225	0.982	0.989	0.9855	
478.8	24.54	2450	2450	1:02	0.255	0.227	0.241	0.992	0.004	0.498	unload
81.4	4.17	412	400	1:08	0.725	0.73	0.7275	1.207	1.245	1.226	
0.0	0	0	0		0.843	0.835	0.839	1.258	1.286	1.272	

Table I3. Load test data for group load test one, pier three

Stress	Load	Gauge Pressure (psi)		time	Dial Reading (in)			Tell-Tale Reading (in)			Remarks
(kPa)	(tons)	planned	actual	hr:min	#1	#2	Avg.	#1	#2	Avg.	
24	1.23	121.5	120	3:19	1.894	1.929	1.9115	1.859	1.97	1.9145	
81	4.17	412	400	3:39	1.878	1.904	1.891	1.855	1.968	1.9115	
158	8.1	800.4	800	4:16	1.846	1.834	1.84	1.834	1.938	1.886	
239	12.27	1212.4	1200	4:48	1.805	1.769	1.787	1.816	1.915	1.8655	
321	16.44	1624.5	1625	5:57	1.73	1.706	1.718	1.768	1.877	1.8225	
397	20.37	2050	2050	7:16	1.647	1.625	1.636	1.714	1.822	1.768	
479	24.54	2450	2450	8:30	1.543	1.524	1.5335	1.629	1.739	1.684	
560	28.72	2900	2900	9:56	1.293	1.286	1.2895	1.41	1.525	1.4675	
637	32.64	3250	3250	11:01	0.86	0.882	0.871	1	1.131	1.0655	
637	32.64	3250	3250	12:01	1.913	1.948	1.9305	1.843	1.815	1.829	zero dials
718	36.82	3700	3700	12:51	0.59	0.668	0.629	0.563	0.592	0.5775	
479	24.54	2450	2450	1:02	0.573	0.649	0.611	0.548	0.596	0.572	unload
81	4.17	412	400	1:08	0.686	0.769	0.7275	0.638	0.673	0.6555	
0	0	0	0		0.984	1.119	1.0515	0.821	0.847	0.834	

Table I4. Load test data for group load test one, pier four

	Stress	Load	Gauge Pressure (psi)		time	Dial Reading (in)			Remarks
Stress (psf)	(kPa)	(tons)	planned	actual	hr:min	#1	#2	Avg.	
500	24	1.23	121.5	120	3:19	1.838	1.873	1.8555	
1700	81	4.17	412	400	3:39	1.834	1.867	1.8505	
3300	158	8.1	800.4	800	4:16	1.78	1.826	1.803	
5000	239	12.27	1212.4	1200	4:48	1.703	1.752	1.7275	
6700	321	16.44	1624.5	1625	5:57	1.653	1.69	1.6715	
8300	397	20.37	2050	2050	7:16	1.576	1.605	1.5905	
10000	479	24.54	2450	2450	8:30	1.461	1.49	1.4755	
11700	560	28.72	2900	2900	9:56	1.194	1.208	1.201	
13300	637	32.64	3250	3250	11:01	0.701	0.675	0.688	
13301	637	32.64	3250	3250	12:01	1.938	1.982	1.96	zero dials
15000	718	36.82	3700	3700	12:51	0.557	0.573	0.565	
10000	479	24.54	2450	2450	1:02	0.574	0.59	0.582	unload
1700	81	4.17	412	400	1:08	0.916	0.981	0.9485	
0	0	0	0	0		1.023	1.041	1.032	

Table I5. Inclinometer data for group test one at 32 ton total load

Depth (ft)	initial	diff	change	change	deflection (in)
34	-45	-42	3	3	0.0018
32	-96	-88	8	11	0.0066
30	-104	-107	-3	8	0.0048
28	-148	-150	-2	6	0.0036
26	-180	-177	3	9	0.0054
24	-115	-117	-2	7	0.0042
22	-150	-153	-3	4	0.0024
20	-154	-156	-2	2	0.0012
18	-161	-155	6	8	0.0048
16	-121	-115	6	14	0.0084
14	-7	-24	-17	-3	-0.0018
12	34	14	-20	-23	-0.0138
10	55	47	-8	-31	-0.0186
8	92	87	-5	-36	-0.0216
6	147	149	2	-34	-0.0204
4	194	231	37	3	0.0018
2	207	276	69	72	0.0432

Table I6. Inclinometer data for group test one at 98 ton total load

Depth (ft)	diff	change	change	deflection (in)
34	-41	4	4	0.0024
32	-89	7	11	0.0066
30	-110	-6	5	0.003
28	-153	-5	0	0
26	-180	0	0	0
24	-124	-9	-9	-0.0054
22	-155	-5	-14	-0.0084
20	-154	0	-14	-0.0084
18	-158	3	-11	-0.0066
16	-119	2	-9	-0.0054
14	-55	-48	-57	-0.0342
12	-15	-49	-106	-0.0636
10	19	-36	-142	-0.0852
8	69	-23	-165	-0.099
6	158	11	-154	-0.0924
4	308	114	-40	-0.024
2	414	207	167	0.1002

Table I7. Inclinometer data for group test one at 129.6 ton total load

Depth (ft)	diff	change	change	deflection (in)
34	-34	11	11	0.0066
32	-85	11	22	0.0132
30	-110	-6	16	0.0096
28	-154	-6	10	0.006
26	-177	3	13	0.0078
24	-121	-6	7	0.0042
22	-156	-6	1	0.0006
20	-170	-16	-15	-0.009
18	-201	-40	-55	-0.033
16	-197	-76	-131	-0.0786
14	-195	-188	-319	-0.1914
12	-79	-113	-432	-0.2592
10	108	53	-379	-0.2274
8	146	54	-325	-0.195
6	197	50	-275	-0.165
4	540	346	71	0.0426
2	882	675	746	0.4476

Table I8. Stress cell readings at load increments for group test one

	Stress Cell Readings (kPa)							
tons	440	439	438	436	50657	50661	50666	50662
0	11.0316	5.7226425	11.0316	12.41055	11.075331	11.053285	11.056037	11.0336
0	25.027943	4.41264	1.93053	7.72212	2.6484497	8.4718115	12.389718	17.876872
0	27.647948	13.23792	12.893183	21.649515	6.0727504	0.7026112	4.5025356	18.36087
0	26.062155	10.342125	13.375815	20.822145	4.7030868	-2.1081427	1.8279319	11.979405
48.0	106.86863	56.054318	45.022718	57.36432	30.348897	28.721044	48.206191	111.07741
65.6	141.54922	76.11804	59.156955	74.73909	37.143783	35.373741	58.911472	155.19954
81.0	162.57821	100.7323	71.912243	91.355438	44.483812	42.240396	70.806674	196.73653
81.0	168.3698	105.97231	72.739613	92.38965	44.89406	42.896186	72.226334	202.33074
98.0	175.81613	129.13867	80.737523	103.14546	49.13289	47.660237	83.977452	239.43084
115.0	169.74875	157.82083	92.66544	120.79602	55.603682	53.033313	100.89972	290.50254
130.0	179.12561	195.39722	105.21389	140.6529	62.346085	61.283571	122.13473	349.71579
130.0	172.2998	191.94984	100.52546	132.58604	59.977342	59.756287	117.13852	307.49322
147.0	182.57298	228.35412	129.69025	189.67457	77.919467	72.79571	141.21901	394.47934
147.0	177.05718	222.28674	126.31182	186.2272	75.825373	71.967653	138.08425	392.81493
0.0	-59.777483	-0.27579	4.826325	12.755288	7.579293	-4.0410141	10.563129	-27.878107

Table I9. Load test data for group load test two, pier one

	Stress	Load	Gauge Pressure (psi)		time	Dial Reading (in)			Remarks
Stress (psf)	(kPa)	(tons)	planned	actual	hr:min	#1	#2	Avg.	
500	24	1.23	121.5	500	2:20	1.878	1.906	1.892	
1700	81	4.17	412	500	3:39	1.877	1.904	1.8905	
3300	158	8.1	800.4	800	4:16	1.838	1.875	1.8565	
5000	239	12.27	1212.4	1200	4:48	1.754	1.764	1.759	
6700	321	16.44	1624.5	1640	5:57	1.755	1.758	1.7565	
8300	397	20.37	2050	2100	7:16	1.665	1.66	1.6625	
10000	479	24.54	2450	2450	8:30	1.595	1.578	1.5865	
11700	560	28.72	2900	2900	9:56	1.438	1.39	1.414	
13300	637	32.64	3250	3250	11:01	1.245	1.174	1.2095	
15000	718	36.82	3700	3700	12:51	0.872	0.744	0.808	
15001	718	36.82	3700	3700	13:51	1.622	1.722	1.672	reset
18333	878	45	4500	4500	12:56	0.652	0.634	0.643	
18334	878	45	4500	4500	1:02	1.229	1.344	1.2865	reset
20000	958	49	4800	4800	1:08	0.649	0.687	0.668	
15000		36.82	3500	3500		0.645	0.676	0.6605	unload
10000		24.54	2450	2450		0.673	0.689	0.681	
8300		20.37	2050	2100		0.715	0.731	0.723	
5000		12.27	1212.4	1200		0.775	0.795	0.785	
0		0	0			1.095	1.146	1.1205	

Table I10. Load test data for group load test two, pier two

Stress	Load	Gauge Pressure (psi)		time	Dial Reading (in)			Tell-Tale Reading (in)			Remarks
(kPa)	(tons)	planned	actual	hr:min	#1	#2	Avg.	#1	#2	Avg.	
24	1.23	121.5	500	2:20	2.004	1.917	1.9605	1.916	1.89	1.903	
81	4.17	412	500	3:39	1.998	1.91	1.954	1.916	1.888	1.902	
158	8.1	800.4	800	4:16	1.962	1.874	1.918	1.911	1.886	1.8985	
239	12.27	1212.4	1200	4:48	1.898	1.776	1.837	1.918	1.88	1.899	
321	16.44	1624.5	1640	5:57	1.905	1.77	1.8375	1.918	1.88	1.899	
397	20.37	2050	2100	7:16	1.835	1.674	1.7545	1.908	1.87	1.889	
479	24.54	2450	2450	8:30	1.786	1.599	1.6925	1.905	1.862	1.8835	
560	28.72	2900	2900	9:56	1.638	1.418	1.528	1.899	1.847	1.873	
637	32.64	3250	3250	11:01	1.508	1.235	1.3715	1.891	1.846	1.8685	
718	36.82	3700	3700	12:51	1.265	0.908	1.0865	1.857	1.801	1.829	
718	36.82	3700	3700	12:51	1.723	1.567	1.645	1.857	1.801	1.829	reset
878	45	4500	4500	12:56	1.057	0.779	0.918	1.77	1.72	1.745	
878	45	4500	4500	1:02	1.789	1.679	1.734	1.77	1.72	1.745	reset
958	49	4800	4800	1:08	1.367	1.284	1.3255	1.712	1.636	1.674	
	36.82	3500	3500		1.36	1.277	1.3185	1.714	1.635	1.6745	unload
	24.54	2450	2450		1.381	1.282	1.3315	1.731	1.647	1.689	
	20.37	2050	2100		1.411	1.312	1.3615	1.741	1.675	1.708	
	12.27	1212.4	1200		1.478	1.376	1.427	1.762	1.376	1.707	
	0	0	0		1.83	1.693	1.7615	1.792	1.758	1.775	

Table I11. Load test data for group load test two, pier three

Stress	Load	Gauge Pressure (psi)		time	Dial Reading (in)			Tell-Tale Reading (in)			Remarks
(kPa)	(tons)	planned	actual	hr:min	#1	#2	Avg.	#1	#2	Avg.	
24	1.23	121.5	500	2:20	1.955	1.933	1.944	1.947	1.911	1.929	
81	4.17	412	500	3:39	1.952	1.93	1.941	1.942	1.905	1.9235	
158	8.1	800.4	800	4:16	1.931	1.911	1.921	1.941	1.906	1.9235	
239	12.27	1212.4	1200	4:48	1.813	1.775	1.794	1.931	1.905	1.918	
321	16.44	1624.5	1640	5:57	1.817	1.772	1.7945	1.933	1.907	1.92	
397	20.37	2050	2100	7:16	1.706	1.634	1.67	1.93	1.892	1.911	
479	24.54	2450	2450	8:30	1.612	1.531	1.5715	1.929	1.889	1.909	
560	28.72	2900	2900	9:56	1.413	1.297	1.355	1.929	1.881	1.905	
637	32.64	3250	3250	11:01	1.177	1.029	1.103	1.92	1.868	1.894	
718	36.82	3700	3700	12:51	0.718	0.523	0.6205	1.898	1.83	1.864	
718	36.82	3700	3700	13:51	1.665	1.667	1.666	1.898	1.83	1.864	reset
878	45	4500	4500	12:56	0.47	0.323	0.3965	1.836	1.708	1.772	
878	45	4500	4500	1:02	1.68	1.559	1.6195	1.836	1.708	1.772	reset
958	49	4800	4800	1:08	0.98	0.755	0.8675	1.8	1.646	1.723	
	36.82	3500	3500		0.875	0.745	0.81	1.803	1.646	1.7245	unload
	24.54	2450	2450		0.997	0.783	0.89	1.8	1.648	1.724	
	20.37	2050	2100		1.041	0.829	0.935	1.81	1.654	1.732	
	12.27	1212.4	1200		1.109	0.906	1.0075	1.821	1.661	1.707	
	0	0	0		1.475	1.335	1.405	1.833	1.679	1.756	

Table I12. Load test data for group load test two, pier four

Stress	Load	Gauge Pressure (psi)		time	Dial Reading (in)			Remarks
(kPa)	(tons)	planned	actual	hr:min	#1	#2	Avg.	
24	1.23	121.5	500	2:20	1.941	1.971	1.956	
81	4.17	412	500	3:39	1.931	1.958	1.9445	
158	8.1	800.4	800	4:16	1.893	1.915	1.904	
239	12.27	1212.4	1200	4:48	1.778	1.814	1.796	
321	16.44	1624.5	1640	5:57	1.775	1.801	1.788	
397	20.37	2050	2100	7:16	1.662	1.671	1.6665	
479	24.54	2450	2450	8:30	1.567	1.567	1.567	
560	28.72	2900	2900	9:56	1.378	1.348	1.363	
637	32.64	3250	3250	11:01	1.181	1.128	1.1545	
718	36.82	3700	3700	12:51	0.818	0.725	0.7715	
0	36.82	3700	3700	13:51	1.8	1.579	1.6895	reset
878	45	4500	4500	12:56	0.969	0.575	0.772	
878	45	4500	4500	1:02	1.491	1.614	1.5525	reset
958	49	4800	4800	1:08	0.96	0.998	0.979	
	36.82	3500	3500		0.948	0.982	0.965	unload
	24.54	2450	2450		0.961	1.007	0.984	
	20.37	2050	2100		0.989	1.033	1.011	
	12.27	1212.4	1200		1.061	1.108	1.0845	
	0	0	0		1.439	1.539	1.489	

APPENDIX J

SETTLEMENT CALCULATIONS

Table J1. Total unreinforced settlement estimate using void ratio relationship and oedometer data

Parameter	Value	Units
Density of soft clay	1876.00	kg/m3
Thickness	7.50	m
Stress at mid-depth	68.94	kPa
Effective Stress at mid-depth	32.20	kPa
Density fill material	1600.00	kg/m3
Fill height	8.00	m
Stress from fill	125.44	kPa
Influence coefficient (Boussinesq)	0.24	
Stress increase at mid-depth	120.40	kPa
Initial void ratio (from Figure 25)	0.90	
Final void ratio (Figure 25)	0.74	
Using height-void ratio relationship		
Change in clay thickness	0.63	m

Table J2. Calculation of unreinforced 90% consolidation period using oedometer data and Terzaghi consolidation theory

Parameter	Value	Units
Coefficient of consolidation (from Table 2)	0.07	m2/day
Thickness of clay layer	7.5	m
Drainage distance	3.75	m
Time factor	0.848	
Percentage of consolidation	90%	
Using Terzaghi consolidation theory		
Time for 90% consolidation	170	days

Table J3. Calculation of reinforced 90% consolidation period using oedometer data and Terzaghi consolidation theory (drainage distance is one-half distance between piers)

Parameter	Value	Units
Coefficient of consolidation (from Table 2)	0.07	m2/day
Thickness of clay layer	7.5	m
Drainage distance	0.75	m
Time factor	0.848	
Percentage of consolidation	90%	
Using Terzaghi consolidation theory		
Time for 90% consolidation	7	days

APPENDIX K

RADIAL STRESS-STRAIN SETTLEMENT PREDICTION

Table K1. Settlement prediction values using Hughes and Withers (1975)

Load	156.9	kPa	Kps =	6.44	
Depth (m)	Vert stress	hor stress	rad strain	layer thick	settlement
1.125	40	6.2111801	0	250	0
1.375	35	5.4347826	0	250	0
1.625	30	4.6583851	0	250	0
1.875	25	3.8819876	0	250	0
2.125	25	3.8819876	0	250	0
				total	
Load	237.7	kPa	Kps =	6.44	
Depth (m)	Vert stress	hor stress	rad strain	layer thick	settlement
1.125	70	10.869565	0	250	0
1.375	50	7.7639752	0	250	0
1.625	45	6.9875776	0	250	0
1.875	40	6.2111801	0	250	0
2.125	40	6.2111801	0	250	0
				total	0
Load	318.5	kPa	Kps =	6.44	
Depth (m)	Vert stress	hor stress	rad strain	layer thick	settlement
1.125	95	14.751553	0	250	0
1.375	75	11.645963	0	250	0
1.625	65	10.093168	0	250	0
1.875	60	9.3167702	0	250	0
2.125	60	9.3167702	0	250	0
				total	0
Load	394.5	kPa	Kps =	6.44	
Depth (m)	Vert stress	hor stress	rad strain	layer thick	settlement
1.125	140	21.73913	0.007	250	3.5
1.375	105	16.304348	0	250	0
1.625	85	13.198758	0	250	0
1.875	80	12.42236	0	250	0
2.125	80	12.42236	0	250	0
				total	3.5

Table K1 (continued). Settlement prediction values using Hughes and Withers (1975)

Load	475.4	kPa	Kps =	6.44	
Depth (m)	Vert stress	hor stress	rad strain	layer thick	settlement
1.125	210	32.608696	0.011	250	5.5
1.375	150	23.291925	0.007	250	1.75
1.625	115	17.857143	0	250	0
1.875	105	16.304348	0	250	0
2.125	100	15.52795	0	250	0
				total	7.25
Load	556.9	kPa	Kps =	6.44	
Depth (m)	Vert stress	hor stress	rad strain	layer thick	settlement
1.125	270	41.925466	0.017	250	8.5
1.375	210	32.608696	0.011	250	5.5
1.625	165	25.621118	0.007	250	3.5
1.875	145	22.515528	0	250	0
2.125	130	20.186335	0	250	0
				total	17.5
Load	632.9	kPa	Kps =	6.44	
Depth (m)	Vert stress	hor stress	rad strain	layer thick	settlement
1.125	345	53.571429	0.026	250	13
1.375	280	43.478261	0.018	250	9
1.625	220	34.161491	0.012	250	6
1.875	180	27.950311	0.008	250	4
2.125	150	23.291925	0	250	0
				total	32
Load	713.7	kPa	Kps =	6.44	
Depth (m)	Vert stress	hor stress	rad strain	layer thick	settlement
1.125	415	64.440994	0.031	250	15.5
1.375	375	58.229814	0.028	250	14
1.625	310	48.136646	0.022	250	11
1.875	250	38.819876	0.015	250	7.5
2.125	185	28.726708	0.008	250	4
				total	52

APPENDIX L

PIER INSTALLATION INSPECTION LOG

geopier™

PETERSON CONTRACTORS, INC.

HEAVY & HIGHWAY CONTRACTORS

Weather: ____________

Project Name & Location: PoH Co Box Culvert

Equipment Used: ____________

PCI #: J327

GFC #: ____________

GEOPIERS INSTALLED

Location	#	Bottom Footing El, ft	Geopier Shaft Length, ft	Ground Surface El, ft	Geopier Bottom El, ft	Geopier Drill Depth, ft		Geopier Top El, ft	Geopier Top Depth, ft		Geopier Stone Lifts		Tamp Time/ Lift	Install Date	Soil Material*		Stiffness	
						Planned	Actual		Planned	Actual	#1	#2			In Shaft	at Tip	BST 2% min.	DCPT 10% min.
ZONE D	1	1059.4	7	1060.40	1052.4	8.00	7.6	1060.4	0.00	0	7		15	9/5	CL	CH		
	2	1059.4	7	1060.40	1052.4	8.00	8.0	1060.4	0.00	0	8		25	9/5	CL	CH		
	3	1059.4	7	1060.40	1052.4	8.00	8.2	1060.4	0.00	0	11		20	9/5	CL	CH		
	4	1059.4	7	1060.40	1052.4	8.00	7.9	1060.4	0.00	0	7		25	9/4	CL	CH		
	5	1059.4	7	1060.40	1052.4	8.00	8	1060.4	0.00	0	6		25	9/4	CL	CH		
	6	1059.4	7	1060.40	1052.4	8.00	8.3	1060.4	0.00	0	9		25	9/5	CL	CH		
	7	1059.4	7	1060.40	1052.4	8.00	7.5	1060.4	0.00	0	8		20	9/5	CL	CH		
	8	1059.4	7	1060.40	1052.4	8.00	7.9	1060.4	0.00	0	6		24	9/5	CL	CH		
	9	1059.4	7	1060.40	1052.4	8.00	7.5	1060.4	0.00	0	7		24	9/4	CL	CH		
	10	1059.4	7	1060.40	1052.4	8.00	8	1060.4	0.00	0	6		20	9/5	CL	CH		
	11	1059.4	7	1060.40	1052.4	8.00	8	1060.4	0.00	0	8		20	9/5	CL	CH		
	12	1059.4	7	1060.40	1052.4	8.00	8.5	1060.4	0.00	0	8		25	9/5	CL	CH		
	13	1059.4	7	1060.40	1052.4	8.00	7.6	1060.4	0.00	0	7		25	9/4	CL	CH		
	14	1059.4	7	1060.40	1052.4	8.00	7.5	1060.4	0.00	0	9		20	9/4	CL	CH		
	15	1059.4	7	1060.40	1052.4	8.00	8.2	1060.4	0.00	0	7		26	9/5	CL	CH		
	16	1059.4	7	1060.40	1052.4	8.00	8.0	1060.4	0.00	0	7		19	9/5	CL	CH		
	17	1059.4	7	1060.40	1052.4	8.00	7.5	1060.4	0.00	0	8		20	9/4	CL	CH		
	18	1059.4	7	1060.40	1052.4	8.00	8.1	1060.4	0.00	0	9		15	9/5	CL	CH		
	19	1059.4	7	1060.40	1052.4	8.00	8.2	1060.4	0.00	0	16		15	9/5	CL	CH		
	20	1059.4	7	1060.40	1052.4	8.00	8.0	1060.4	0.00	0	8		30	9/5	CL	CH		
	21	1059.4	7	1060.40	1052.4	8.00	7.5	1060.4	0.00	0	7		20	9/4	CL	CH		

7.5 ft min

*SOIL MATERIAL:

GW: WELL-GRADED GRAVELS
GP: POORLY GRADED GRAVELS
GM: SILTY GRAVELS
GC: CLAYEY GRAVELS

SW: WELL-GRADED SANDS
SP: POORLY GRADED SANDS
SM: SILTY SANDS
SC: CLAYEY SANDS

ML: INORGANIC SILTS
CL: INORGANIC CLAYS, LOW PI Lean
OL: ORGANIC SILTS AND CLAYS, LOW PI
F: RUBBLE FILL

MH: INORGANIC SILTS, HIGH PI
CH: INORGANIC CLAYS, HIGH PI Fat
OH: ORGANIC SILTS AND CLAYS, HIGH PI
PT: PEAT AND HIGHLY ORGANIC SOILS

PCI QC REPRESENTATIVE:

OWNER'S QA REPRESENTATIVE:

Project Name & Location: Polk Co Bui
Equipment Used:
PCI #: J327
GFC #

GEOPIERS INSTALLED

Location	#	Bottom Footing El, ft	Geopier Shaft Length, ft	Ground Surface El, ft	Geopier Bottom El, ft	Geopier Drill Depth, ft Planned	Geopier Drill Depth, ft Actual	Geopier Top El, ft.	Geopier Top Depth, ft Planned	Geopier Top Depth, ft Actual	Geopier Stone Lifts #1	Geopier Stone Lifts #2	Tamp Time/Lift	Install Date	Soil Material In Shaft	Soil Material at Tip	Stiffness BST 2% min.	Stiffness DCPT 10% min.
~~ZONE C~~	22	1059.5	12	1060.50	1047.5	13.00	9	1060.5	0.00	0	15		15	9/5	CL	CH		
	23	[illegible]	[illegible]	1060.50	1047.5	13.00	8.8	1060.5	0.00	0	8		20	9/5	CL	CH		
	24	[illegible]	12	1060.50	1047.5	13.00	8.7	1060.5	0.00	0	8		25	9/5	CL	CH		
ZONE C	25	1059.[illegible]	12	1060.50	1047.5	13.00	12.2	1060.5	0.00	0	12		20	9/5	CL	CH		
	26	1059.5	12	1060.50	1047.5	13.00	12.7	1060.5	0.00	0	12		20	9/5	CL	CH		
	27	1059.5	12	1060.50	1047.5	13.00	12.5	1060.5	0.00	0	12		22	9/6	CL	CH		
	28	1059.5	12	1060.50	1047.5	13.00	12.2	[illegible]	[illegible]	0	12		25	9/5	CL	CH		
	29	1059.5	12	1060.50	1047.5	13.00	12.7	1060.5	0.00	1.0	12		22	9/5	CL	CH		
	30	1059.5	12	1060.50	1047.5	13.00	12.5	1060.5	0.00	1.0	12		22	9/5	CL	CH		
C	31	1059.5	12	1060.50	1047.5	13.00	12.9	1060.5	0.00	1.0	12		25	9/5	CL	CH		
	32	1059.5	12	1060.50	1047.5	13.00	12.4	1060.5	0.00	1.0	12		25	9/5	CL	CH		
	33	1059.5	12	1060.50	1047.5	13.00	12.5	1060.5	0.00	0	12.5		20	9/6	CL	CH		
	34	1059.5	12	1060.50	1047.5	13.00	13.4	1060.5	0.00	1.0	13		25	9/5	CL	CH		
	35	1059.5	12	1060.50	1047.5	13.00	12.5	1060.5	0.00	1.0	12		20	9/5	CL	CH		
	36	1059.5	12	1060.50	1047.5	13.00	12.4	1060.5	0.00	1.0	12.5		20	9/5	CL	CH		
	37	1059.5	12	1060.50	1047.5	13.00	13.8	1060.5	0.00	0	11		20	9/5	CL	CH		
	38	1059.5	12	1060.50	1047.5	13.00	12.6	1060.5	0.00	0	12		25	9/5	CL	CH		
	39	1059.5	12	1060.50	1047.5	13.00	12.7	1060.5	0.00	0	11		15	9/5	CL	CH		
~~ZONE B~~	40	1059.6	17	1060.60	1042.6	18.00	13.0	1060.6	0.00	0.0	12		25	9/5	CL	CH		
	41	1059.6	17	1060.60	1042.6	18.00	12.5	1060.6	0.00	0	13		20	9/5	CL	CH		
	42	1059.6	17	1060.60	1042.6	18.00	12.[illegible]	1060.6	0.00	0	11		15	9/5	CL	CH		
ZONE B	43	1059.6	17	1060.60	1042.6	18.00	18	1060.6	0.00	0	17		24	9/6	CL	CH		
	44	1059.6	17	1060.60	1042.6	18.00	17.4	1060.6	0.00	0	17		25	9/6	CL	CH		
	45	1059.6	17	1060.60	1042.6	18.00	17.2	1060.6	0.00	0	17		30	9/11	CL	CH		
	46	1059.6	17	1060.60	1042.6	18.00	17.2	1060.6	0.00	0	17		25	9/6	CL	CH		
	47	1059.6	17	1060.60	1042.6	18.00	17.1	1060.6	0.00	0	16		25	9/6	CL	CH		
	48	1059.6	17	1060.60	1042.6	18.00	17.4	1060.6	0.00	0	17		25	9/11	CL	CH	X	
	49	1059.6	17	1060.60	1042.6	18.00	17.7	1060.6	0.00	0	17		23	9/6	CL	CH		
	50	1059.6	17	1060.60	1042.6	18.00	17.1	1060.6	0.00	0	16		22	9/6	CL	CH		
	51	1059.6	17	1060.60	1042.6	18.00	18	1060.6	0.00	0	18		18	9/6	CL	CH		
	52	1059.6	17	1060.[illegible]	1042.6	18.00	17.2	1060.6	0.00	0	16		15	9/5	CL	CH		
	53	1059.6	17	1060.[illegible]	1042.6	18.00	17.1	1060.6	0.00	0	17		22	9/6	CL	CH	X	
	54	1059.6	17	1060.60	1042.6	18.00	17.	1060.6	0.00	0	18		18	9/6	CL	CH		
	55	1059.6	17	1060.60	1042.6	18.00	17.6	1060.6	0.00	0	16		25	9/6	CL	CH		
	56	1059.6	17	1060.60	1042.6	18.00	18	1060.6	0.00	0	17		15	9/6	CL	CH		
	57	1059.6	17	1060.60	1042.6	18.00	17.1	1060.6	0.00	0	16		20	9/6	CL	CH		
~~ZONE A~~	58	1059.7	20	1060.70	1039.7	21.00	18	1060.7	0.00	0	17		25	9/6	CL	CH		
	59	1059.7	20	1060.70	1039.7	21.00	17.6	1060.7	0.00	0	17		19	9/6	CL	CH		
	60	1059.7	20	1060.70	1039.7	21.00	17.4	1060.7	0.00	0	16		20	9/6	CL	CH		
ZONE A	61	1059.7	20	1060.70	1039.[illegible]	21.00	20.3	1060.7	0.00	0	24		25	9/12	CL	CH		
	62	1059.8	20	1060.80	103[illegible]	21.00	20.2	1060.8	0.00	0	19		30	9/13	CL	CH		

9/11
9/11

PCI QC REPRESENTATIVE:

OWNER'S QA REPRESENTATIVE:

Location: Yott Co Box Used: PCI #:

GEOPIERS INSTALLED

Location	#	Bottom Footing El, ft	Geopier Shaft Length, ft	Ground Surface El, ft	Geopier Bottom El, ft	Geopier Drill Depth, ft Planned	Geopier Drill Depth, ft Actual	Geopier Top El, ft	Geopier Top Depth, ft Planned	Geopier Top Depth, ft Actual	Geopier Stone Lifts #1	Geopier Stone Lifts #2	Tamp Time/Lift	Install Date	Soil Material In Shaft	Soil Material at [illegible]	Stiffness BST 2% min.	Stiffness DCPT 10% min.
ZONE A	63	1059.8	[illegible]	1060.80	1039.8	21.00	22.1	1060.8	0.00	0	16		25	9/7	CL	CH		
	64	1059.8	20	1060.80	1039.8	21.00	20.1	1060.8	0.00	0	16		18	9/7	CL	CH		
	65	1059.8	20	1060.80	1039.8	21.00	18.3	1060.8	0.00	0	16		18	9/19	CL	CH		
	66	1059.9	20	1060.90	1039.9	21.00	20	1060.9	0.00	0	22		25	9/21	CL	CH		
	67	[illegible]	20	1061.00	1040	21.00	18	1061	0.00	0	22		17	9/21	CL	CH		
	68	1060	20	1061.00	1040	21.00	22	1061	0.00	0	20		20	9/27	CL	CH		
	69	1060	20	1061.00	1040	21.00	20.3	1061	0.00	0	20		25	9/27	CL	CH		
	70	1060	20	1061.00	1040	21.00	20.5	1061	0.00	0	24		15	9/27	CL	CH		
	71	1060	20	1061.00	1040	21.00	20.2	1061	0.00	0	22		15	9/27	CL	CH		
	72	1060	20	1061.00	1040	21.00	21.6	1061	0.00	0	16		15	9/19	CL	CH		
	73	1060	20	1061.00	1040	21.00	20.5	1061	0.00	0	16		25	9/14	CL	CH		
	74	1060	20	1061.00	1040	21.00	18.9	1061	0.00	0	18		25	9/7	CL	CH		
	75	1060	20	1061.00	1040	21.00	20.5	1061	0.00	0	22		25	9/14	CL	CH		
	76	1059.6	20	1060.60	1039.6	21.00	20.3	1060.6	0.00	0	16		22	9/14	CL	CH		
	77	1059.7	20	1060.70	1039.7	21.00	20.4	1060.7	0.00	0	19		20	9/13	CL	CH		
	78	1059.7	20	1060.70	1039.7	21.00	20	1060.7	0.00	0	20		30	9/11	[illegible]	CH		
	79	1059.7	20	1060.70	1039.7	21.00	[illegible]	1060.7	0.00	0	19		25	9/12	CL/CH	CH		
	80	1059.7	20	1060.70	1039.7	21.00	20.3	1060.7	0.00	0	19		35	9/13	CL	CH		
	81	1059.8	20	1060.80	1039.8	21.00	19.5	1060.8	0.00	0	16		20	9/7	CL	CH		
	82	1059.8	20	1060.80	1039.8	21.00	17	1060.8	0.00	0	13		25	9/19	CL	CH		
	83	1059.8	20	1060.80	1039.8	21.00	19.6	1060.8	0.00	0	14		27	9/19	CL	CH		
	84	1059.9	20	1060.90	1039.9	21.00	19.4	1060.9	0.00	0	16		20	9/20	CL	CH		
	85	1059.9	20	1060.90	1039.9	21.00	19	1060.9	0.00	0	20		20	9/21	CL	CH		
	86	1059.9	20	1060.90	1039.9	21.00	19	1060.9	0.00	0	18		21	9/21	CL	CH		
	87	1060	20	1061.00	1040	21.00	17.2	1061	0.00	0	16		16	9/21	CL	CH		
	88	1060	20	1061.00	1040	21.00	20.5	1061	0.00	0	22		25	9/27	CL	CH		
	89	1060	20	1061.00	1040	21.00	18	1061	0.00	0	16		15	9/21	CL	CH		
	90	1060	20	1061.00	1040	21.00	21.4	1061	0.00	0	18		10	9/20	CL	CH		
	91	1060	20	1061.00	1040	21.00	17	1061	0.00	0	16		20	9/19	CL	CH		
	92	1060	20	1061.00	1040	21.00	20.7	1061	0.00	0	22		20	9/19	CL	CH		
	93	1060	20	1061.00	1040	21.00	20.9	1061	0.00	0	30		21	9/17	CL	CH		
	94	1060	20	1061.00	1040	21.00	18.3	1061	0.00	0	28		15	9/17	CL	CH		
	95	1060	20	1061.00	1040	21.00	20.1	1061	0.00	0	22		21	9/14	CL	CH		
	96	1060	20	1061.00	1040	21.00	20.5	1061	0.00	0	28		25	9/14	CL	CH		
	97	1059.7	20	1060.70	1039.7	21.00	15.8	1060.7	0.00	0	17		25-30	8/31	CH	[illegible]		
	98	1059.7	20	1060.70	1039.7	21.00	20.5	1060.7	0.00	0	22		25	9/11	CL	CH		
	99	1059.7	20	1060.70	1039.7	21.00	20.3	1060.7	0.00	0	20		25	9/12	CL	CH		
	100	1059.7	20	1060.70	1039.7	21.00	20.3	1060.7	0.00	0	16		25	9/18	CL	CH		
	101	1059.8	20	1060.80	1039.8	21.00	20.	1060.8	0.00	0	26		20	9/17	CL	CH		
	102	1059.8	20	1060.80	1039.8	21.00	20.7	1060.8	0.00	0	[illegible]		20	9/18	CL	CH		
	103	1059.8	20	1060.80	1039.8	21.00	21	1060.8	0.00	0	[illegible]		15	[illegible]	CL	[illegible]		

1/4

12:30-@1060

186

PCI QC REPRESENTATIVE:

OWNER'S QA REPRESENTATIVE:

3/11

Location: Hot! Io Dox Used: [illegible] PCI #: [illegible] GFC #

GEO[illegible]INSTALLED

Location	#	Bottom Footing El, ft	Geopier Shaft Length, ft	Ground Surface El, ft	Geopier Bottom El, ft	Geopier Drill Depth, ft Planned	Geopier Drill Depth, ft Actual	Geopier Top El, ft	[illegible] Top Depth, ft Planned	[illegible] Top Depth, ft Actual	Geopier Stone Lifts #1	Geopier Stone Lifts #2	Temp Time/Lift	Install Date	*Soil Material In Shaft	*Soil Material at Tip	Stiffness BST 2% min.	Stiffness DCPT 10% min.
ZONE A	104	1059.9	[illegible]	1060.90	1039.9	21.00	18	1060.9	0.00	0	28		23	9/21	CL	CH		
	105	1059.9	20	1060.90	1039.9	21.00	17	1060.9	0.00	0	24		23	9/21	CL	CH		
	106	1059.9	20	1060.90	1039.9	21.00	20.5	1060.9	0.00	0	22		16	9/27	CL	CH		
	107	[illegible]	20	1061.00	1040	21.00	19.0	1061	0.00	0	20		22	9/22	CL	CH		
	108	[illegible]	20	1061.[illegible]	1040	21.00	19.1	1061	0.00	0	26		20	9/27	CL	CH		
	109	1060	20	1061.00	1040	21.00	17.5	1061	0.00	0	18		10	9/20	CL	CH		
	110	1060	20	1061.00	1040	21.00	21.4	1061	0.00	0	22		11	9/19	CL	CH		
	111	1060	20	1061.00	1040	21.00	20.9	1061	0.00	0	18		18	9/19	CL	CH		
	112	1060	20	1061.00	1040	21.00	20.9	1061	0.00	0	16		20	9/17	CL	CH		
	113	1060	20	1061.00	1040	21.00	20.2	1061	0.00	0	20		25	9/14	CL	CH		
	114	1060	20	1061.00	1040	21.00	20.1	1061	0.00	0	18		15	9/14	CL	CH		
	115	1060	20	1061.00	1040	21.00	20.4	1061	0.00	0	27		22	9/14	CL	CH		
	116	1060	20	1061.00	1040	21.00	20.5	1061	0.00	0	20		22	9/14	CL	CH		
	117	1059.7	20	1060.70	1039.7	21.00	20.5	1060.7	0.00	0	20		15	9/13	CL	CH		
	118	1059.7	20	1060.70	1039.7	21.00	20.7	1060.7	0.00	0	18		30	9/11	CL	CH		
	119	1059.7	20	1060.70	1039.7	21.00	20.1	1060.7	0.00	0	22		25	9/12	CL	CH		
	120	1059.7	20	1060.70	1039.7	21.00	20.2	1060.7	0.00	0	17		25	9/13	CL	CH		
	121	1059.8	20	1060.80	1039.8	21.00	20.6	1060.8	0.00	0	22		20	9/17	CL	CH		
	122	1059.8	20	1060.80	1039.8	21.00	17.5	1060.8	0.00	0	26		22	9/4	CL	CH		
	123	1059.8	20	1060.80	1039.8	21.00	19.3	1060.8	0.00	0	26		20	9/10	CL	CH		
	124	1059.9	20	1060.90	1039.9	21.00	17	1060.9	0.00	0	GEO	TRENCH		9/20	CL	CH		
	125	1059.9	20	1060.90	1039.9	21.00	18	1060.9	0.00	0	GEO	TRENCH		9/20	CL	CH		
	126	1059.9	20	1060.90	1039.9	21.00	19	1060.9	0.00	0	26		20	9/28	CL	CH		
	127	1060	20	1061.00	1040	21.00	21	1061	0.00	0	24		20	9/26	CL	CH		
	128	1060	20	1061.00	1040	21.00	20.5	1061	0.00	0	18		15	9/26	CL	CH		
	129	1060	20	1061.00	1040	21.00	20.5	1061	0.00	0	20		25	9/26	CL	CH		
	130	1060	20	1061.00	1040	21.00	20.8	1061	0.00	0	20		10	9/20	CL	CH		
	131	1060	20	1061.00	1040	21.00	21	1061	0.00	0	18		25	9/19	CL	CH		
	132	1060	20	1061.00	1040	21.00	20.4	1061	0.00	0	26		20	9/17	CL	CH		
	133	1060	20	1061.00	1040	21.00	20.7	1061	0.00	0	22		20	9/26	CL	CH		
	134	1060	20	1061.00	1040	21.00	20.1	1061	0.00	0	20		20	9/26	CL	CH		
	135	1060	20	1061.00	1040	21.00	20.3	1061	0.00	0	22		20	9/26	CL	CH		
	136	1060	20	1061.00	1040	21.00	20.3	1061	0.00	0	24		17	9/26	CL	CH		
	137	1059.7	20	1060.70	1039.7	21.00	20.5	1060.7	0.00	0	22		15	9/26	CL	CH		
	138	1059.7	20	1060.70	1039.7	21.00	20.	1060.7	0.00	0	18		25	9/11	CL	CH		
	139	1059.7	20	1060.70	1039.7	21.00	20.3	1060.7	0.00	0	21		25	9/12	CL	CH		
	140	1059.7	20	1060.70	1039.7	21.00	20.3	1060.7	0.00	0	19		30	9/13	CL	CH		
	141	1059.8	20	1060.80	1039.8	21.00	20.2	1060.8	0.00	0	28		18	9/11	CL	CH		
	142	1059.8	20	1060.80	1039.8	21.00	17	1060.8	0.00	0	14		25	9/4	CL	CH		
	143	1059.9	20	1060.90	1039.9	21.00	17	1060.9	0.00	0	18		30	9/4	CL	CH		
	144	1059.9	20	1060.90	1039.9	21.00	18.7	1060.9	0.00	0	18		25	9/4	CL	CH		

PCI QC REPRESENTATIVE:

OWNER'S QA REPRESENTATIVE

Location: Y6H to DOY Used: PCI #: 9527 GFC #

GEOPIERS INSTALLED

Location	#	Bottom Footing El, ft	Geopier Shaft Length, ft	Ground Surface El, ft	Geopier Bottom El, ft	Geopier Drill Depth, ft		Geopier Top El, ft	Geopier Top Depth, ft		Geopier Stone Lifts		Temp Time/ Lift	Install Date	Soil Material		Stiffness	
						Planned	Actual		Planned	Actual	#1	#2			in Shaft	at Tip	BST 2% min.	DCPT 10% min.
ZONE A	145	1059.9	20	1060.90	1039.9	21.00	18	1060.9	0.00	0	Geo	Trench		9/20	CL	CH		
	146	1059.9	20	1060.90	1039.9	21.00	20.4	1060.9	0.00	0	20		15	9/27	CL	CH		
	147	1059.9	20	1060.90	1039.9	21.00	20.3	1060.9	0.00	0	22		15	9/27	CL	CH		
	148	1060	20	1061.00	1040	21.00	20.1	1061	0.00	0	20		13	9/26	CL	CH		
	149	1060	20	1061.00	1040	21.00	21.3	1061	0.00	0	20		25	9/26	CL	CH		
	150	1060	20	1061.00	1040	21.00	21.0	1061	0.00	0	22		10	9/20	CL	CH		
	151	1060	20	1061.00	1040	21.00	[illegible]	1061	0.00	0	18		20	9/19	CL	CH		
	152	1060	20	1061.00	1040	21.00	21.2	1061	0.00	0	20		15	9/19	CL	CH		
	153	1060	20	1061.00	1040	21.00	20.5	1061	0.00	0	22		20	9/25	CL	CH		
	154	1060	20	1061.00	1040	21.00	20.7	1061	0.00	0	20		20	9/25	CL	CH		
	155	1060	20	1061.00	1040	21.00	20.3	1061	0.00	0	18		20	9/25	CL	CH		
	156	1060	20	1061.00	1040	21.00	21	1061	0.00	0	20		20	9/25	CL	CH		
	157	1059.7	20	1060.70	1039.7	21.00	20.7	1060.7	0.00	0	18		24	9/25	CL	CH		
	158	1059.7	20	1060.70	1039.7	21.00	21.2	1060.7	0.00	0	18		24	9/25	CL	CH		
	159	1059.7	20	1060.70	1039.7	21.00	20.9	1060.7	0.00	0	26		25	9/21	CL	CH		
	160	1059.7	20	1060.70	1039.7	21.00	20.0	1060.7	0.00	0	12		[illegible]	9/12	CL	CH		
	161	1059.8	20	1060.80	1039.8	21.00	20.3	1060.8	0.00	0	22		25	9/17	CL	CH		
	162	1059.8	20	1060.80	1039.8	21.00	20.4	1060.8	0.00	0	20		16	9/17	CL	CH		
	163	1059.9	20	1060.90	1039.9	21.00	20.4	1060.9	0.00	0	32		17	9/17	CL	CH		
	164	1059.9	20	1060.90	1039.9	21.00	20.6	1060.9	0.00	0	16		15	[illegible]	CL	CH		
	165	1059.9	20	1060.90	1039.9	21.00	[illegible]	1060.9	0.00	0	11		15	[illegible]	CL	CH		
	166	1059.9	20	1060.90	1039.9	21.00	20.7	1060.9	0.00	0	22		15	9/26	CL	CH		
	167	1059.9	20	1060.90	1039.9	21.00	[illegible]	1060.9	0.00	0	18		19	9/26	CL	CH		
	168	1059.9	20	1060.90	1039.9	21.00	[illegible]	1060.9	0.00	0	24		20	9/26	CL	CH		
	169	1059.9	20	1060.90	1039.9	21.00	[illegible]	1060.9	0.00	[illegible]	[illegible]		15	[illegible]	CL	CH		
	170	1059.9	20	1060.90	1039.9	21.00	[illegible]	1060.9	0.00	0	[illegible]		15	[illegible]	CL	CH		
	171	1059.9	20	1060.90	1039.9	21.00	21.0	1060.9	0.00	0	20		23	[illegible]	CL	CH		
	172	1059.9	20	1060.90	1039.9	21.00	20.9	1060.9	0.00	0	20		23	9/25	CL	CH		
	173	1059.9	20	1060.90	1039.9	21.00	21.5	1060.9	0.00	0	18		25	9/25	CL	CH		
	[redacted]	1059.9	20	1060.90	1039.9	21.00	22.2	1060.9	0.00	[illegible]	20		25	9/25	CL	CH		
	[redacted]	1059.9	20	1060.90	1039.9	21.00	[illegible]	1060.9	0.00	[illegible]	[illegible]		25	9/25	CL	CH		
	[redacted]	1059.9	20	1060.90	1039.9	21.00	20.9	1060.9	0.00	0	20		20	9/25	CL	CH		
	[redacted]	1059.9	20	1060.90	1039.9	21.00	22	1060.9	0.00	0	24		24	9/26	CL	CL	X	
*	[redacted]	1059.9	20	1060.90	1039.9	21.00	24	1060.9	0.00	0	18		18	10/1	CL	CH		
*	[redacted]	1059.9	20	1060.90	1039.9	21.00	24.1	1060.9	0.00	0	20		12	10/2	CL	CH		
*	[redacted]	1059.9	20	1060.90	1039.9	21.00	23.7	1060.9	0.00	[illegible]	[illegible]		21	10/2	CL	CH		
*	[redacted]	1059.9	20	1060.90	1039.9	21.00	24.5	1060.9	0.00	[illegible]	[illegible]		22	10/2	CL	CH		
*	[redacted]	1059.9	20	1060.90	1039.9	21.00	23.9	1060.9	0.00	[illegible]	22		25	10/2	CL	CH		
*	[redacted]	1059.9	20	1060.90	1039.9	21.00	24.3	1060.9	0.00	[illegible]	[illegible]		23	10/2	CL	CH		
*	[redacted]	1059.9	20	1060.90	1039.9	21.00	24.6	1060.9	0.00	0	[illegible]		22	10/2	CL	CH		
*	[redacted]	1059.9	20	1060.90	1039.9	21.00	24.2	1060.9	0.00	0	16		20	10/1	CL	CH		

PCI QC REPRESENTATIVE: * Cut was not subtracted

OWNER'S QA REPRESENTATIVE:

Location: 10 to Bay   Used: PCI #   GFC #

GEOPIERS INSTALLED

Location	#	Bottom Footing El, ft	Geopier Shaft Length, ft	Ground Surface El, ft	Geopier Bottom El, ft	Geopier Drill Depth, ft Planned	Geopier Drill Depth, ft Actual	Geopier Top El, ft.	Geopier Top Depth, ft Planned	Geopier Top Depth, ft Actual	Geopier Stone Lifts #1	Geopier Stone Lifts #2	Tamp Time/ Lift	Install Date	Soil Material In Shaft	Soil Material at Tip	Stiffness BST 2% min.	Stiffness DCPT 10% min.
*	[illegible]	1059.9	20	1060.90	1039.9	21.00	24.3	1060.9	0.00	0	15		27	[illegible]	CL	CH		
*	[illegible]	1059.9	20	1060.90	1039.9	21.00	24.5	1060.9	0.00	0	18		25	10/1	CL	CH		
*	[illegible]	1059.9	20	1060.90	1039.9	21.00	23	1060.9	0.00	0	12		20	10/1	CL	CH		
*	[illegible]	1059.9	20	1060.90	1039.9	21.00	24.2	1060.9	0.00	0	18		20	10/2	CL	CH		
*	[illegible]	1059.9	20	1060.90	1039.9	21.00	23.4	1060.9	0.00	0	19		25	10/2	CL	CH		
*	[illegible]	1059.9	20	1060.90	1039.9	21.00	23.2	1060.9	0.00	0	16		17	10/1	CL	[illegible]		
*	[illegible]	1059.9	20	1060.90	1039.9	21.00	23.1	1060.9	0.00	0	22		21	10/1	CL	[illegible]		
*	[illegible]	1059.9	20	1060.90	1039.9	21.00	24.5	1060.9	0.00	0	16		25	10/1	CL	[illegible]		
*	[illegible]	1059.9	20	1060.90	1039.9	21.00	22.5	1060.9	0.00	0	14		22	10/1	CL	[illegible]		
*	[illegible]	1059.9	20	1060.90	1039.9	21.00	21.6	1060.9	0.00	0	[illegible]		25	9/27	CL	[illegible]		
*	[illegible]	1059.9	20	1060.90	1039.9	21.00	23.1	1060.9	0.00	0	14		27	10/2	CL	CH		
*	[illegible]	1059.9	20	1060.90	1039.9	21.00	22	1060.9	0.00	0	18		20	9/18	CL	CH		
*	[illegible]	1059.9	20	1060.90	1039.9	21.00	20.1	1060.9	0.00	0	24		25	9/21	CL	CH		
*	[illegible]	1059.9	20	1060.90	1039.9	21.00	18.6	1060.9	0.00	0	20		17	9/22	CL	CH		
*	[illegible]	1059.9	20	1060.90	1039.9	21.00	25.4	1060.9	0.00	0	18		20	10/1	CL	CH		
*	[illegible]	1059.9	20	1060.90	1039.9	21.00	26.4	1060.9	0.00	0	18		22	10/1	CL	CH		
*	[illegible]	1059.9	20	1060.90	1039.9	21.00	22.7	1060.9	0.00	0	18		25	10/1	CL	CH		
*	[illegible]	1059.9	20	1060.90	1039.9	21.00	27.2	1060.9	0.00	0	18		25	10/2	CL	CH		
*	[illegible]	1059.9	20	1060.90	1039.9	21.00	27.6	1060.9	0.00	0	17		25	10/2	CL	CH		
*	[illegible]	1059.9	20	1060.90	1039.9	21.00	27.8	1060.9	0.00	0	18		20	10/2	CL	CH		
*	[illegible]	1059.9	20	1060.90	1039.9	21.00	27.8	1060.9	0.00	0	[illegible]		20	10/2	CL	CH		
	[illegible]	1059.9	20	1060.90	1039.9	21.00	20	1060.9	0.00	0	20		15	9/27	CL	CH		
	[illegible]	1059.9	20	1060.90	1039.9	21.00	21	1060.9	0.00	0	15		25	9/27	CL	CH		
*	[illegible]	1059.9	20	1060.90	1039.9	21.00	27.9	1060.9	0.00	0	16		20	10/2	CL	CH		
*	[illegible]	1059.9	20	1060.90	1039.9	21.00	27.6	1060.9	0.00	0	17		25	10/2	CL	CH		
*	[illegible]	1059.9	20	1060.90	1039.9	21.00	27.9	1060.9	0.00	0	19		25	10/2	CL	CH		
*	[illegible]	1059.9	20	1060.90	1039.9	21.00	28.6	1060.9	0.00	0	20		25	10/2	CL	CH		
*	[illegible]	1059.9	20	1060.90	1039.9	21.00	29.4	1060.9	0.00	0	16		15	9/28	CL	CH		
*	[illegible]	1059.9	20	1060.90	1039.9	21.00	26.0	1060.9	0.00	0	18		23	9/28	CL	CH		
*	[illegible]	1059.9	20	1060.90	1039.9	21.00	26.3	1060.9	0.00	0	16		15	9/28	CL	CH		
	[illegible]	1059.9	20	1060.90	103[illegible]	21.00	21.9	1060.9	0.00	0	18		15	9/19	CL	CH		
* ZONE B *	217	1060.3	17	1061.30	1043.3	18.00	26.8	1061.3	0.00	0	14		15	9/28	CL	CH		
*	218	1060.3	17	1061.30	1043.3	18.00	28.5	1061.3	0.00	0	14		15	9/28	CL	CH		
*	219	1060.3	17	1061.30	1043.3	18.00	28.1	1061.3	0.00	0	18		15	9/28	CL	CH		
	220	1060.3	17	1061.30	1043.3	18.00	20.6	1061.3	0.00	0	17		20	9/13	CL	CH		
	221	1060.3	17	1061.30	1043.3	18.00	17.4	1061.3	0.00	0	18		25	9/13	CL	CH		
	222	1060.3	17	1061.30	1043.3	18.00	17.6	1061.3	0.00	0	17		20	9/13	CL	CH		
	223	1060.3	17	1061.30	1043.3	18.00	17.5	1061.3	0.00	0	17		26	9/13	CL	[illegible]		
	224	1060.3	17	1061.30	1043.3	18.00	17.9	1061.3	0.00	0	17		25	9/13	CL	CH		
	225	1060.3	17	1061.30	1043.3	18.00	17.6	1061.3	0.00	0	20		26	9/13	CL	CH		
	226	1060.3	17	1061.30	1043.3	18.00	17.5	1061.3	0.00	0	18		25	9/13	CL	CH		

PCI QC REPRESENTATIVE:

*Cut was not subtracted

REPRESENTATIVE:

Location: [illegible] Used: PCI #: [illegible] GFC #

GEOPIERS INSTALLED

Location	#	Bottom Footing El, ft	Geopier Shaft Length, ft	Ground Surface El, ft	Geopier Bottom El, ft	Geopier Drill Depth, ft Planned	Geopier Drill Depth, ft Actual	Geopier Top El, ft	Geopier Top Depth, ft Planned	Geopier Top Depth, ft Actual	Geopier Stone Lifts #1	Geopier Stone Lifts #2	Tamp Time/Lift	Install Date	* Soil Material In Shaft	* Soil Material at Tip	Stiffness BST 2% min.	Stiffness DCPT 10% min.
	227	1060.3	17	1061.30	1043.3	18.00	17.2	1061.3	0.00	0	17		25	9/13	CL	CH		
	228	1060.3	17	1061.30	1043.3	18.00	17.4	1061.3	0.00	0	16		20	9/13	CL	CH		
	229	1060.3	17	1061.30	1043.3	18.00	18	1061.3	0.00	0	16		20	9/26	CL	CH		
	230	1060.3	17	1061.30	1043.3	18.00	17.2	1061.3	0.00	0	18		15	9/26	CL	CH		
	231	1060.3	17	1061.30	1043.3	18.00	20	1061.3	0.00	0	20		21	9/25	CL	CH		
	232	1060.3	17	1061.30	1043.3	18.00	17.9	1061.3	0.00	0	20		22	9/25	CL	CH		
	233	1060.3	17	1061.30	1043.3	18.00	18	1061.3	0.00	0	18		20	9/25	CL	CH		
	234	1060.3	17	1061.30	1043.3	18.00	[illegible]	1061.3	0.00	0	22		25	9/24	CL	CH		
ZONE C	235	1060.4	12	1061.40	1048.4	13.00	17.4	1061.4	0.00	0	19		16	9/25	CL	CH		
	236	1060.4	12	1061.40	1048.4	13.00	17.8	1061.4	0.00	0	18		15	9/25	CL	CH		
	237	1060.4	12	1061.40	1048.4	13.00	18.1	1061.4	0.00	0	20		20	9/24	CL	CH		
	238	1060.4	12	1061.40	1048.4	13.00	12.9	1061.4	0.00	0	11		20	9/13	CL	CH		
	239	1060.4	12	1061.40	1048.4	13.00	12	1061.4	0.00	0	12		20	9/13	CL	CH		
	240	1060.4	12	1061.40	1048.4	13.00	11.4	1061.4	0.00	0	13		20	9/13	CL	CH		
	241	1060.4	12	1061.40	1048.4	13.00	11.3	1061.4	0.00	0	13		20	9/13	CL	CH		
	242	1060.4	12	1061.40	1048.4	13.00	17.9	1061.4	0.00	0	15		25	9/13	CL	CH		
	243	1060.4	12	1061.40	1048.4	13.00	[illegible]	1061.4	0.00	0	[illegible]		20	[illegible]	CL	CH		
	244	1060.4	12	1061.40	1048.4	13.00	12.5	1061.4	0.00	0	12		25	9/13	CL	CH		
	245	1060.4	12	1061.40	1048.4	13.00	12.6	1061.4	0.00	0	12		25	9/13	CL	CH		
	246	1060.4	12	1061.40	1048.4	13.00	12.3	1061.4	0.00	0	12		25	9/13	CL	CH		
	247	1060.4	12	1061.40	1048.4	13.00	13.6	1061.4	0.00	0	21		20	9/24	CL	CH		
	248	1060.4	12	1061.40	1048.4	13.00	14.2	1061.4	0.00	0	22		20	9/24	CL	CH		
	249	1060.4	12	1061.40	1048.4	13.00	12.5	1061.4	0.00	0	16		17	9/24	CL	CH		
	250	1060.4	12	1061.40	1048.4	13.00	12.8	1061.4	0.00	0	18		15	9/24	CL	CH		
	251	1060.4	12	1061.40	1048.4	13.00	13.0	1061.4	0.00	0	19		20	9/24	CL	CH		
	252	1060.4	12	1061.40	1048.4	13.00	[illegible]	1061.4	0.00	0	12		15	9/24	CL	CH		
ZONE D	253	1060.6	7	1061.60	1053.6	8.00	14	1061.6	0.00	0	19		15	9/24	CL	CH		
	254	1060.6	7	1061.60	1053.6	8.00	13.5	1061.6	0.00	0	22		25	9/24	CL	CH		
	255	1060.6	7	1061.60	1053.6	8.00	13.9	1061.6	0.00	0	15		15	9/24	CL	CH		
	256	1060.6	7	1061.60	1053.6	8.00	7.5	1061.6	0.00	0	7		18	9/13	CL	CH		
	257	1060.6	7	1061.60	1053.6	8.00	7.5	1061.6	0.00	0	6		20	9/13	CL	CH		
	258	1060.6	7	1061.60	1053.6	8.00	8.0	1061.6	0.00	0	7		15	9/13	CL	CH		
	259	1060.6	7	1061.60	1053.6	8.00	7.8	1061.6	0.00	0	7		25	9/13	CL	CH		
	260	1060.6	7	1061.60	1053.6	8.00	7.8	1061.6	0.00	0	7		18	9/13	CL	CH		
	261	1060.6	7	1061.60	1053.6	8.00	7.5	1061.6	0.00	0	7		22	9/13	CL	CH		
	262	1060.6	7	1061.60	1053.6	8.00	8.0	1061.6	0.00	0	7		16	9/13	CL	CH		
	263	1060.6	7	1061.60	1053.6	8.00	9.5	1061.6	0.00	0	9		25	9/13	CL	CH		
	264	1060.6	7	1061.60	1053.6	8.00	7.5	1061.6	0.00	0	8		25	9/13	CL	CH		
	265	1060.6	7	1061.60	1053.6	8.00	7.5	1061.6	0.00	0	7		21	9/13	CL	CH		
	266	1060.6	7	1061.60	1053.6	8.00	8.4	1061.6	0.00	0	8		15	9/24	CL	CH		
	267	1060.6	7	1061.60	1053.6	8.00	9.1	1061.6	0.00	0	10		25	9/24	CL	CH		

190

[illegible]

PCI QC REPRESENTATIVE:

OWNER'S QA REPRESENTATIVE:

Location: VOH (O DOY   Used: ________   PCI #: [illegible]   GFC #: ________

GEOPIERS INSTALLED

Location	#	Bottom Footing El, ft	Geopier Shaft Length, ft	Ground Surface El, ft	Geopier Bottom El, ft	Geopier Drill Depth, ft Planned	Geopier Drill Depth, ft Actual	Geopier Top El, ft.	Geopier Top Depth, ft Planned	Geopier Top Depth, ft Actual	Geopier Stone Lifts #1	Geopier Stone Lifts #2	Tamp Time/ Lift	Install Date	* Soil Material In Shaft	* Soil Material at Tip	Stiffness BST 2% min.	Stiffness DCPT 10% min.
	268	1060.6	7	1061.60	1053.6	8.00	8.8	1061.6	0.00	0	12		17	9/24	CL	CH		
	269	1060.6	7	1061.60	1053.6	8.00	8.6	1061.6	0.00	0	12		25	9/24	CL	CH		
	270	1060.6	7	1061.60	1053.6	8.00	8.9	1061.6	0.00	0	12		24	9/24	CL	CH		
	271	1060.6	7	1061.60	1053.6	8.00	8.7	1061.6	0.00	0	13		20	9/24	CL	CH		
	272	1060.6	7	1061.60	1053.6	8.00	8.7	1061.6	0.00	0	18		23	9/24	CL	CH		
	273	1060.6	7	1061.60	1053.6	8.00	8.9	1061.6	0.00	0	14		25	9/24	CL	CH		
	274	1060.6	7	1061.60	1053.6	8.00	9	1061.6	0.00	0	10		21	9/24	CL	CH		
	275	1060.6	7	1061.60	1053.6	8.00	8.9	1061.6	0.00	0	10		21	9/24	CL	CH		
	276	1060.6	7	1061.60	1053.6	8.00	8.7	1061.6	0.00	0	10		23	9/24	CL	CH		
	277				0	0.00		1	0.00									
	278				0	0.00		1	0.00									
	279				0	0.00		1	0.00									
	280				0	0.00		1	0.00									
	281				0	0.00		1	0.00									
	282				0	0.00		1	0.00									
	283				0	0.00		1	0.00									
	284				0	0.00		1	0.00									
	285				0	0.00		1	0.00									
	286				0	0.00		1	0.00									
	287				0	0.00		1	0.00									
	288				0	0.00		1	0.00									
	289				0	0.00		1	0.00									
	290				0	0.00		1	0.00									
	291				0	0.00		1	0.00									
	292				0	0.00		1	0.00									
	293				0	0.00		1	0.00									
	294				0	0.00		1	0.00									
	295				0	0.00		1	0.00									
	296				0	0.00		1	0.00									
	297				0	0.00		1	0.00									
	298				0	0.00		1	0.00									
	299				0	0.00		1	0.00									
	300				0	0.00		1	0.00									
	301				0	0.00		1	0.00									
	302				0	0.00		1	0.00									
	303				0	0.00		1	0.00									
	304				0	0.00		1	0.00									
	305				0	0.00		1	0.00									
	306				0	0.00		1	0.00									
	307				0	0.00		1	0.00									
	308				0	0.00		1	0.00									

PCI QC REPRESENTATIVE: ________

OWNER'S QA REPRESENTATIVE: ________

REFERENCES

Aboshi, H., Suematsu, N. (1985),"Sand compaction pile method: state of the art paper." *Proc. 3^{rd} Intl. Geotechnical Seminar on Soil Improvement Methods*, Nanyang Technological Institute, Singapore.

ASCE (1984), "Committee on deep foundations report", ASCE Press, New York, New York.

Balaam, N. P., and Booker, J. R. (1981). "Analysis of rigid rafts supported by granular piles." *Int. J. Num. Anal. Methods in Geomechanics*, Vol. 5, p. 379-403.

Balaam, N. P., and Booker, J. R. (1985). "Effect of stone column yield on settlement of rigid foundations in stabilized clay." *Int. J. Num. Anal. Methods in Geomechanics*, Vol. 9, No. 4, p. 331-351.

Barksdale, R.D., Bachus R.C. (1983). "Design and construction of stone column.", Vol. 1, Report No. FHWA RD-83-026, NTIS, Virginia, USA.

Barron, R.A. (1947). "Consolidation of fine-grained soils by drain wells." *Proceedings ASCE*, Vol. 73, No. 6, p. 811-835.

Bergado, D.T., Rantucci, G., and Widodo, S. (1984). "Full scale load tests on granular piles and sand drains in the soft Bangkok clay.", Proc. Intl. Conf. on In-situ Soil and Rock Reinforcement, Paris, p. 111-118.

Bergado, D.T., Anderson, L.R., Miura, N., and Balasubramaniam, A.S. (1996) *Soft ground improvement in lowland and other environments*, ASCE Press, New York, N.Y., 1996.

Bergado, D.T., Lam, F.L. (1987). "Full scale load tests of granular piles with different densities and different proportions of gravel and sand on soft Bangkok clay, *Soils and Foundations*, Vol. 27, No. 1, p. 86-93.

Bergado, D.T., Sim, S.H., and Kalvade, S. (1987). "Improvement of soft Bangkok clay using granular piles in subsiding environment", Proc 5^{th} Intl. Geotechnical Seminar on Case Histories in Soft Clay, Singapore, p. 219-226.

Bergado, D.T., Miura, N., Panichayatum, B., and Sampaco, C.L. (1988). "Reinforcement of soft Bangkok clay using granular piles, Proc. Intl. Geotechnical Symp. on Theory and Practice of Earth Reinforcement, Fukuoka, Japan, p. 179-184.

Bowles, J. E. (1996). *Foundation analysis and design*, 5^{th} Edition. McGraw-Hill, New York, New York.

Briaund, Jean-Louis. (1989). "The pressuremeter test for highway applications." Federal Highway Administration Report No. FHWA –IP-89-008.

Brinoli, Enrico, Garassino, Angelo, and Renzo, Pietro. (1994). "The usefulness of stone columns to reduce settlements and distortions – A Case History." *Vertical and Horizontal Deformations of Foundations and Embankments,* Vol. 1, Geotechnical Special Publication No. 40, ASCE, New York, New York, p. 561-570.

Buggy, Fintan J., Martinez, Ramon E., Hussin, James D., and Deschamps, Richard J. (1994). "Performance of oil storage tanks on vibroflotation improved hydraulic fill in the Port of Tampa, Florida." *Vertical and Horizontal Deformations of Foundations and Embankments,* Vol. 1, Geotechnical Special Publication No. 40, ASCE, New York, New York, p. 561-570.

Carillo, N. (1942). "Simple two and three dimensional cases in the theory of consolidation of soils.", *Journal of Math and Physics*, Vol. 21, No. 1, p. 1-5.

Castelli, F., Maugeri, M. (2002). "Simplified non-linear analysis for settlement prediction of pile groups." *Journal of Geotechnical and Geoenvironmental Engineering*, Vol. 128, No. 1, p. 76-83.

Gaul, A.J. (2001). "Evaluation of rammed aggregate piers for highway applications in Iowa soils.", Iowa State University M.S. Thesis.

Goughnour, R. R. (1983). "Settlement of vertically loaded stone columns in soft ground." *Improvement of Ground*, Rotterdam, p. 235-240.

Greenwood, D. A. (1970). "Mechanical improvement of soils below ground surface." *Proc. Conf. On Ground Engineering*, London, ICE, p. 11-22.

Greenwood, D.A. and Kirsch, K. (1983). "Specialized ground treatment by vibratory and dynamic methods." *Proc. Conf. On Advances in Piling and Ground Treatment for Foundations*, London, Institution of Civil Engineers, p. 17-45.

Han, J., Ye, S.L. (1991). "Field tests of soft clay stabilized by stone columns in coastal areas in China." *Proc. 4th Intl. Conf. on Piling and Deep Foundations*, Balkema, Rotterdam, The Netherlands, 243-248.

Han, J., Ye, S.L. (2001). "Simplified method for consolidation rate of stone column reinforced foundations." *Journal of Geotechnical and Geoenvironmental Engineering*, Vol. 127, No. 7, p. 597-603.

Handy, R.L. (1976). "Discussion: Measurement of in-situ shear strength, in-situ measurement of soil properties." ASCE, Vol. II, p. 143-149.

Handy, Richard L. (2001). "Does lateral stress really influence settlement?" *Journal of Geotechnical Engineering*, (Accepted for Publication).

Hughes, J.M.O., and Withers, N.J. (1974). "Reinforcing of soft cohesive soils with stone columns." *Ground Engineering*, Vol. 7, No. 3, May, p. 42-49.

Hughes, J.M.O., Withers, N.J., Greenwood, D.A. (1975). "A field trial of the reinforcing effect of a stone column in soil.", Vol. 25, No. 1, p. 31-44.

Jamiolkowski, M., Baldi, G., Bellotti, R., Ghionna, V., and Pasqualini, E. (1985). "Penetration resistance and liquefaction of sand." *Proceedings 11th International Conference on Soil Mechanics and Foundation Engineering*, Vol. 4, San Francisco, p. 1891-1896.

Juran, I., Guermazi, A. (1988). "Settlement response of soft soils reinforced by compacted sand columns.", *Journal of Geotechnical Engineering*, ASCE, Vol. 114, No. 8, p. 930-943.

Kulhawy, F.H., and Mayne, P.W. (1990). "Manual on estimating soil properties for foundation design." EL-6800 Electric Power Research Institute, Palo Alto, California.

Lambe, T. W. and Whitman, Robert V. (1969). *Soil mechanics*. John Wiley & Sons, New York, New York.

Lawton, E.C. (1999). "Performance of Geopier™ foundations during simulated seismic tests at South Temple Bridge on Interstate 15, Salt Lake City, Utah." UUCVEEN, Report No. 99-06.

Lawton, Evert C., and Fox, Nathaniel S. (1994). "Settlement of structures supported on marginal or inadequate soils stiffened with short aggregate piers." *Vertical and Horizontal Deformations of Foundations and Embankments,* Vol. 2, Geotechnical Special Publication No. 40, ASCE, New York, New York, 962-974.

Lawton, Evert C., Fox, Nathaniel S., and Handy, Richard L. (1994). "Control of settlement and uplift of structures using short aggregate piers." *In-Situ Deep Soil Improvement*, Geotechnical Special Publication No. 45, ASCE, New York, New York, p. 121-132.

Madhav, M.R., Vitkar, R.P. (1978). "Strip footing on weak clay stabilized with granular trench or pile." *Canadian Geotechnical Journal*, Vol.15, No. 4, p. 605-609.

Marchetti, S. (1980). "In-situ tests by flat dilatometer." *Journal of Geotechnical Engineering Division*, ASCE, Vol. 106, GT 3, p. 299-321.

Mattes, N.S., and Poulos, H.G. (1969). "Settlement of single compressible piles.", *Journal of Soil Mechanics and Foundations*, ASCE, Vol. 95, p. 189-207.

Meyerhof, G.G. (1956). "Penetration tests and bearing capacity of cohesionless soils.", *Journal of Soil Mechanics and Foundation Division*, ASCE, Vol. 82, SM 1, p. 1-19.

Robertson, P.K, and Campanella, R.G. (1986). "Guidelines for use, interpretation, and application of the CPT and CPTU." 3rd ed., Hogentogler and Co., Inc.

Schmertmann, J.H. (1976). "Measurement of in-situ shear strength, in-situ measurement of soil properties." ASCE, Vol. II, p. 57-138.

Skempton, A.W. (1944). "Notes on compressibility of clays." *Quarterly Journal of the Geological Society of London*, p. 119-135.

Stewart, D., and Fahey, M. (1984). "An investigation of the reinforcing effect of stone columns in soft clay." *Vertical and Horizontal Deformations of Foundations and Embankments,* Vol. 1, Geotechnical Special Publication No. 40, ASCE, New York, New York, p. 513-524.

Terzaghi, K., Peck, R.B. (1967). *Soil mechanics in engineering practice.* 2nd edition, John Wiley and Sons, New York.

Van Impe, W. F. (1989). *Soil Improvement Techniques and Their Evolution*, Balkema, Rotterdam, The Netherlands.

White, David J., Lawton, Evert C., and Pitt, John M. (2000). "Lateral earth pressure induced by rammed aggregate piers." *Proceedings of the 53rd Canadian Geotechnical Conference,* Montreal, Vol. 2, p. 871-876.

Wineland, J.D. (1976). "Borehole shear device, in-situ measurement of soil properties." ASCE, Vol. II, p. 57-138.

Zhang, T., Tang, S., Ng, T. (2001). "Reliability of axially loaded driven pile groups.", *Journal of Geotechnical and Geoenvironmental Engineering*, Vol. 127, No. 12, p. 1051-1057.

ACKNOWLEDGMENTS

The author wishes to extend gratitude to the Iowa Highway Research Board for funding this research and to the Iowa DOT, Geopier™ Foundation Company, and Peterson Contractors Inc. for their full support, cooperation and assistance throughout this investigation. Several individual employees from each organization were absolutely invaluable including: Scott, Iowa DOT, Cork, PCI, Walt, PCI, Dan, PCI, Brendan, GFC.

The author is indebted to Dr. David J. White, my major professor, for the enormous amount of effort he put forth during the course of this project. His hard work was well beyond anything I could have expected.

The author wishes to thank Terracon and Dr. John M. Pitt for providing the financial support to complete my graduate studies. With their help I was able to focus on my studies to a much higher degree.

The author is heavily indebted to Aaron J. Gaul for several things including: encouragement to seek a Master's in geotechnical engineering (the best decision I've made in my education), the Terracon connection, surveying help at the project, a fantastic reference thesis, and generally being a righteous dude.

Finally, the author would like to thank his mother. You picked me up when I was down. I would not be writing this without you. Big brother Tim, the same goes for you.